(NASA-CR-160355) NUMERICAL SIMULATION OF DYNAMICS OF BRUSHLESS DC MOTORS FOR AEROSPACE AND OTHER APPLICATIONS. VOLUME 1: MODEL DEVELOPMENT AND APPLICATIONS, PART B Final Report (Virginia Polytechnic Inst. and G3/33

N80-14339

Unclas
46337

Virginia Polytechnic Institute and State University

Electrical Engineering

BLACKSBURG, VIRGINIA 24061

Final Report on Contract No. NAS 9-15091

NUMERICAL SIMULATION OF DYNAMICS OF BRUSHLESS DC MOTORS FOR AEROSPACE AND OTHER APPLICATIONS

VOLUME (I) - MODEL DEVELOPMENT AND APPLICATIONS - PART (B)

Submitted to NASA-Johnson Space Center

Control Systems Development Division

Houston, Texas 77058

by

Principal Investigator

N. A. O. Demerdash

N. A. O. Demerdash

and

Research Associate

T. W. Nehl

T. W. Nehl

Department of Electrical Engineering

Virginia Polytechnic Institute and State University

Blacksburg, VA 24061

5.0 MODEL VERIFICATION

In order to establish the validity of the EMA model, comparisons are made between results obtained from lab tests on the actual EMA and those from equivalent computer simulations. The computer program has several run options as described earlier in Section 4.5, for this reason, the following verification schedule will be followed:

1. Verification of the Power Conditioner and Machine Model
   - Motoring
   - Regeneration
   - Plugging
2. Verification of the Fourteenth Order EMA Model
3. Verification of the Tenth Order EMA Model

Table (5.0-1) catalogs the various computer runs which are used in this verification procedure. The results of these runs are presented in the twelve appendices: A.1-A.3, B.1, C.1-C.3, D.1, E.1-E.4. In terms of the aforementioned verification program, these appendices are organized as follows:

1. Power Conditioner and Machine Model
   - Motoring: Appendices A.1, A.2, and A.3
   - Regeneration: Appendix B.1
   - Plugging: Appendices C.1, C.2, and C.3
2. Fourteenth Order EMA Model: Appendix D.1
3. Tenth Order EMA Model: Appendices E.1, E.2, E.3, and E.4.

The tests on the actual hardware were performed by Delco Electronics and are described in References (2), (3), and (4).

A summary of each computer run is given on the first page of each of the twelve appendices. The results of these computer simu-

TABLE 5.0-1

RUN NUMBER	CALCOMP FIGURES	MODE	ROTOR SPEED (RPM)	CURRENT COMMAND ICMD (amps)	COMMUTATION SHIFT SHIFT: mech rad, mech deg COM. ADVANCE: elec deg	FLAP POSITION COMMAND (DC) (flap deg)
A.1	A.1-1,20	Motoring	5000	31.5 ± 4	0.0 rad, 0.0 (30) deg	--
A.2	A.2-1,5	Motoring	5000	31.5 ± 4	0.0349 rad, 2.0 (38) deg	--
A.3	A.3-1,5	Motoring	5000	31.5 ± 4	-0.0349 rad, -2.0 (22) deg	--
B.1	B.1-1,20	Regeneration	5101	-38.0 ± 4	--	--
C.1	C.1-1,20	Plugging	240	32.0 ± 4	0.0 rad, 0.0 (30) deg	--
C.2	C.2-1,5	Plugging	240	32.0 ± 4	0.0349 rad, 2.0 (38) deg	--
C.3	C.3-1,5	Plugging	240	32.0 ± 4	-0.0349 rad, -2.0 (22) deg	--
D.1	D.1-1,14	14^{th} Order EMA Model	0-10159	$-40 \rightarrow +40 \pm 4$	0.0 rad, 0.0 (30) deg	2.75
E.1	E.1-1,8	10^{th} Order EMA Model	0-9500	$-40 \rightarrow +40$	--	1.1
E.2	E.2-1,8	10^{th} Order EMA Model	0-9500	$-40 \rightarrow +40$	--	1.65
E.3	E.3-1,8	10^{th} Order EMA Model	0-9500	$-40 \rightarrow +40$	--	2.2
E.4	E.4-1,8	10^{th} Order EMA Model	0-9500	$-40 \rightarrow +40$	--	2.75

lations are plotted by a CalComp pen type plotter. Tables 5.0-2 and 5.0-3 contain listings and descriptions of the CalComp plots. Figures (A.1-1), (A.2-1), (A.3-1), (B.1-1), (C.1-1), (C.2-1), (C.3-1), (D.1-1) (E.1-1), (E.2-1), (E.3-1), and (E.4-1) give the status of the logic signals versus time for each of the twelve computer runs. These (5.0-4) signals are defined in Table (5.0-4). With these logical variables the reader can easilty follow the status of each solid state power conditioner element as time progresses.

A few conventions must be established to facilitate the comparison and discussion which will follow. It will be agreed upon, in the language of this report, that the time origin in all the waveforms included here is at the farthest left hand side of the figures. Also, positive time is measured to the right hand side of the origin. The edge of a positive half-waveform closer to the time origin will be referred to as the "leading edge". On the other hand, the edge of a positive half-waveform farther from the time origin will be referred to as the "trailing edge". The waveform for various currents and voltages which are obtained from computer simulations will be referred to by the abbreviation CSWF. It should be pointed out that various CSWFs and their corresponding oscillogram counterparts have been obtained under slightly different operating conditions (speed, current command, etc.). Also it must be made clear that these investigators had no control over the experimental test procedures and conditions, since they were performed at a different facility.

TABLE 5.0-2

EMA Logic Signals	A.1-1	A.2-1	A.3-1	B.1-1	C.1-1	C.2-1	C.3-1
Machine Electromagnetic Torque (TEM)	A.1-2	A.2-2	A.3-2	B.1-2	C.1-2	C.2-2	C.3-2
Capacitor Voltage (VB5)	A.1-3	---	---	B.1-3	C.1-3	---	---
Phase A Machine Current (C1A)	A.1-4	A.2-3	A.3-3	B.1-4	C.1-4	C.2-3	C.3-3
Phase B Machine Current (C1B)	A.1-5	---	---	B.1-5	C.1-5	---	---
Phase C Machine Current (C1C)	A.1-6	---	---	B.1-6	C.1-6	---	---
Phase A Back EMF (E1)	A.1-7	A.2-4	A.3-4	B.1-7	C.1-7	C.2-4	C.3-4
Phase B Back EMF (E2)	A.1-8	---	---	B.1-8	C.1-8	---	---
Phase C Back EMF (E3)	A.1-9	---	---	B.1-9	C.1-9	---	---
Line to Line Machine Voltage VAB	A.1-10	A.2-5	A.3-5	B.1-10	C.1-10	C.2-5	C.3-5
Q1-D1 Current (IB9)	A.1-11	---	---	B.1-11	C.1-11	---	---
Q1-D1 Voltage (VB9)	A.1-12	---	---	B.1-12	C.1-12	---	---
QM-DB Current (IB17)	A.1-13	---	---	B.1-13	C.1-13	---	---
QM-DB Voltage (VB17)	A.1-14	---	---	B.1-14	C.1-14	---	---
QB-DM Current (1b6)	A.1-15	---	---	B.1-15	C.1-15	---	---
QB-DM Voltage (VB6)	A.1-16	---	---	B.1-16	C.1-16	---	---
DR Current (IB7)	A.1-17	---	---	B.1-17	C.1-17	---	---
DR Voltage (VB7)	A.1-18	---	---	B.1-18	C.1-18	---	---
Chopper Inductor Current	A.1-19	---	---	B.1-19	C.1-19	---	---
Machine Line Current (IM)	A.1-20	---	---	B.1-20	C.1-20	---	---

TABLE 5.0-3

EMA Logic Signals	D.1-1	E.1-1	E.2-1	E.3-1	E.4-1
Machine Torque (TM)	D.1-2	E.1-2	E.2-2	E.3-2	E.4-2
Flap Position Angle (FANG)	D.1-3	E.1-3	E.2-3	E.3-3	E.4-3
Machine Current (IM)	D.1-4	- - -	- - -	- - -	- - -
Machine Current |IM|	- - -	E.1-4	E.2-4	E.3-4	E.4-4
Velocity Error (VE)	D.1-5	E.1-5	E.2-5	E.3-5	E.4-5
Commanded Machine Current (IMC)	D.1-6	- - -	- - -	- - -	- - -
ICMD1/5 (XV(2))	D.1-7	- - -	- - -	- - -	- - -
Velocity FB-Loop Output (XV(3))	D.1-8	- - -	- - -	- - -	- - -
Current Rate Limiter (XV(5))	D.1-9	E.1-6	E.2-6	E.3-6	E.4-6
Rotor Velocity (XM(1))	D.1-10	E.1-7	E.2-7	E.3-7	E.4-7
EMA Mount Reaction Torque (TACT - XM(2))	D.1-11	- - -	- - -	- - -	- - -
Flap Velocity (XM(3))	D.1-12	- - -	- - -	- - -	- - -
Flap Position (XM(4))	D.1-13	- - -	- - -	- - -	- - -
Amplified Position Error (PE - XM(5))	D.1-14	E.1-8	E.2-8	E.3-8	E.4-8

TABLE 5.0-4 Description of the Logical Variables

LOGICAL VARIABLES	DESCRIPTION
DR	STATUS OF DIODE DR
DM	STATUS OF DIODE DM
DB	STATUS OF DIODE DB
D(6)	STATUS OF DIODE D6
D(5)	STATUS OF DIODE D5
D(4)	STATUS OF DIODE D4
D(3)	STATUS OF DIODE D3
D(2)	STATUS OF DIODE D2
D(1)	STATUS OF DIODE D1
QBON	STATUS OF TRANSISTOR QB
QMON	STATUS OF TRANSISTOR QM
Q(6)	STATUS OF TRANSISTOR Q6
Q(5)	STATUS OF TRANSISTOR Q5
Q(4)	STATUS OF TRANSISTOR Q4
Q(3)	STATUS OF TRANSISTOR Q3
Q(2)	STATUS OF TRANSISTOR Q2
Q(1)	STATUS OF TRANSISTOR Q1
CC	OUTPUT OF ROTOR POSITION SENSOR C
BB	OUTPUT OF ROTOR POSITION SENSOR B
AA	OUTPUT OF ROTOR POSITION SENSOR A
PLUG2	PLUGGING REGION 2
RGN2	REGENERATION REGION 2
MTRG3	MOTORING REGION 3
PLUG 4	PLUGGING REGION 4
RGN4	REGENERATION REGION 4
MTRG1	MOTORING REGION 1
TNEG	POSITIVE MACHINE TORQUE
TPOS	NEGATIVE MACHINE TORQUE
SPDNEG	NEGATIVE MACHINE VELOCITY
SPDPOS	POSITIVE MACHINE VELOCITY
SPDLO	RGN2 VELOCITY RANGE
SPDHI	RGN4 VELOCITY RANGE

5.1 VERIFICATION OF THE POWER CONDITIONER AND MACHINE MODEL

The power conditioner and machine model is verified by comparisons of simulation runs with actual oscillograms obtained from tests performed on the EMA. These comparisons are made for each of the three modes, as follows:

Motoring	5000 rpm	ICMD = 31.5
Regeneration	5101 rpm	ICMD = -38
Plugging	240 rpm	ICMD = 32

The input data used for the power conditioner and machine is given in Table (5.1-1).

Computer simulations were obtained for the three basic modes of operation for the brushless DC machine-power conditioner package. The first mode is the forward motoring case at a rotor speed of 5000 r.p.m. The corresponding current and voltage waveforms through and across the numerous elements of the network for various commutation angles are given in Appendices A.1, A.2, and A.3, respectively. The second mode given here, is the generator (regenerative braking) case at a rotor speed of 5101 r.p.m. The corresponding current and voltage waveforms are given in Appendix B.1. The third mode studied is the forward braking case at a rotor speed of 240 r.p.m. The various waveforms obtained during this mode are displayed in Appendices C.1, C.2, and C.3. For the sake of convenience and comparison purposes some of the figures given in these appendices are repeated here with their corresponding experimentally obtained counterparts.

Figure (5.1-1) shows experimentally obtained oscillograms of the machine phase currents at a speed of 5000 r.p.m. and with a comm-

TABLE 5.1-1 The Values of the Parameters for the Power Conditioner and Machine Model

R1	.0333333/333.3333 (ON/OFF)
R2	.0333333/333.3333
R3	.0333333
R4	.0333333/333.3333
R5	.0333333/333.3333
R6	.0333333/333.3333
R7	.0596
R8	.0596
R9	.0596
R10	.0333333
R11	.0333333/333.3333
R12	.0333333/333.3333
R13	.0333333/333.3333
R14	.0333333/333.3333
L1	.000286
L2	.000486 (NONLINEAR)
L3	.000286
L4	.000286
C1	.00099
E4	270
UNITS: Ohms, Henries, Farads, and Volts.	

utation advance of 30 electrical degrees. The corresponding CSWF of the currents through phase A for commutation advance angles of 30, 22, and 38 electrical degrees are shown in Figures (5.1-3), (5.1-4), and (5.1-5). Figure (5.1-2) shows the spatial relationship between the output AA of the RPS for phase A and the command to inject current into phase A, Q(1), for the chosen commutation angles. Examination of the current waveforms reveals the same characteristic over-shoot and under-shoot at the leading and trailing edges of the oscillogram and the CSWF. The positive peaks of the current oscillograms shown in Figure (5.1-1) are indicated by an (X) on the corresponding CSWF, Figure (5.1-3). Notice the excellent agreement between the measured and computed current peaks. The transients in Figure (5.1-3) may appear exaggerated in comparison with Figure (5.1-1), but this is due to the "horizontal squeeze" and "vertical stretch" of the CSWF caused by the horizontal and vertical scaling of the plot. Both the oscillogram and the CSWF display the same chopper frequency of nine peaks per half cycle. Notice also the two slope current transient present in both cases in the middle of the positive and negative current cycle. Figures (5.1-4) and (5.1-5) demonstrate the effects of varying the commutation angle on the nature of the phase currents. This commutation angle also has a great effect on the electromagnetic torque of the machine as shown in Figures (A.1-1), (A.3-1), and (A.2-1), respectively.

The lower trace in Figure (5.1-6) depicts the oscillogram of the current through one of the transistor-diode switches in the six legged inverter-converter bridge leading to the machine phases. A corresponding CSWF is given in Figure (5.1-7). Excellent correlation between the various ripples and pulses in the oscillogram and the CSWF are self evident upon examining these figures. Time congruence between the occurance of the various ripples and pulses is also evident in these figures.

Figure (5.1-8) depicts the oscillogram of the main DC line current for a motoring mode. Notice the current dips which are occuring at regular intervals. The almost identical ripple and dip pattern is also evident in the CSWF given here in Figure (5.1-9). Again the agreement between the numerical and test results is excellent.

Figure (5.1-10) gives the phase current for the generating (or regenerative braking) mode at a rotor speed of 5101 r.p.m., Figure (5.1-11) depicts the corresponding CSWF of one of the three phase currents at a constant rotor speed of 5101. Again agreement between the oscillogram and the CSWF is excellent.

The last oscillogram, Figure (5.1-12) was made while the machine-power conditioner was operating in the braking mode at a speed of 240 r.p.m. The upper trace of this oscillogram shows a typical phase current for this mode of operation. The corresponding CSWF is given in Figure (5.1-13). The lower trace of Figure (5.1-12) shows the waveform of the current through one of the transistor switches connected to the permanent magnet machine. The corresponding CSWF is given in Figure (5.1-17). The CSWF shown in Figure (5.1-13) was obtained by using a reduced emf waveform, see Reference (15).
The CSWFs of Figures (5.1-14), (5.1-15), and (5.1-16) where obtained using the magnetized and demagnetized back emfs described earlier in Section 2.4. The reduced emfs are better in this case because

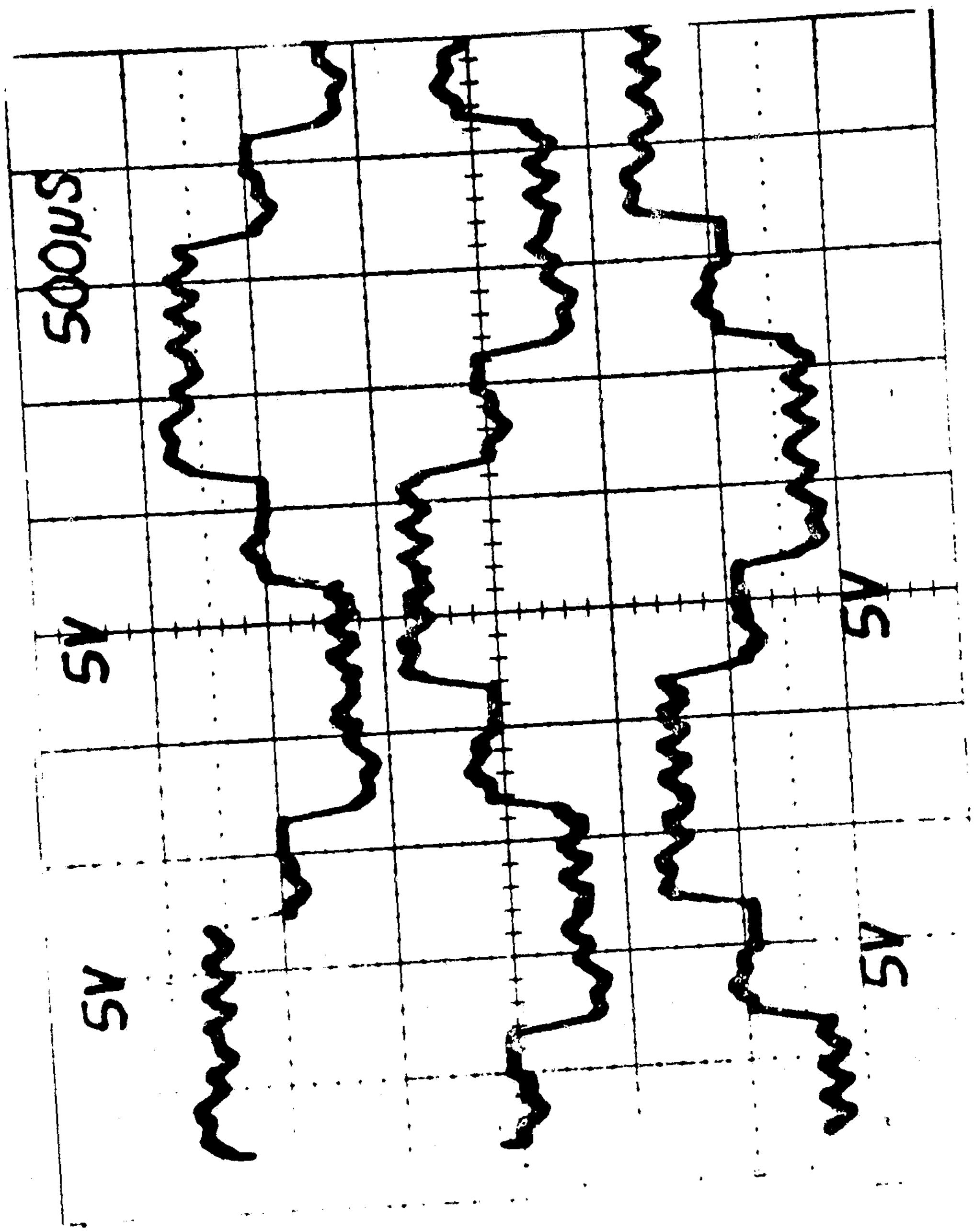

Figure 5.1-1. Oscillogram of Phase Currents during Motoring 5000rpm, ICMD = 31.5 amps, and 30° Com. Adv.

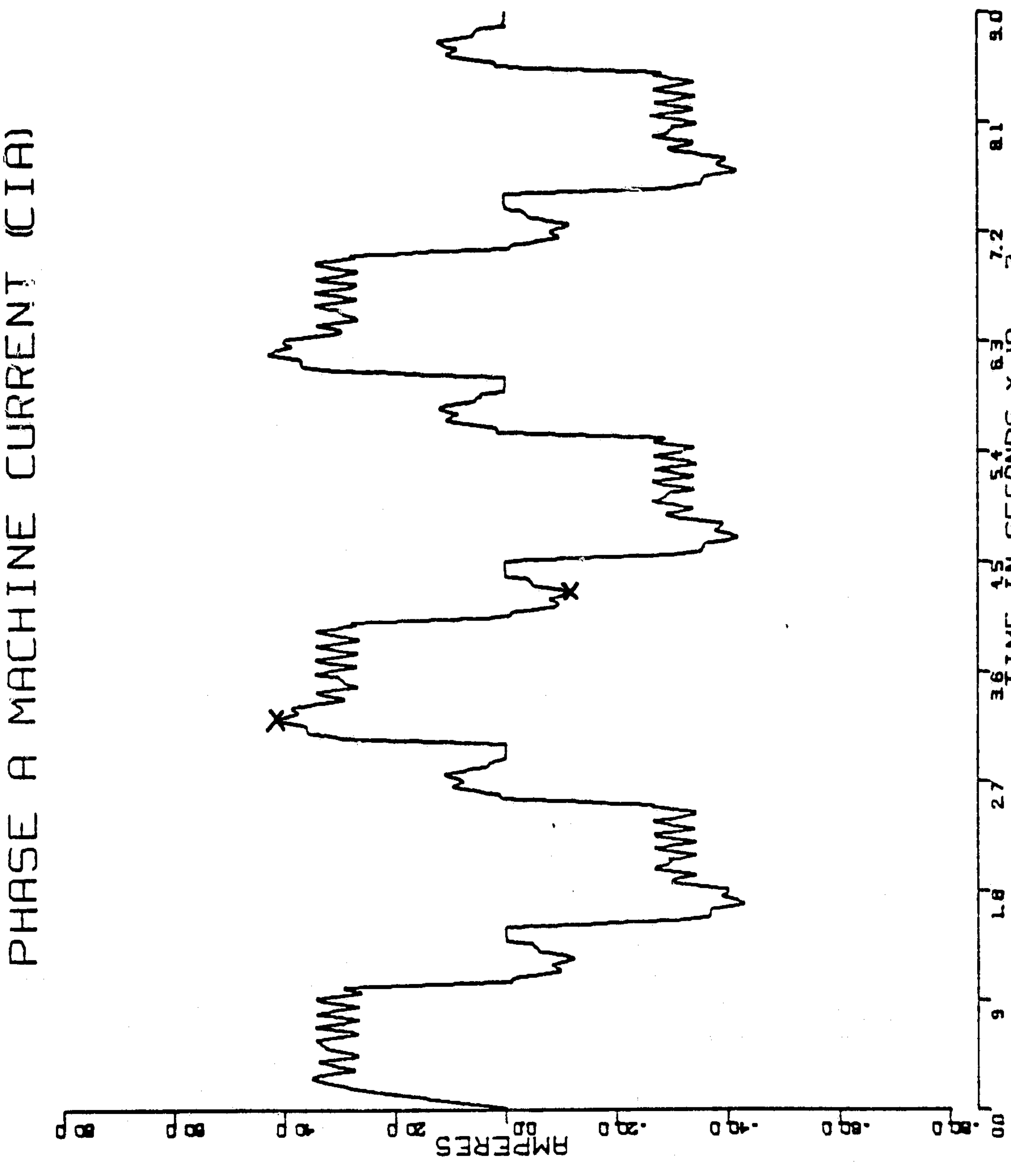

× Measured from Oscillogram

Figure 5.1-2. Simulated Phase A Current during Motoring
5000 rpm, ICMD = 31.5 amps, 30° Com. Adv.

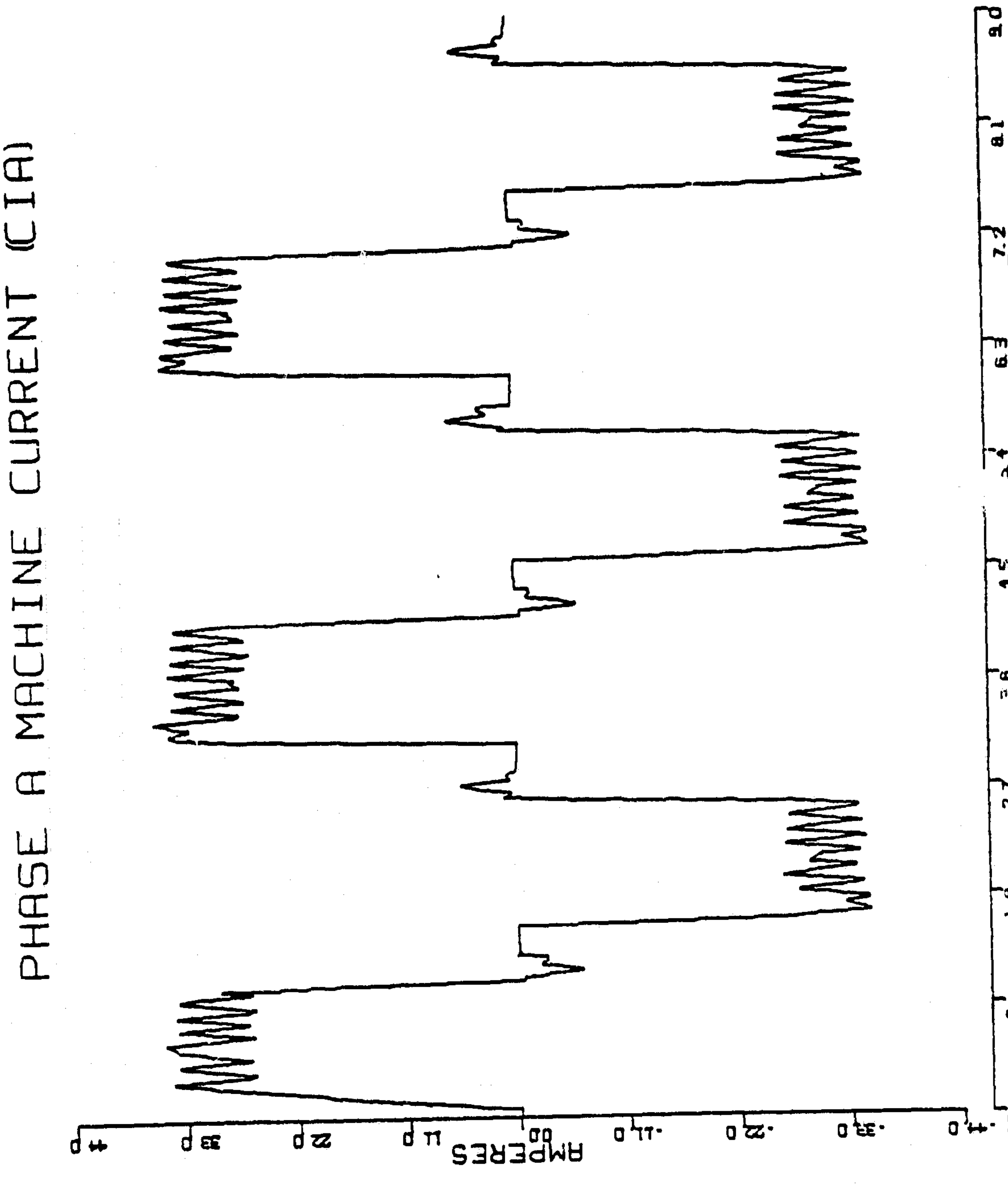

Figure 5.1-3. Simulated Phase A Current during Motoring at 5000 rpm, ICMD = 31.5 amps, and 22° Com. Adv.

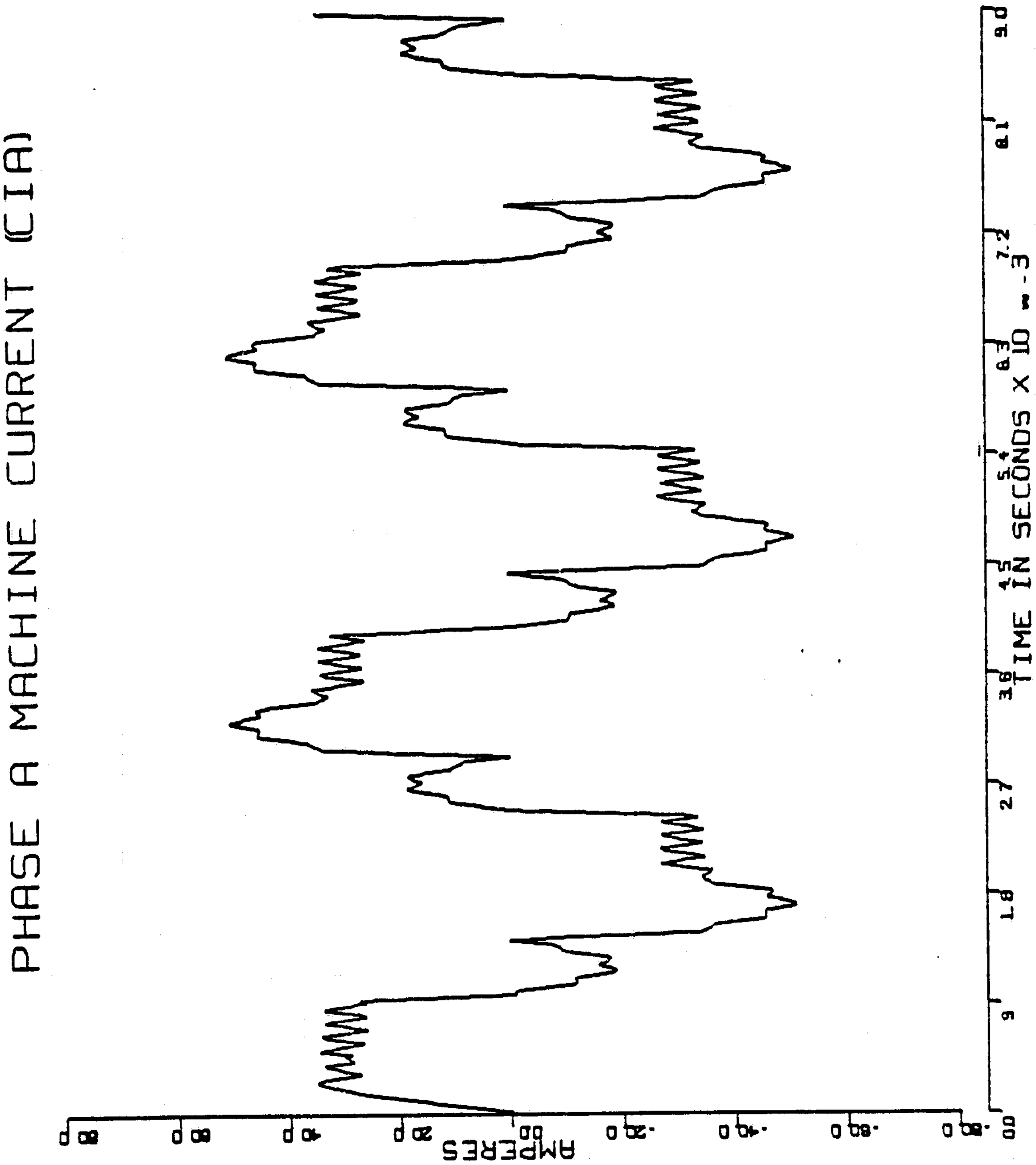

Figure 5.1-4. Simulated Phase A Current during Motoring 5000 rpm, ICMD = 31.5, and 38° Com. Adv.

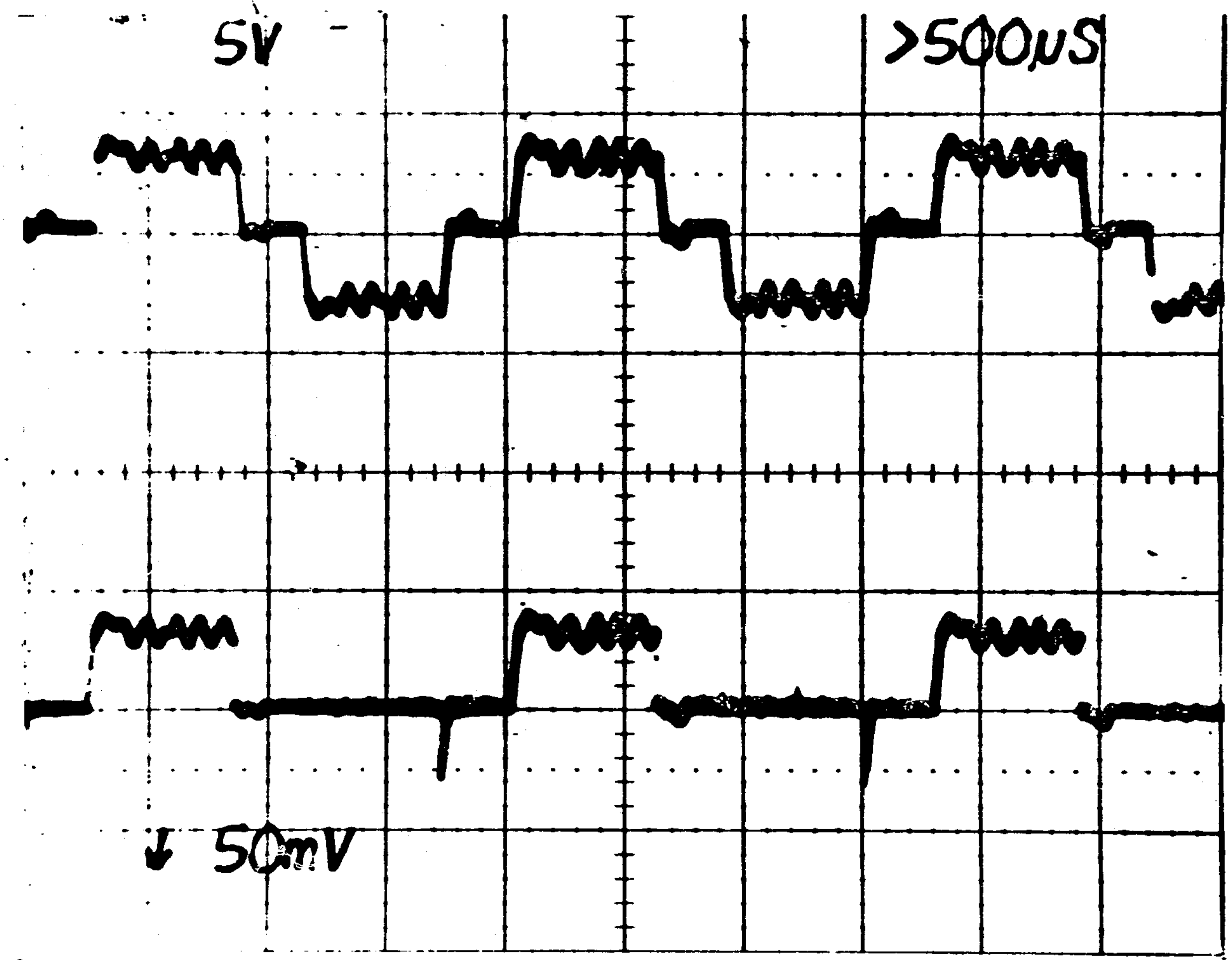

Figure 5.1-5. Oscillogram of the Currents through Phase B (Top) and through the (Q2-D2) Inverter Switch during Motoring 5025 rpm, ICMD = 32.5 amps, and 30° Com. Adv.

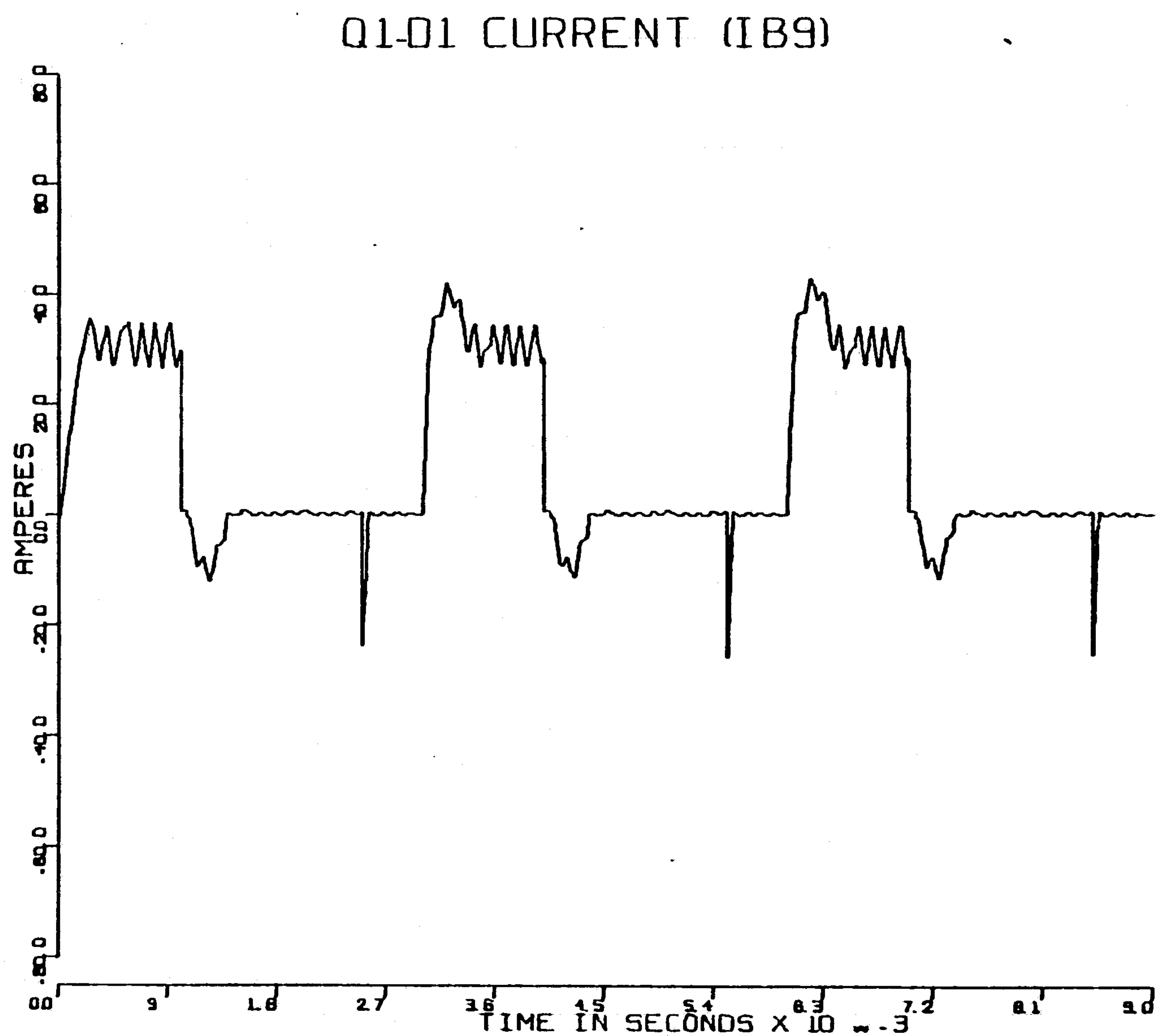

Figure 5.1-6. Simulation of the Current through the (Q1-D1) Inverter Switch during Motoring
5000 rpm, ICMD = 31.5 amps and 30° Com. Adv.

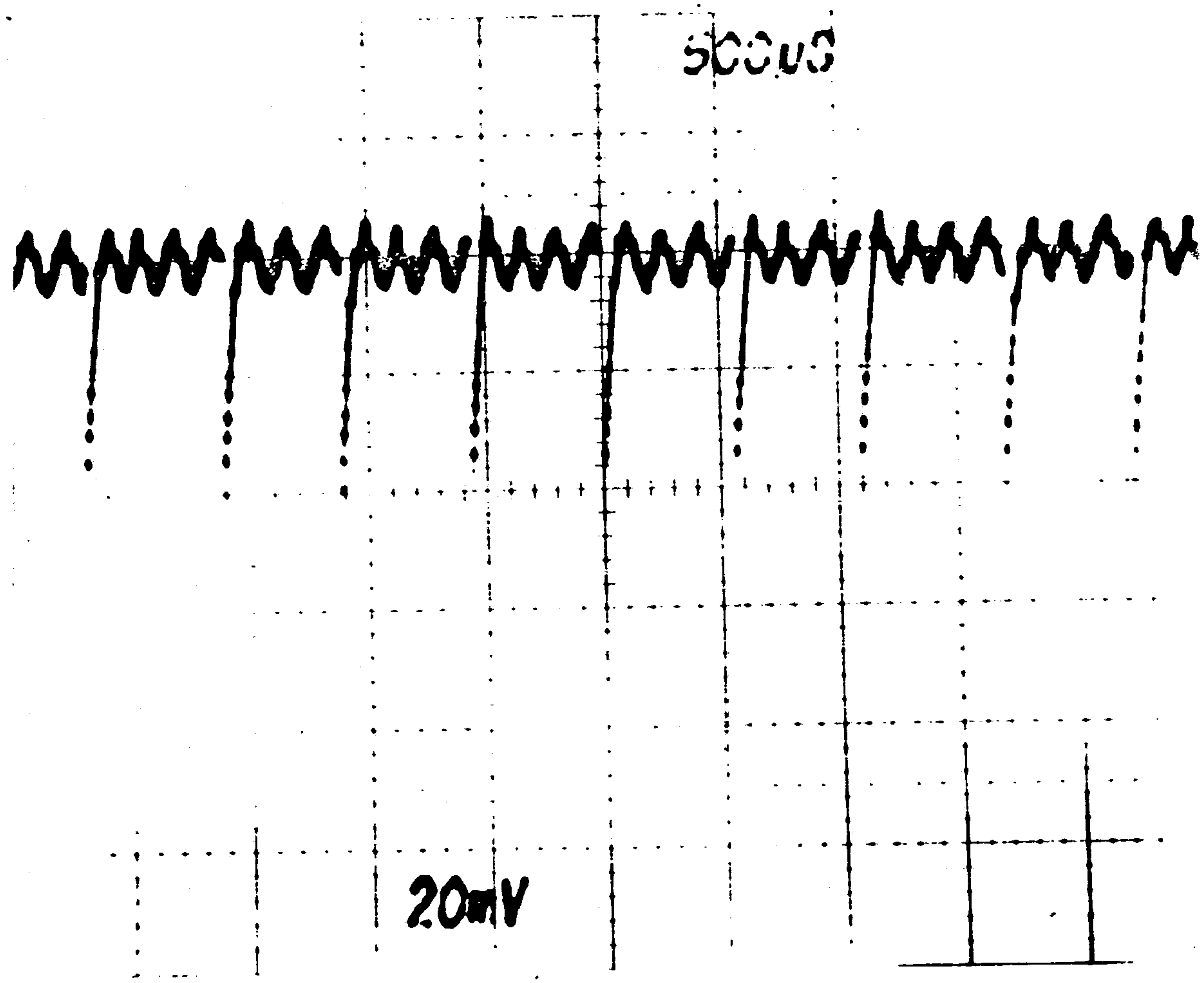

Figure 5.1-7. Oscillogram of the Machine Line Current during Motoring +500 rpm, ICMD = 41.5 amps, 30° Com. Adv.

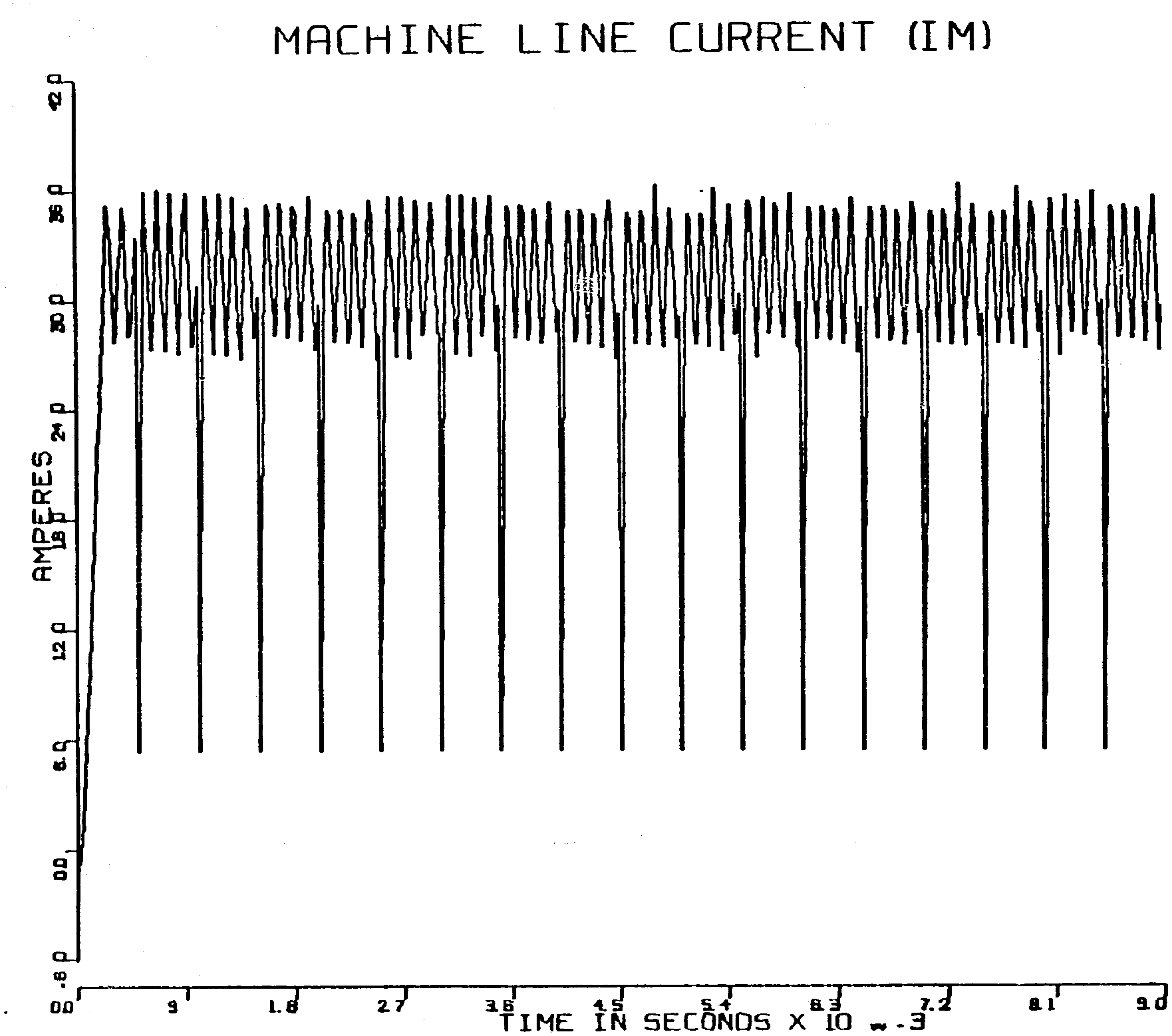

Figure 5.1-8. Simulation of the Machine Line Current during Motoring
5000 rpm, ICMD = 3 amps, 30° Com. Adv.

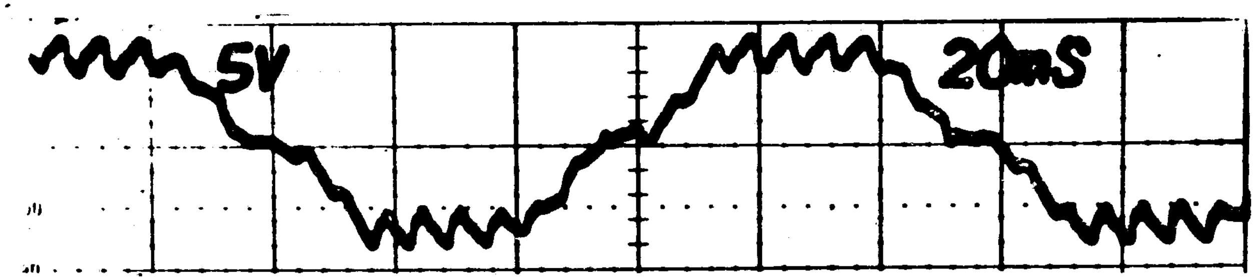

Figure 5.1-9. Oscillogram of a Machine Phase Current during Regeneration
5101 rpm, ICMD = -38.0 amps

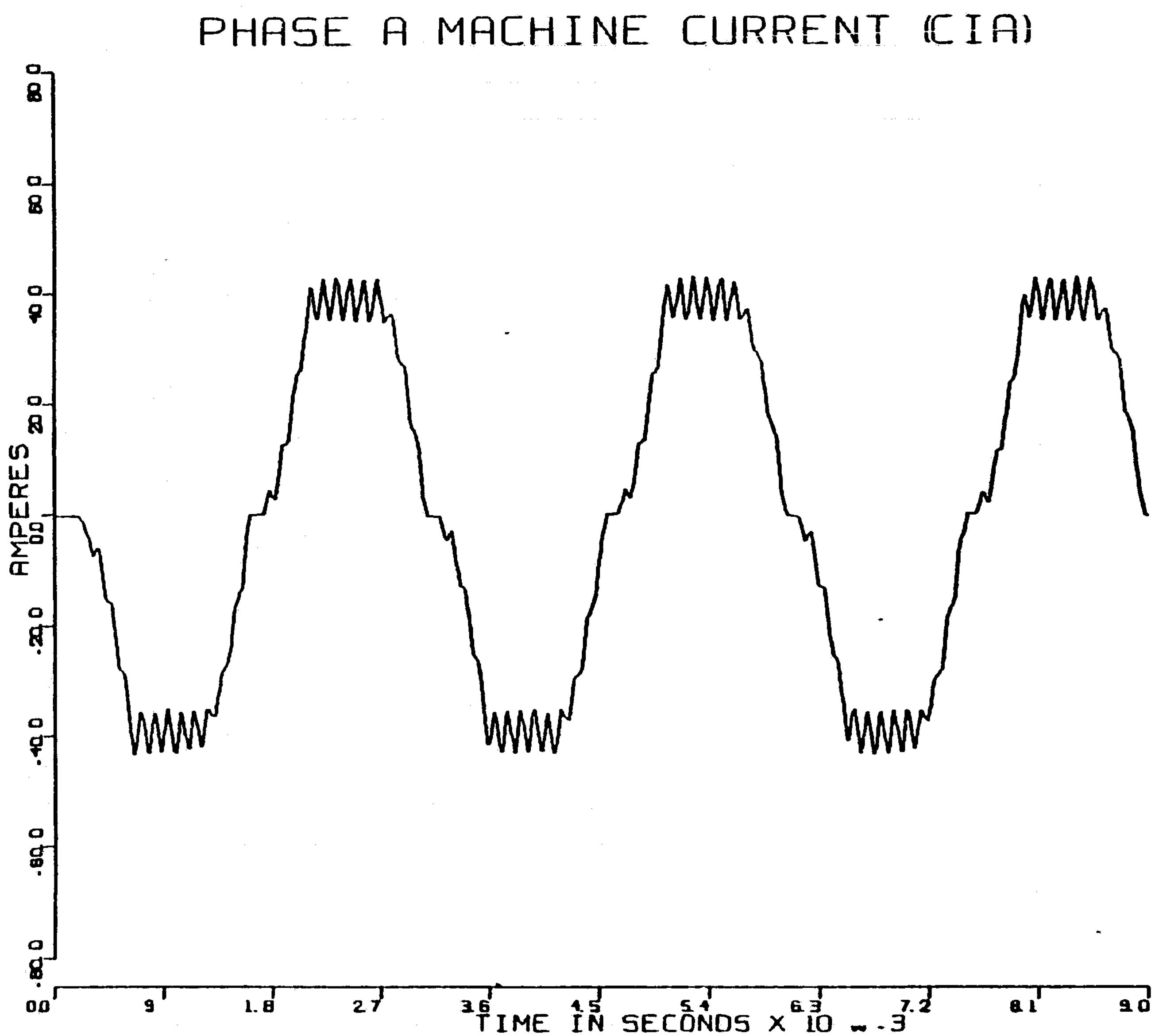

Figure 5.1-10. Simulated Phase A Current during Regeneration
5101 rpm, ICMD = -38.0 amps

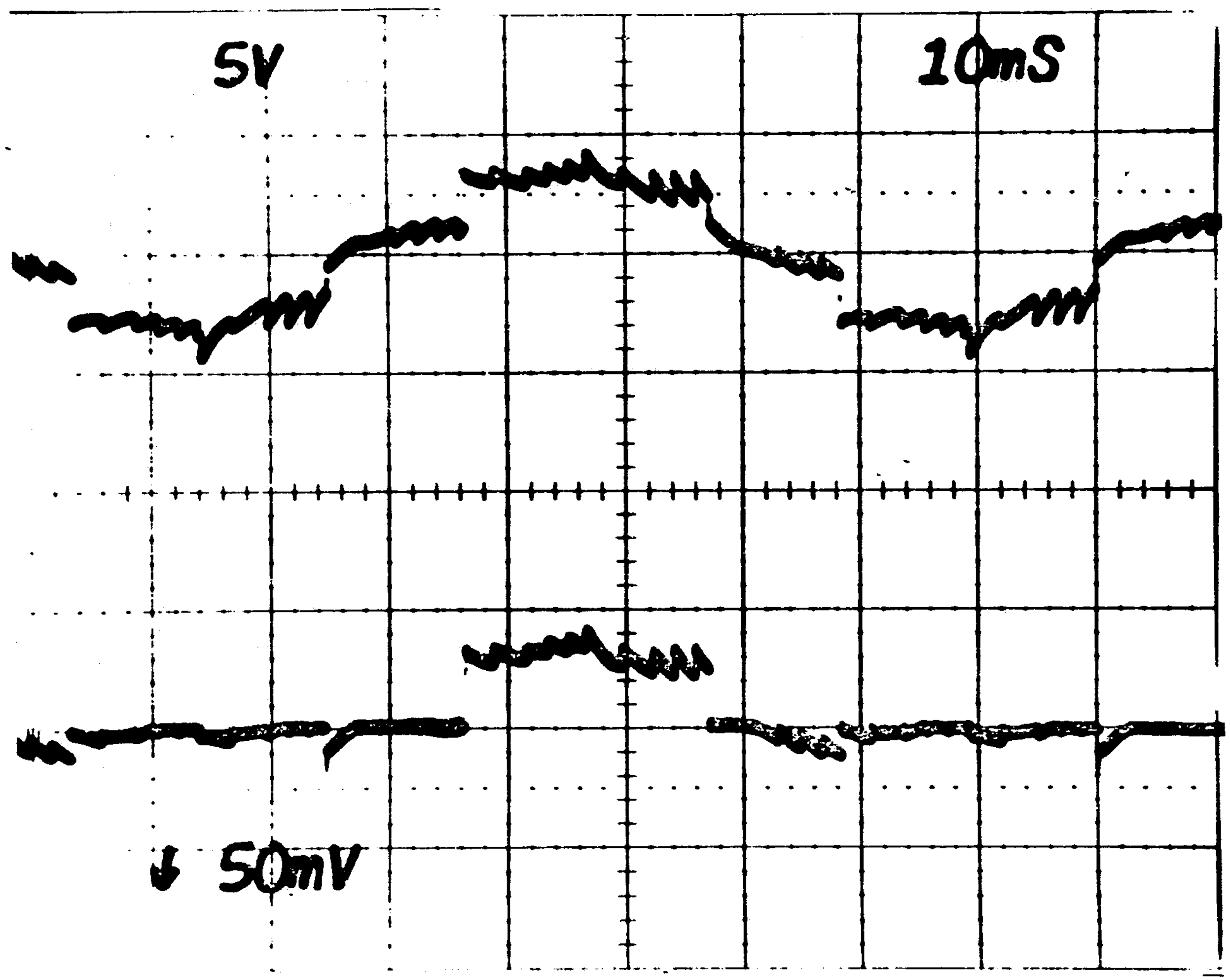

Figure 5.1-11. Oscilloogram of the Currents through Phase B (Top) and through the (Q2-D2) Inverter Switch during Plugging
240 rpm, ICMD = 32 amps, 30° Com. Adv.

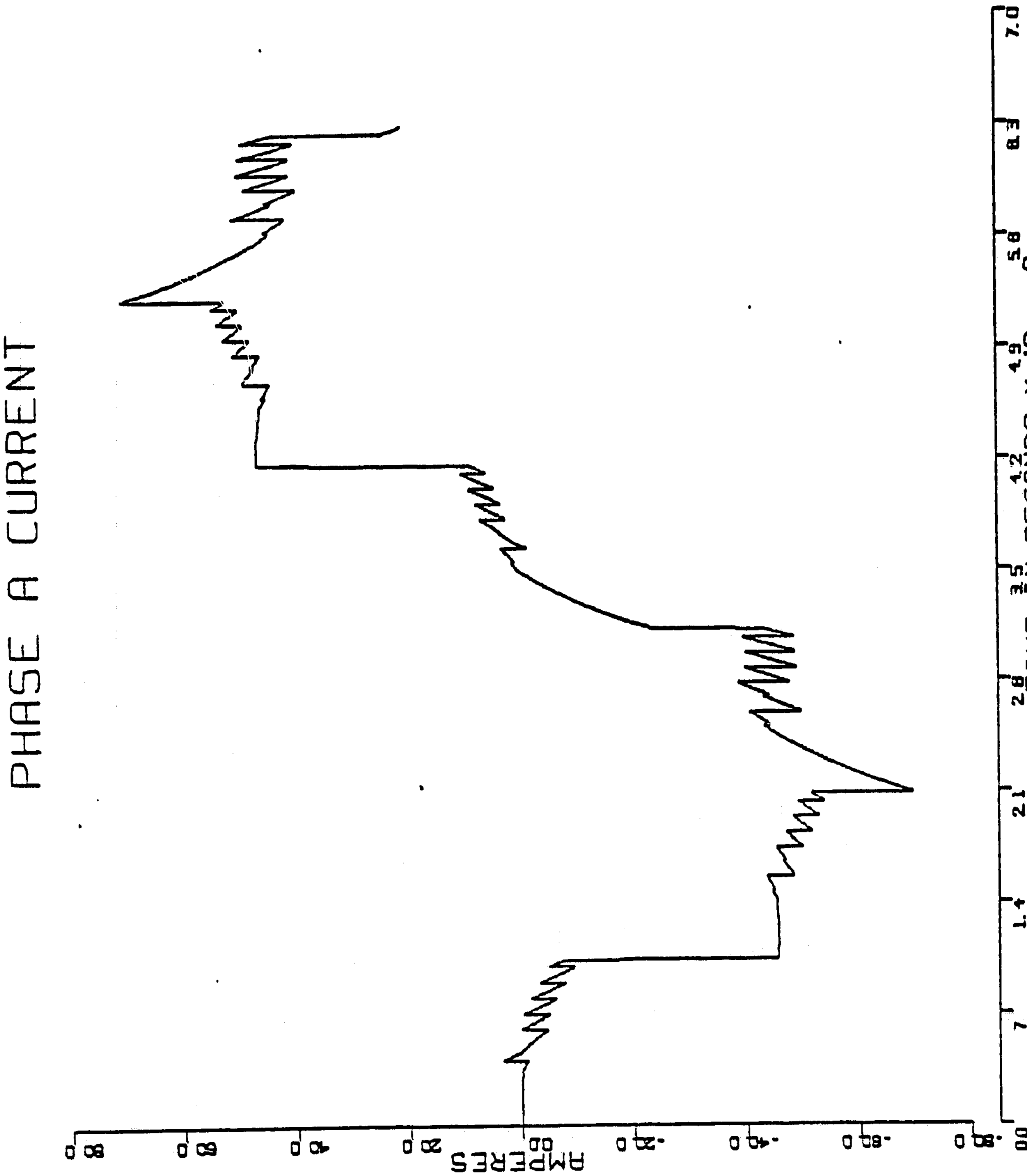

Figure 5.1-12 Simulated Phase A Current during Plugging, 240 rpm ICMD = 40 amps, 30° Com. Adv. Obtained using a Reduced Back Emf of 30 volts peak.

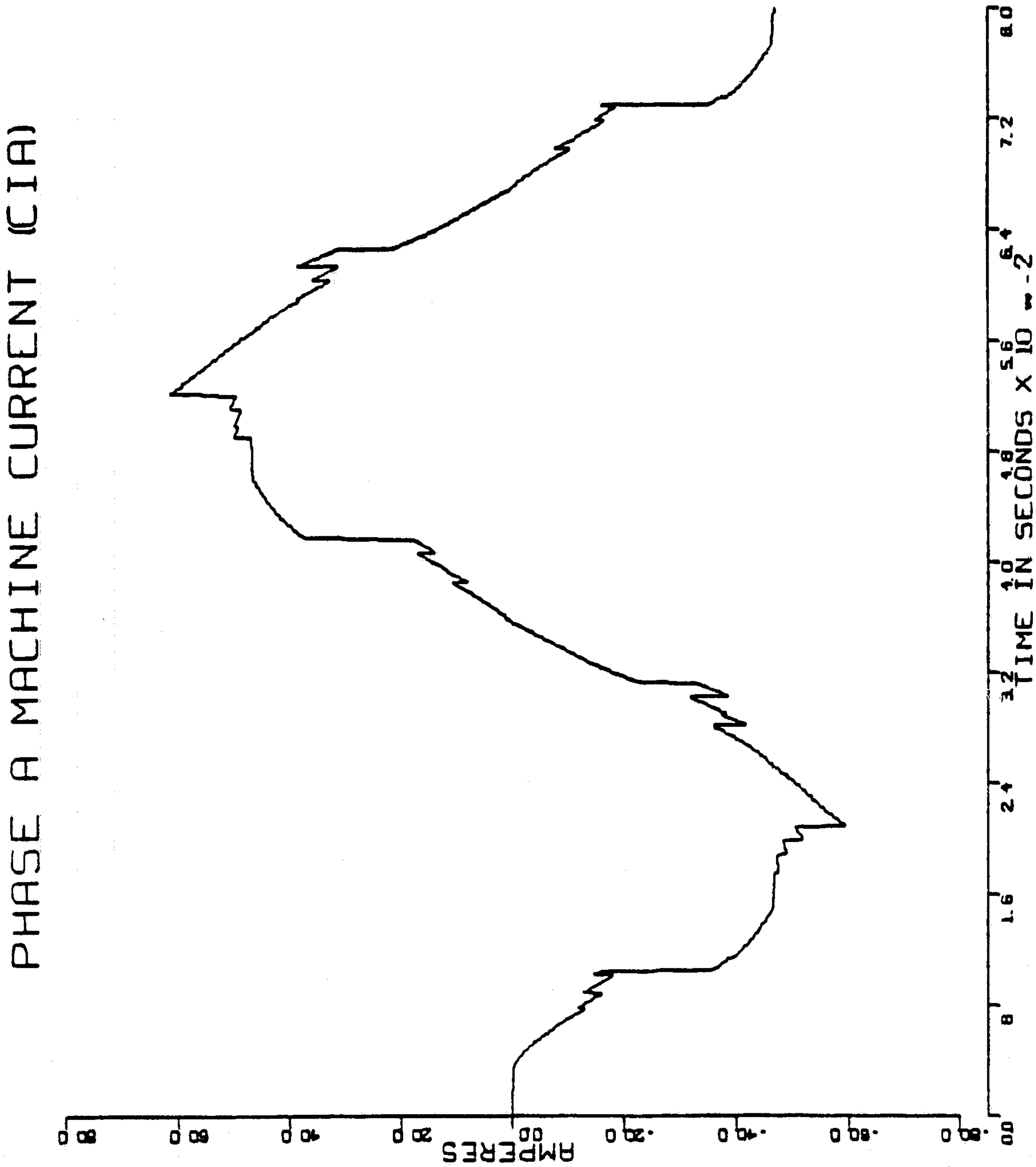

Figure 5.1-13 Simulated Phase A Current during Plugging
240 rpm, ICMD = 32 amps, 30° Com. Adv.
Peak Back Emf = 3.8 volts

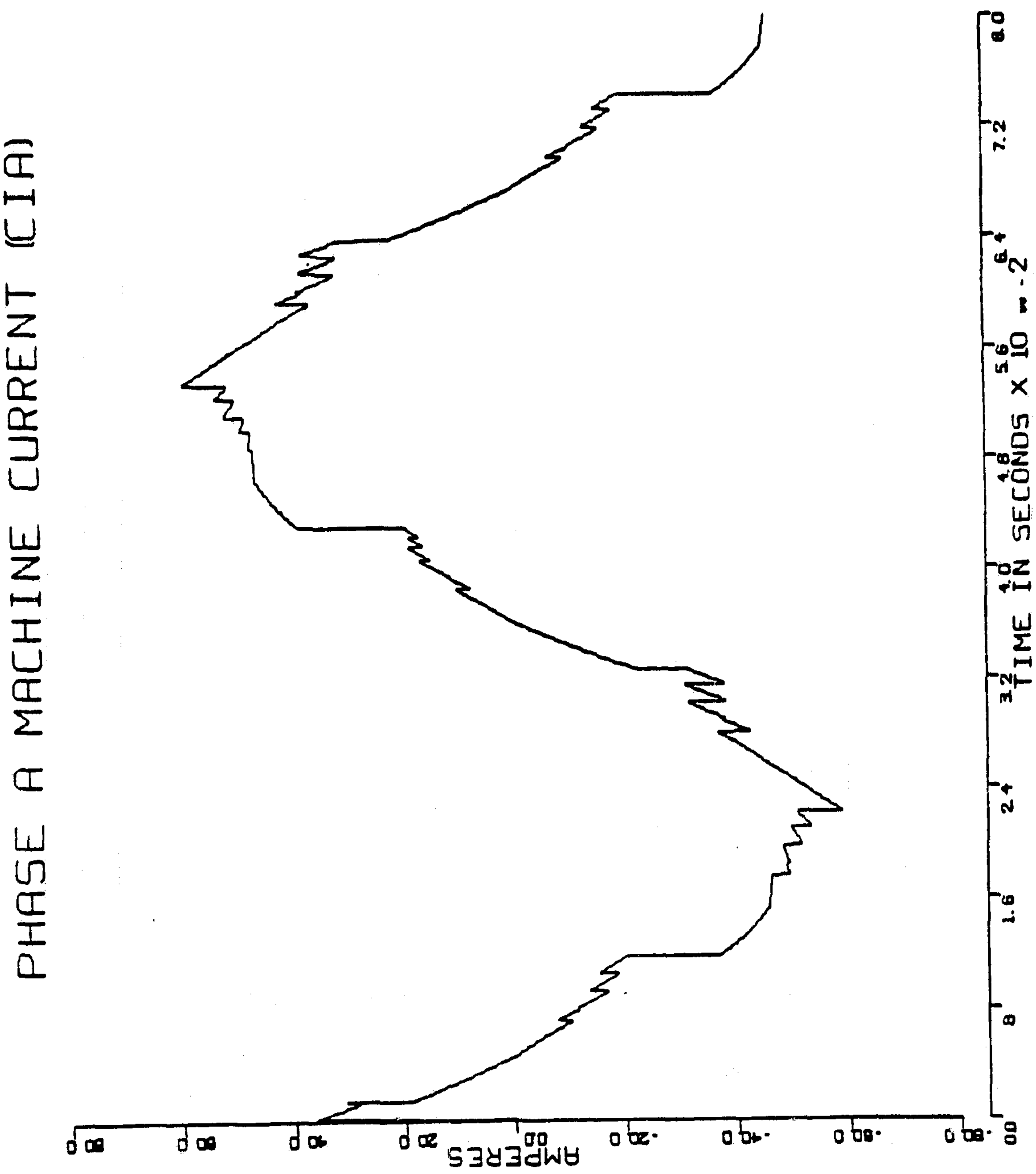

Figure 5.1-14. Simulated Phase A Current during Plugging.
240 rpm, ICMD = 32 amps, 22° Com. Adv.
Peak Back Emf = 3.7 volts peak

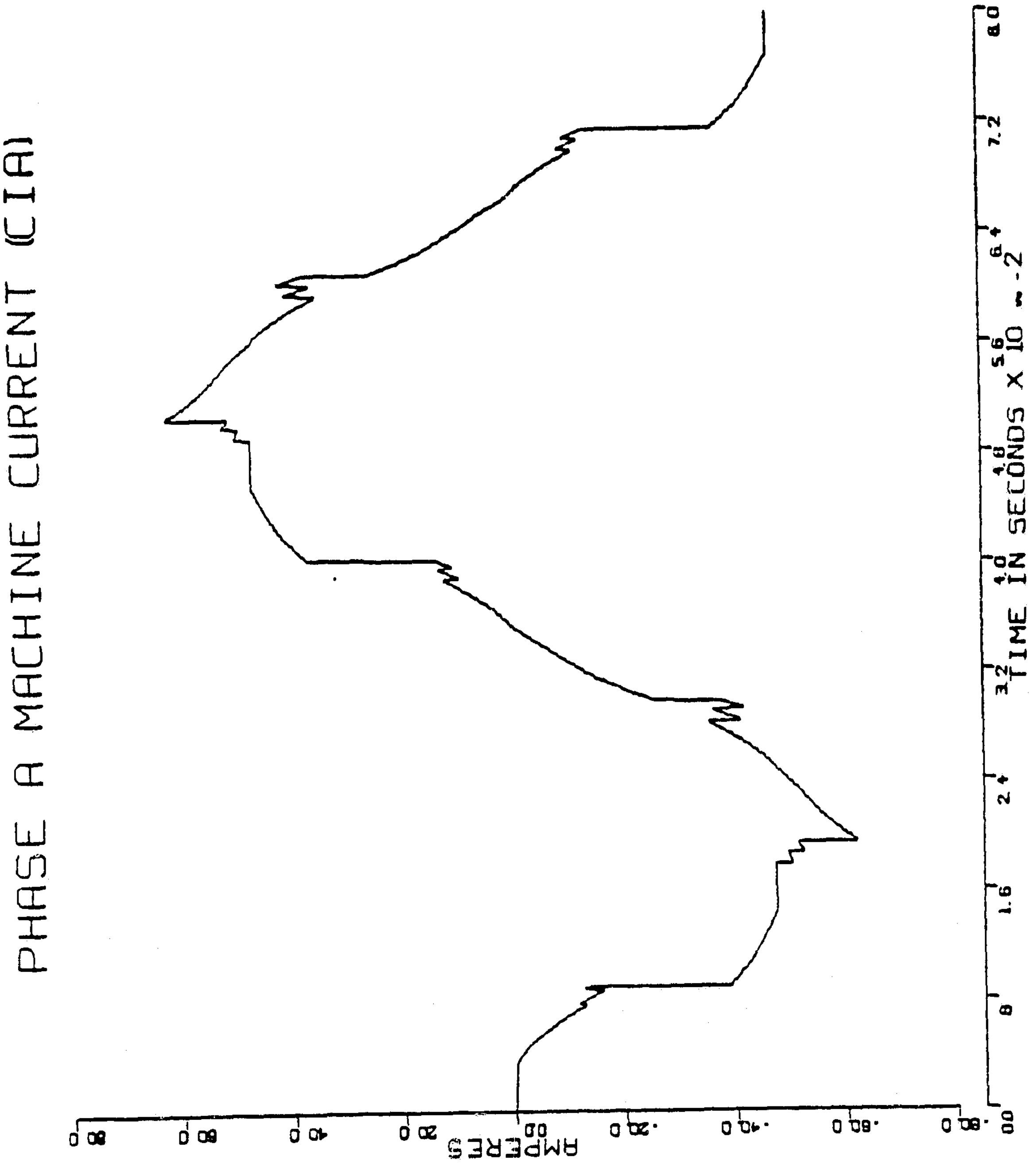

Figure 5.1-15 Simulated Phase A Current during Plugging
240 rpm, ICMD = 32 amps, 38° Com. Adv.
Peak Back Emf = 3.9 volts

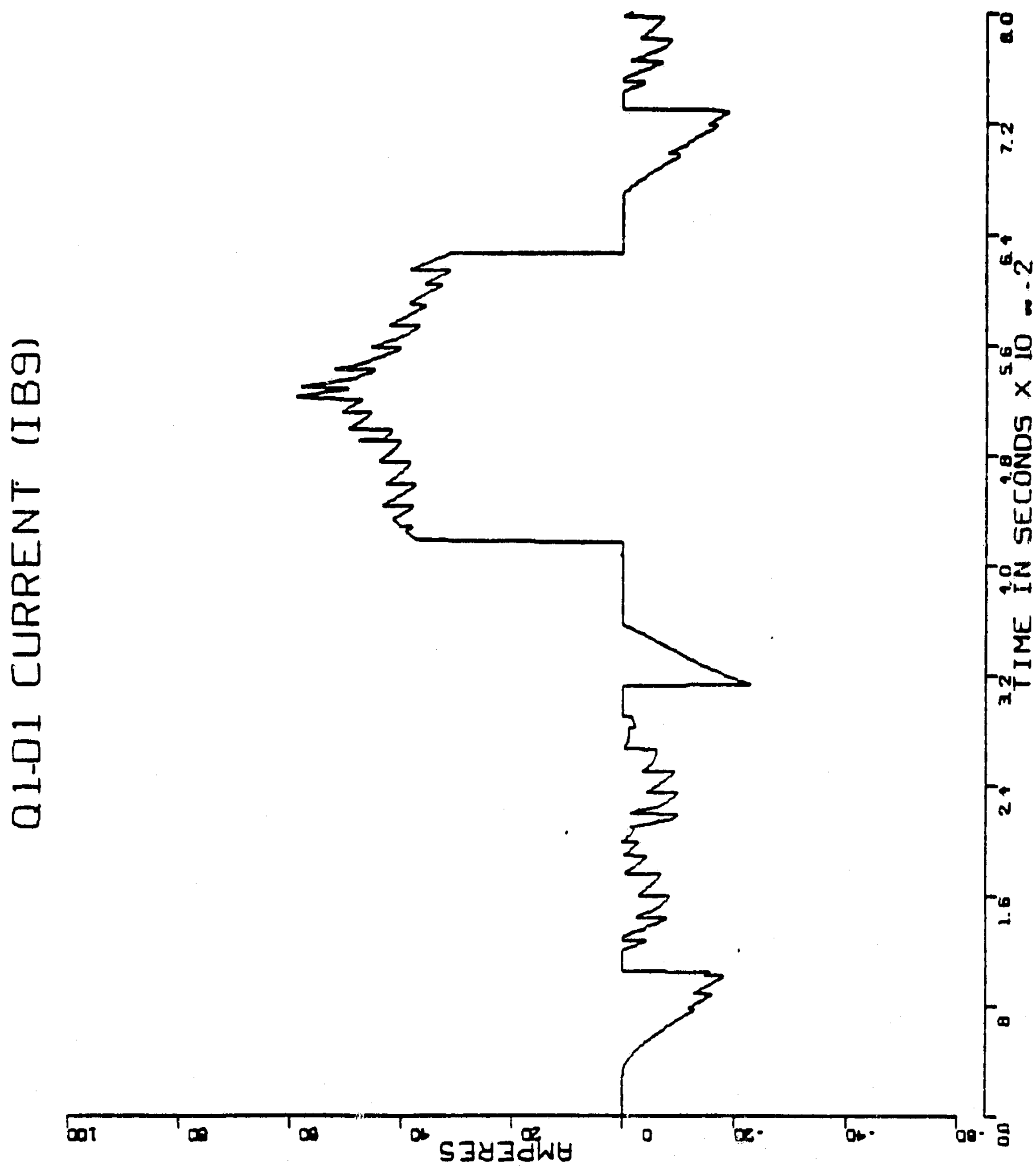

Figure 5.1-16 Simulated Current through Q1-D1 during Plugging
240 rpm, ICMD = 32 amps, 30° Com. Adv.
Peak Back Emf = 3.8 volts

the large circulating phase currents result in the saturation of the stator teeth and yoke thereby increasing the mmf drop across the stator and hence reduced back emfs. The inclusion of this nonlinear stator reluctance in the back emf routine can be accomplished by a Finite Element analysis of the two dimensional nonlinear magnetic fields which govern the electromagnetic behavior of this machine.

5.2 VERIFICATION OV THE TENTH AND FOURTEENTH ORDER EMA MODELS

The overall EMA was modeled using both a detailed and a simplified model of the power conditioner and machine network. Delco electronics, References (2), (3), and (4), performed a series of step responses on the actual hardware using four flap position commands of 1.1, 1.65, 2.2 and 2.75 flap degrees. The results of step responses are tabulated in table (5.2-1). This table contains the times it took the flap to reach the commanded flap positions for the first time. The maximum overshoot is also given. Close examination of this data reveals the excellent agreement between experimental and simulation results.

The results of the 14th order EMA model are given in Appendix (D.1). Figures (D.1-1) through (D.1-14) display some typical waveforms produced by the EMA in response to a step position command. Figure (D.1-1) displays the status of the various EMA logic signals versus time. The extreme variations in rotor speed during such a maneuver is illustrated by the changing width of the RPS outputs (AA, BB, and CC). Since each RPS pulse corresponds to 45 degrees of rotor displacement, the narrow RPS pulses occur at high rotor speeds

TABLE 5.2-1

FLAP ANGLE	1.1		1.65		2.2		2.75		2.75	
RUN	Meas.	E.1	Meas.	E.2	Meas.	E.3	Meas.	E.4	Meas.	D.1
Peak Overshoot	1.38°	1.33°	2.13°	2.14°	2.73°	2.77°	3.37°	3.26°	3.37°	3.23°
First Crossing	.115 sec	.114 sec	.134 sec	.139 sec	.158 sec	.163	.187 sec	.187 sec	.187	.179 sec

and vice versa. The machine torque during the step response is given in Figure (D.1-2). The rapid fluctuations in the torque are due to the sawtooth component of the machine phase currents which is produced by chopper. Notice that as the machine velocity reaches its maximum (at approximately 0.15 sec) value, the average machine torque is significantly reduced. This is due to the increasing machine back emfs with increasing speed. This torque reduction at higher speeds results in velocity saturation which is graphically illustrated in Figure (5.2-1) (Figure (D.1-10)) and in Figure (5.2-2) which shows the corresponding observed velocity, Reference (4).

The response of the flap to the step input is given in Figure (5.2-3). This waveform agrees with the oscillogram of the actual response given in Figure (5.2-4). Because of the linear relationship between machine current, IM, and torque, TM, the machine current, Figure (D.1-4) is very similar to Figure (D.1-2).

The computed velocity error given in Figure (D.1-5) shows how the velocity error approaches zero in time. The position error also approaches zero towards the end of the step response as expected, see Figure (D.1-14).

The filtered current command IMC is displayed in Figure (D.1-6). The rectangular notch at t = .24 seconds is due to the lower current limit during plugging. The rate and magnitude limited current ICMD1/5 is shown in Figure (5.2-5) as well as in Figure (D.1-7). This compares favorably with the actual current command waveform given in Figure (5.2-6).

The action of the current rate limiter is displayed in Figure

(D.1-9). The reaction torque, TACT, given in Figure (D.1-11) shows the spring loading effect due to the nonzero value of the final flap position.

In addition to these runs, the step response to the various position commands of Table (5.2-1) have been determined using a simpler 10th order EMA model. Comparison of these results to test results demonstrates that the simpler model does an excellent job of predicting the step response.

5.3 CONCLUSIONS AND RECOMMENDATIONS

A comparison was made between the experimental test results, Reference (2), and the numerical results presented in Appendices (A) through (E). In all cases excellent agreement was found between the waveforms obtained from the actual machine-power conditioner package and those obtained from the mathematical (numerical) model. This close agreement between the behavior of the actual hardware and the mathematical model strongly suggests that the underlying assumptions and simplifications used in the development of this model are valid and sound.

Future improvements in this model can include the following endeavors:

1. The development of a rigorous magnetic field analysis model for the determination of airgap flux density waveforms under load and no load. This model would constitute the heart of a program for the calculation of the machine back emfs in the machine-power conditioner network, as well as the calculation of the electromagnetic dynamic

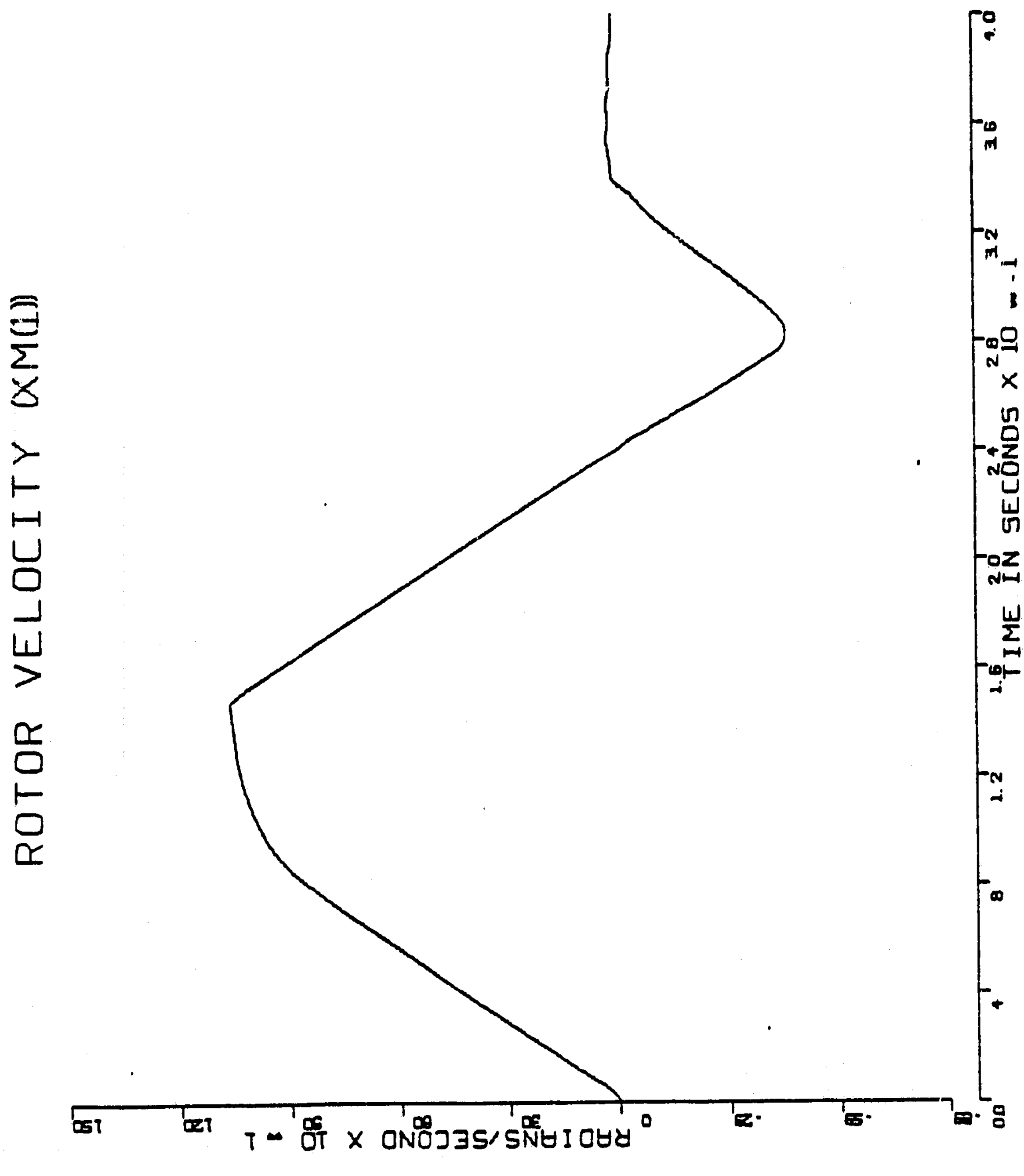

Figure 5.2-1. Simulation of Machine Velocity (14th Order Model)
DC = 2.75°

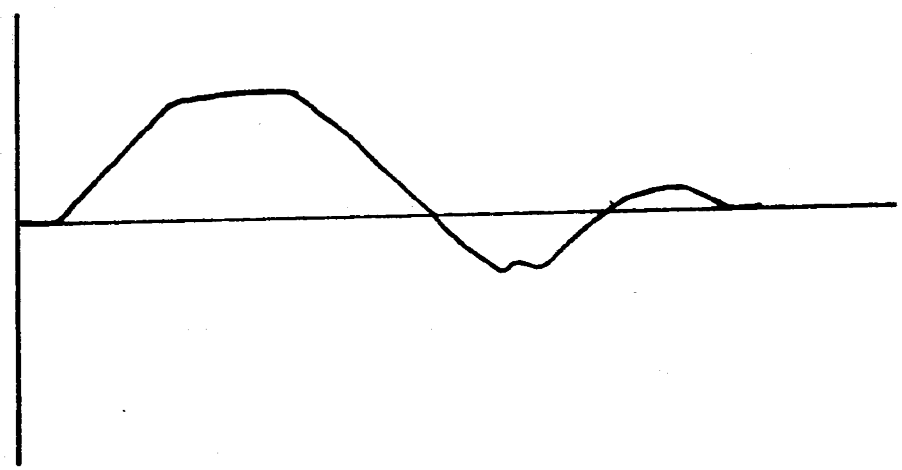

Figure 5.2-2. Copy of Oscillogram of Machine Velocity (scale Not Available)
DC = 2.75°

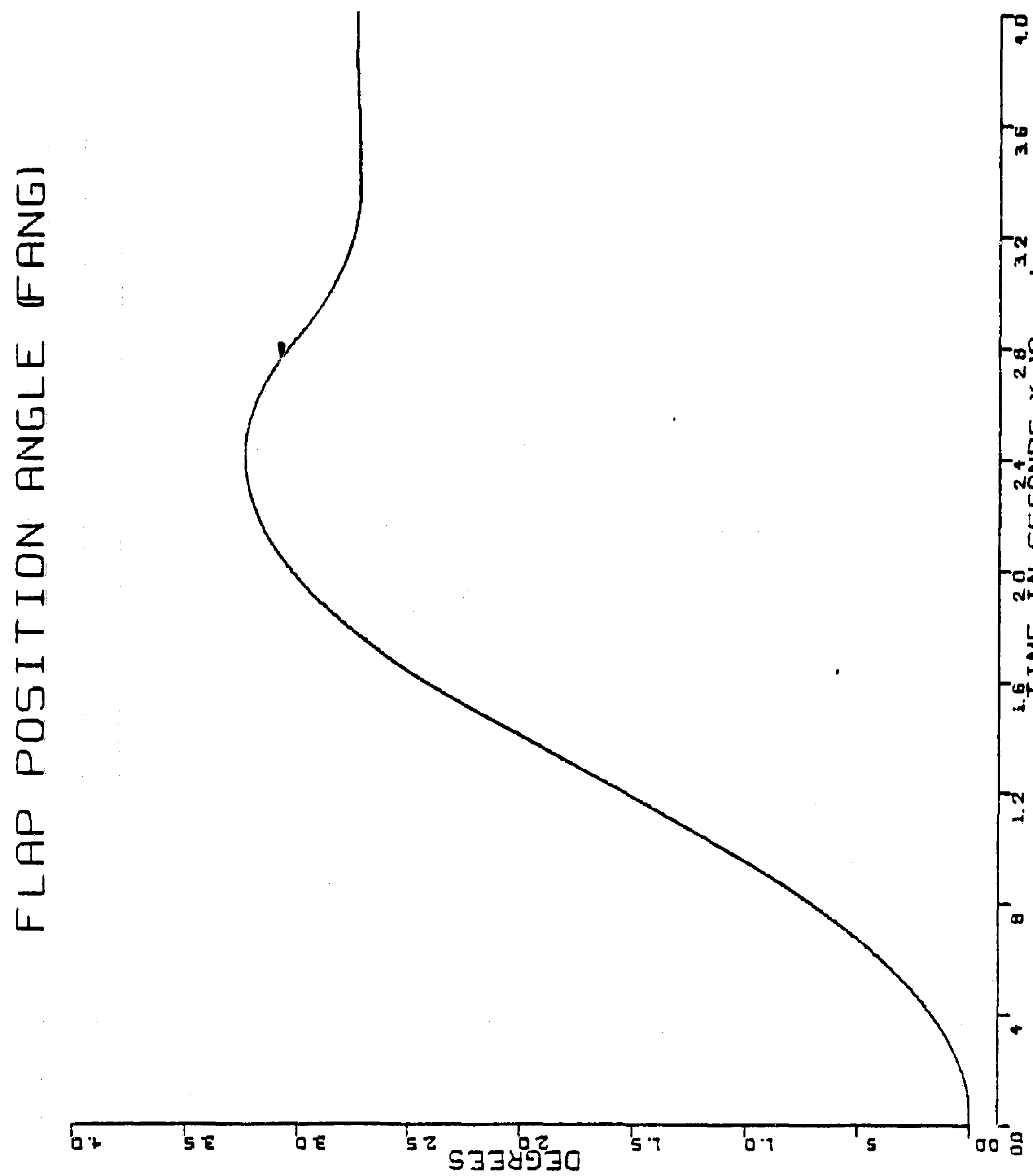

Figure 5.2-3. Simulation of the Flap Position (14th Order Model)
DC = 2.75°

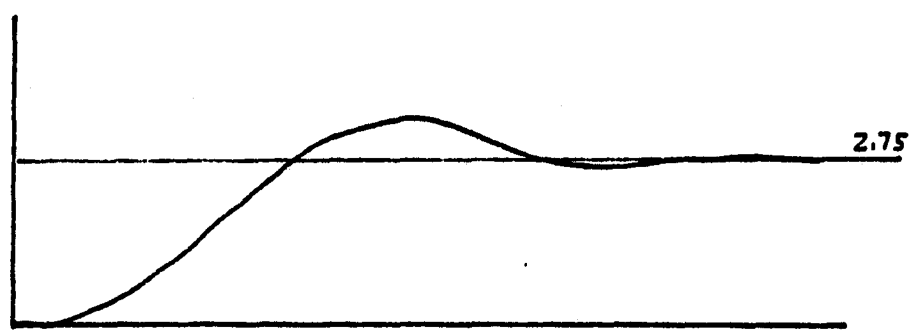

Figure 5.2-3. Simulation of the Flap Position (14^{th} Order Model)
DC = 2.75°

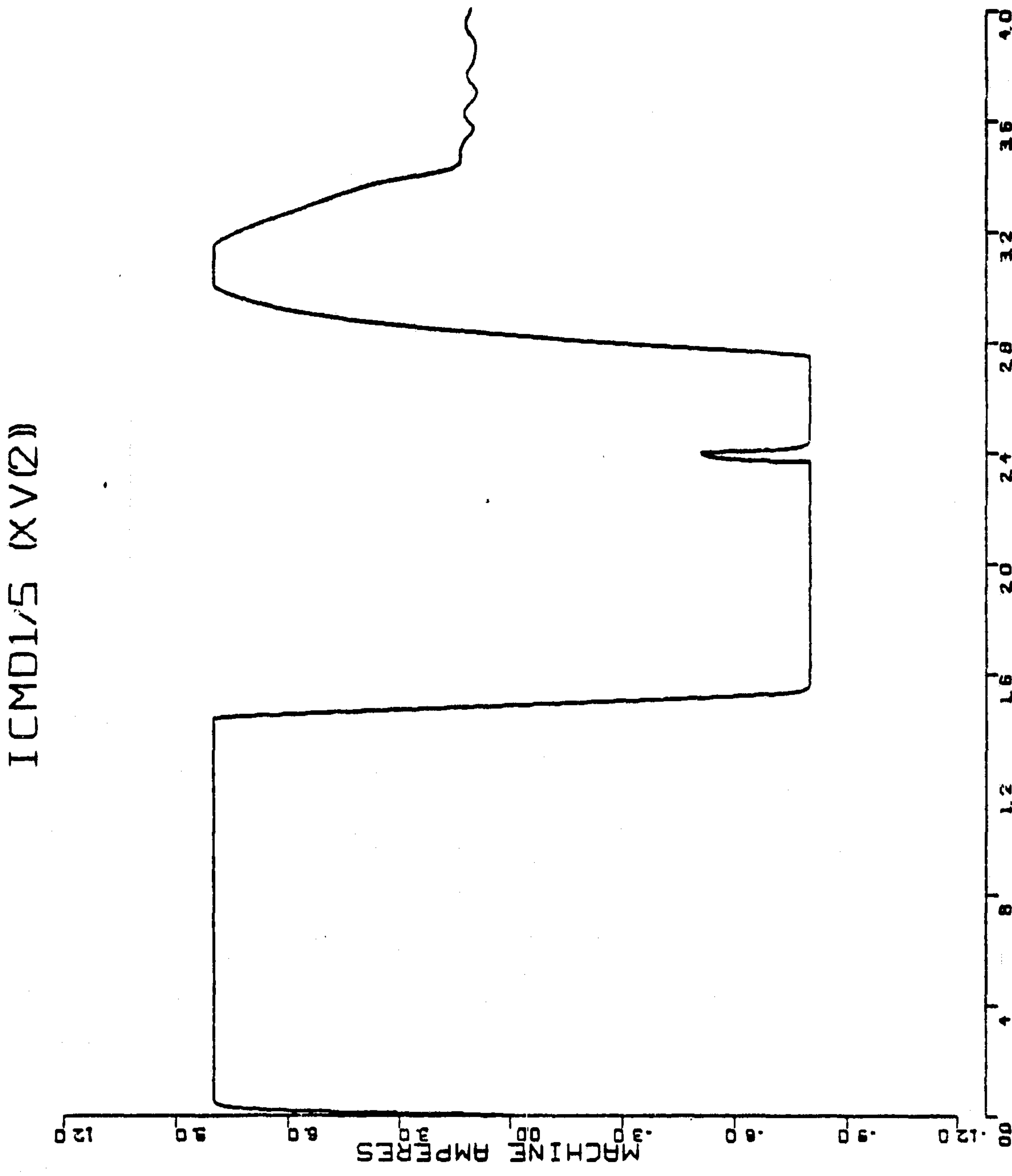

Figure 5.2-5. Simulation of ICMD1/5 (14th Order Model)
DC = 2.75°

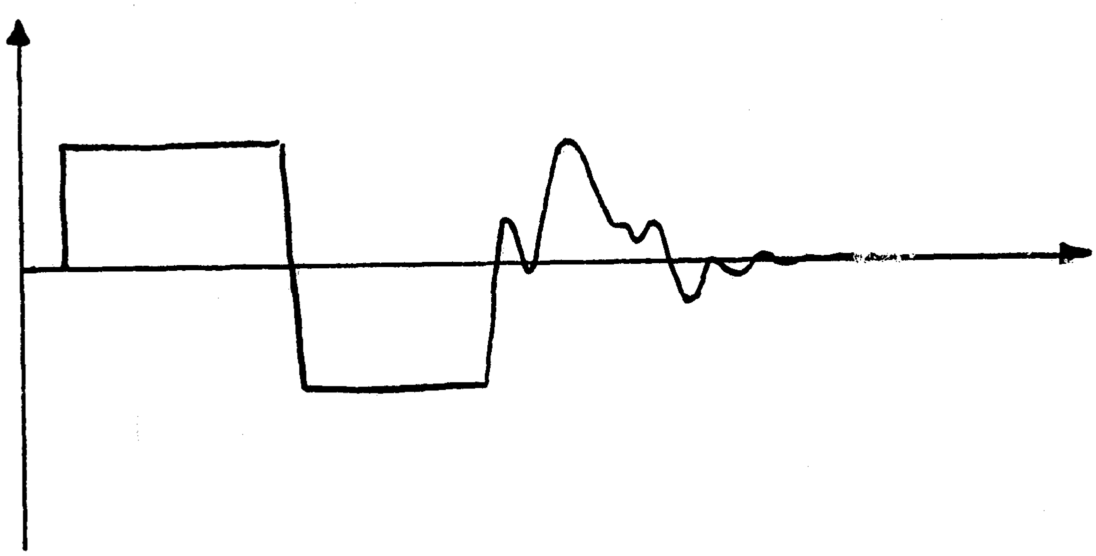

Figure 5.2-6. Copy of Oscillogram of ICMD1/5
DC = 2.75°

torque. Such a package would allow the calculation of more accurate motor leakage inductances, which are necessary for accurate commutation studies. Such a model can also be used for the determination of better magnet-airgap configurations for optimum torque and dynamic characteristics.

2. Increasing the order of the mathematical model in order to include the effects of the various capacitors and inductors which have been neglected in the present model.

3. The incorporation of items (1) and (2) mentioned above into an overall EMA design optimization program. Such a program would determine the optimum system parameters given a set of system constraints. This type of capability would be useful in tailoring the system to a given application.

APPENDIX A.1 CALCOMP PLOTS: MOTORING 5000 rpm 30° ADVANCE

RUN SUMMARY

MODE: MOTORING

PROGRAM MODE: PGMODE = 1

CURRENT COMMAND: ICMD = 31.5 amps

TIME STEP: TSNET = 5 μs

COMMUTATION SHIFT: SHIFT = 0.0 mech rad

CURRENT THRESHOLD: ITOL = 4.0 amps

ROTOR VELOCITY: (5000 rpm) (523.599 rad/sec)

TOTAL NUMBER OF POINTS PLOTTED: NREC = 901

TOTAL NUMBER OF NETWORK CHANGES: NNETSW = 349

TOTAL NUMBER OF INTEGRATIONS: NUMINT = 1800

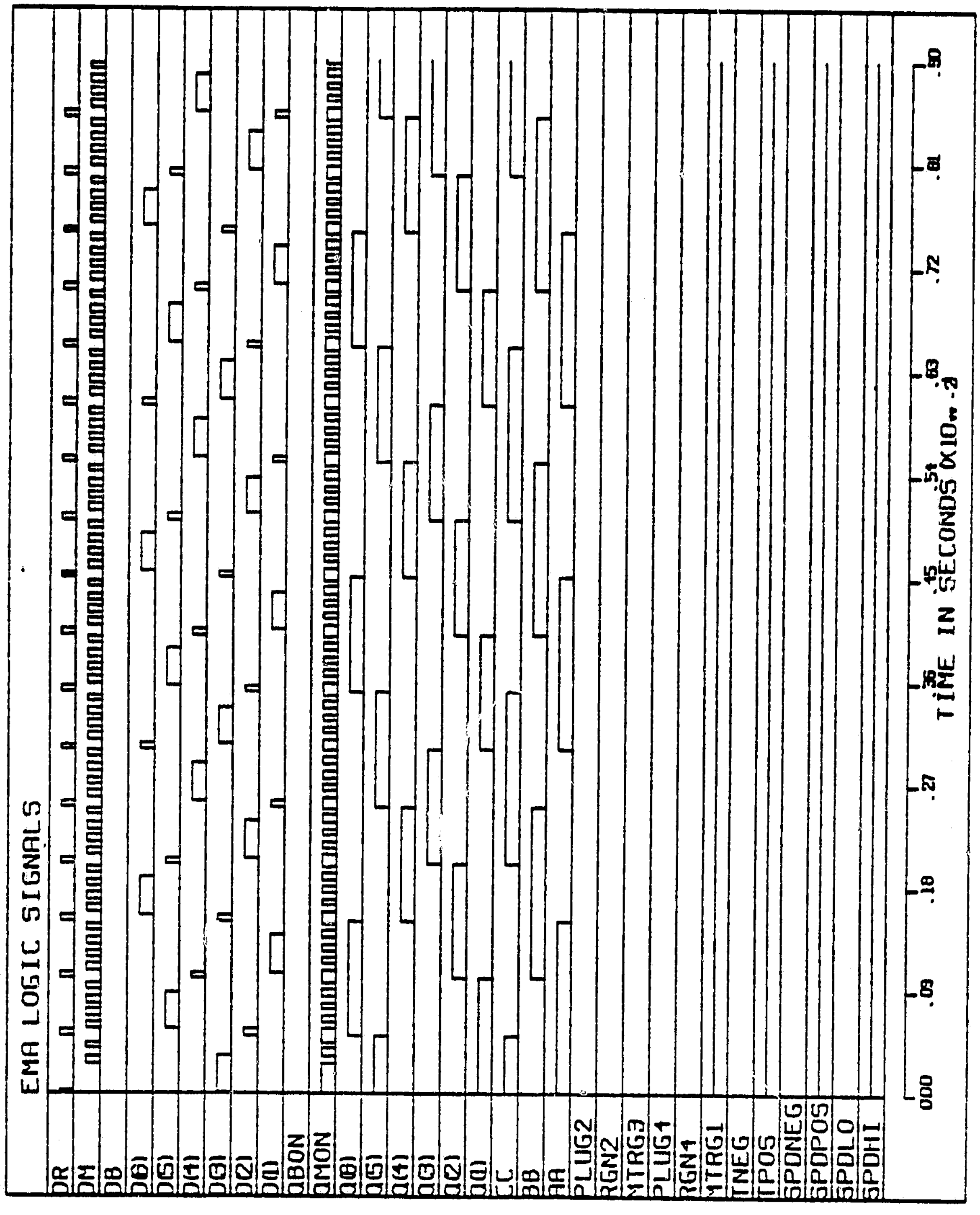
EMA LOGIC SIGNALS
DR
DM
DB
D(6)
D(5)
D(4)
D(3)
D(2)
D(1)
QBON
QMON
Q(6)
Q(5)
Q(4)
Q(3)
Q(2)
Q(1)
CC
BB
AA
PLUG2
RGN2
MTRG3
PLUG4
RGN4
MTRG1
TNEG
TPOS
SPDNEG
SPDPOS
SPDLO
SPDHI
.000
.09
.18
.27
.36
.45
.54
.63
.72
.81
.90
TIME IN SECONDS (X10** -2)

Figure A.1-1

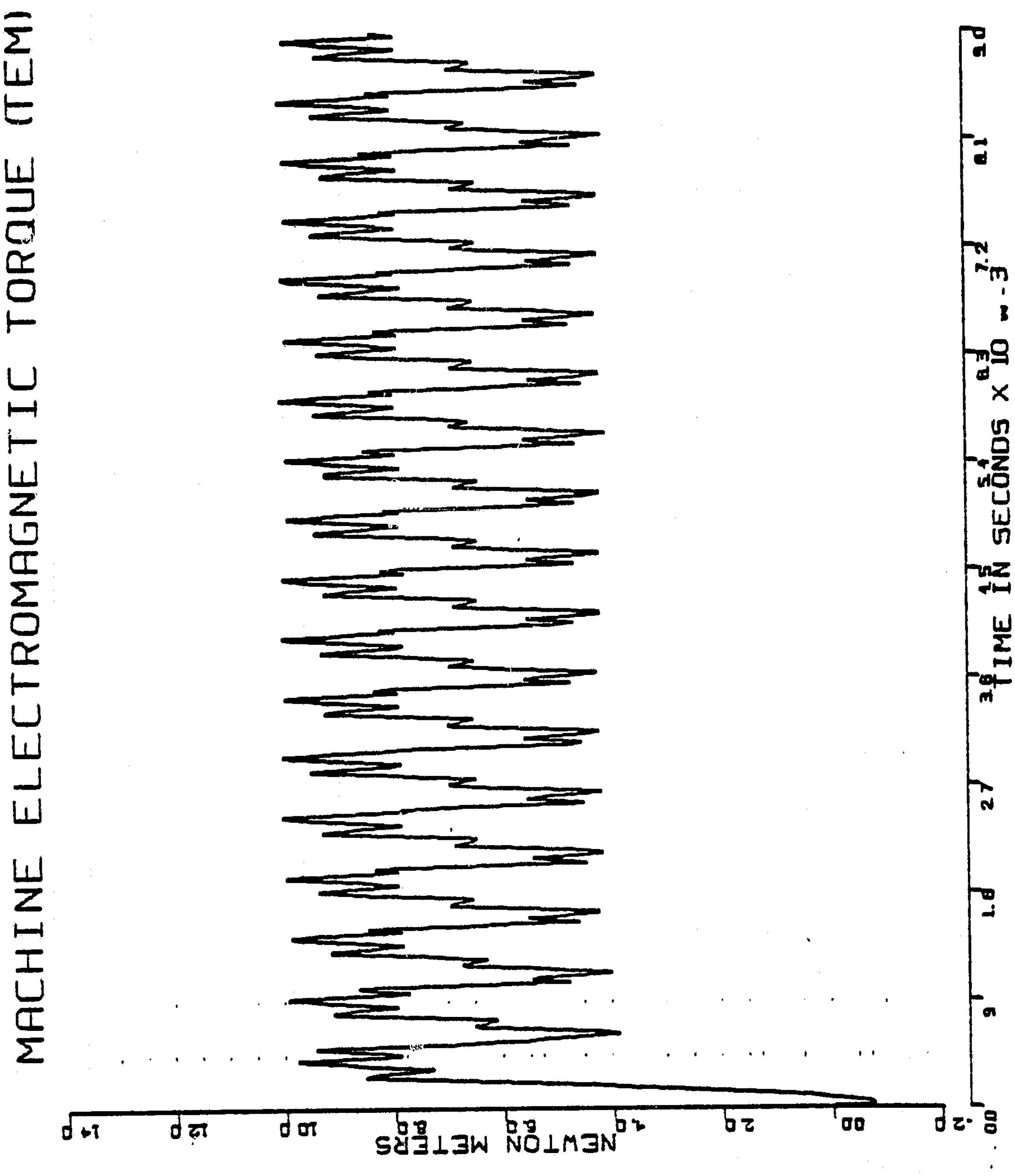
MACHINE ELECTROMAGNETIC TORQUE (TEM)
TIME IN SECONDS X 10 ** -3
NEWTON METERS
.00
.9
1.8
2.7
3.6
4.5
5.4
6.3
7.2
8.1
9.0
-2.0
0.0
2.0
4.0
6.0
8.0
10.0
12.0
14.0

Figure A.1-2

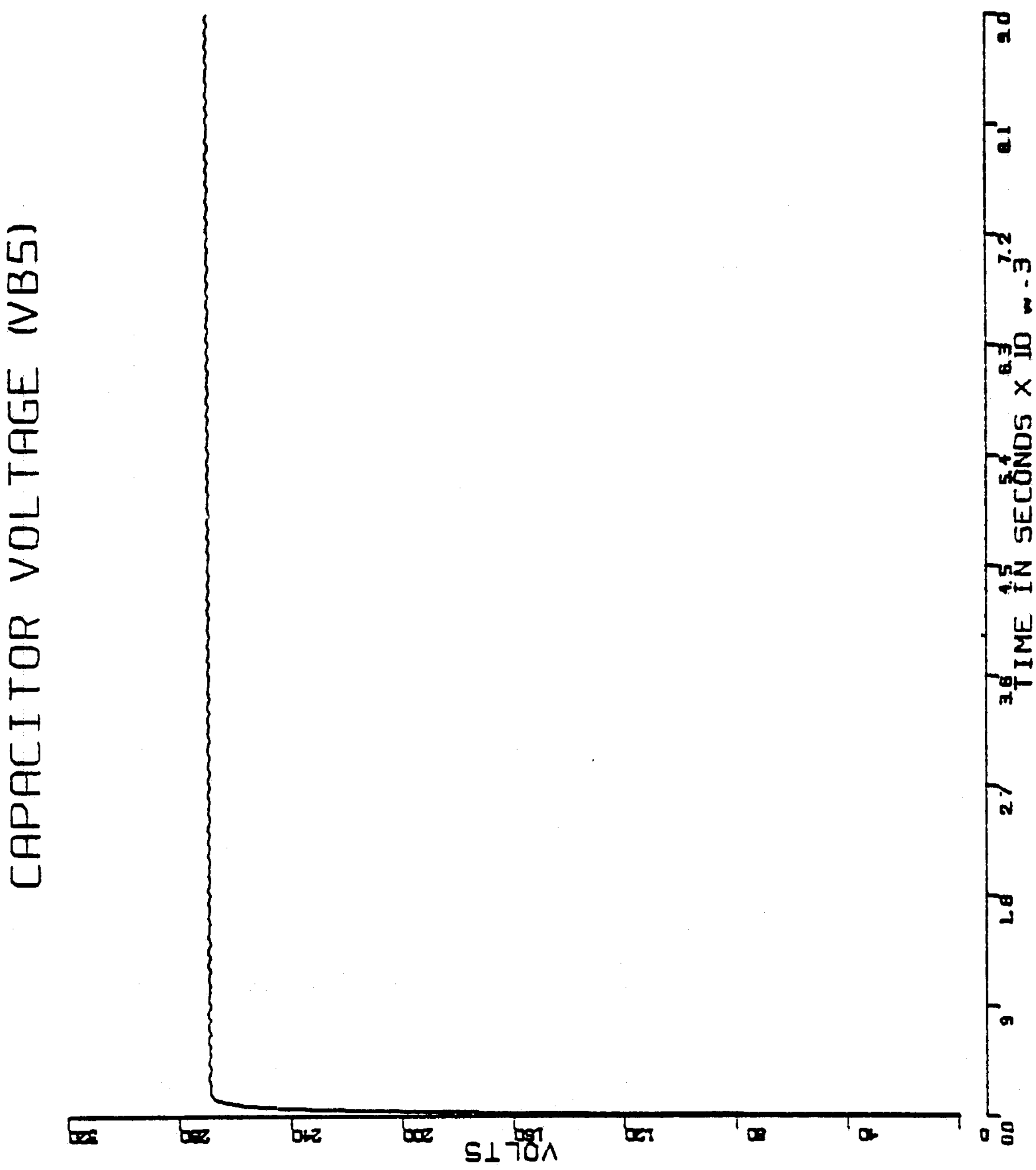

Figure A.1-3

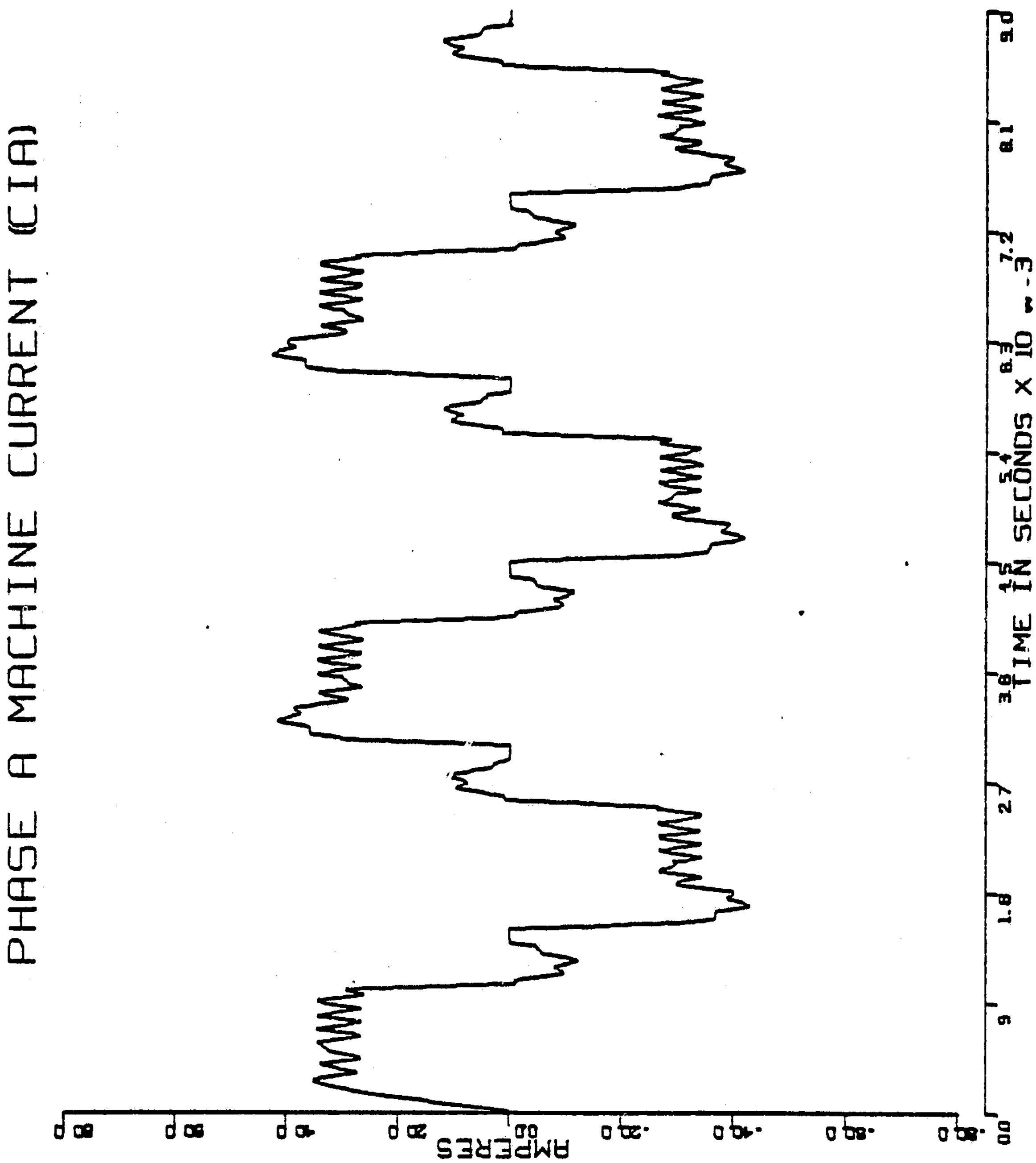
PHASE A MACHINE CURRENT (CIA)
AMPERES
80.0
60.0
40.0
20.0
0.0
-20.0
-40.0
-60.0
-80.0
TIME IN SECONDS X 10 ** -3
0.0
.9
1.8
2.7
3.6
4.5
5.4
6.3
7.2
8.1
9.0

Figure A.1-4

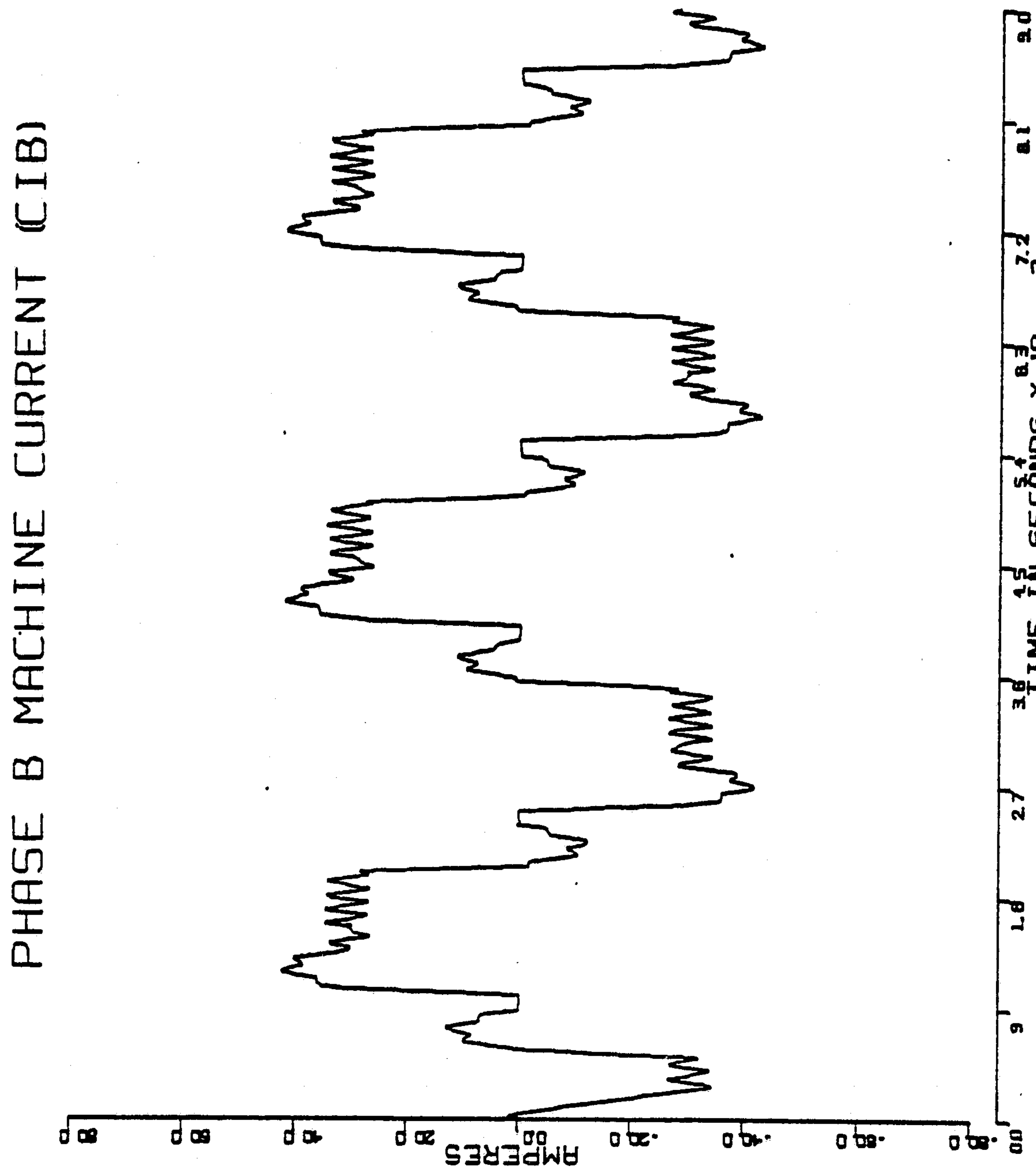
PHASE B MACHINE CURRENT (CIB)
TIME IN SECONDS X 10 ** -3
AMPERES
.00
.9
1.8
2.7
3.6
4.5
5.4
6.3
7.2
8.1
9.0
-80.0
-60.0
-40.0
-20.0
.00
20.0
40.0
60.0
80.0

Figure A.1-5

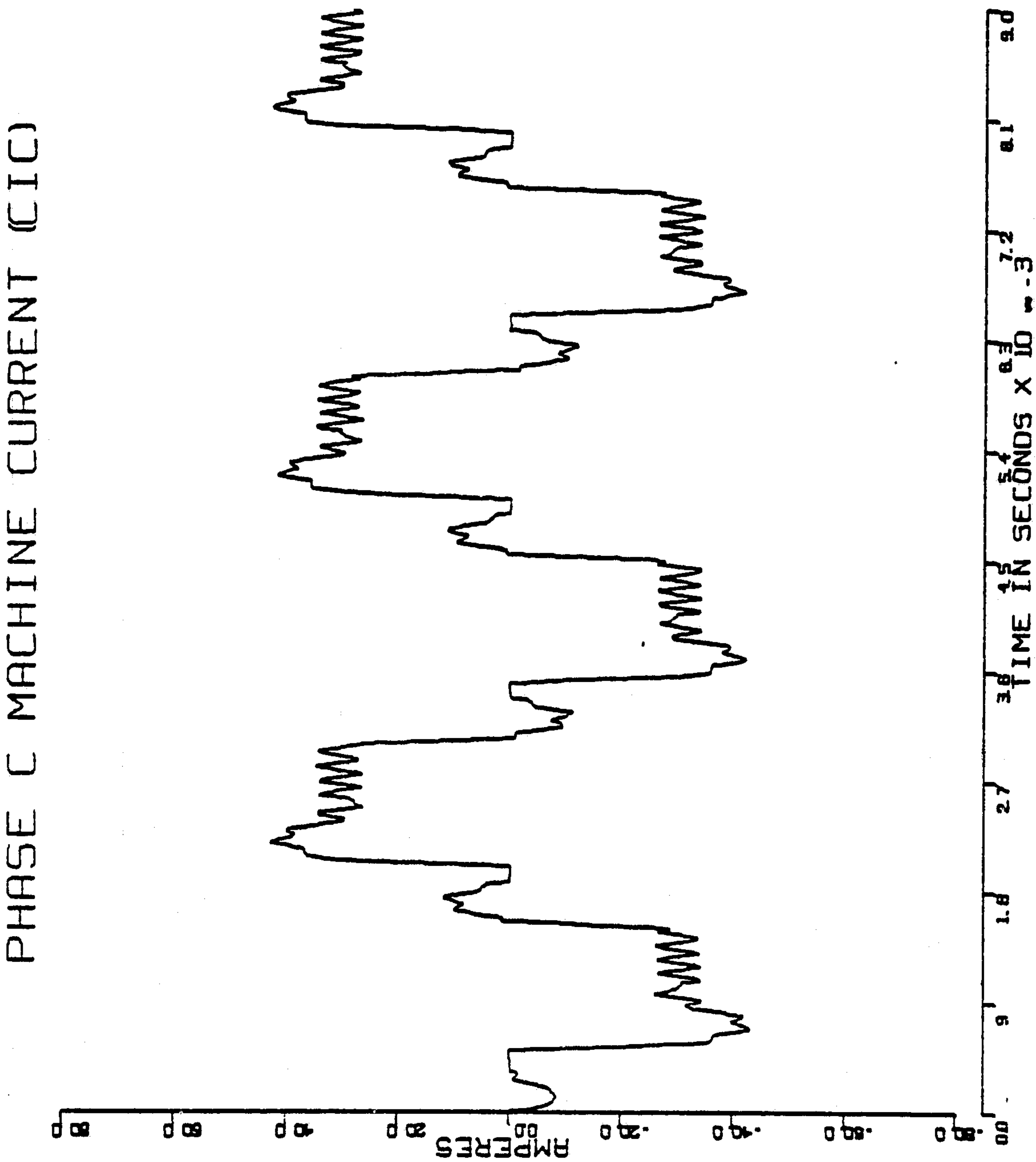

Figure A.1-6

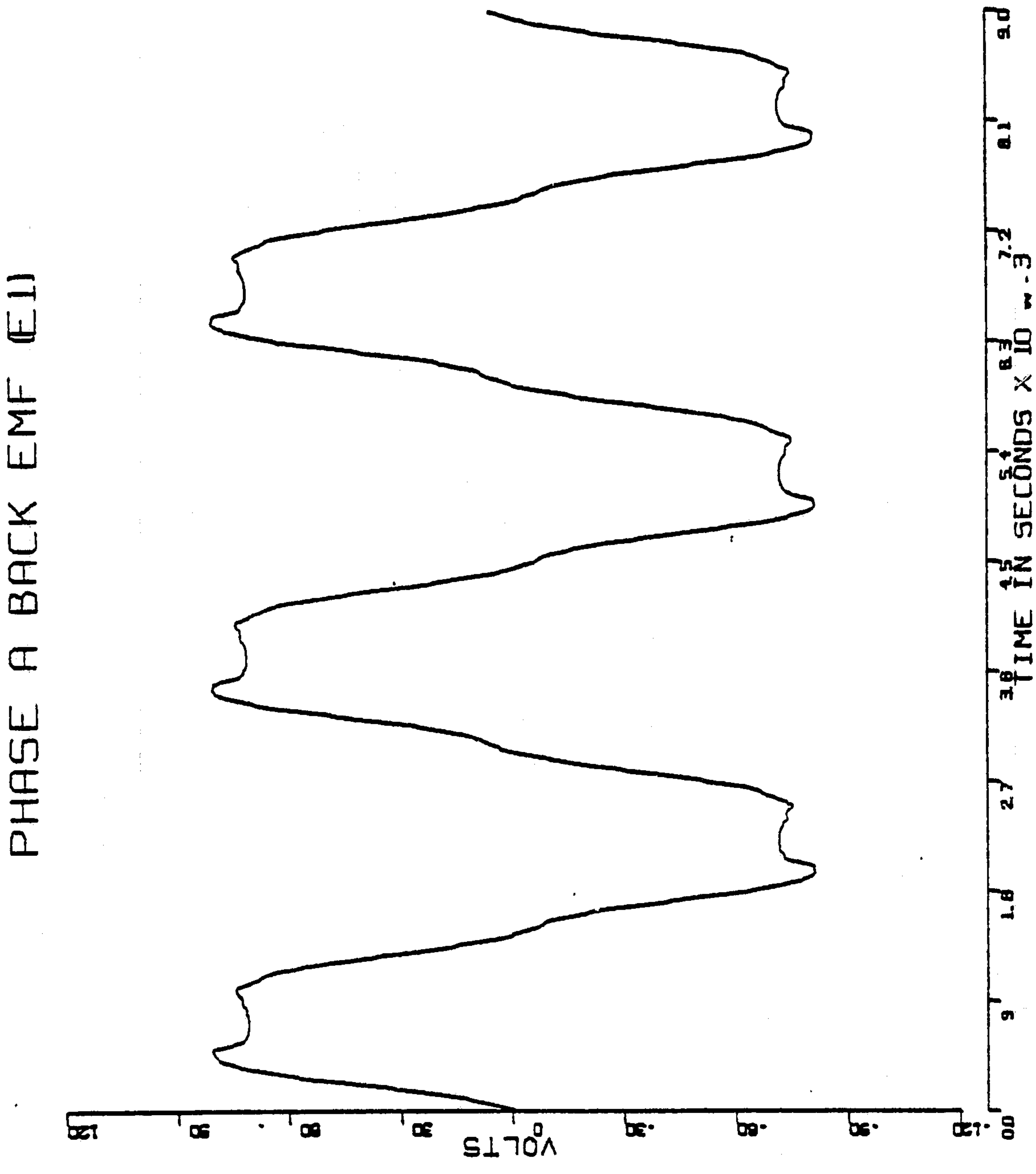
PHASE A BACK EMF (E1)
TIME IN SECONDS X 10 ** -3
VOLTS
0.0
.9
1.8
2.7
3.6
4.5
5.4
6.3
7.2
8.1
9.0
120
90
60
30
0
-30
-60
-90
-120

Figure A.1-7

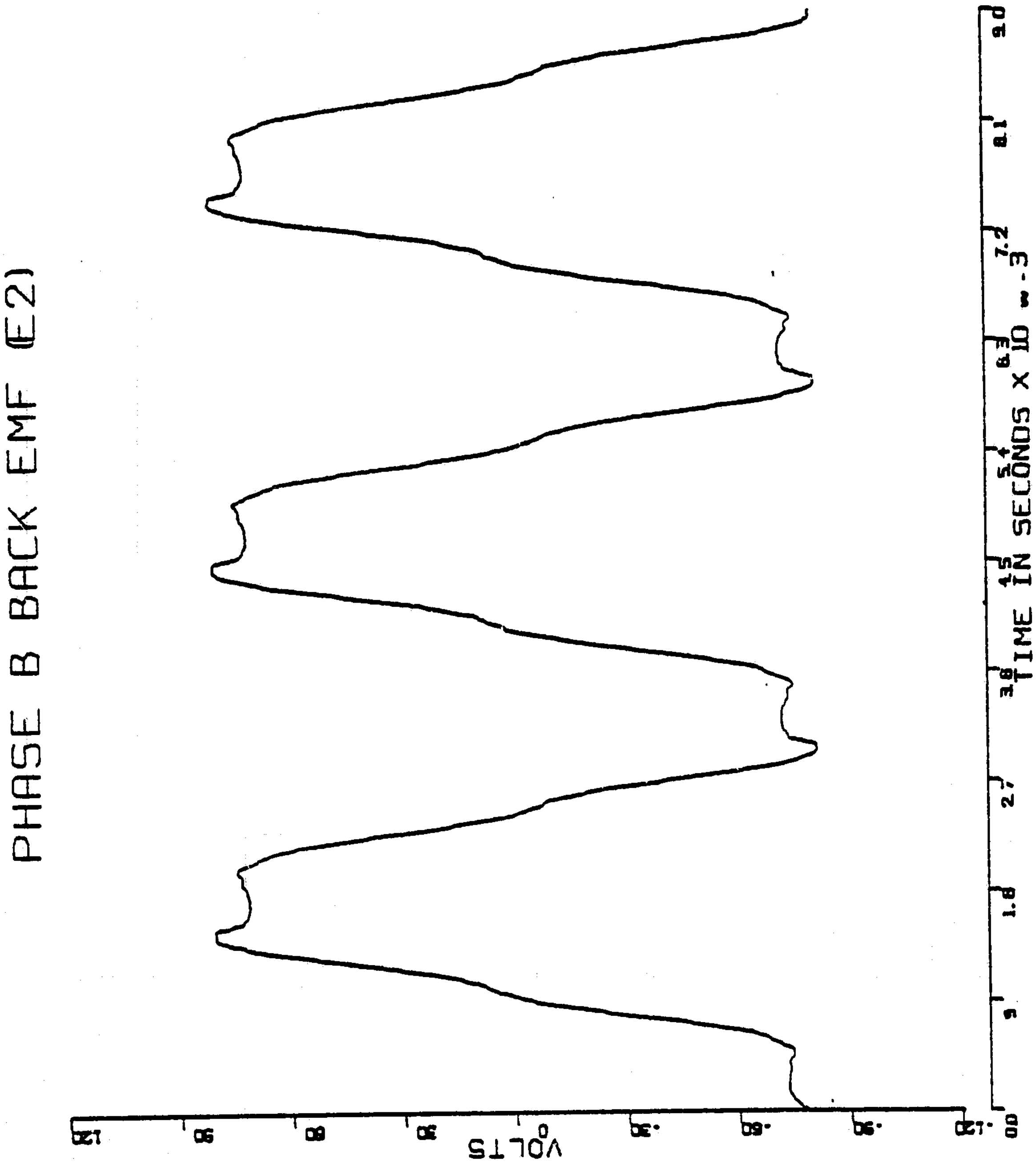
PHASE B BACK EMF (E2)
TIME IN SECONDS X 10 ** -3
VOLTS
0.0
.9
1.8
2.7
3.6
4.5
5.4
6.3
7.2
8.1
9.0
-120
-90
-60
-30
0
30
60
90
120

Figure A.1-8

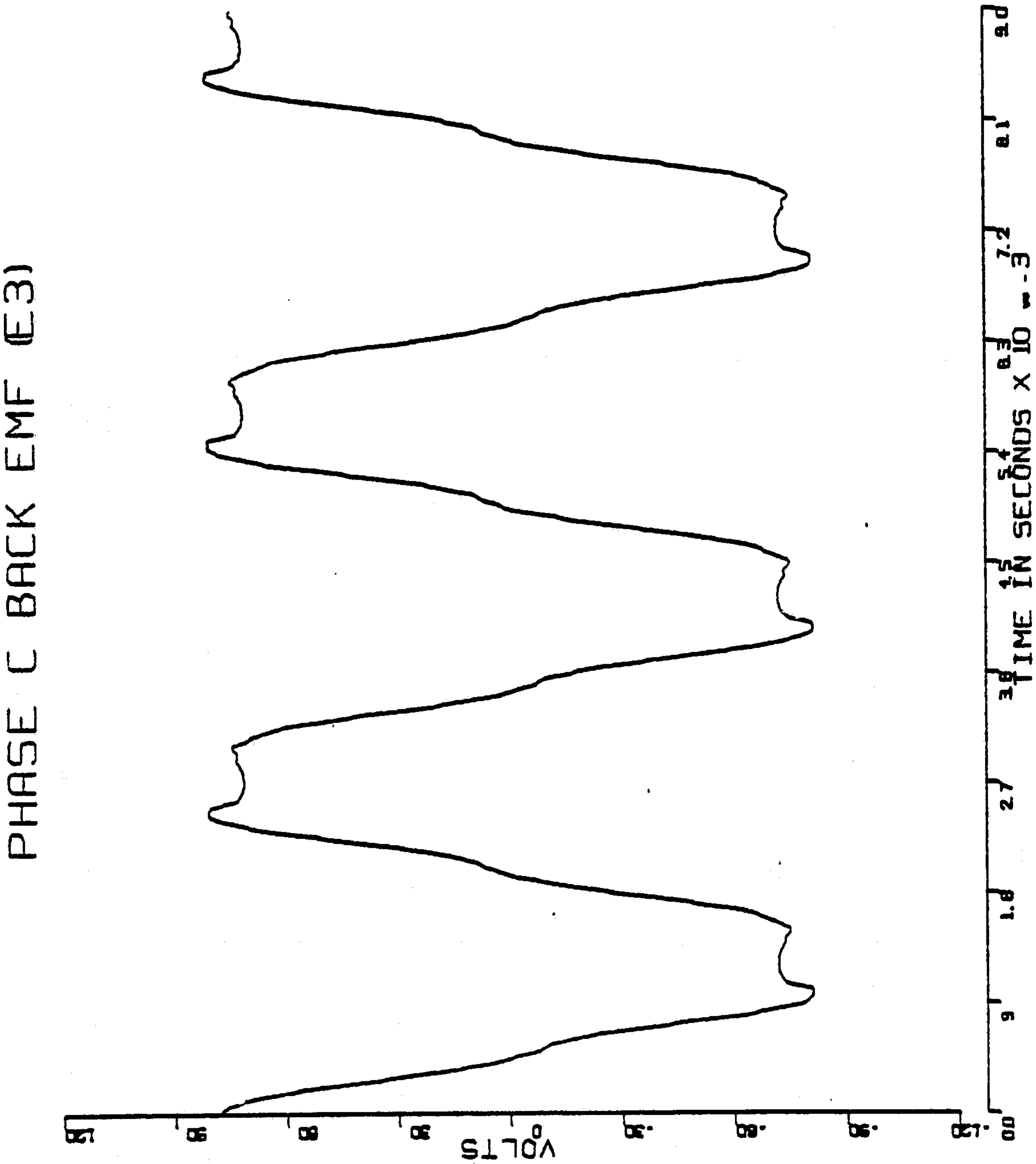
PHASE C BACK EMF (E3)
TIME IN SECONDS X 10 ** -3
0.0
.9
1.8
2.7
3.6
4.5
5.4
6.3
7.2
8.1
9.0
VOLTS
120
90
60
30
0
-30
-60
-90
-120

Figure A.1-9

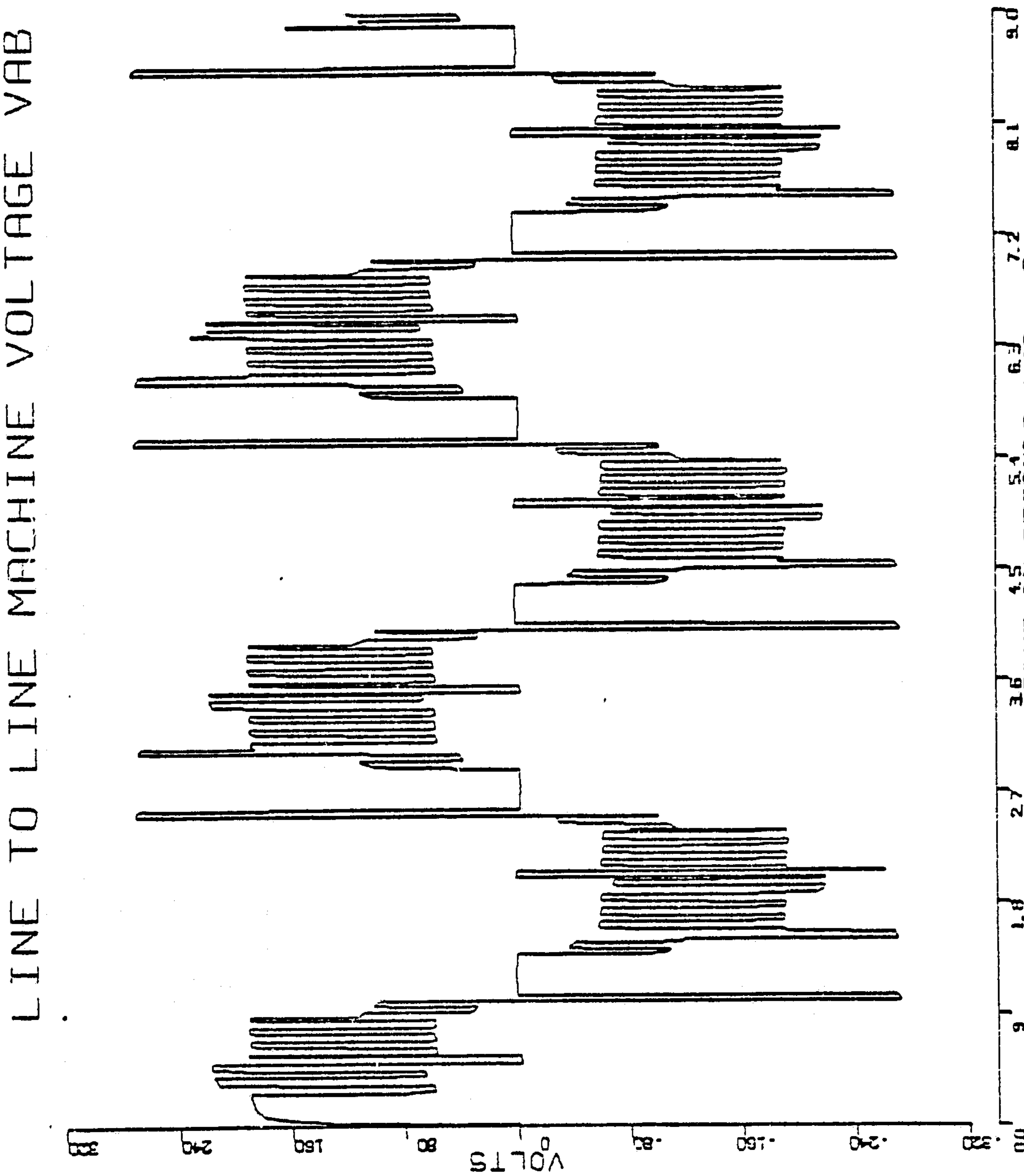
LINE TO LINE MACHINE VOLTAGE VAB
TIME IN SECONDS X 10 ** -3
VOLTS
0.0
.9
1.8
2.7
3.6
4.5
5.4
6.3
7.2
8.1
9.0
320
240
160
80
0
-80
-160
-240
-320

Figure A.1-10

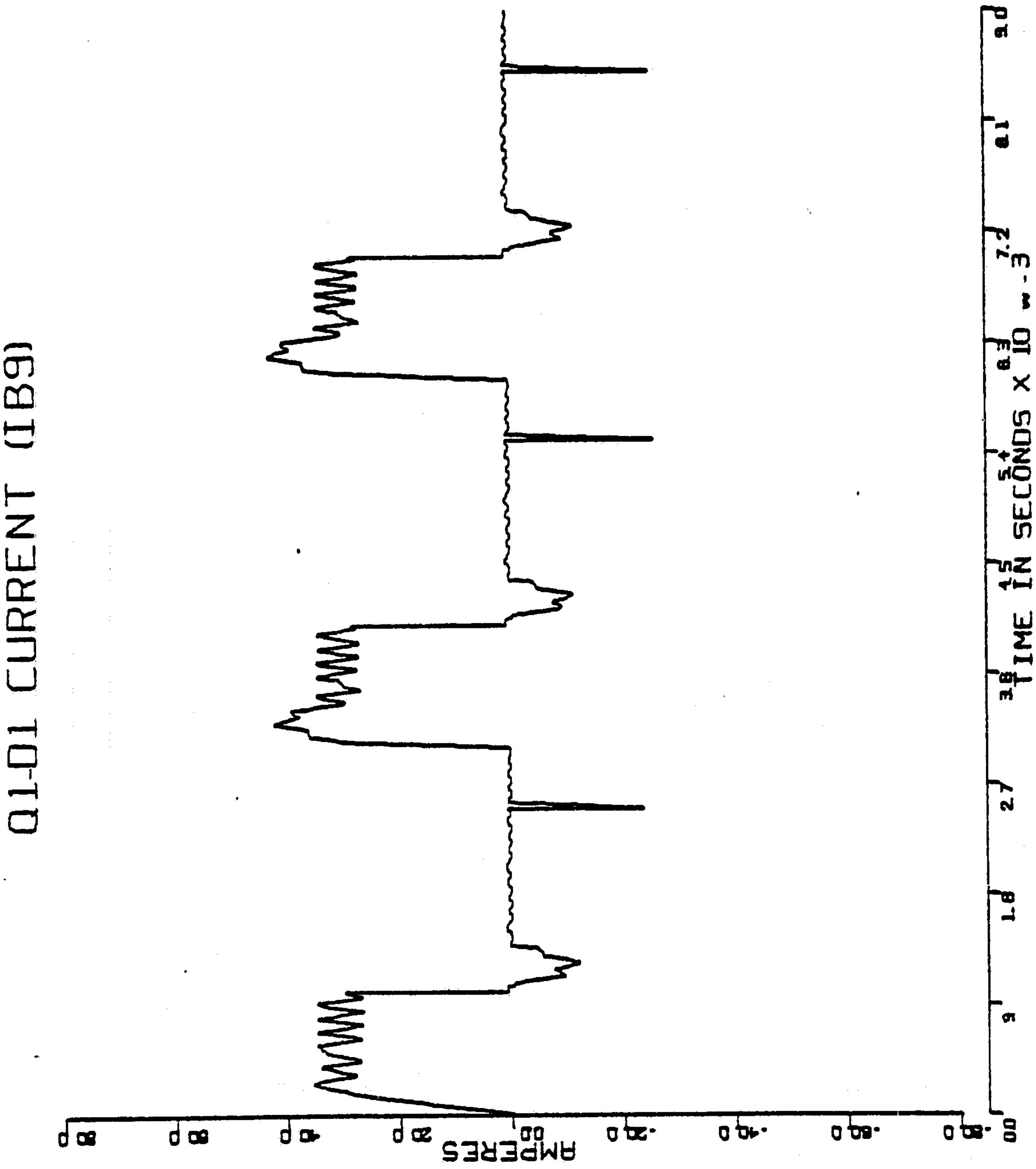

Figure A.1-11

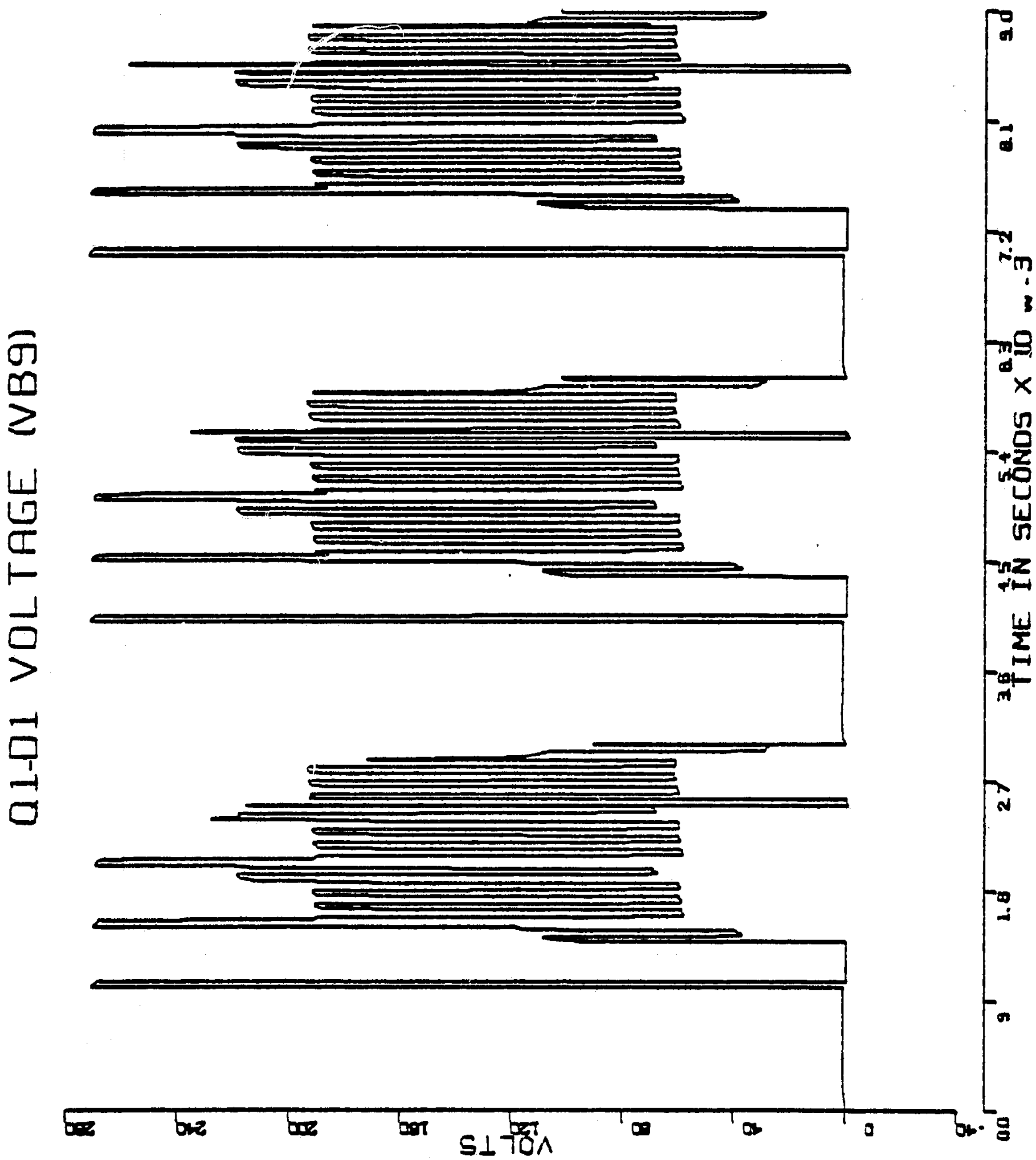
Q1-D1 VOLTAGE (VB9)
TIME IN SECONDS X 10 ** -3
VOLTS
0.0
.9
1.8
2.7
3.6
4.5
5.4
6.3
7.2
8.1
9.0
-40
0
40
80
120
160
200
240
280

Figure A.1-12

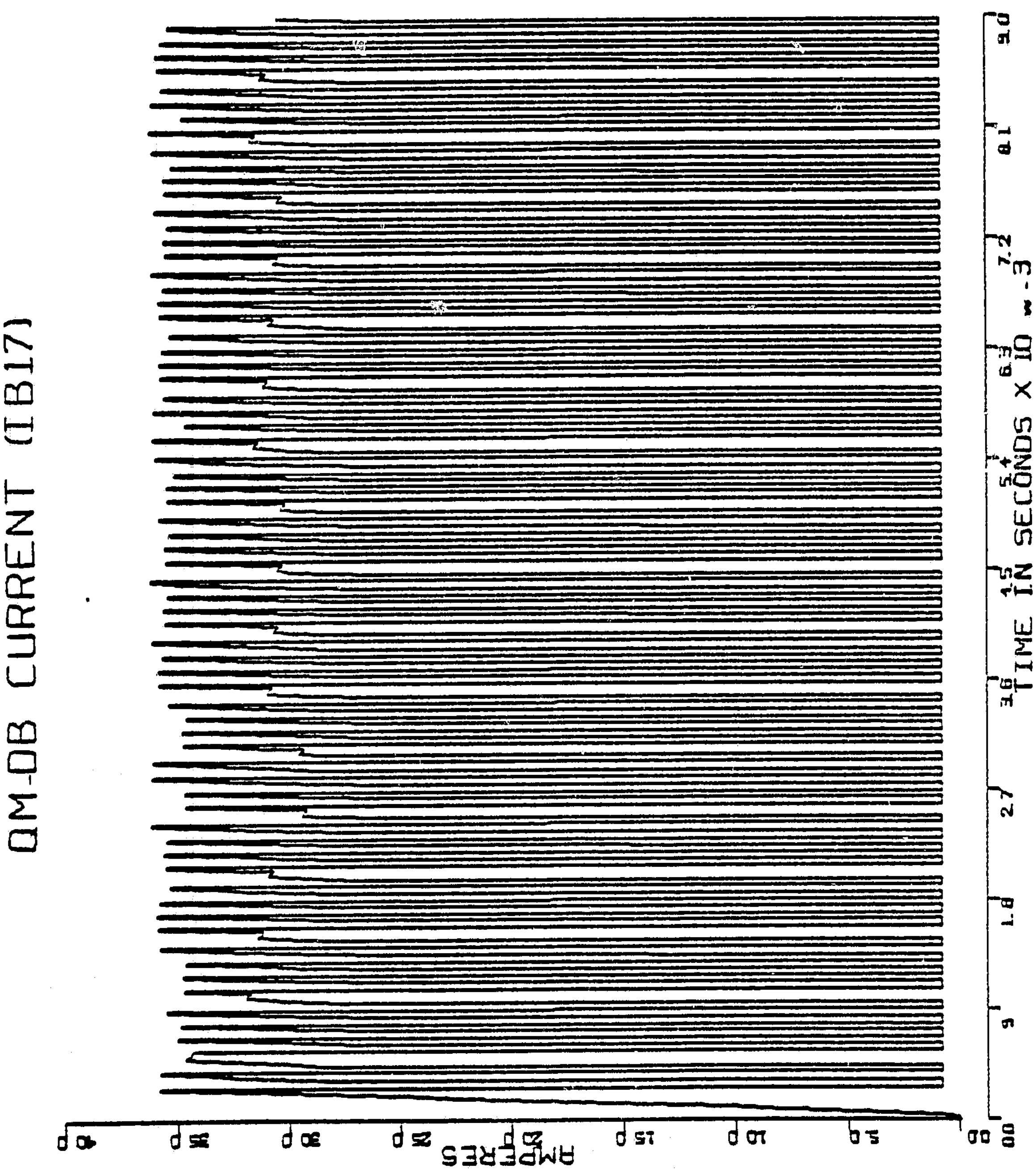
QM-DB CURRENT (IB17)
AMPERES
TIME IN SECONDS X 10 ** -3
0.0
.9
1.8
2.7
3.6
4.5
5.4
6.3
7.2
8.1
9.0
0.0
5.0
10.0
15.0
20.0
25.0
30.0
35.0
40.0

Figure A.1-13

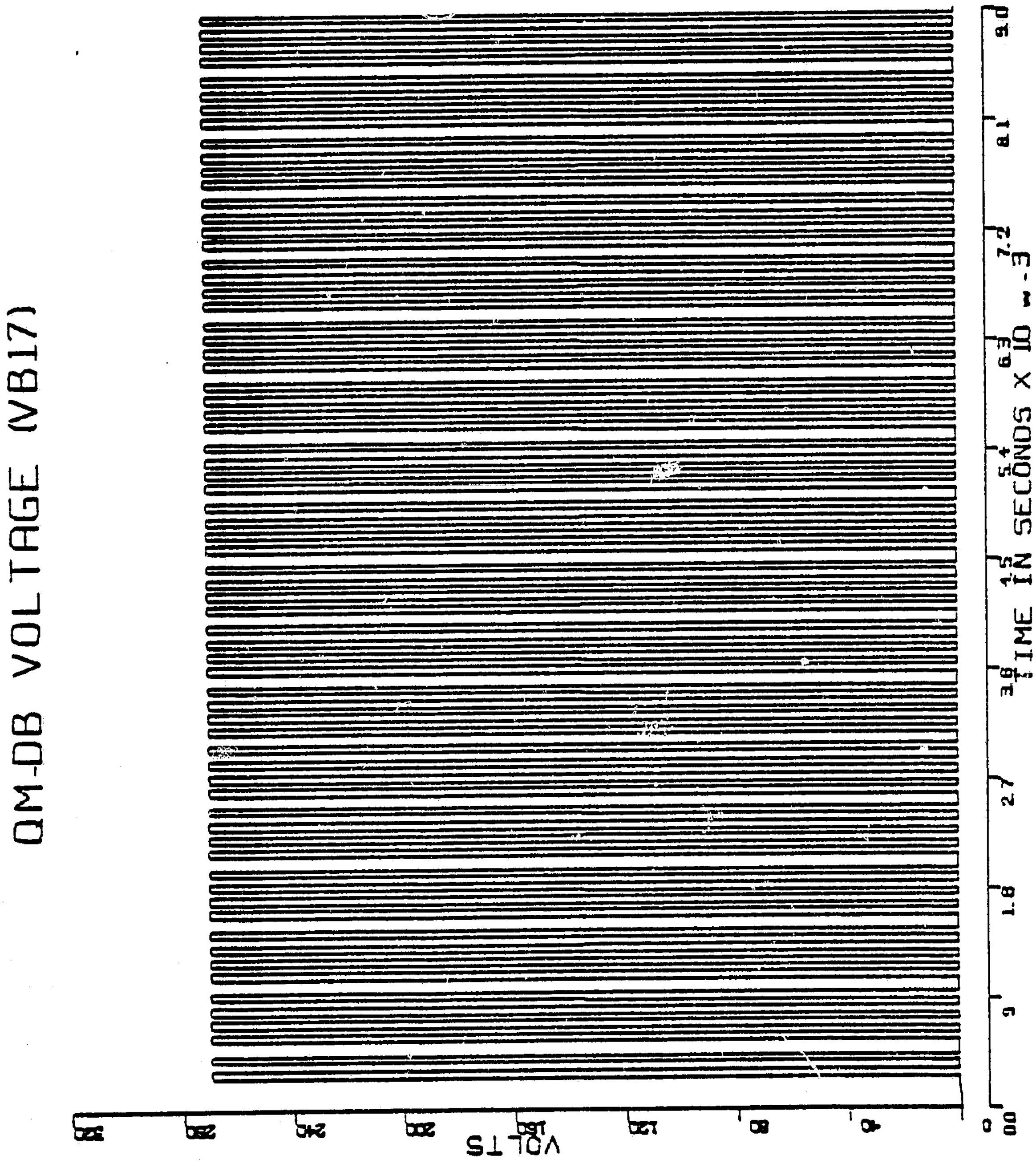
QM-DB VOLTAGE (VB17)
TIME IN SECONDS X 10 ** -3
0.0
.9
1.8
2.7
3.6
4.5
5.4
6.3
7.2
8.1
9.0
VOLTS
0
40
80
120
160
200
240
280
320

Figure A.1-14

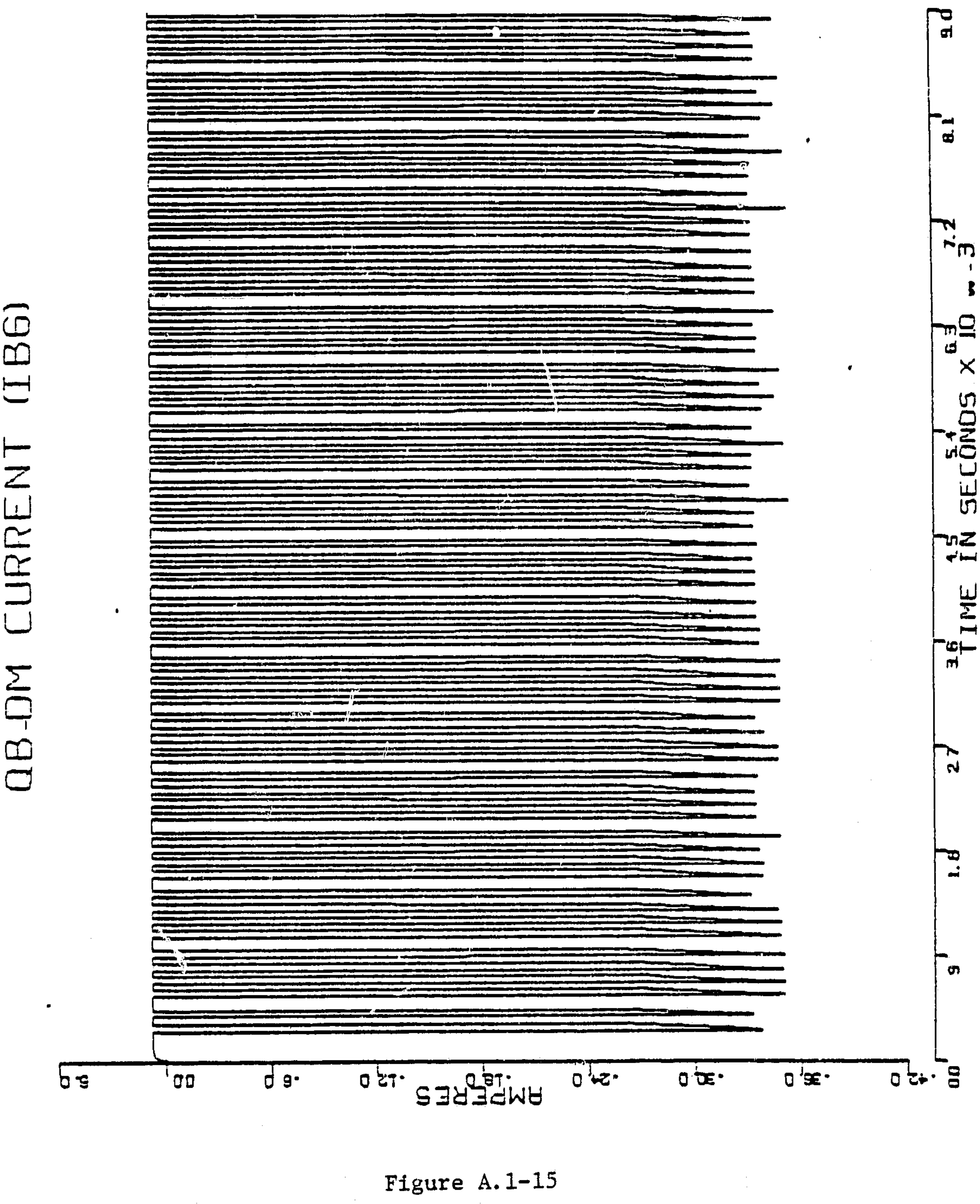

Figure A.1-15

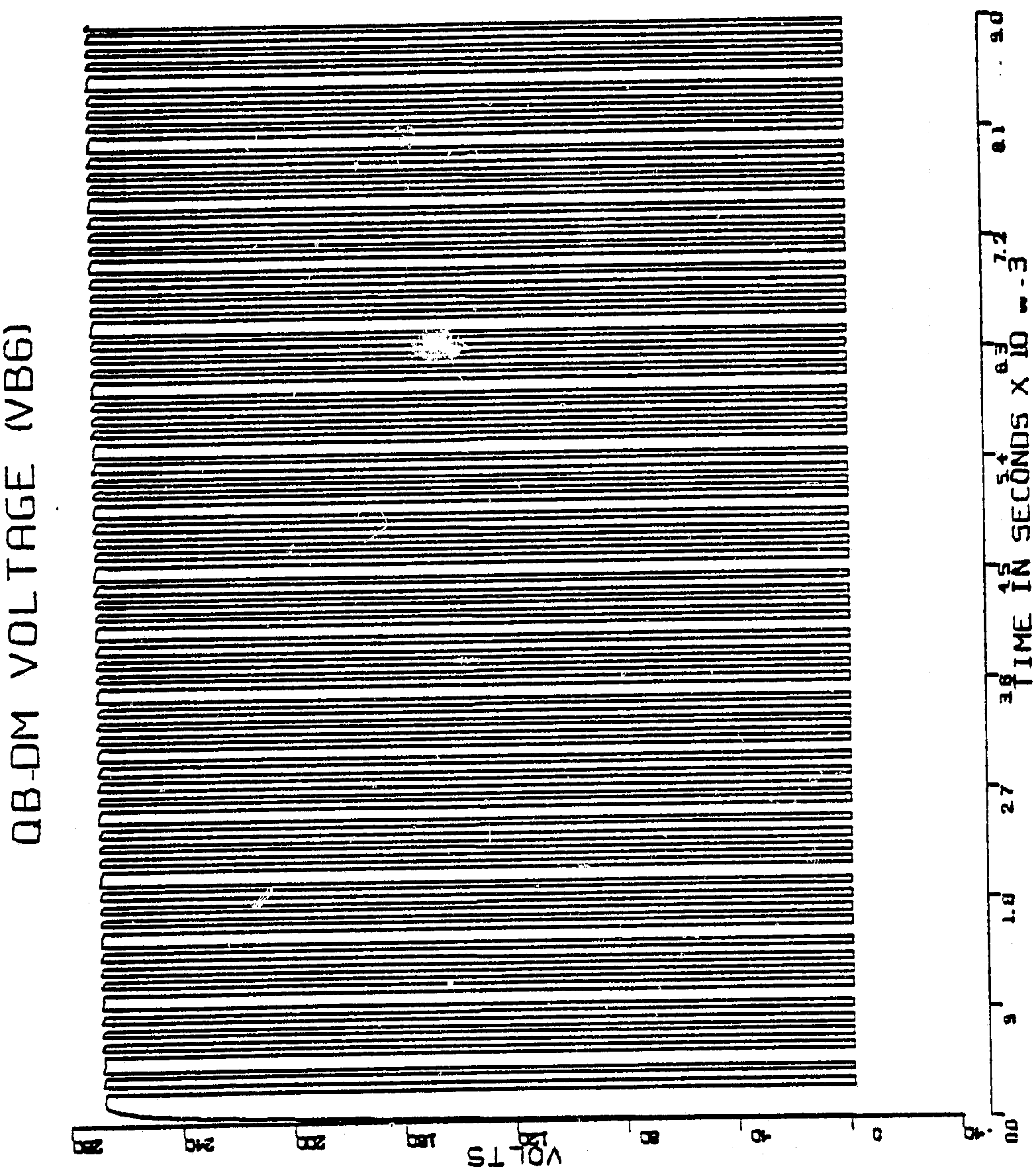
QB-DM VOLTAGE (VB6)
TIME IN SECONDS X 10 ** -3
0.0
.9
1.8
2.7
3.6
4.5
5.4
6.3
7.2
8.1
9.0
VOLTS
-40
0
40
80
120
160
200
240
280

Figure A.1-16

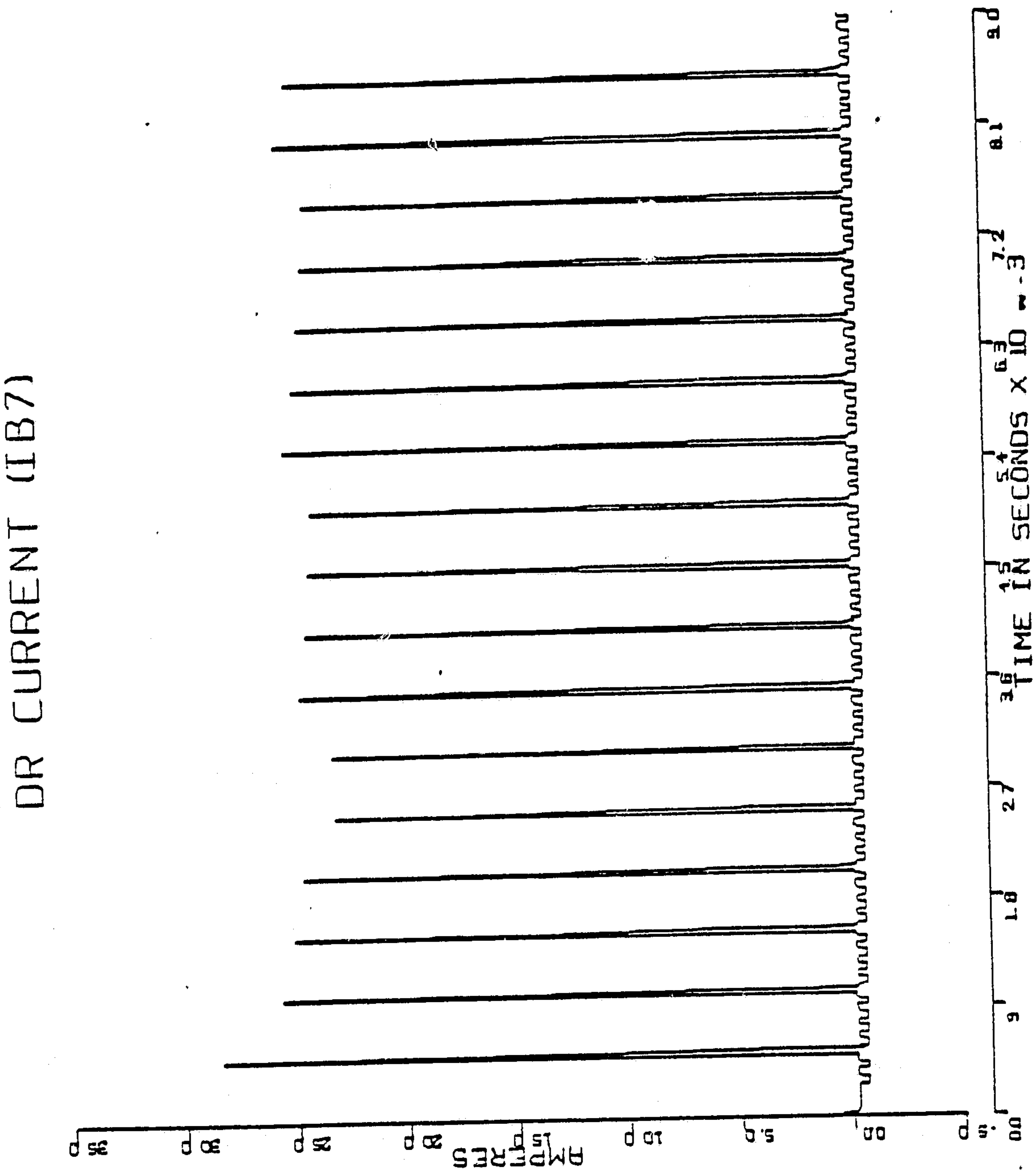

Figure A.1-17

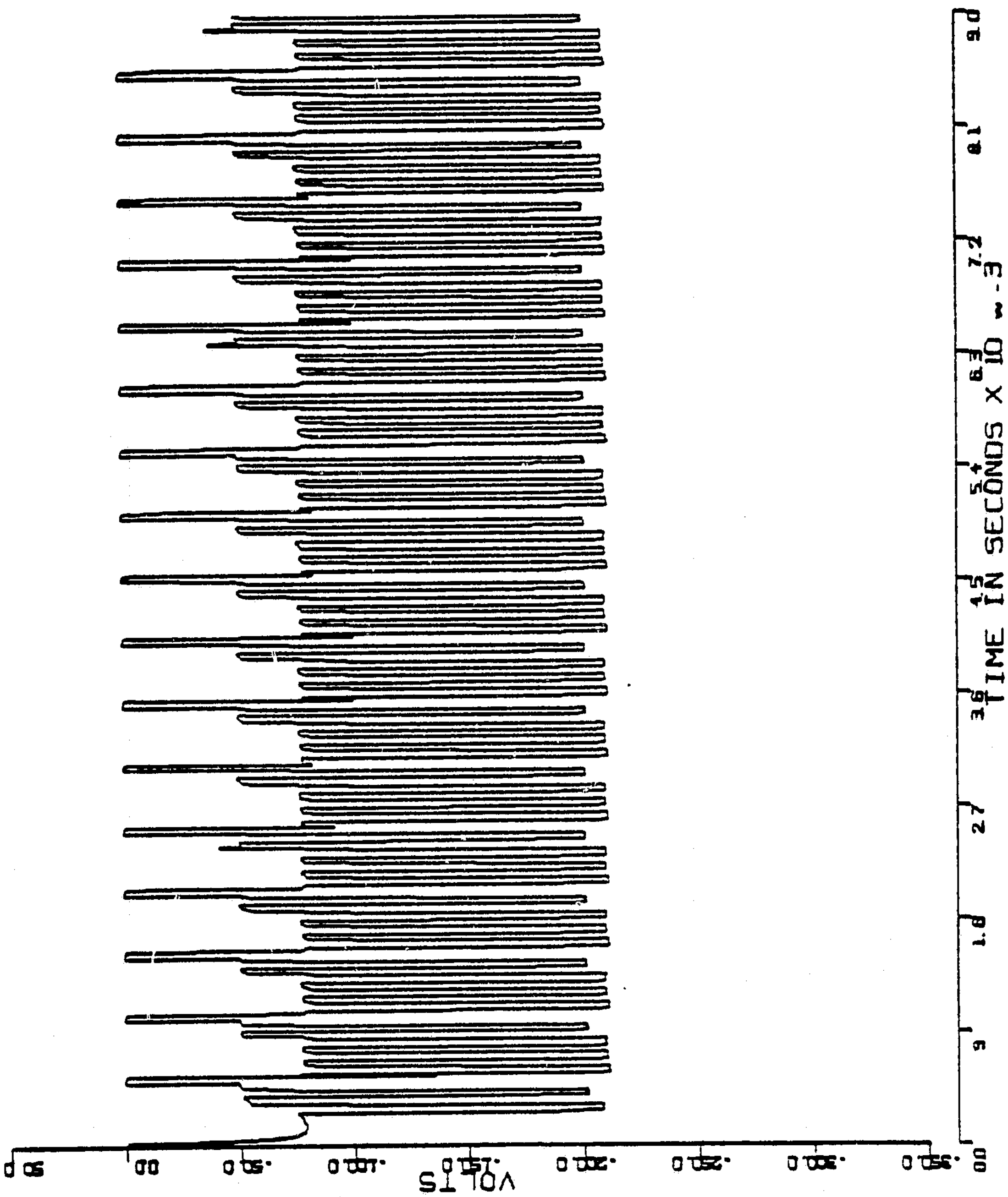
DR VOLTAGE (VB7)
TIME IN SECONDS X 10 ** -3
0.0
.9
1.8
2.7
3.6
4.5
5.4
6.3
7.2
8.1
9.0
VOLTS
50.0
0.0
-50.0
-100.0
-150.0
-200.0
-250.0
-300.0
-350.0

Figure A.1-18

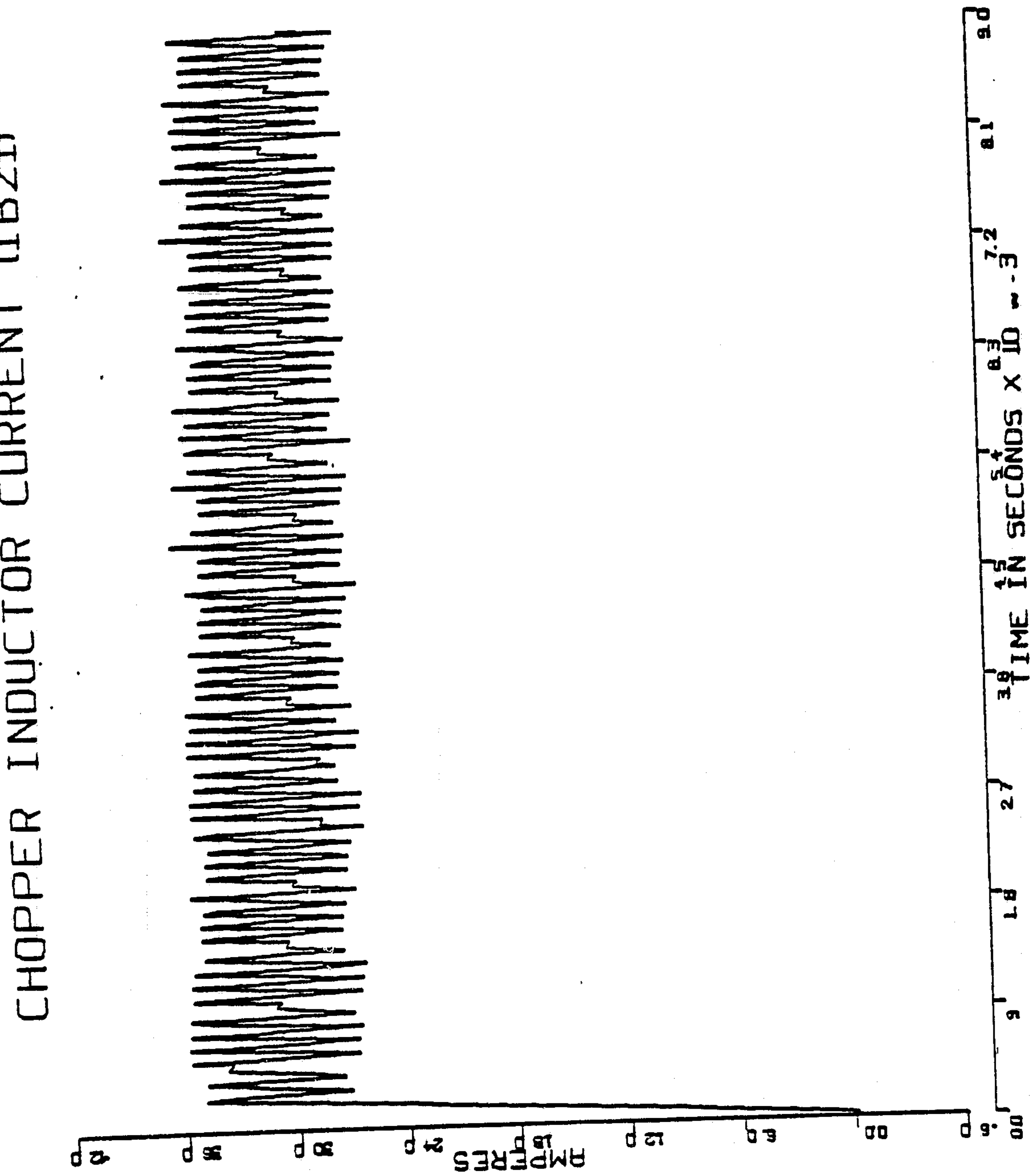
CHOPPER INDUCTOR CURRENT (IB21)
TIME IN SECONDS X 10 ** -3
AMPERES
0.0
.9
1.8
2.7
3.6
4.5
5.4
6.3
7.2
8.1
9.0

Figure A.1-19

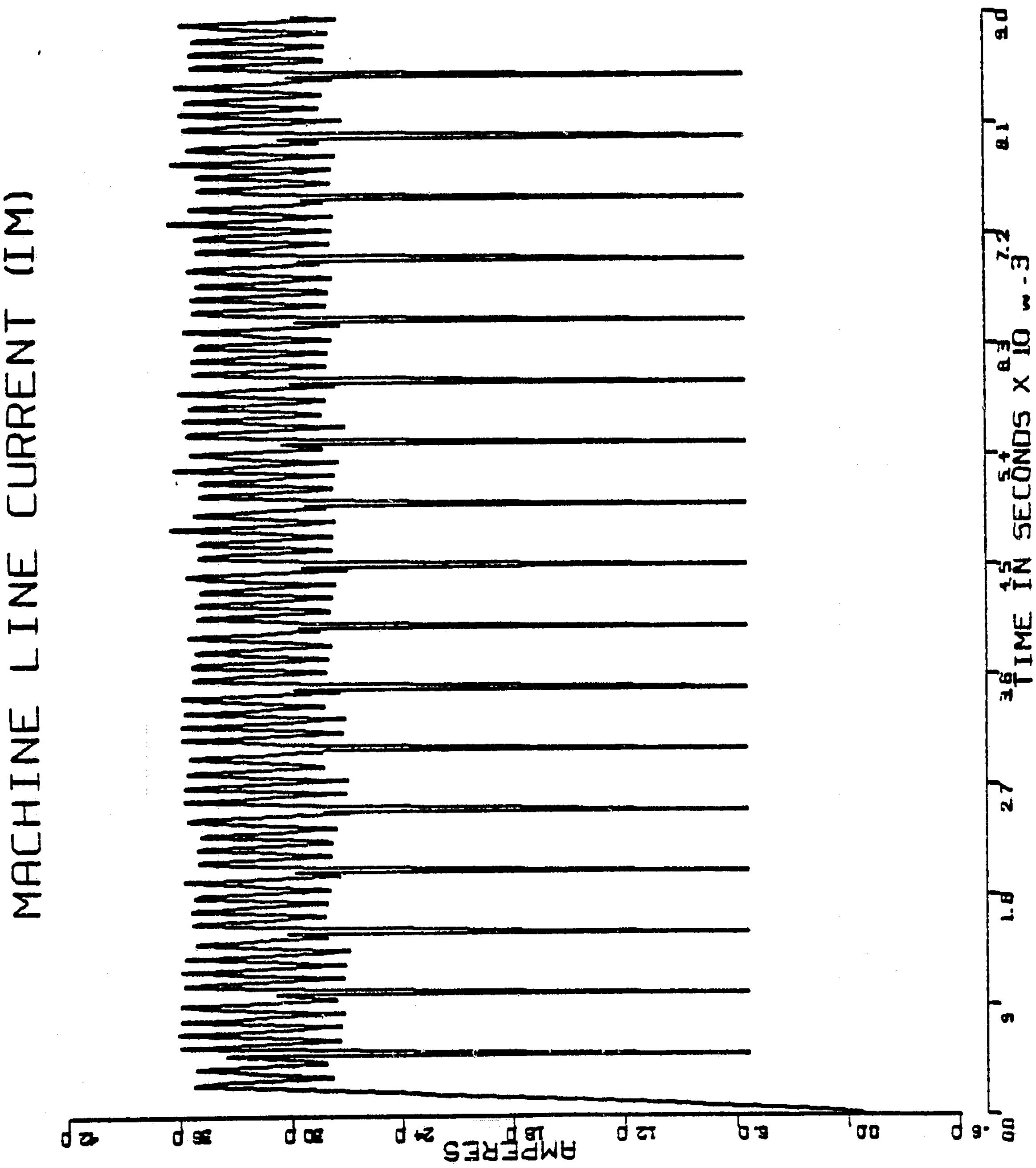

Figure A.1-20

APPENDIX A.2 CALCOMP PLOTS: MOTORING 5000 rpm 38° ADVANCE

RUN SUMMARY

MODE: MOTORING

PROGRAM MODE: PGMODE = 1

CURRENT COMMAND: ICMD = 31.5 amps

TIME STEP: TSNET = 5 μs

COMMUTATION SHIFT: SHIFT = .034906 mech rad

ITOL: 4.0 amps

ROTOR VELOCITY: (5000 rpm) (523.599 rad/sec)

TOTAL NUMBER OF POINTS PLOTTED: NREC = 901

TOTAL NUMBER OF NETWORK CHANGES: NNETSW = 359

TOTAL NUMBER OF INTEGRATIONS: NUMINT = 1800

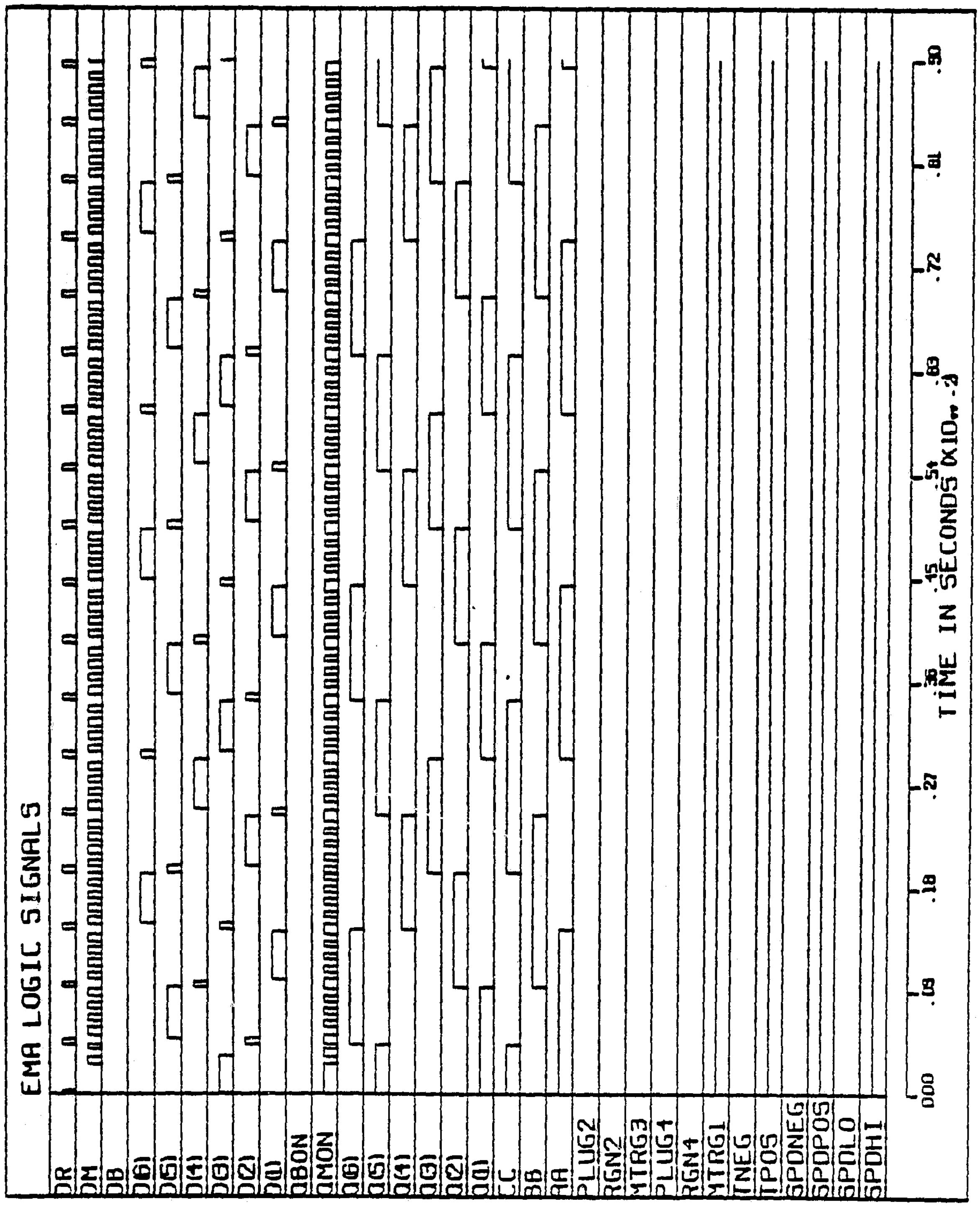
EMA LOGIC SIGNALS
TIME IN SECONDS (X10** -3)
.000
.09
.18
.27
.36
.45
.54
.63
.72
.81
.90
PLUG2
RGN2
MTRG3
PLUG4
RGN4
MTRG1
TNEG
TPOS
SPDNEG
SPDPOS
SPDLO
SPDHI

Figure A.2-1.

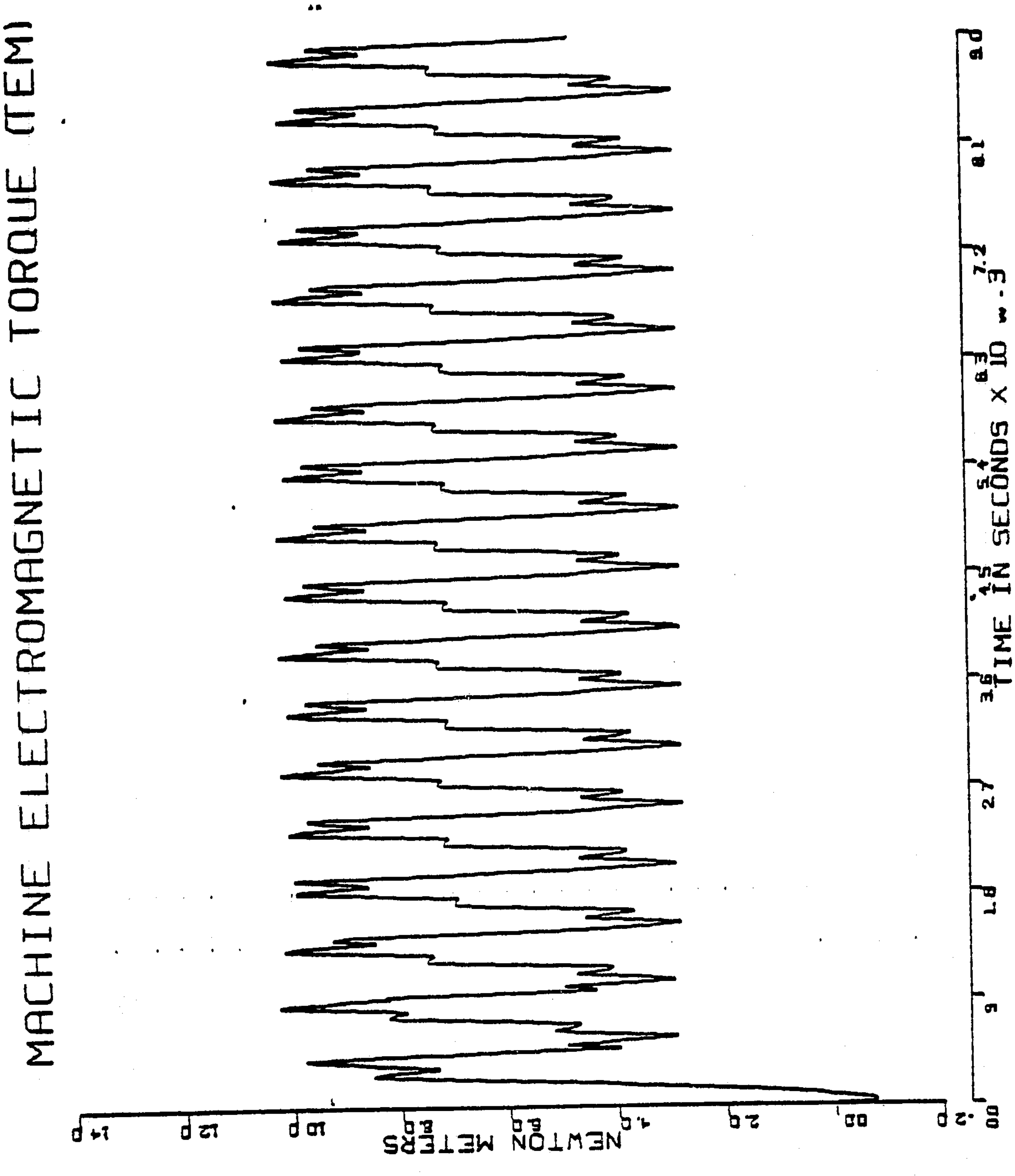
MACHINE ELECTROMAGNETIC TORQUE (TEM)
TIME IN SECONDS X 10 ** -3
NEWTON METERS
0.0
.9
1.8
2.7
3.6
4.5
5.4
6.3
7.2
8.1
9.0
-2.0
0.0
2.0
4.0
6.0
8.0
10.0
12.0
14.0

Figure A.2-2

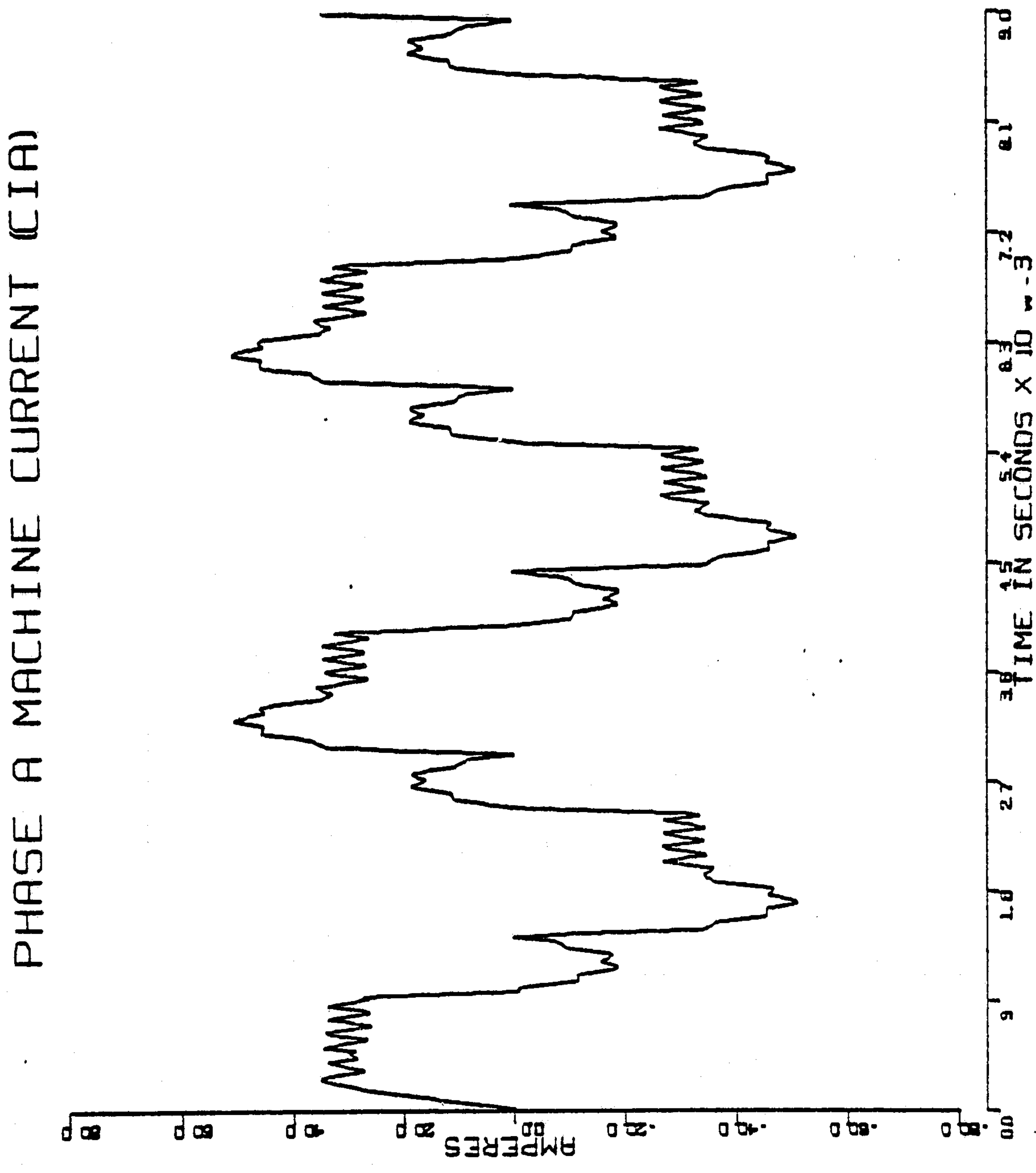

Figure A.2-3

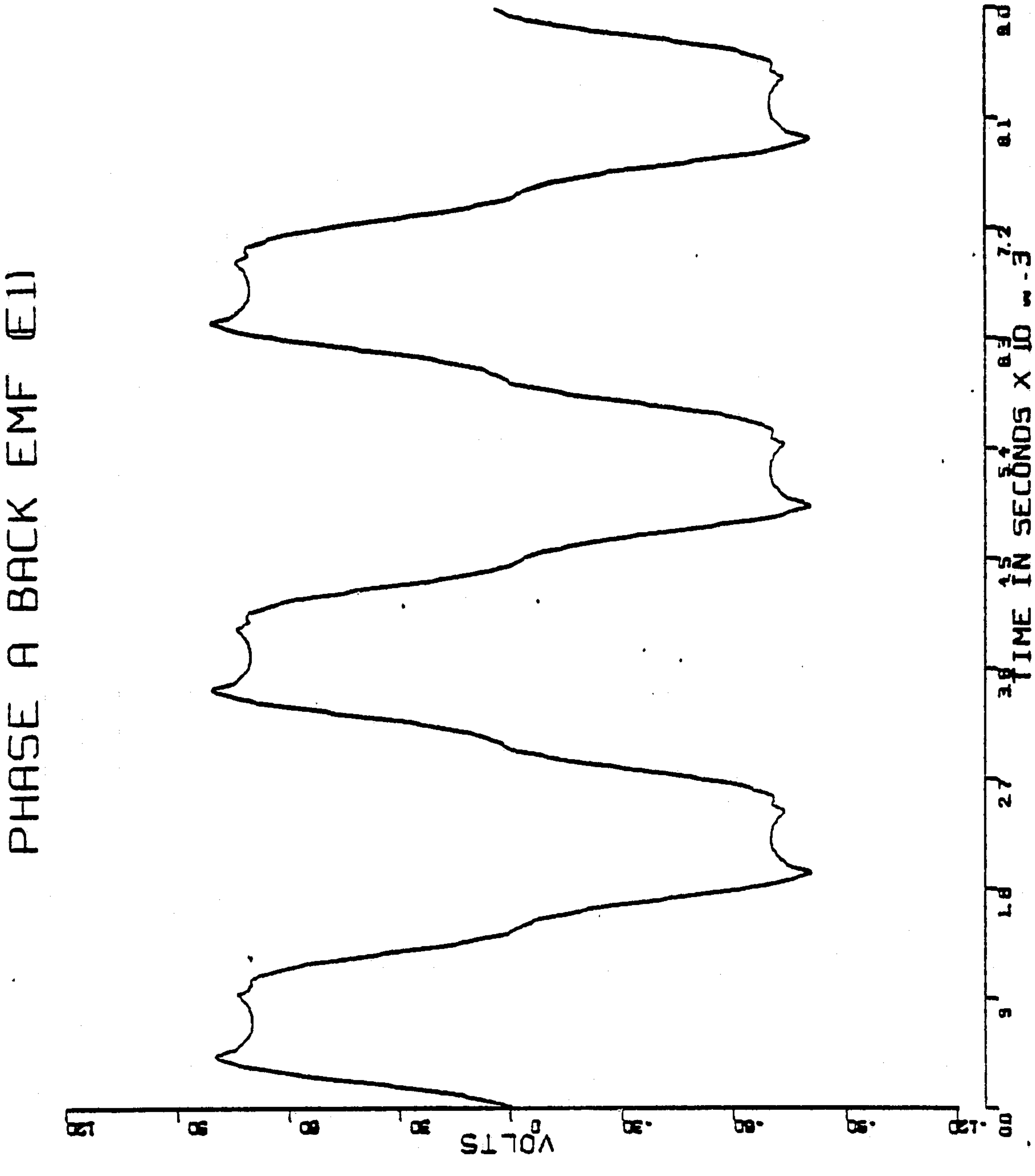

Figure A.2-4

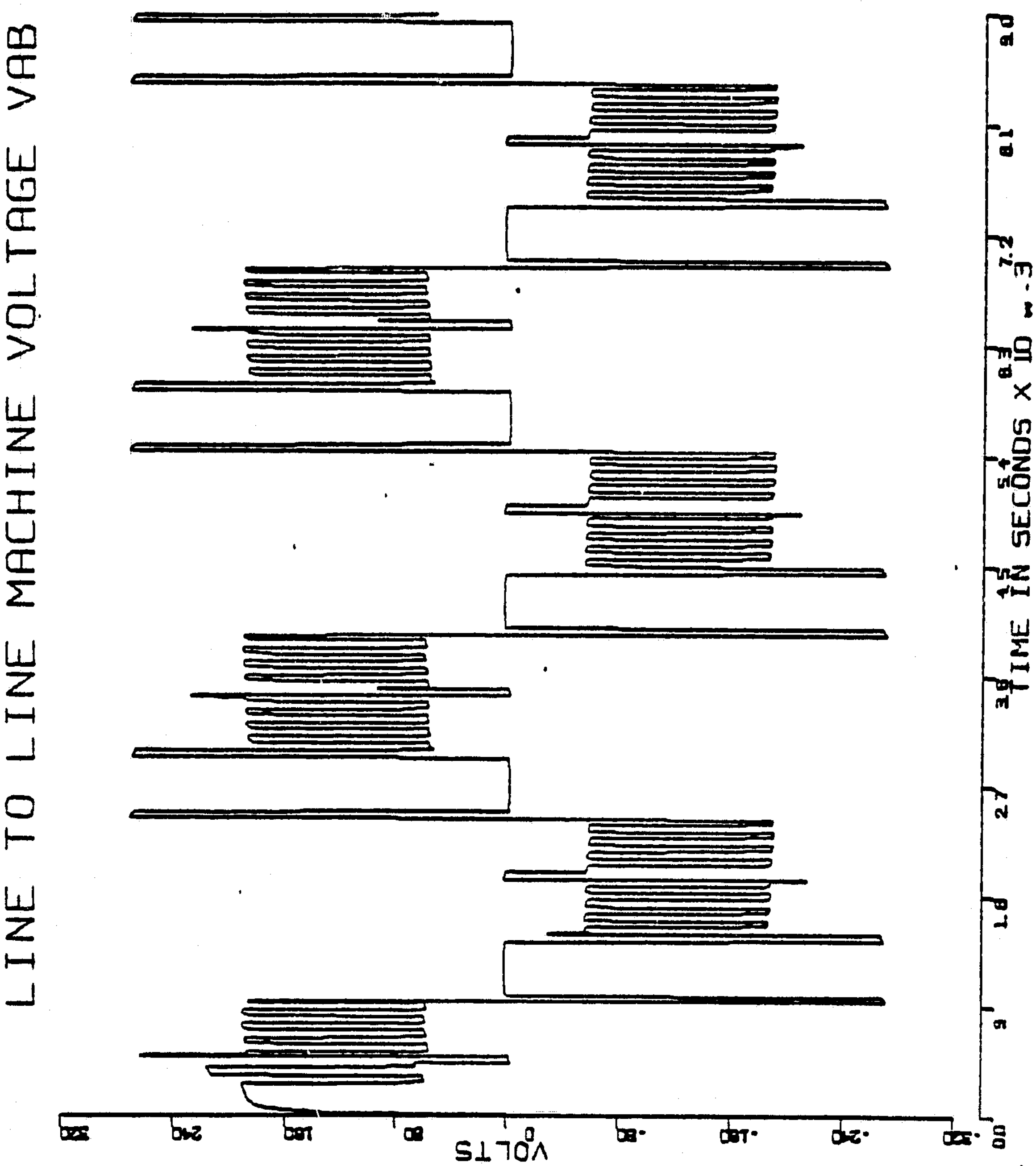
LINE TO LINE MACHINE VOLTAGE VAB
TIME IN SECONDS X 10 ** -3
VOLTS
0.0
.9
1.8
2.7
3.6
4.5
5.4
6.3
7.2
8.1
9.0
320
240
160
80
0
-80
-160
-240
-320

Figure A.2-5

APPENDIX A.3 CALCOMP PLOTS: MOTORING 5000 rpm 22° ADVANCE

RUN SUMMARY

MODE: MOTORING

PROGRAM MODE: PGMOD = 1

CURRENT COMMAND: ICMD = 31.5

TIME STEP: TSNET = 5 μs

COMMUTATION SHIFT: SHIFT = -0.034906 mech rad

CURRENT THRESHOLD: ITOL = 4.0 amps

ROTOR VELOCITY: (5000 rpm), (523,599 rad/sec)

TOTAL NUMBER OF INTEGRATIONS: NUMINT = 1800

NUMBER OF POINTS PLOTTED: NREC = 901

TOTAL NUMBER OF NETWORK CHANGES: NNETSW = 367

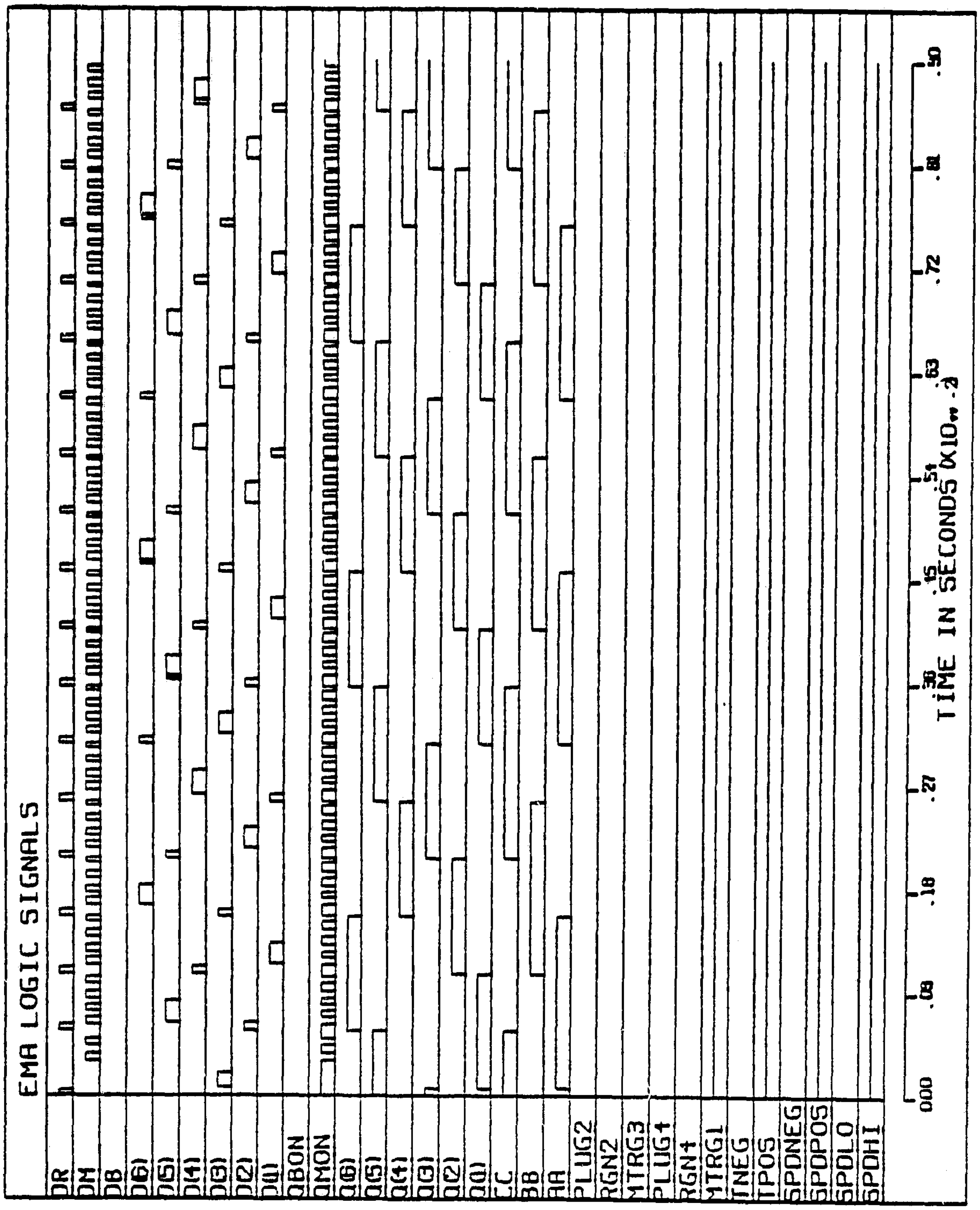
EMA LOGIC SIGNALS
DR
DM
DB
D(6)
D(5)
D(4)
D(3)
D(2)
D(1)
QBON
QMON
Q(6)
Q(5)
Q(4)
Q(3)
Q(2)
Q(1)
CC
BB
AA
PLUG2
RGN2
MTRG3
PLUG4
RGN4
MTRG1
TNEG
TPOS
SPDNEG
SPDPOS
SPDLO
SPDHI
TIME IN SECONDS

Figure A.3-1

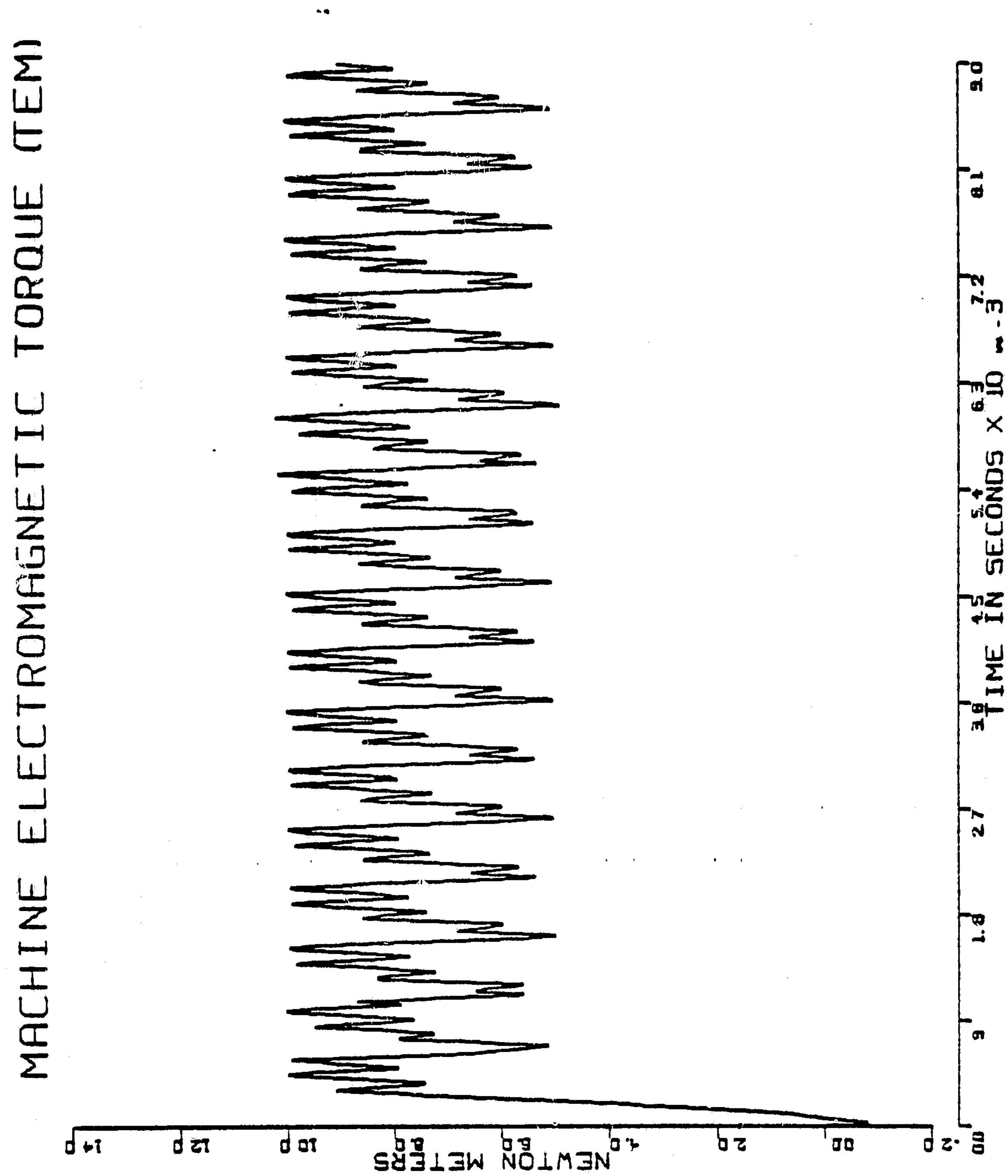
MACHINE ELECTROMAGNETIC TORQUE (TEM)
TIME IN SECONDS X 10 ** -3
NEWTON METERS

Figure A.3-2

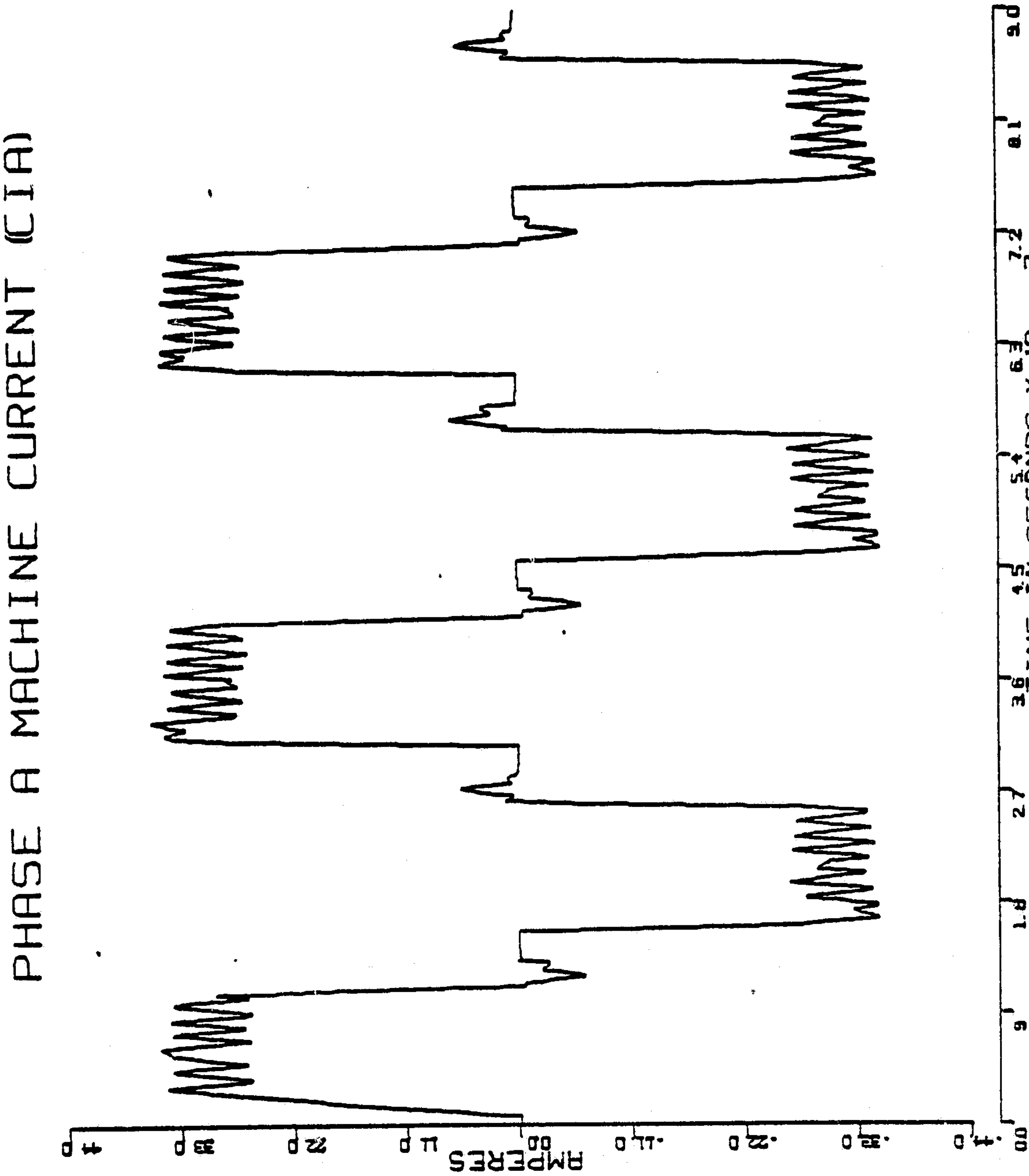

Figure A.3-3

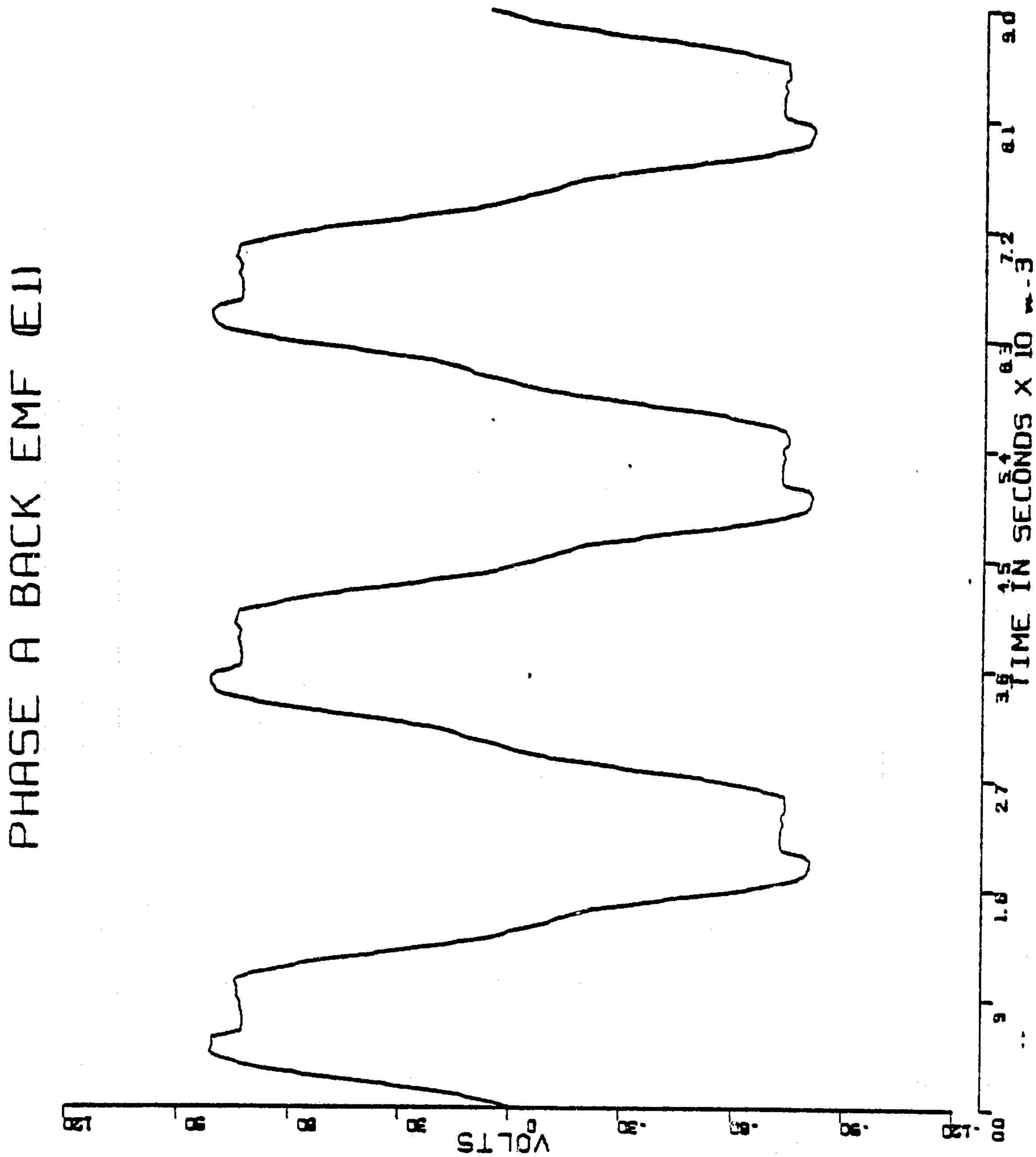

Figure A.3-4

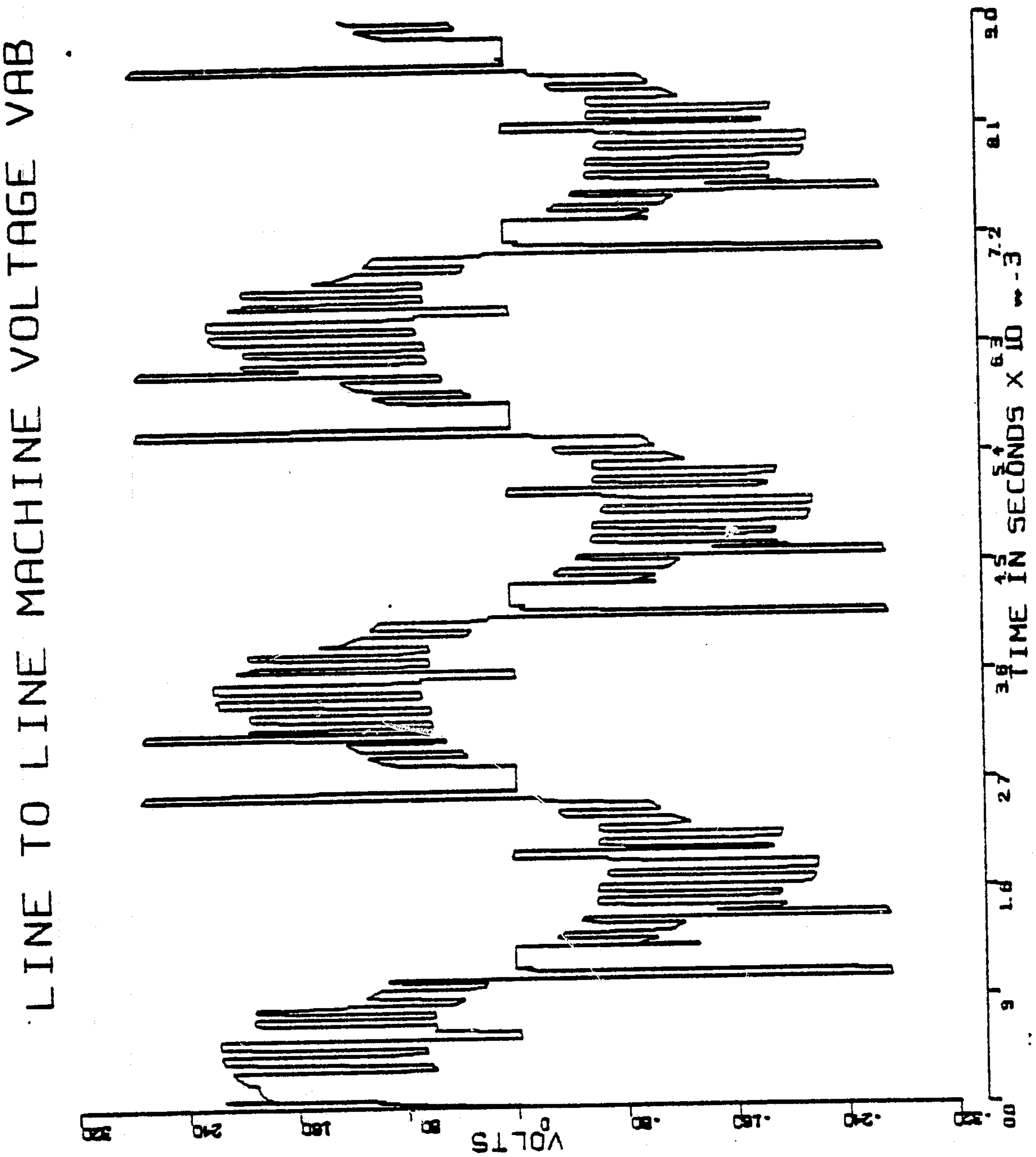
LINE TO LINE MACHINE VOLTAGE VAB
TIME IN SECONDS X 10 ** -3
0.0
.9
1.8
2.7
3.6
4.5
5.4
6.3
7.2
8.1
9.0
VOLTS
320
240
160
80
0
-80
-160
-240
-320

Figure A.3-5

APPENDIX B.1 CALCOMP PLOTS: REGENERATION 5101 rpm

RUN SUMMARY

MODE: REGENERATION

PROGRAM MODE: PGMODE = 1

CURRENT COMMAND: ICMD = -38.0 amps

TIME STEP: TSNET = 5 μs

COMMUTATION SHIFT: SHIFT = 0.0 mech rad

CURRENT THRESHOLD: ITOL = 4.0 amps

ROTOR VELOCITY: (5101 rpm), (534.1756 rad/sec)

TOTAL NUMBER OF POINTS PLOTTED: NREC = 901

TOTAL NUMBER OF NETWORK CHANGES: NNETSW = 415

TOTAL NUMBER OF INTEGRATIONS: NUMINT = 1800

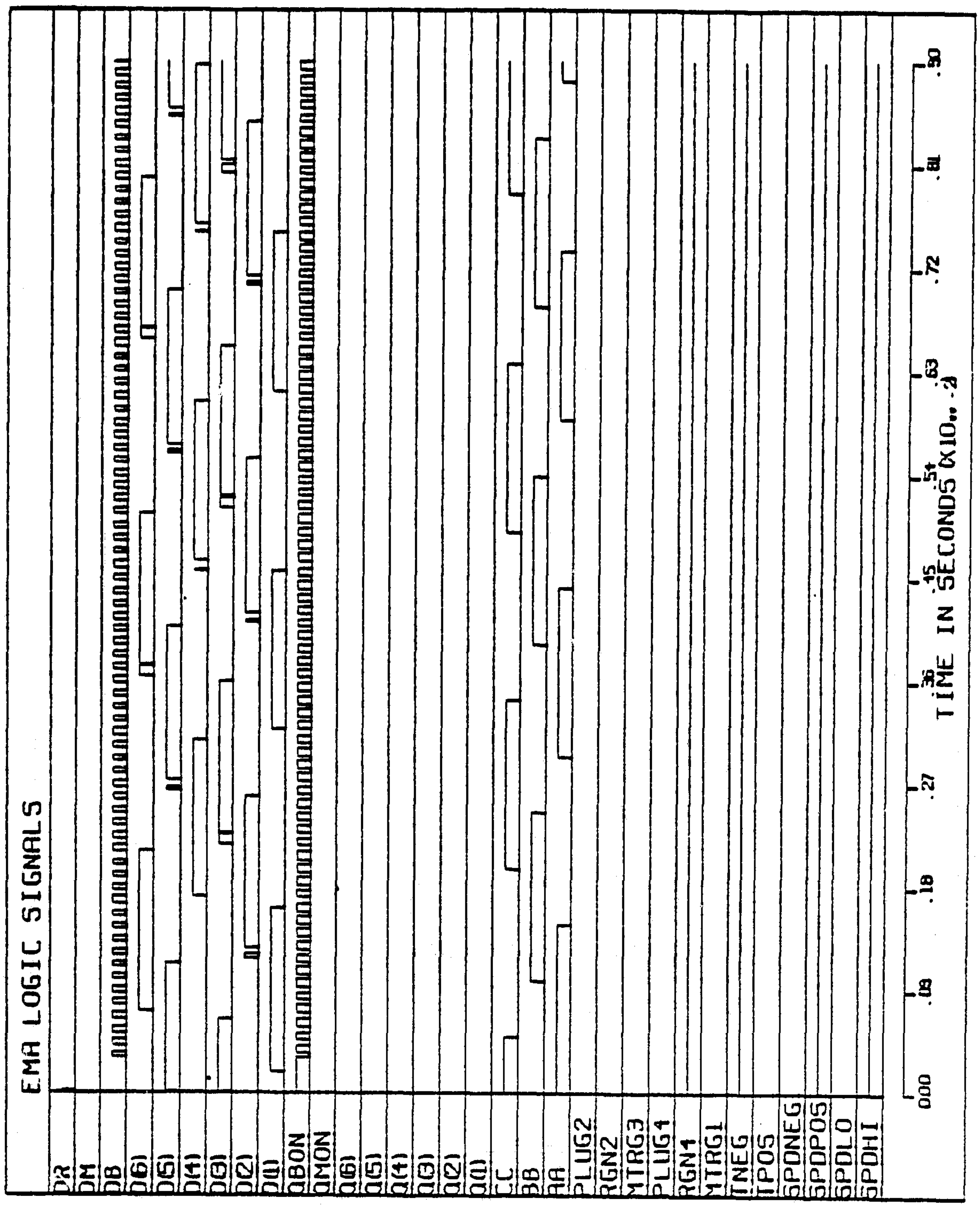
EMA LOGIC SIGNALS
TIME IN SECONDS
.000
.09
.18
.27
.36
.45
.54
.63
.72
.81
.90

Figure B.1-1

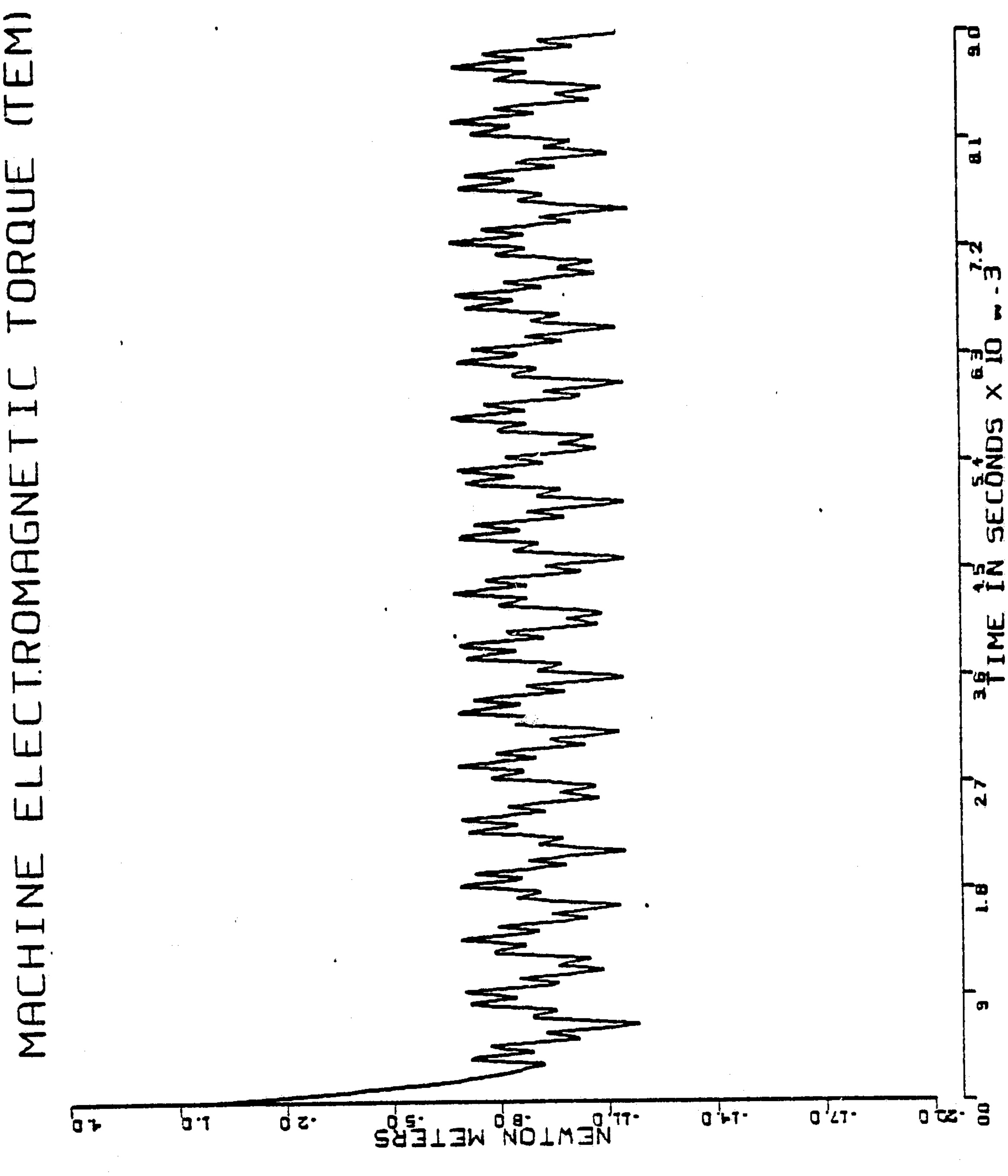
MACHINE ELECTROMAGNETIC TORQUE (TEM)
TIME IN SECONDS X 10 ** -3
NEWTON METERS
0.0
.9
1.8
2.7
3.6
4.5
5.4
6.3
7.2
8.1
9.0
4.0
1.0
-2.0
-5.0
-8.0
-11.0
-14.0
-17.0
-20.0

Figure B.1-2

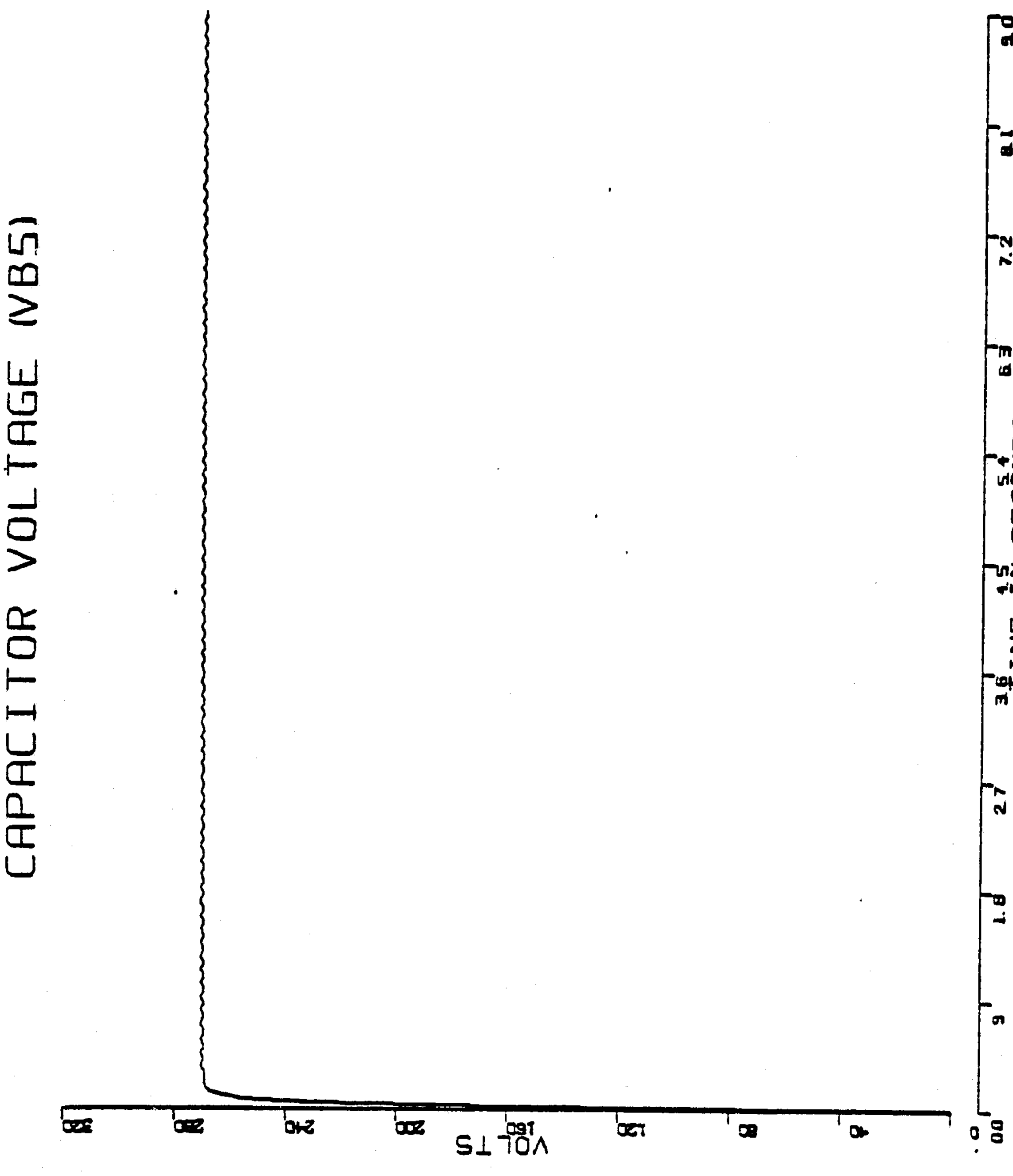
CAPACITOR VOLTAGE (VB5)
TIME IN SECONDS X 10^-3
VOLTS
0.0
.9
1.8
2.7
3.6
4.5
5.4
6.3
7.2
8.1
9.0
0
40
80
120
160
200
240
280
320

Figure B.1-3

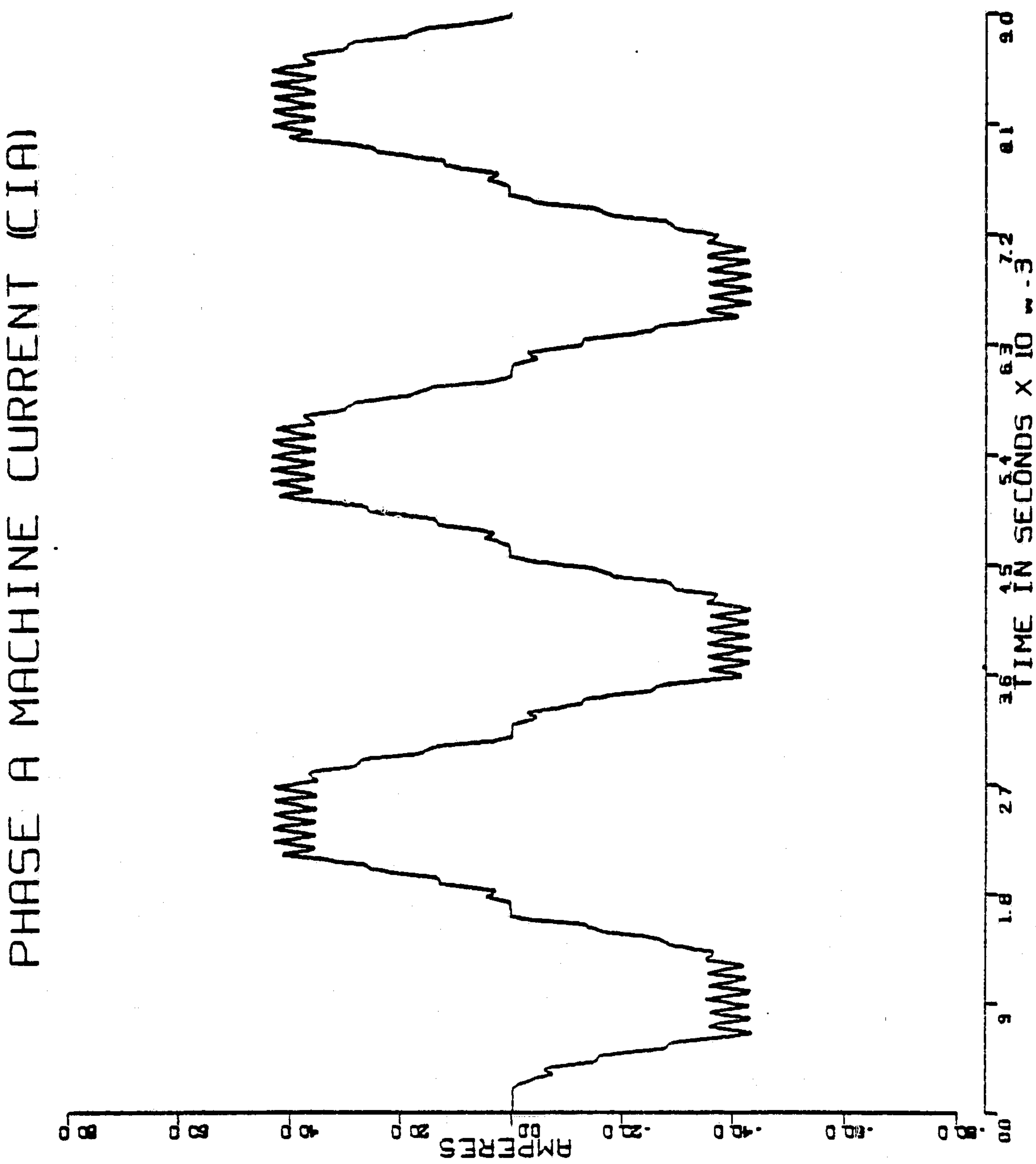

Figure B.1-4

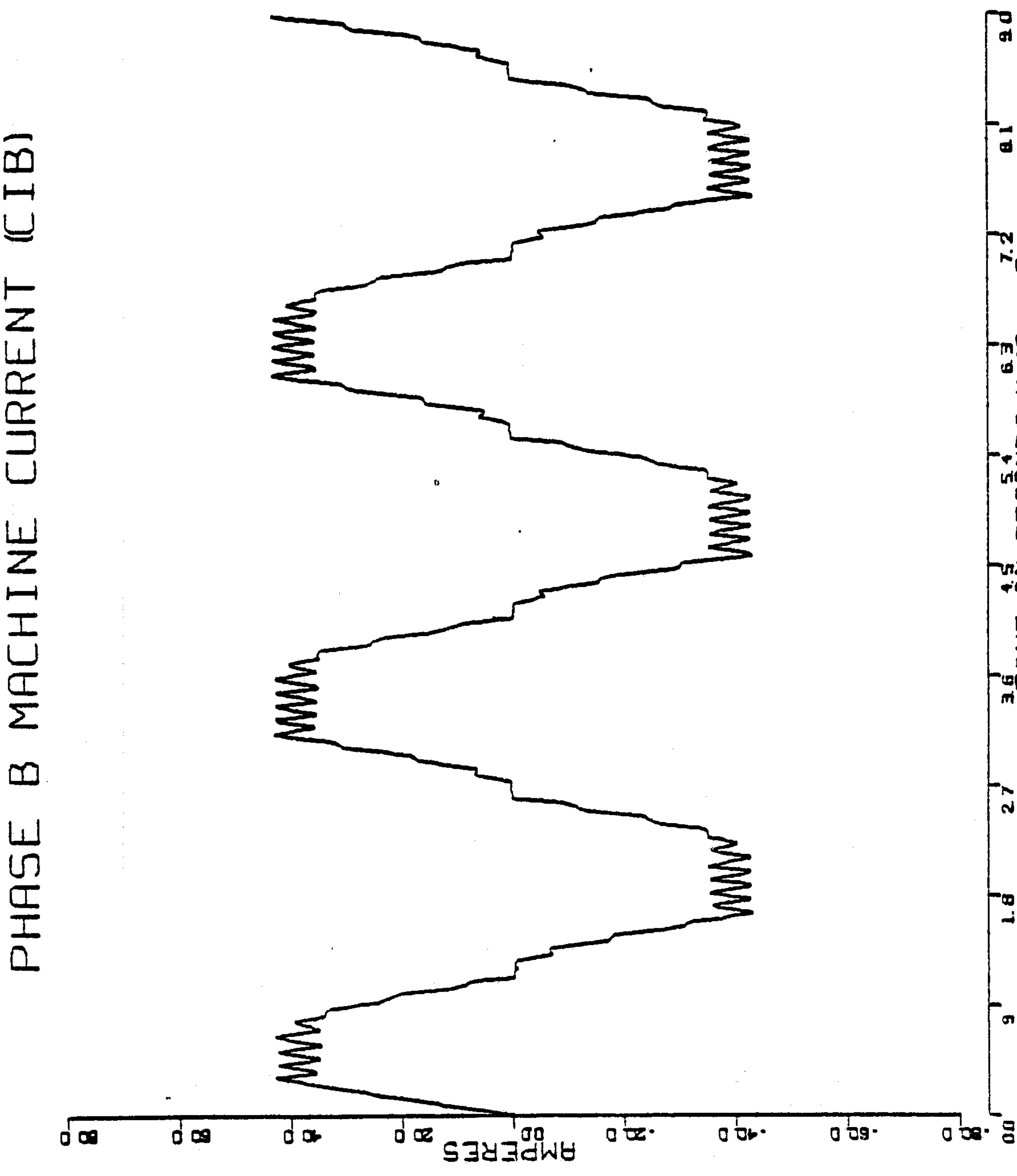
PHASE B MACHINE CURRENT (CIB)
TIME IN SECONDS X 10 ** -3
AMPERES
0.0
.9
1.8
2.7
3.6
4.5
5.4
6.3
7.2
8.1
9.0

Figure B.1-5

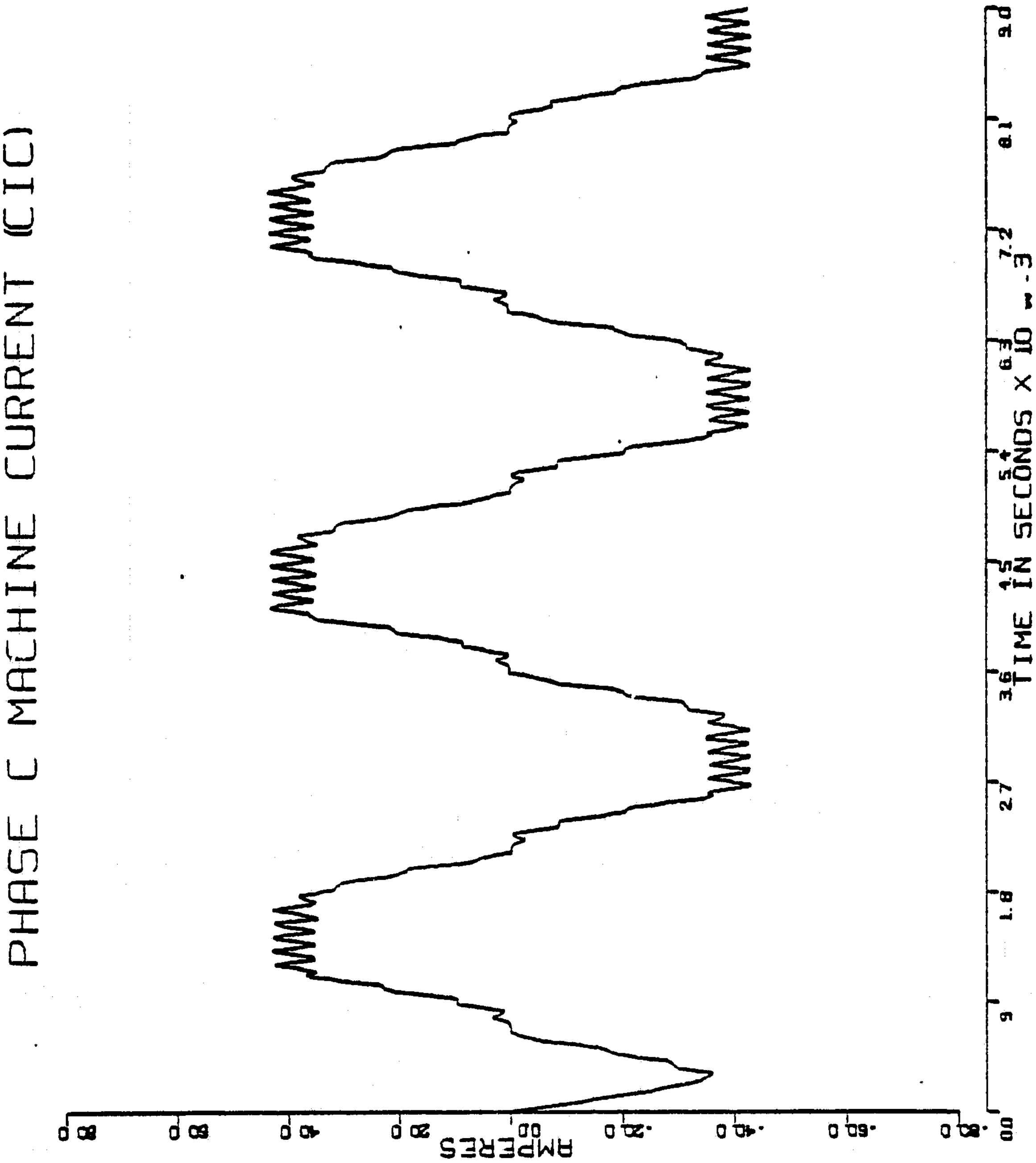
PHASE C MACHINE CURRENT (CIC)
TIME IN SECONDS X 10 ** -3
AMPERES
0.0
.9
1.8
2.7
3.6
4.5
5.4
6.3
7.2
8.1
9.0
-80.0
-60.0
-40.0
-20.0
0.0
20.0
40.0
60.0
80.0

Figure B.1-6

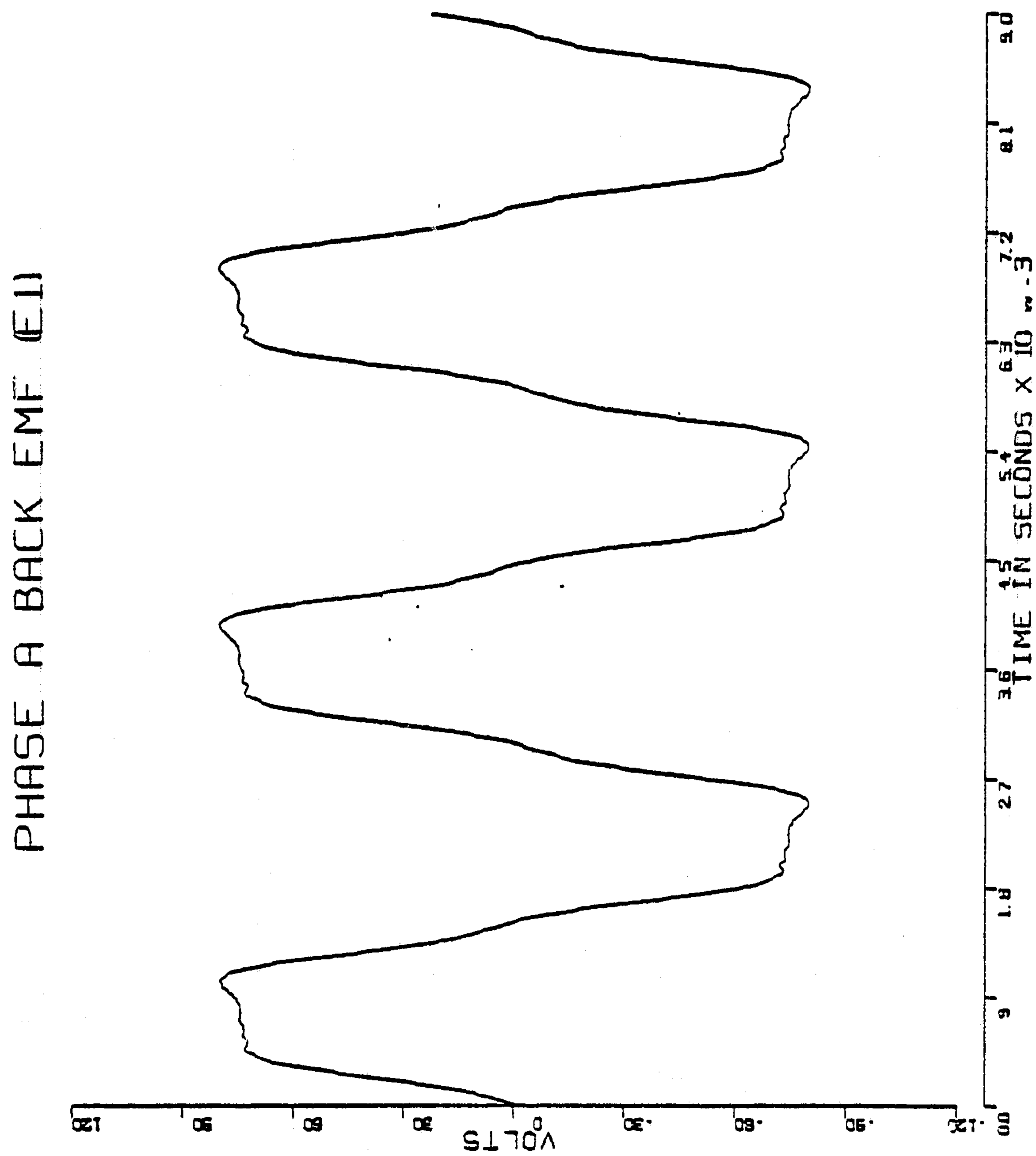

Figure B.1-7

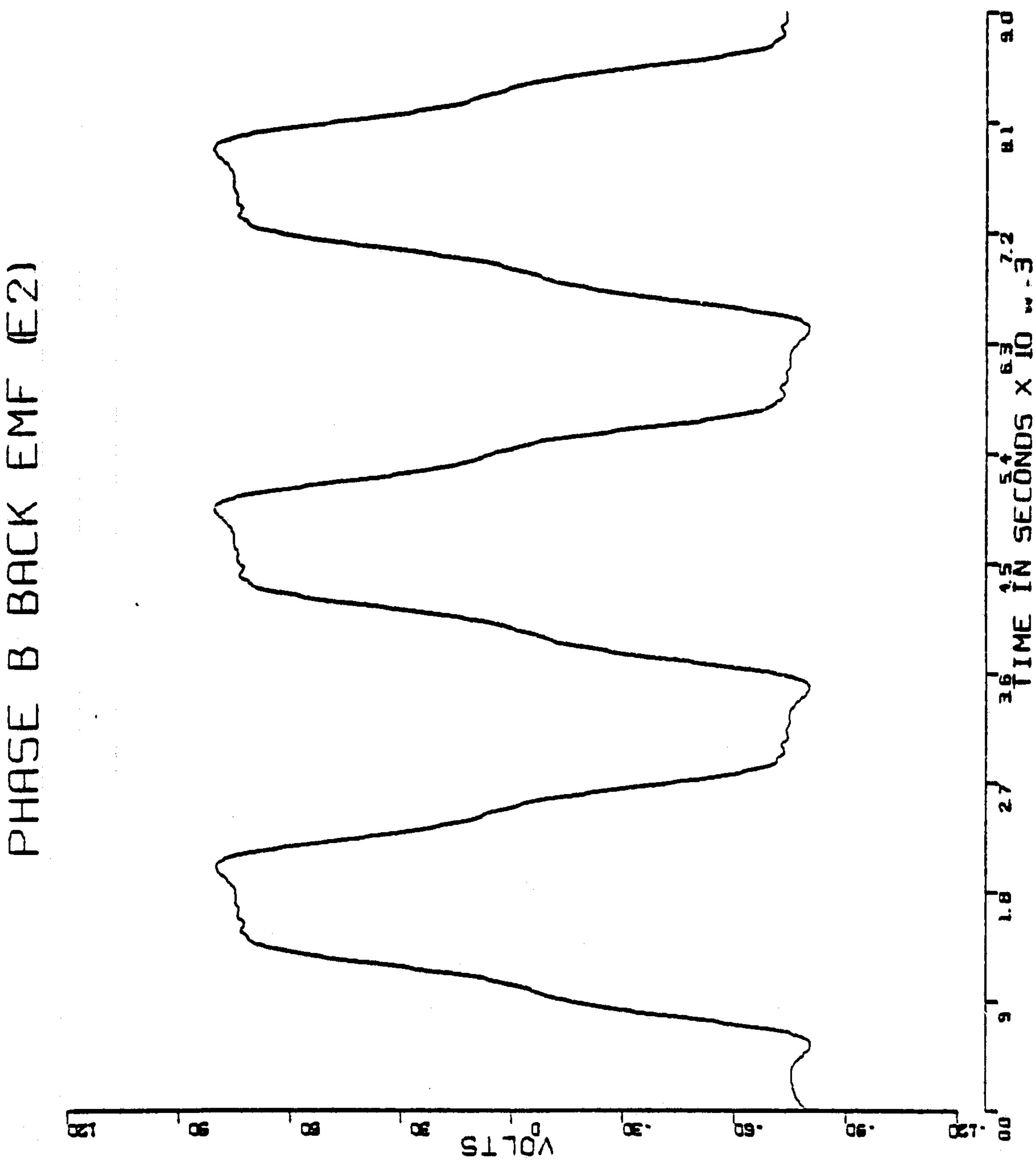
PHASE B BACK EMF (E2)
TIME IN SECONDS x 10 ** -3
VOLTS
0.0
.9
1.8
2.7
3.6
4.5
5.4
6.3
7.2
8.1
9.0

Figure B.1-8

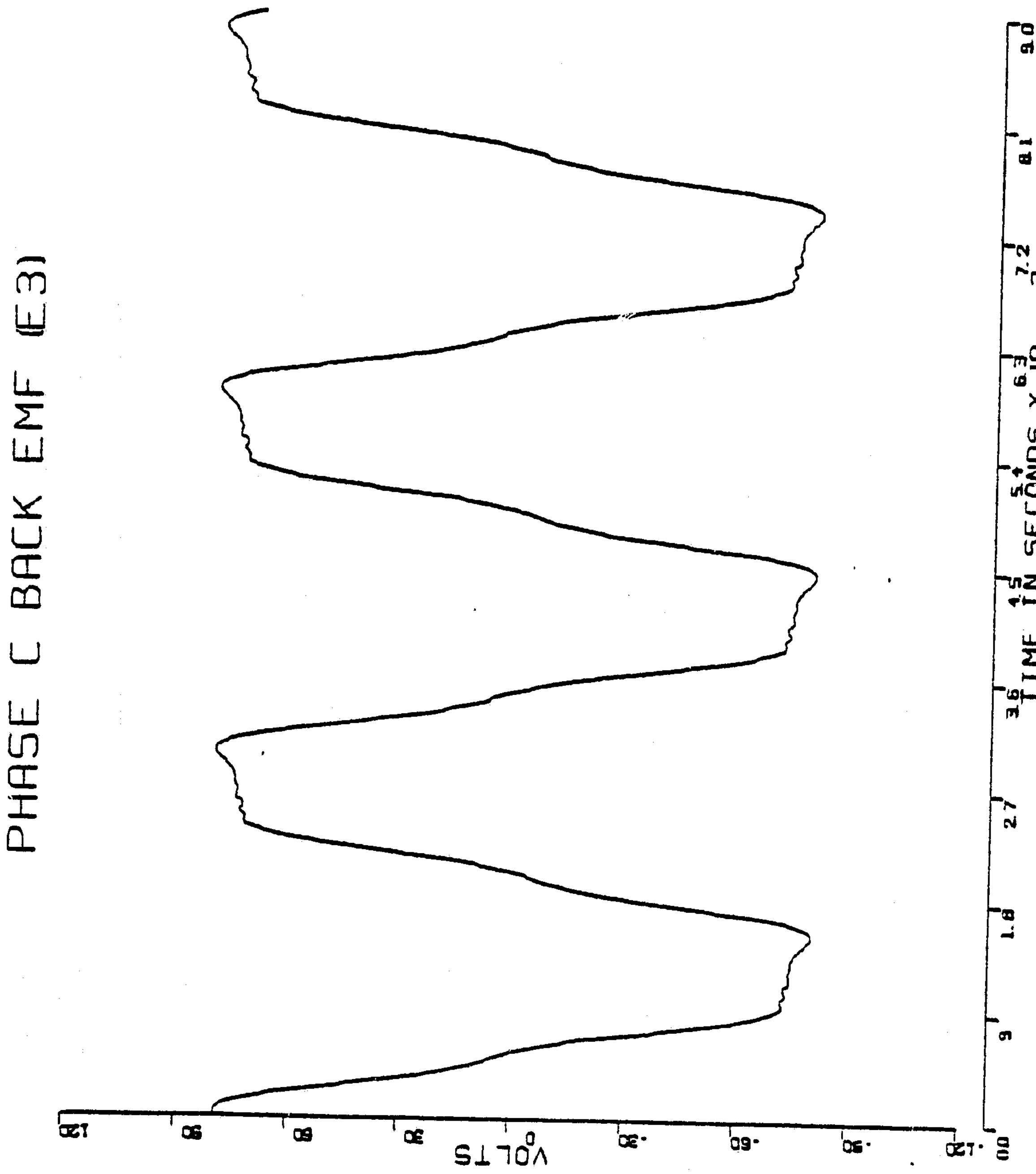

Figure B.1-9

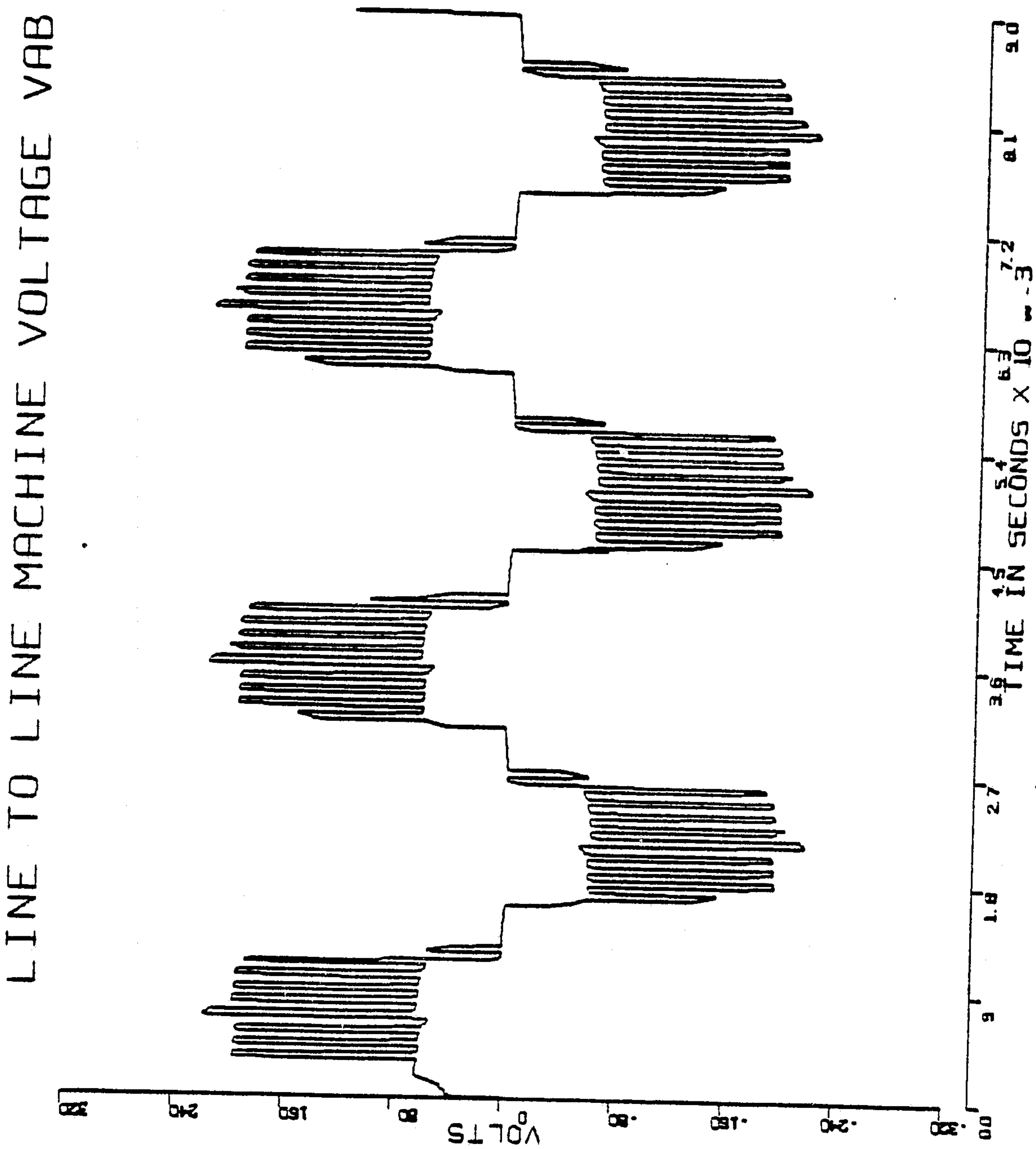
LINE TO LINE MACHINE VOLTAGE VAB
TIME IN SECONDS X 10 ** -3
VOLTS
0.0
.9
1.8
2.7
3.6
4.5
5.4
6.3
7.2
8.1
9.0
320
240
160
80
0
-80
-160
-240
-320

Figure B.1-10

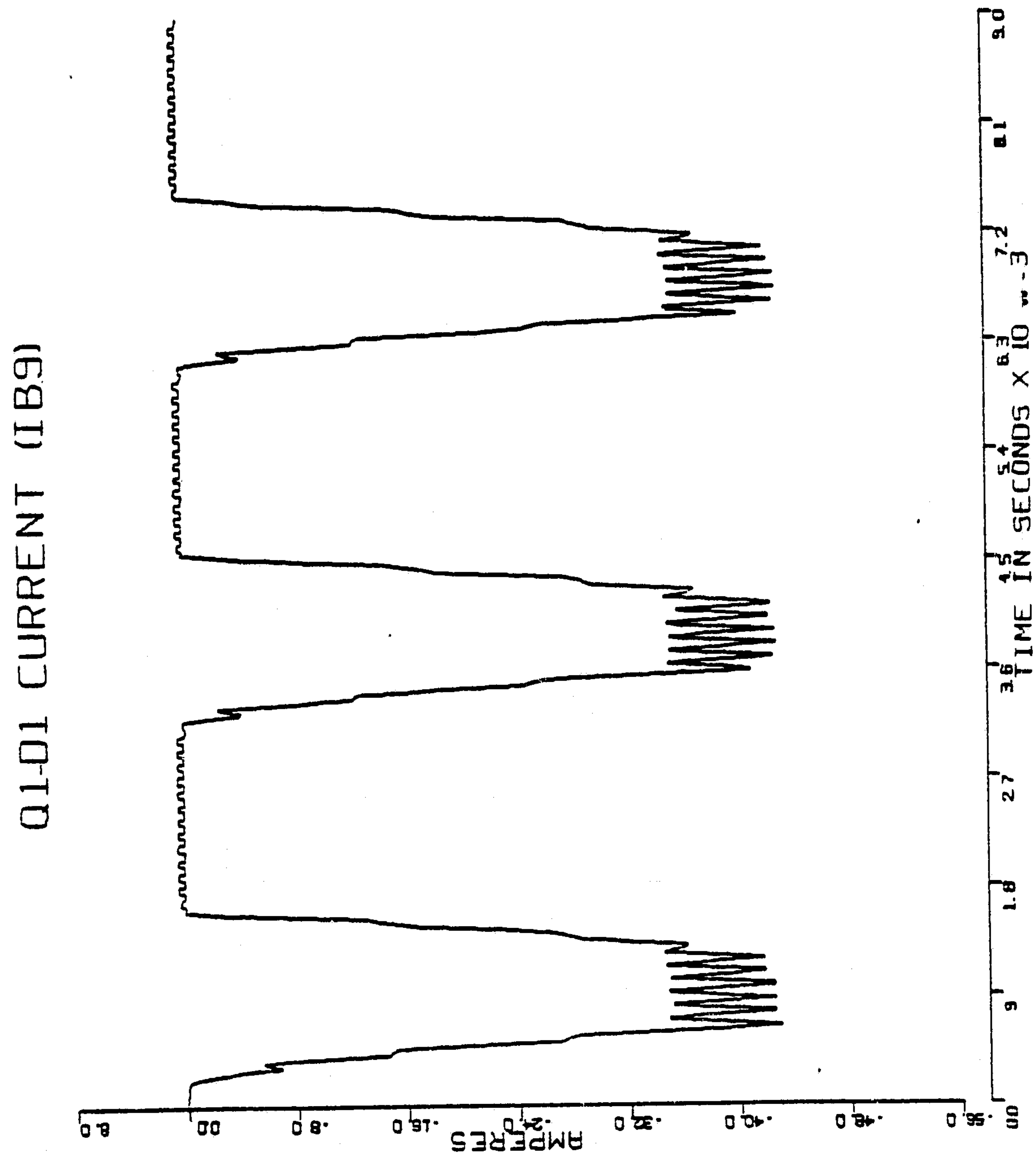
Q1-D1 CURRENT (IB9)
TIME IN SECONDS X 10 ** -3
.9
1.8
2.7
3.6
4.5
5.4
6.3
7.2
8.1
9.0
AMPERES
-56.0
-48.0
-40.0
-32.0
-24.0
-16.0
-8.0
0.0
8.0

Figure B.1-11

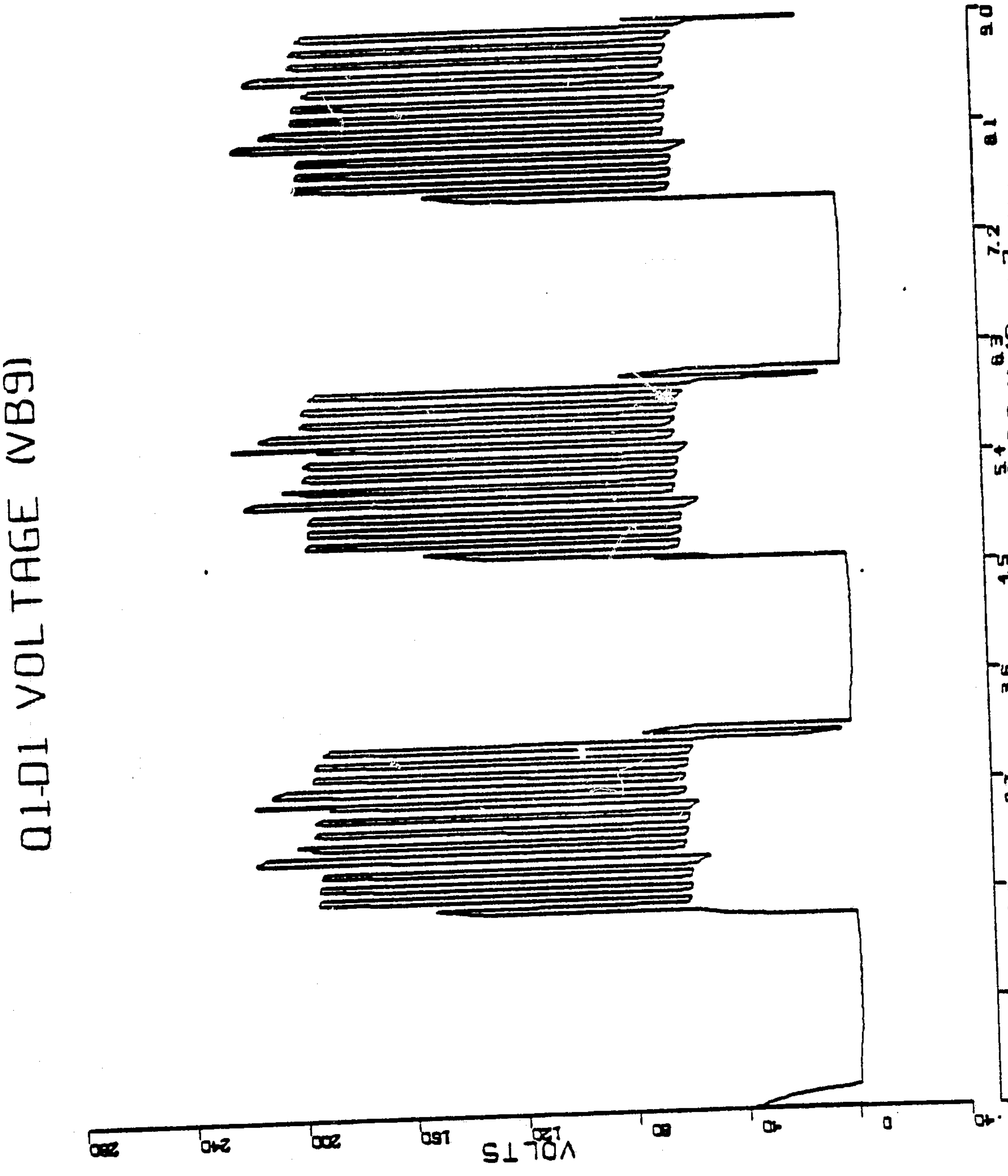
Q1-D1 VOLTAGE (VB9)
TIME IN SECONDS X 10 ** -3
0.0
.9
1.8
2.7
3.6
4.5
5.4
6.3
7.2
8.1
9.0
VOLTS
-40
0
40
80
120
160
200
240
280

Figure B.1-12

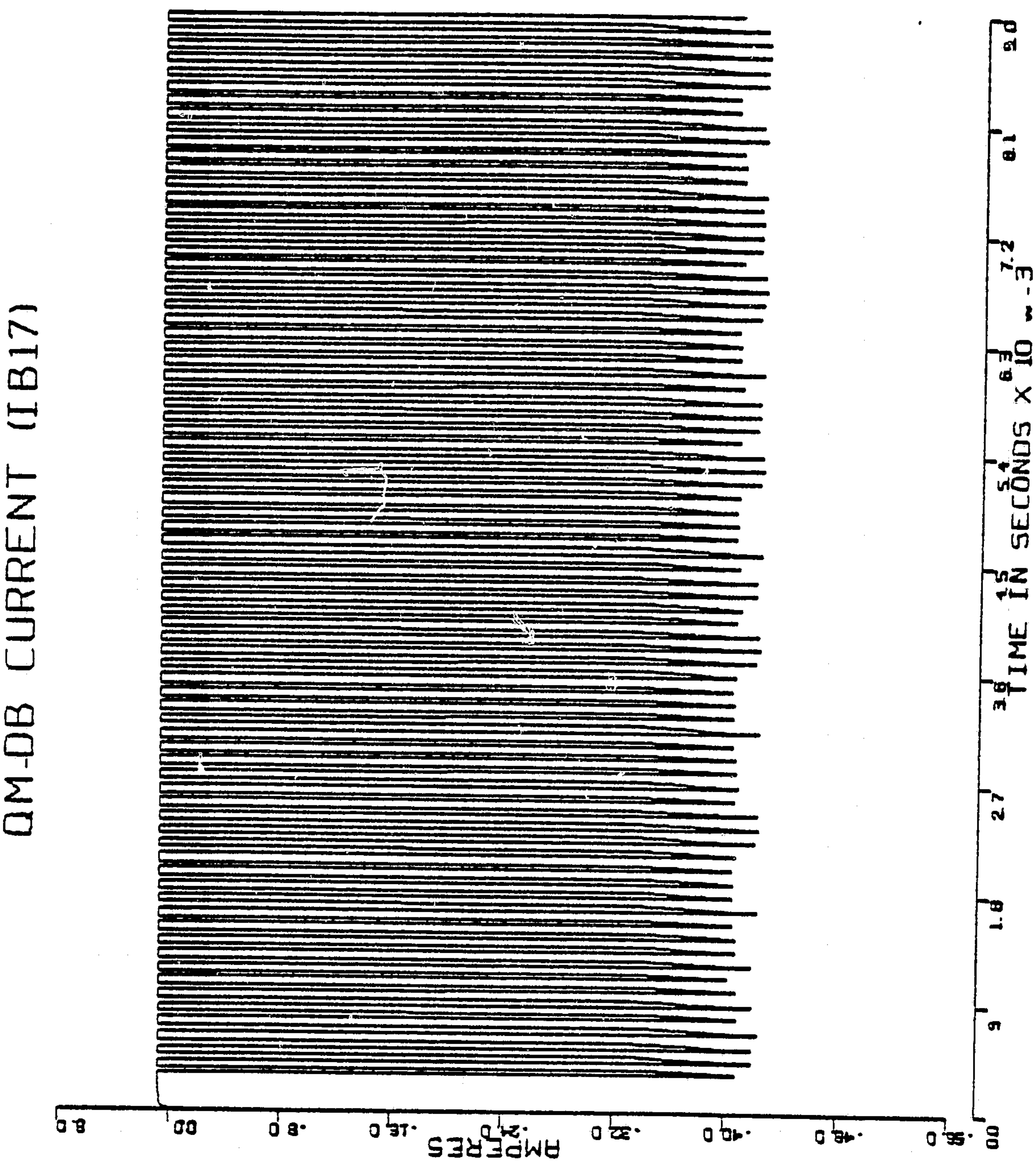

QM-DB CURRENT (IB17)
TIME IN SECONDS X 10 ** -3
0.0
.9
1.8
2.7
3.6
4.5
5.4
6.3
7.2
8.1
9.0
AMPERES
-56.0
-48.0
-40.0
-32.0
-24.0
-16.0
-8.0
0.0
8.0

Figure B.1-13

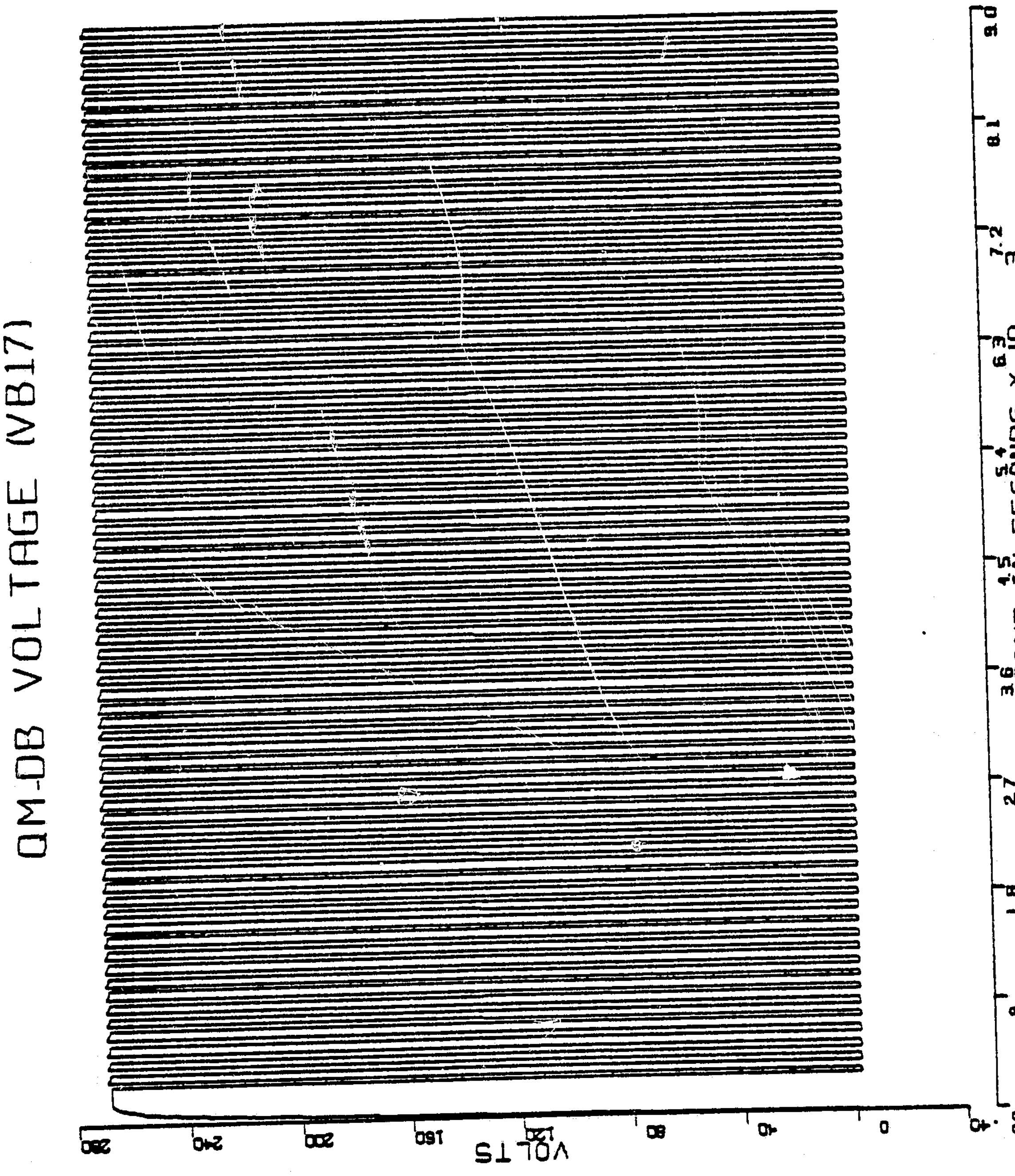
QM-DB VOLTAGE (VB17)
TIME IN SECONDS X 10 ** -3
VOLTS
0.0
.9
1.8
2.7
3.6
4.5
5.4
6.3
7.2
8.1
9.0
-40
0
40
80
120
160
200
240
280

Figure B.1-14

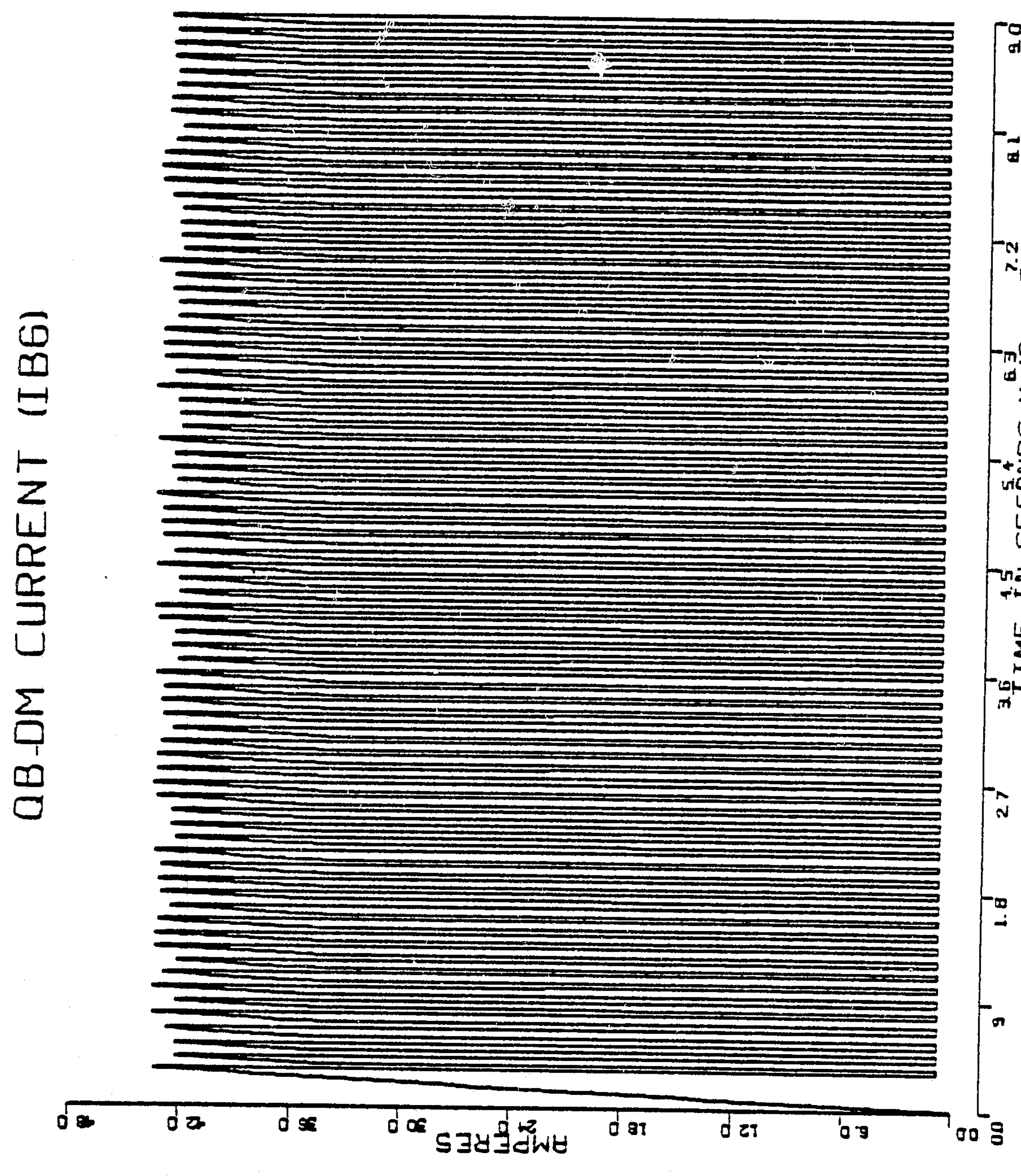
QB-DM CURRENT (IB6)
TIME IN SECONDS X 10 ** -3
AMPERES
0.0
.9
1.8
2.7
3.6
4.5
5.4
6.3
7.2
8.1
9.0
0.0
6.0
12.0
18.0
24.0
30.0
36.0
42.0
48.0

Figure B.1-15

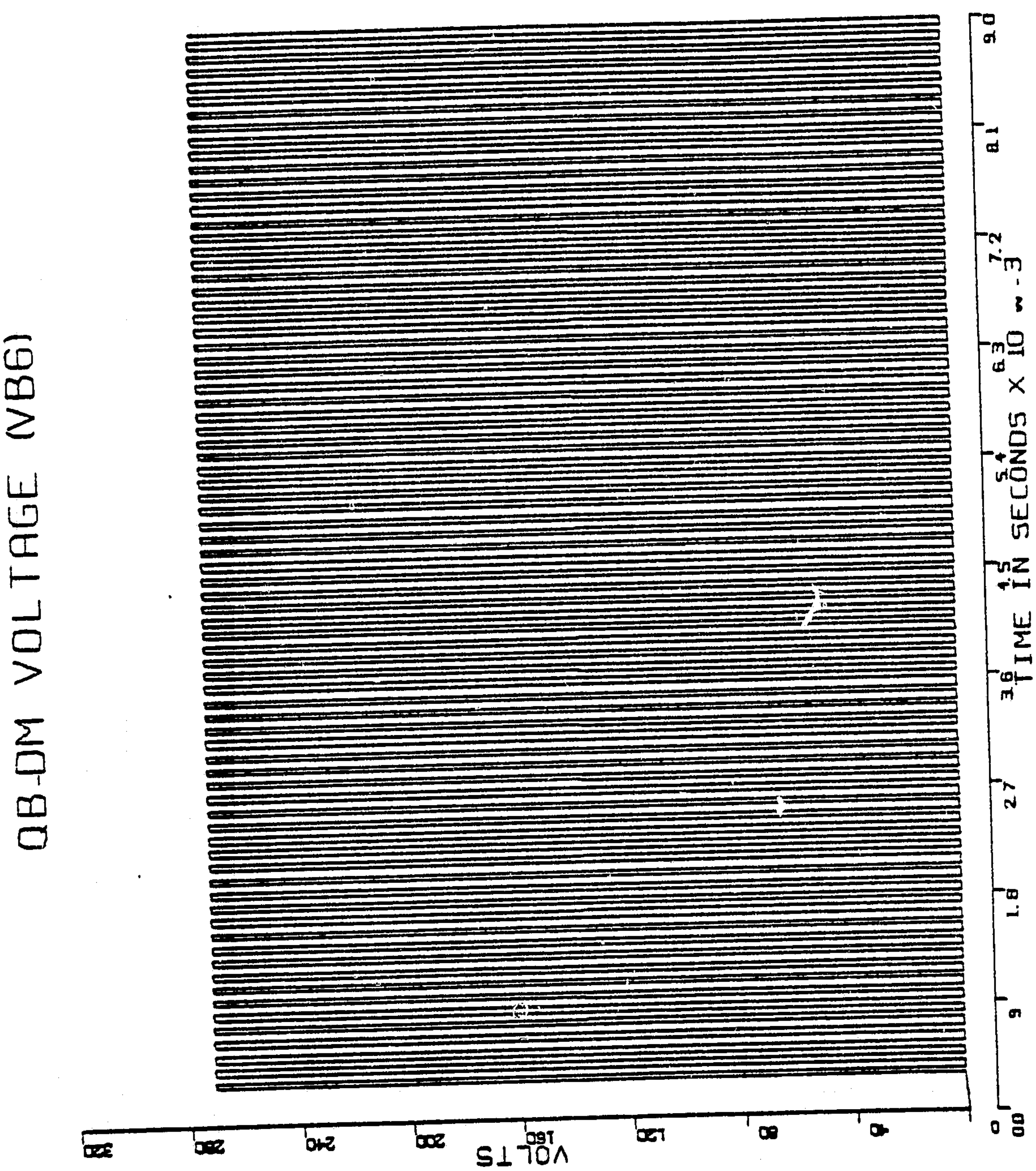
QB-DM VOLTAGE (VB6)
TIME IN SECONDS X 10 ** -3
VOLTS
0.0
.9
1.8
2.7
3.6
4.5
5.4
6.3
7.2
8.1
9.0
40
80
120
160
200
240
280
320

Figure B.1-16

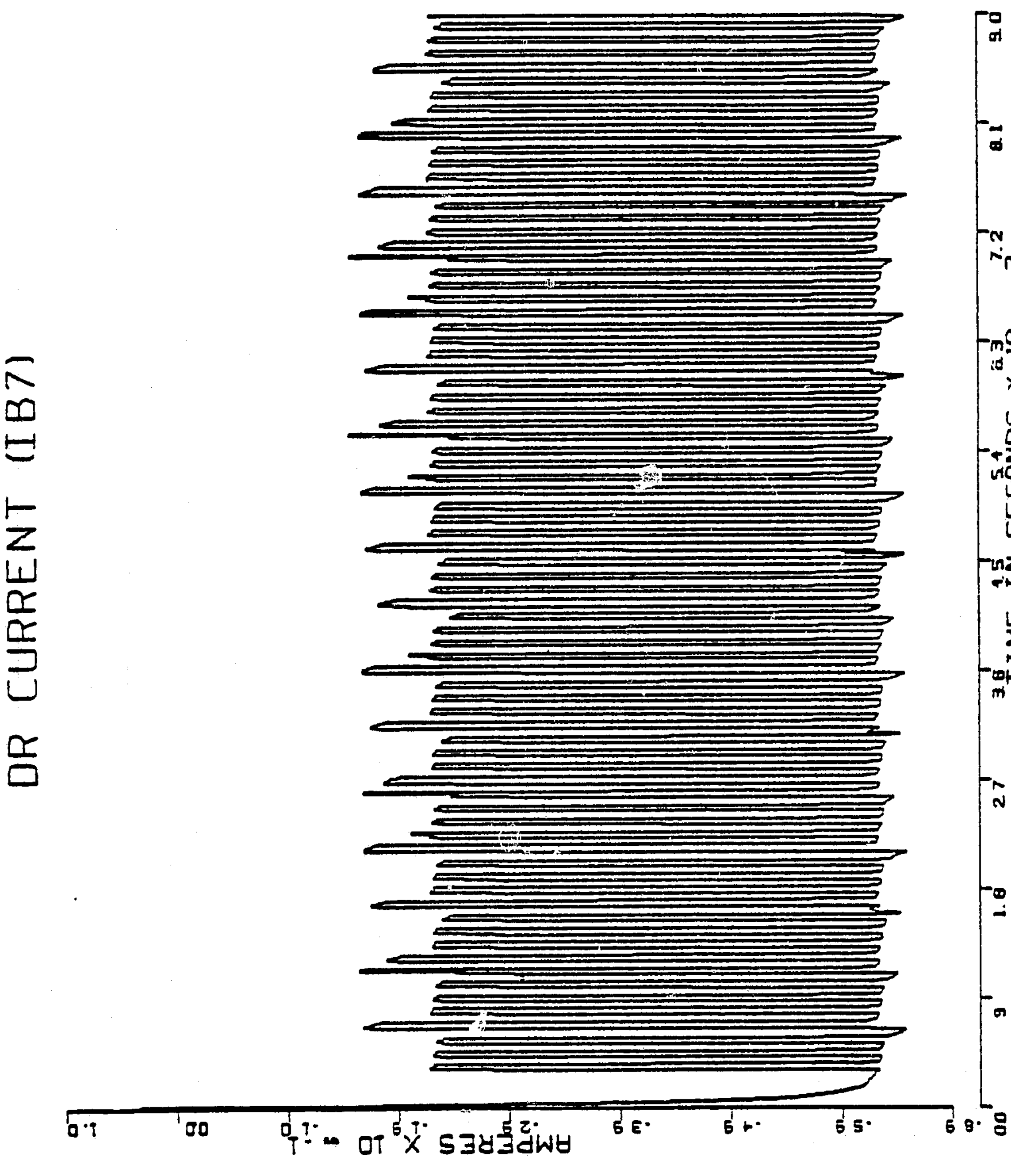
DR CURRENT (IB7)
TIME IN SECONDS X 10 ** -3
0.0
.9
1.8
2.7
3.6
4.5
5.4
6.3
7.2
8.1
9.0
AMPERES X 10 ** -1

Figure B.1-17

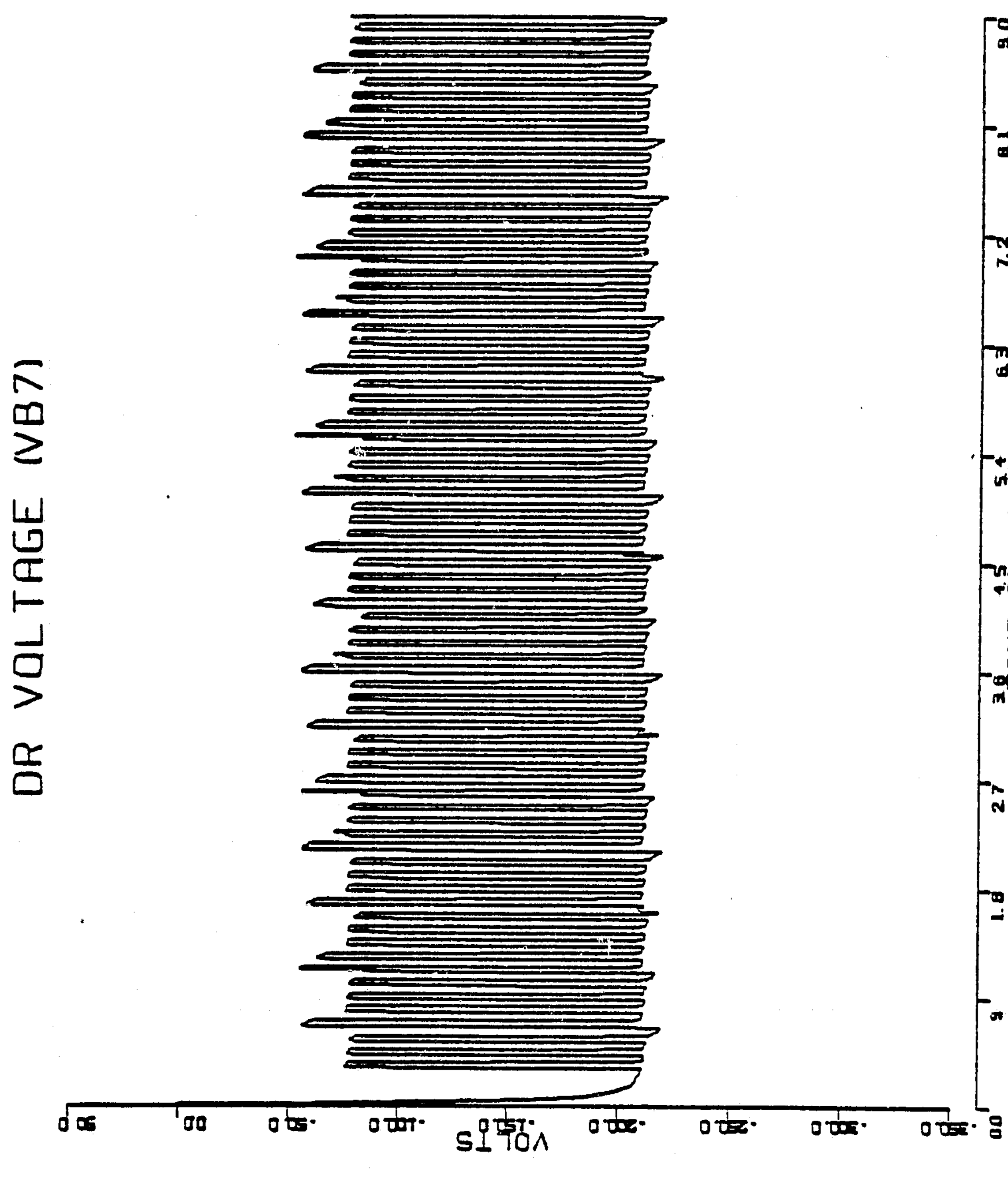
DR VOLTAGE (VB7)
TIME IN SECONDS X 10 ** -3
VOLTS
0.0
.9
1.8
2.7
3.6
4.5
5.4
6.3
7.2
8.1
9.0

Figure B.1-18

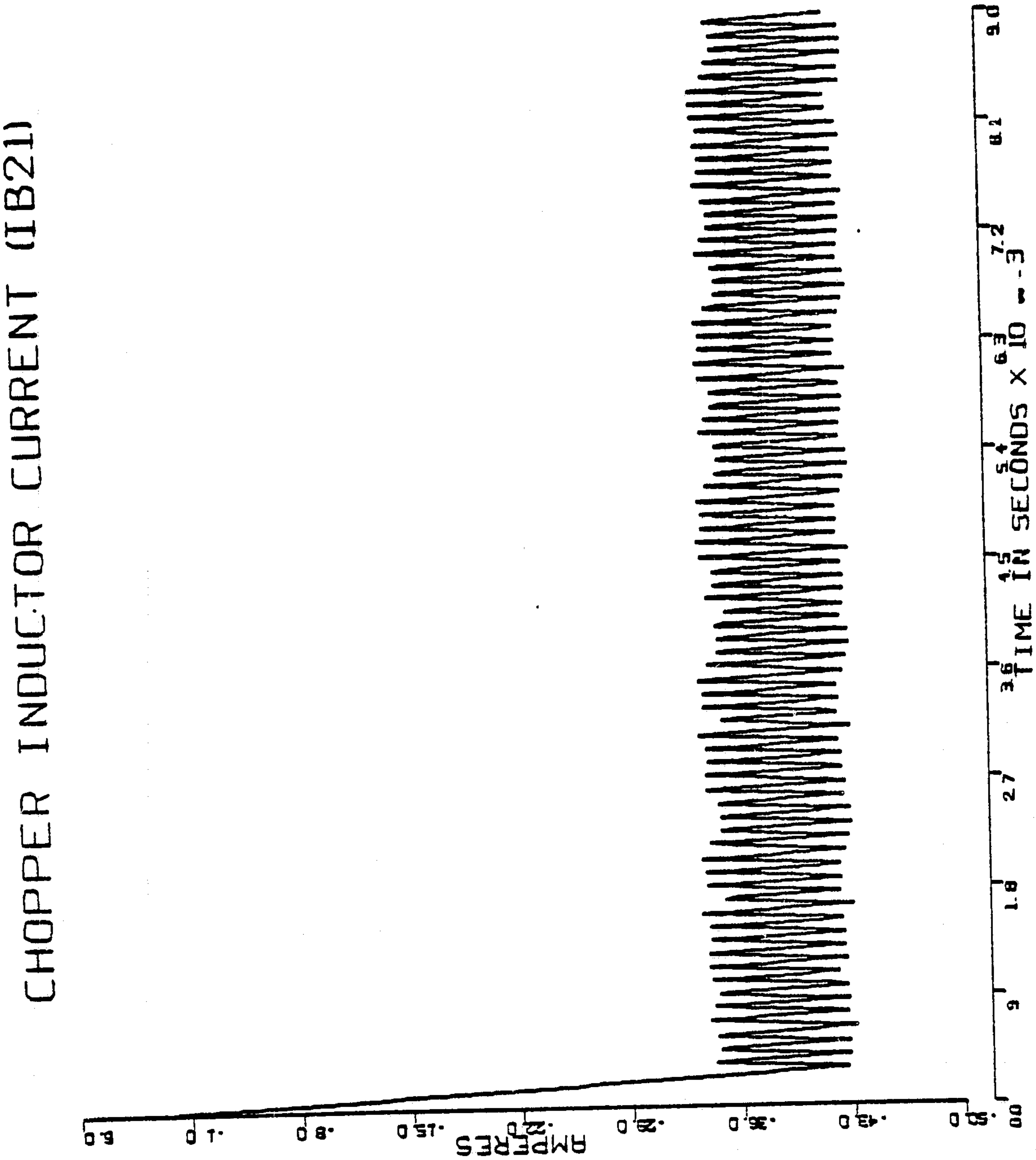
CHOPPER INDUCTOR CURRENT (IB21)
TIME IN SECONDS X 10 ** -3
AMPERES

Figure B.1-19

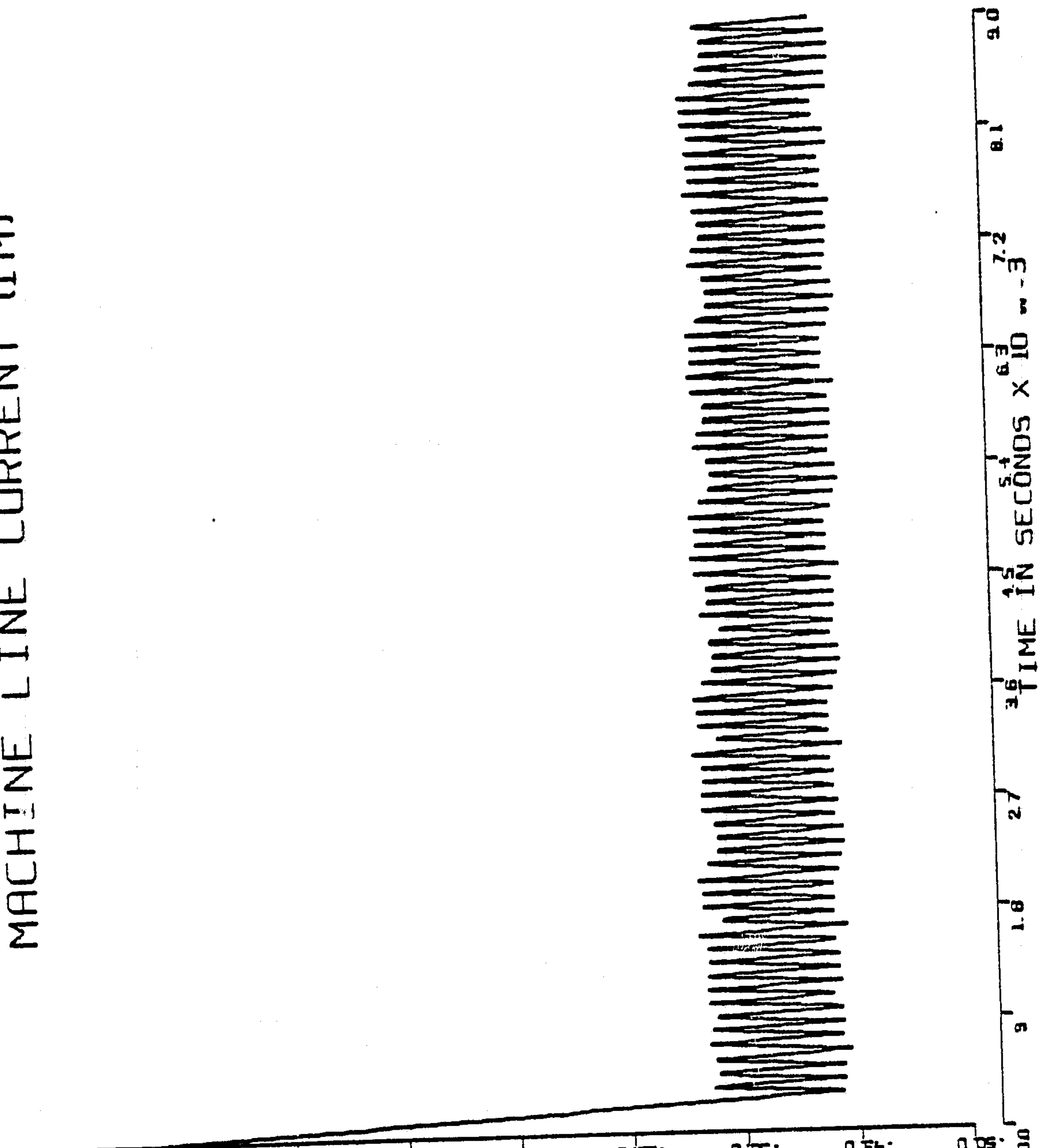
MACHINE LINE CURRENT (IM)
TIME IN SECONDS x 10 ** -3
AMPERES
0.0
.9
1.8
2.7
3.6
4.5
5.4
6.3
7.2
8.1
9.0
-50.0
-43.0
-36.0
-29.0
-22.0
-15.0
-8.0
-1.0
6.0

Figure B.1-20

APPENDIX C.1 CALCOMP PLOTS: PLUGGING 240 rpm 30° ADVANCE

RUN SUMMARY

MODE: PLUGGING

PROGRAM MODE: PGMODE = 1

CURRENT COMMAND: ICMD - 32.0 amps

TIME STEP: TSNET = 10 μs

COMMUTATION SHIFT: SHIFT = 0.0 mech rad, 0.0 mech deg

CURRENT THRESHOLD: ITOL = 4.0

ROTOR VELOCITY: (240 rpm), (24.13274 rad/sec)

TOTAL NUMBER OF POINTS PLOTTED: NREC = 801

TOTAL NUMBER OF NETWORK CHANGES: NNETSW = 360

TOTAL NUMBER OF INTEGRATIONS: NUMINT = 8000

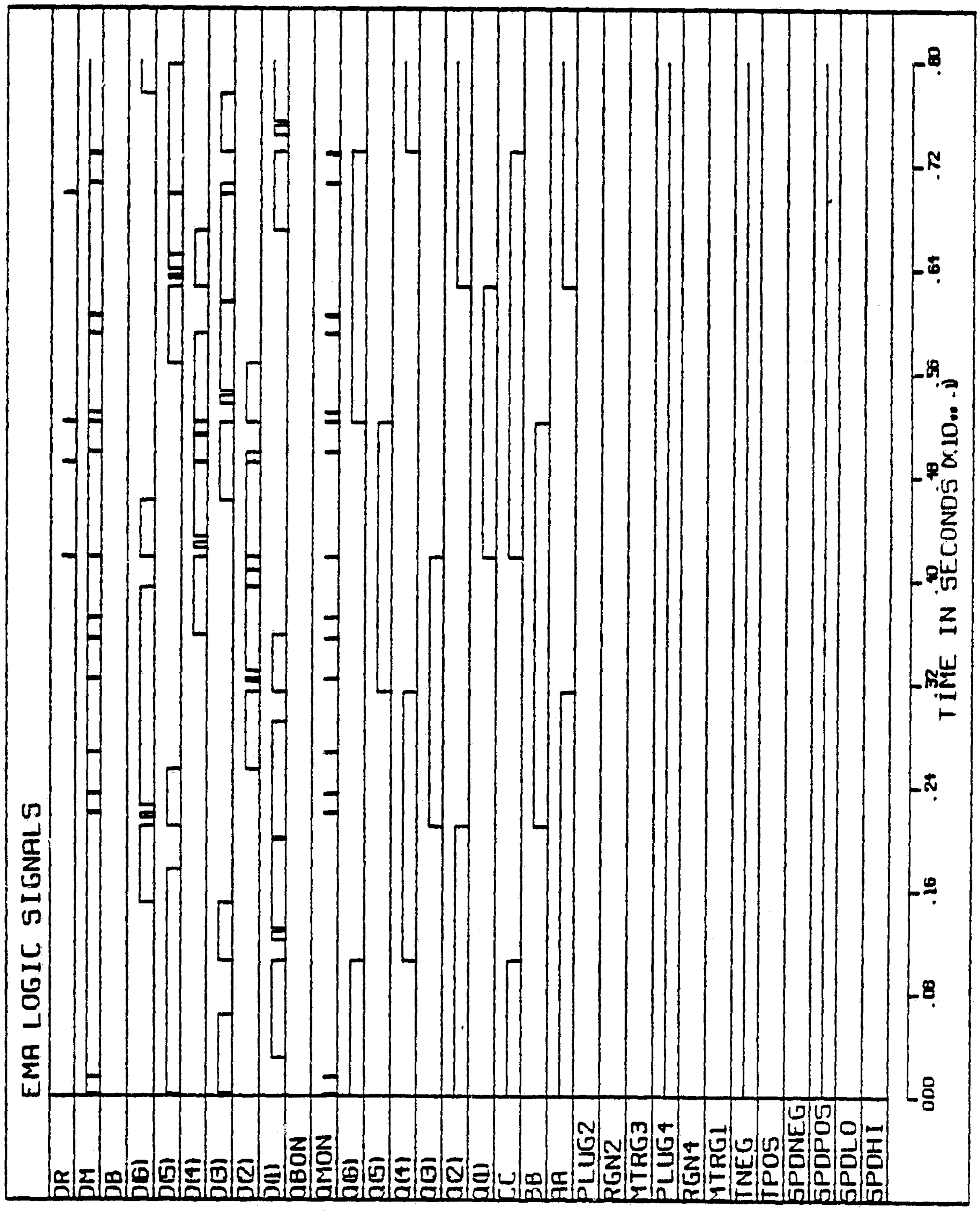
EMA LOGIC SIGNALS
TIME IN SECONDS (X10** 1)
.000
.08
.16
.24
.32
.40
.48
.56
.64
.72
.80

Figure C.1-1

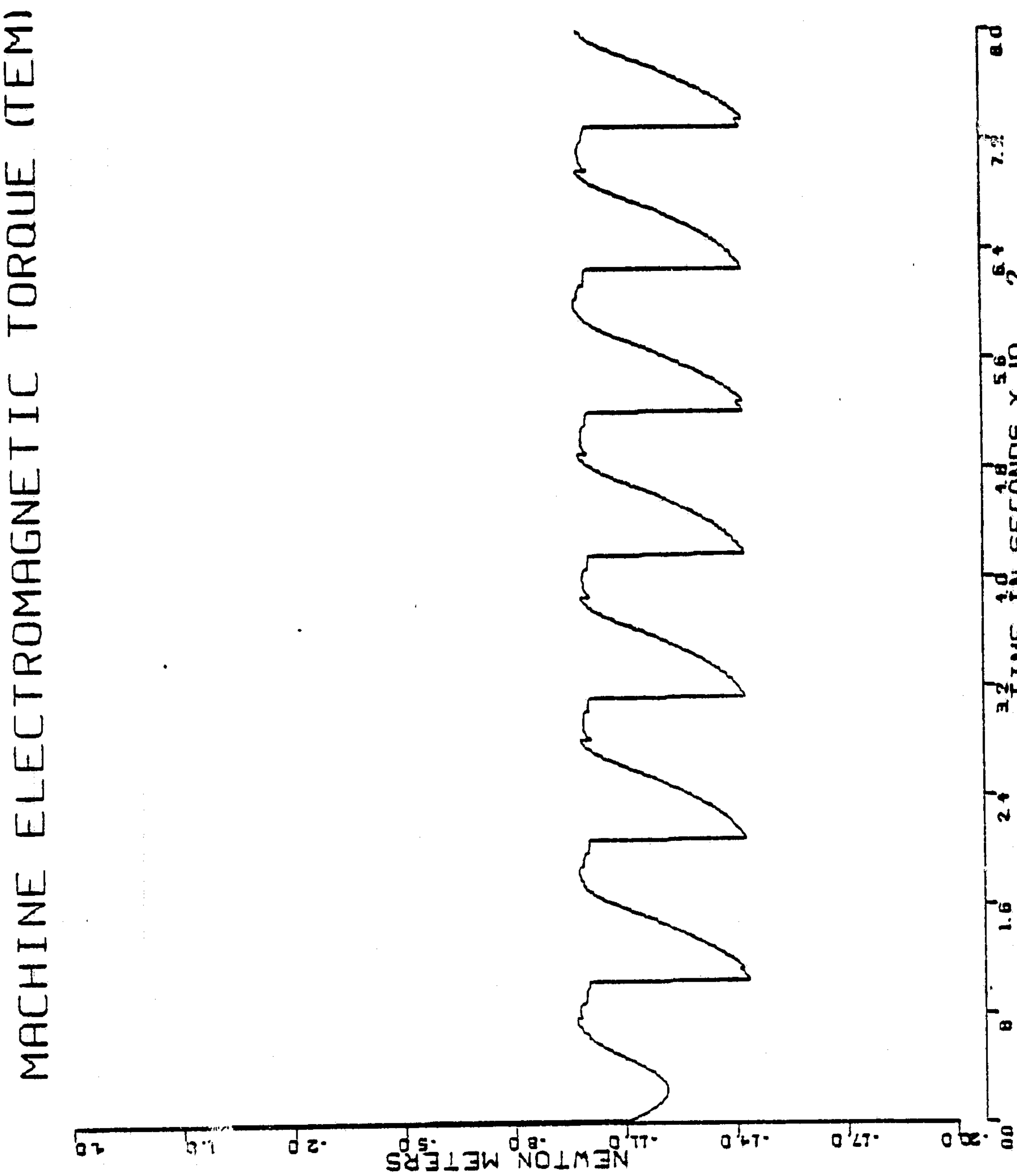
MACHINE ELECTROMAGNETIC TORQUE (TEM)
TIME IN SECONDS X 10 ** -2
NEWTON METERS

Figure C.1-2

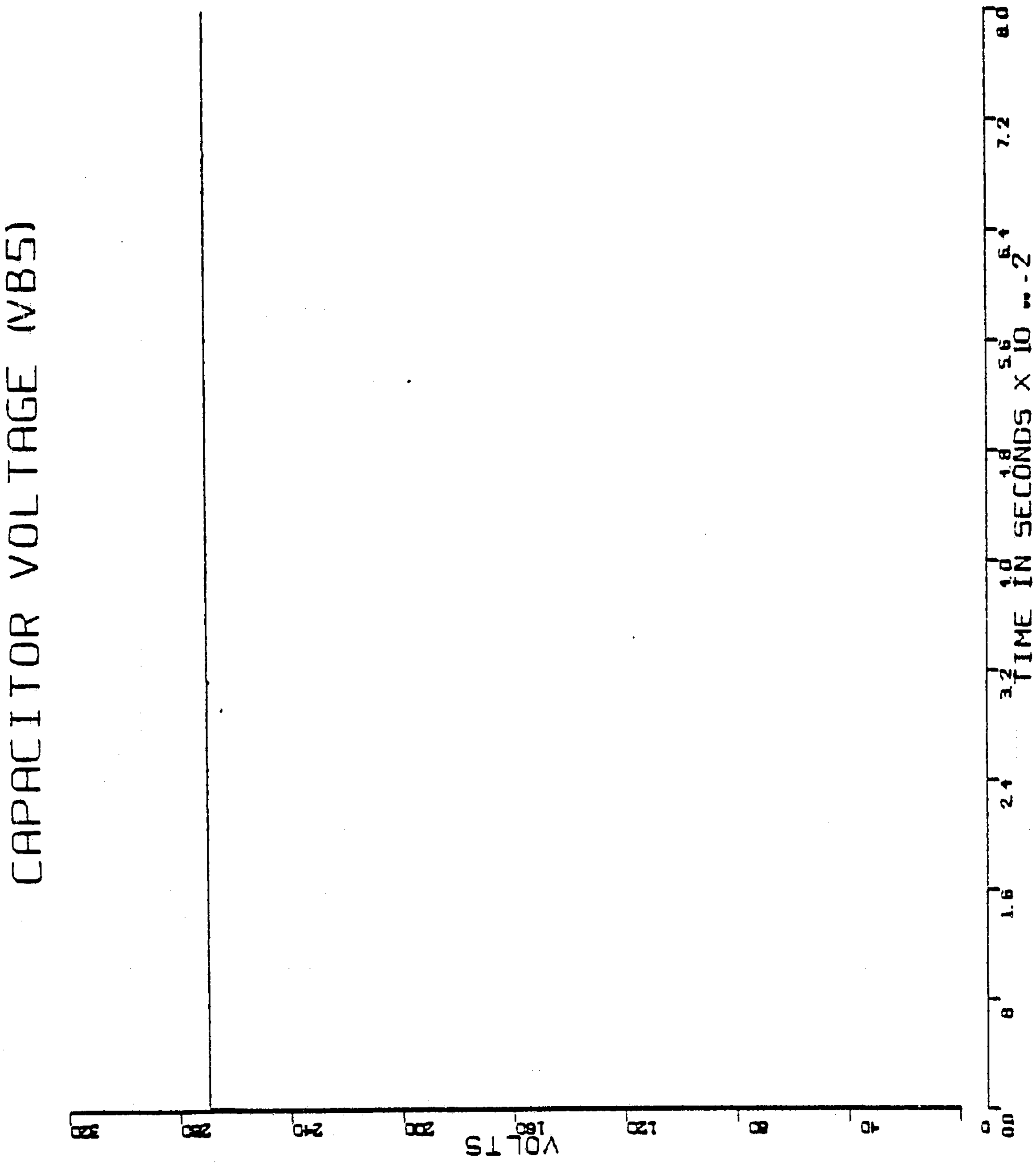

Figure C.1-3

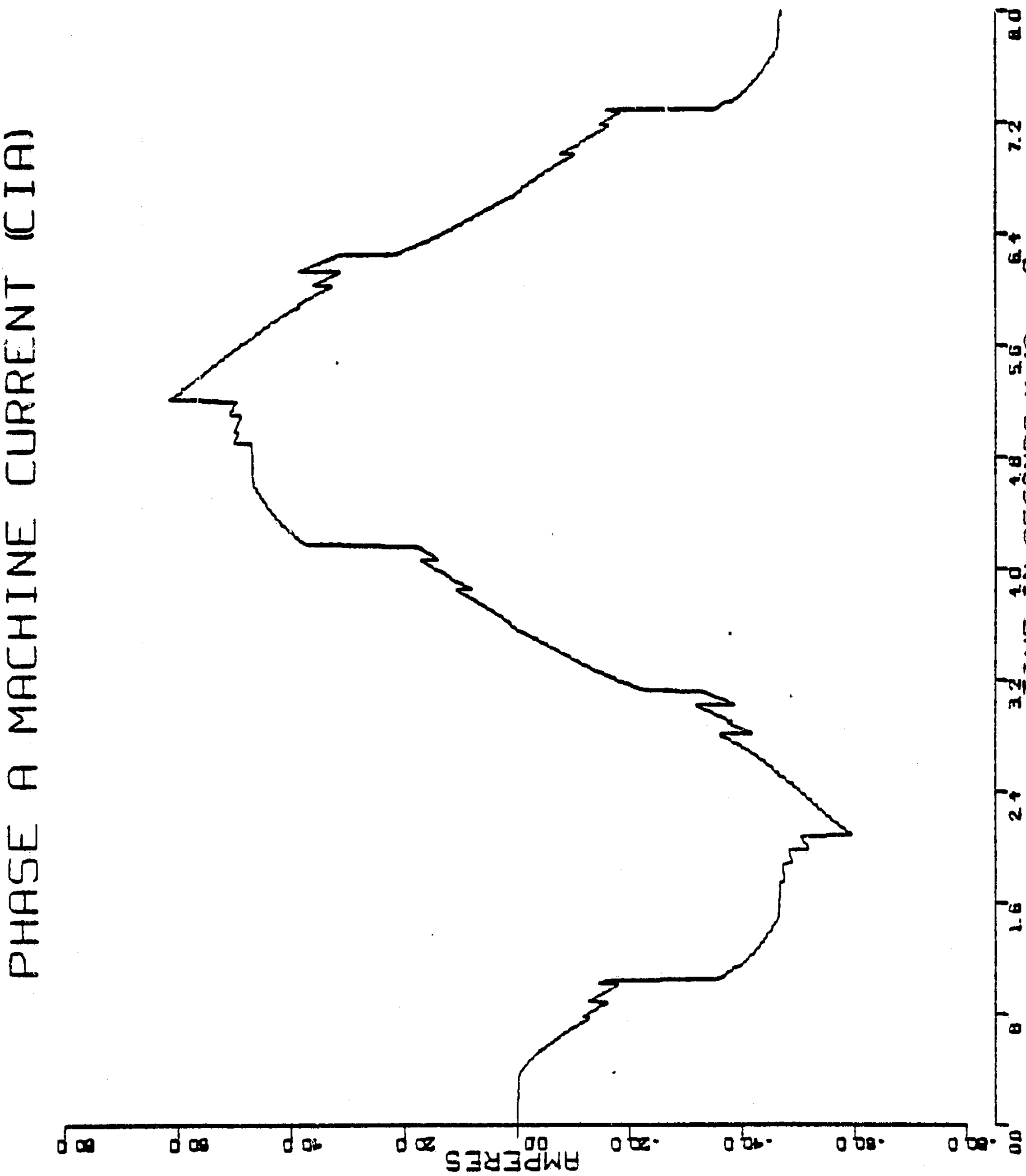

Figure C.1-4

C-2

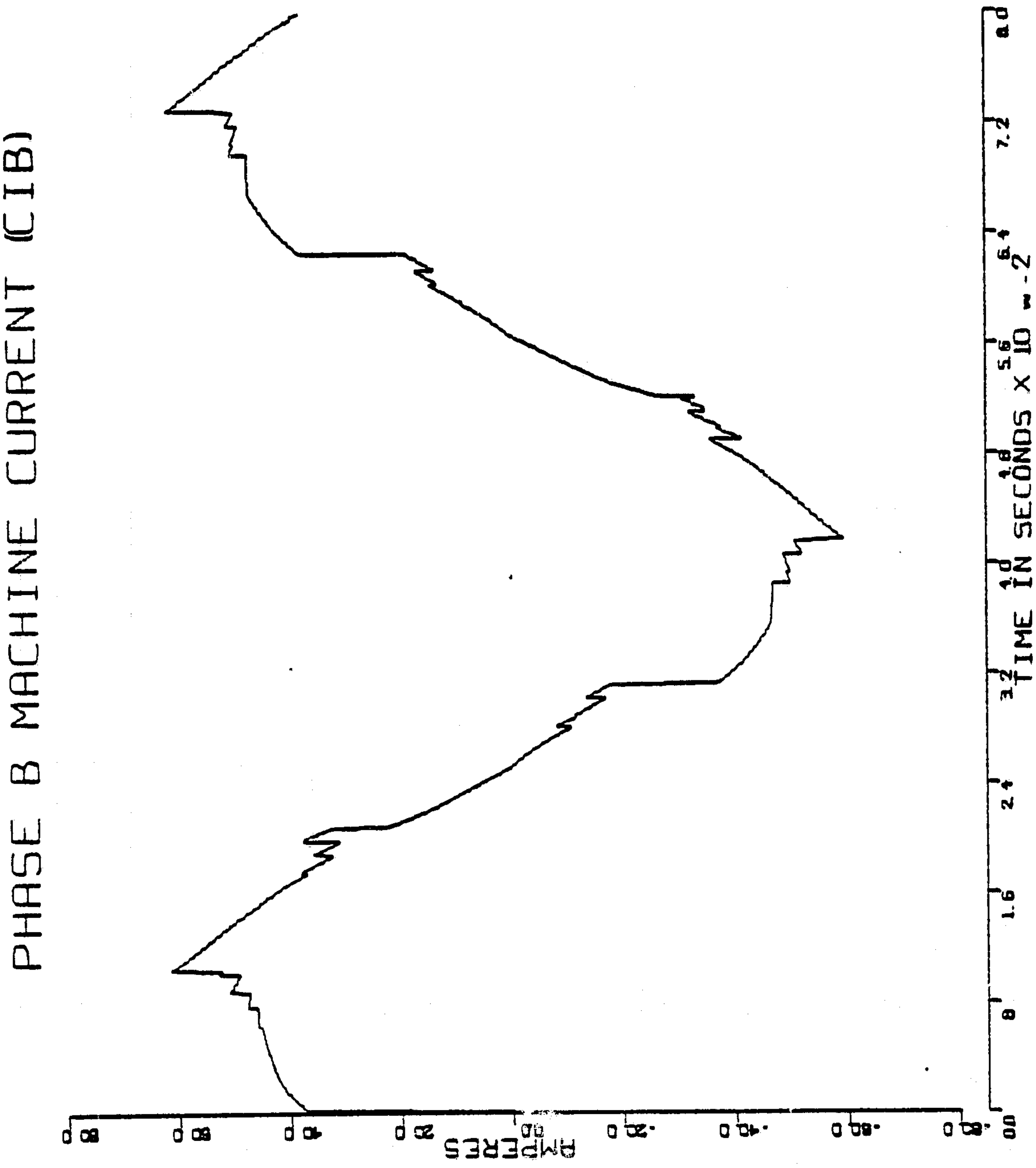
PHASE B MACHINE CURRENT (CIB)
TIME IN SECONDS × 10 ** -2
AMPERES
0.0 .8 1.6 2.4 3.2 4.0 4.8 5.6 6.4 7.2 8.0
-80.0 -60.0 -40.0 -20.0 0.0 20.0 40.0 60.0 80.0

Figure C.1-5

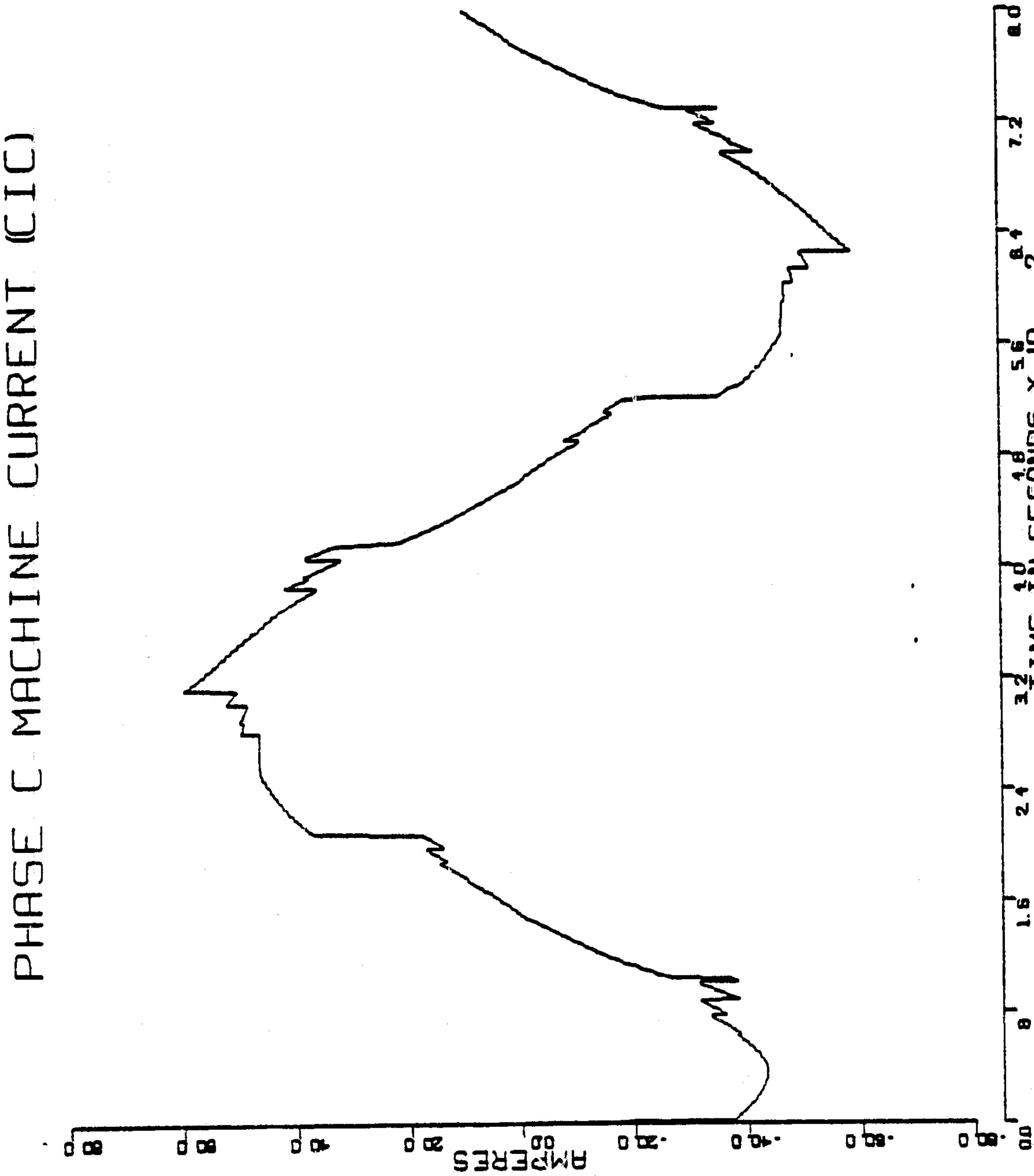

Figure C.1-6

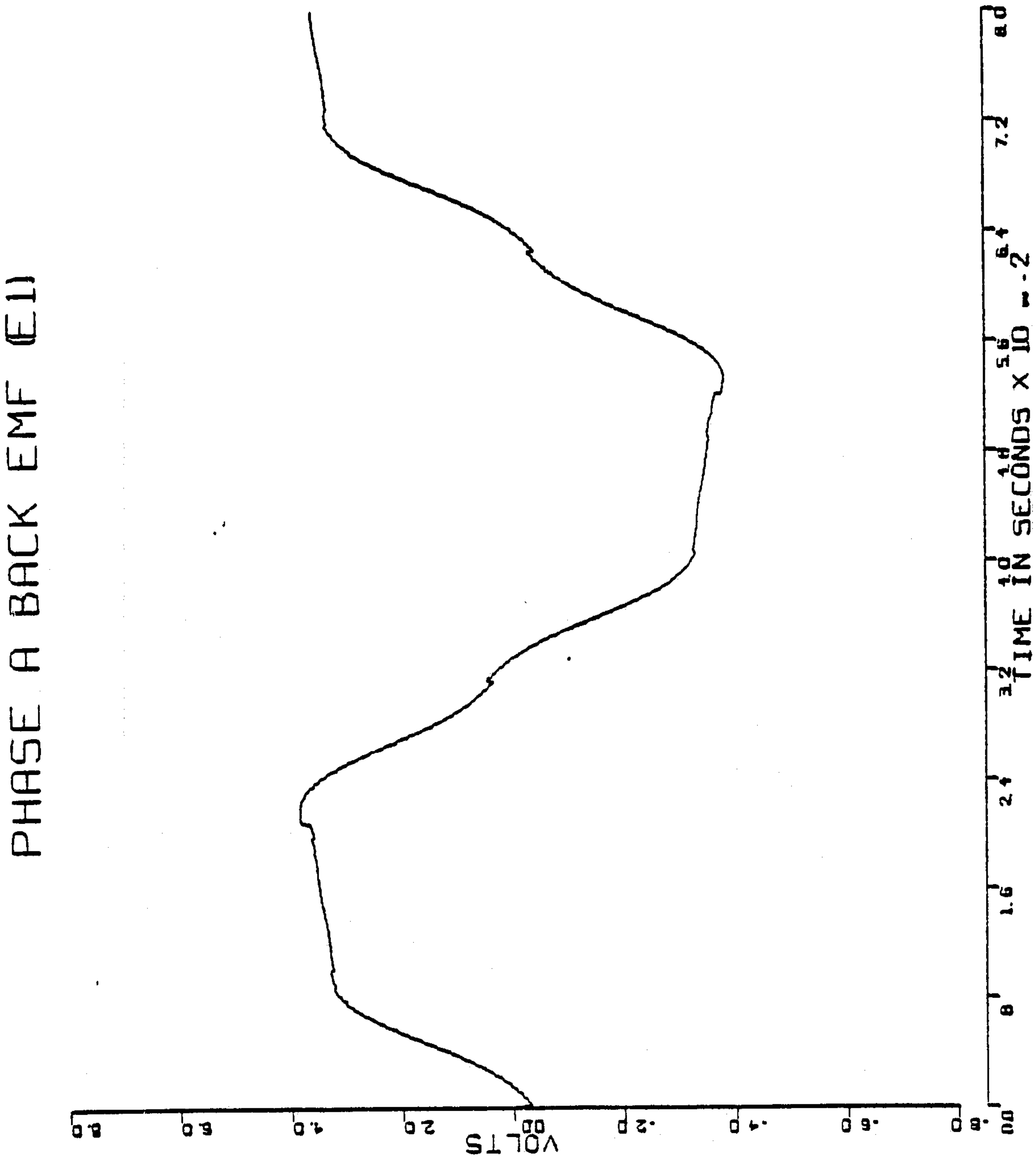

Figure C.1-7

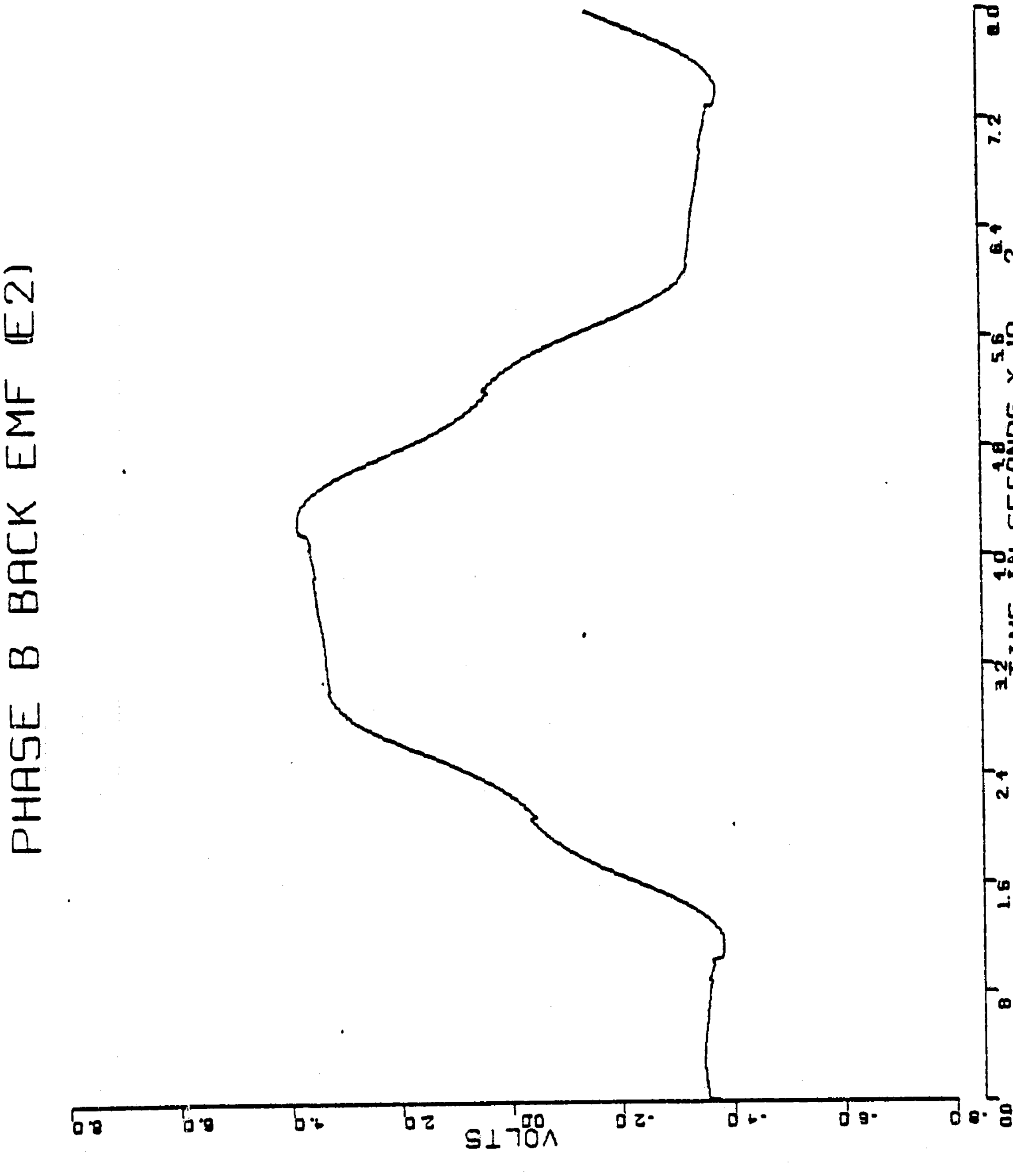

Figure C.1-8

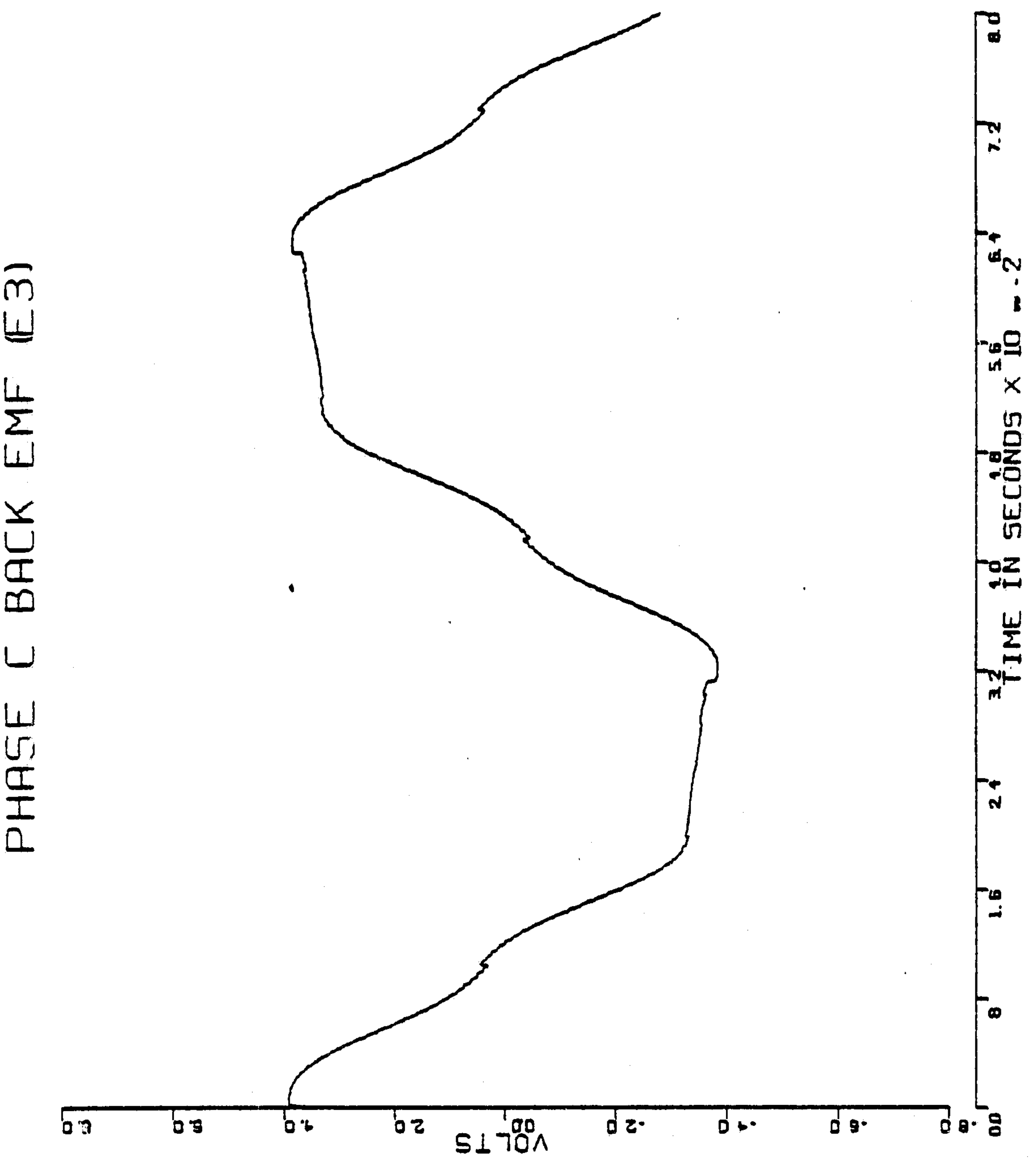

Figure C.1-9

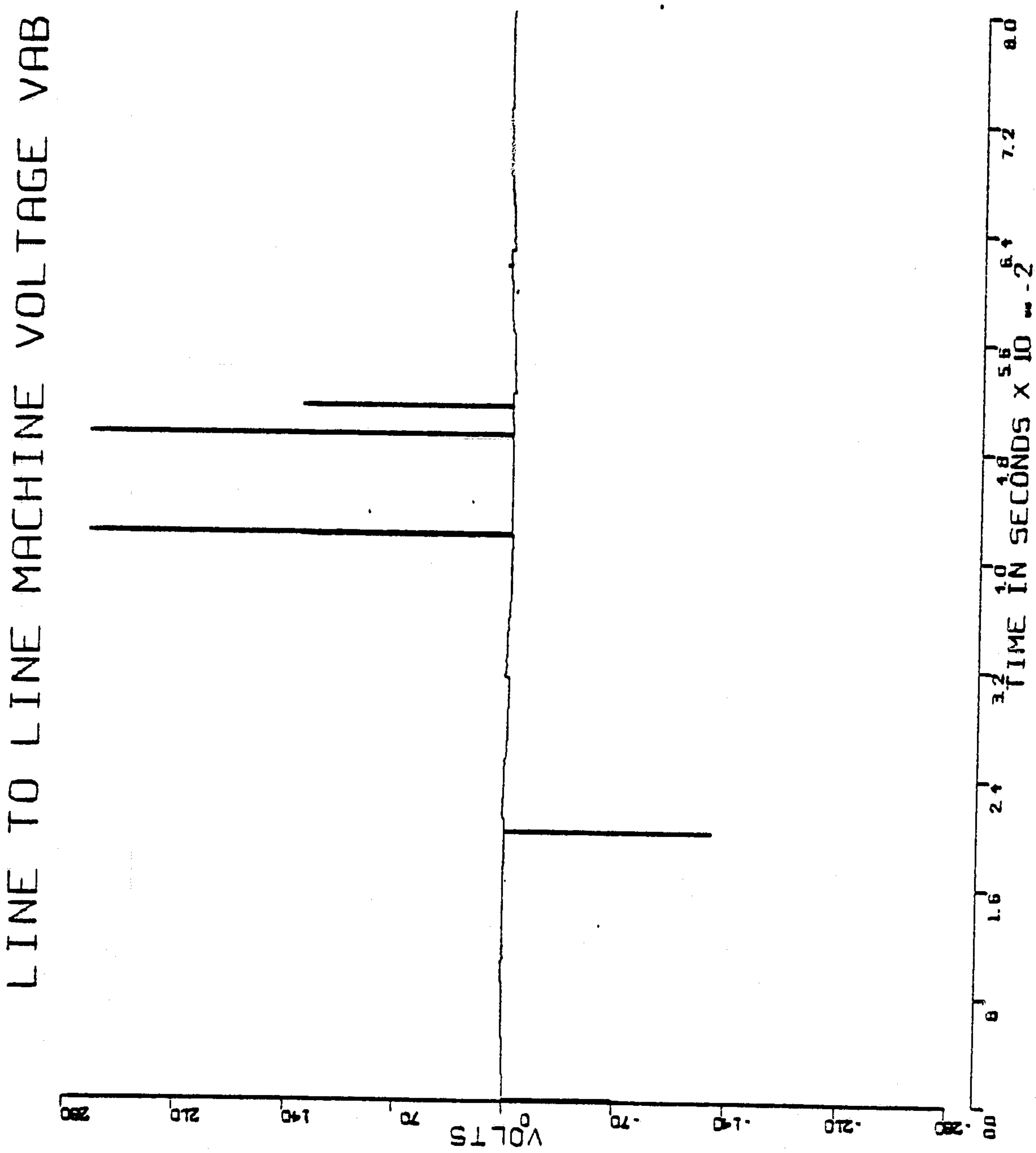

LINE TO LINE MACHINE VOLTAGE VAB
TIME IN SECONDS x 10 ** -2
VOLTS
0.0
.8
1.6
2.4
3.2
4.0
4.8
5.6
6.4
7.2
8.0
280
210
140
70
0
-70
-140
-210
-280

Figure C.1-10

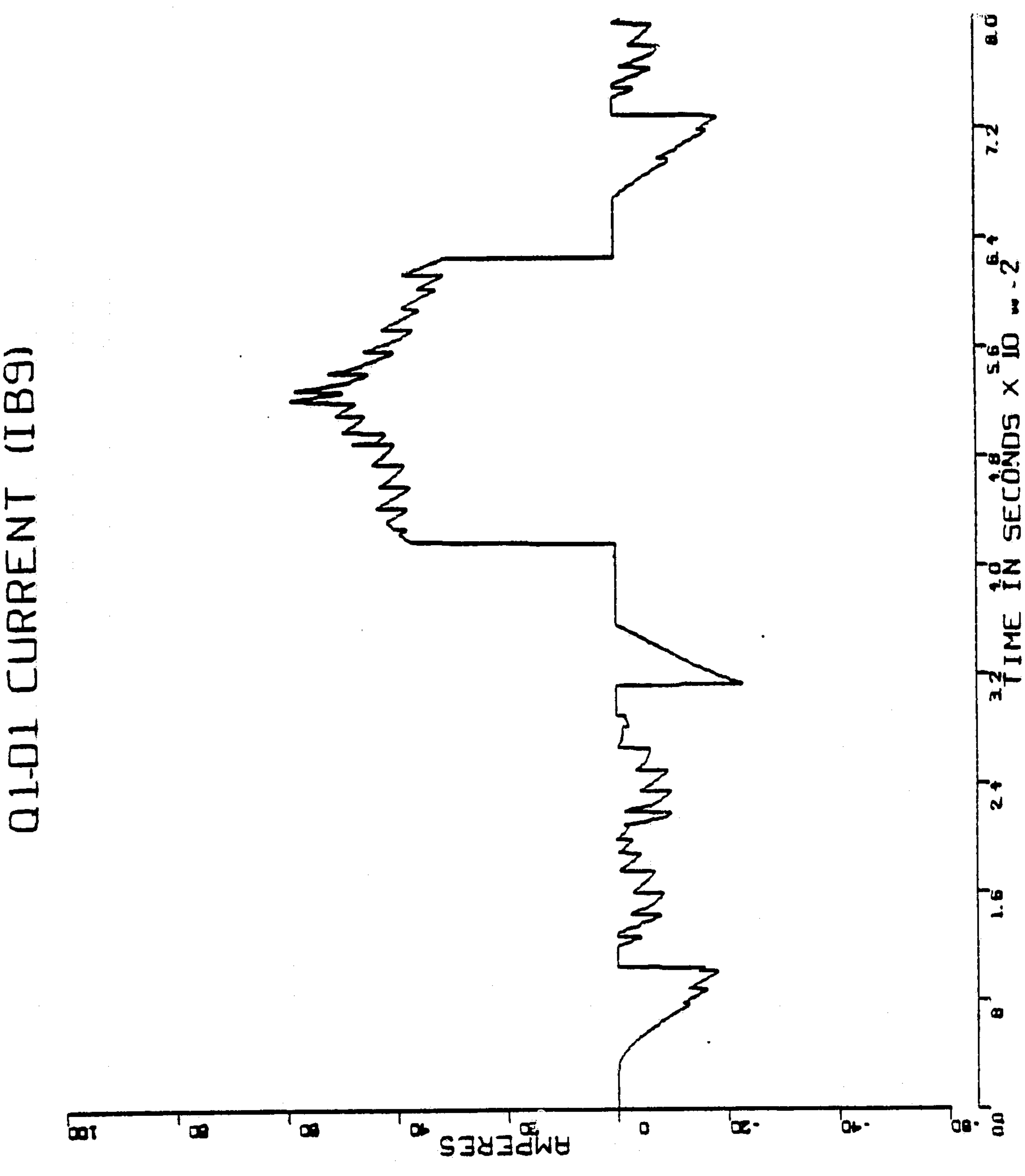

Figure C.1-11

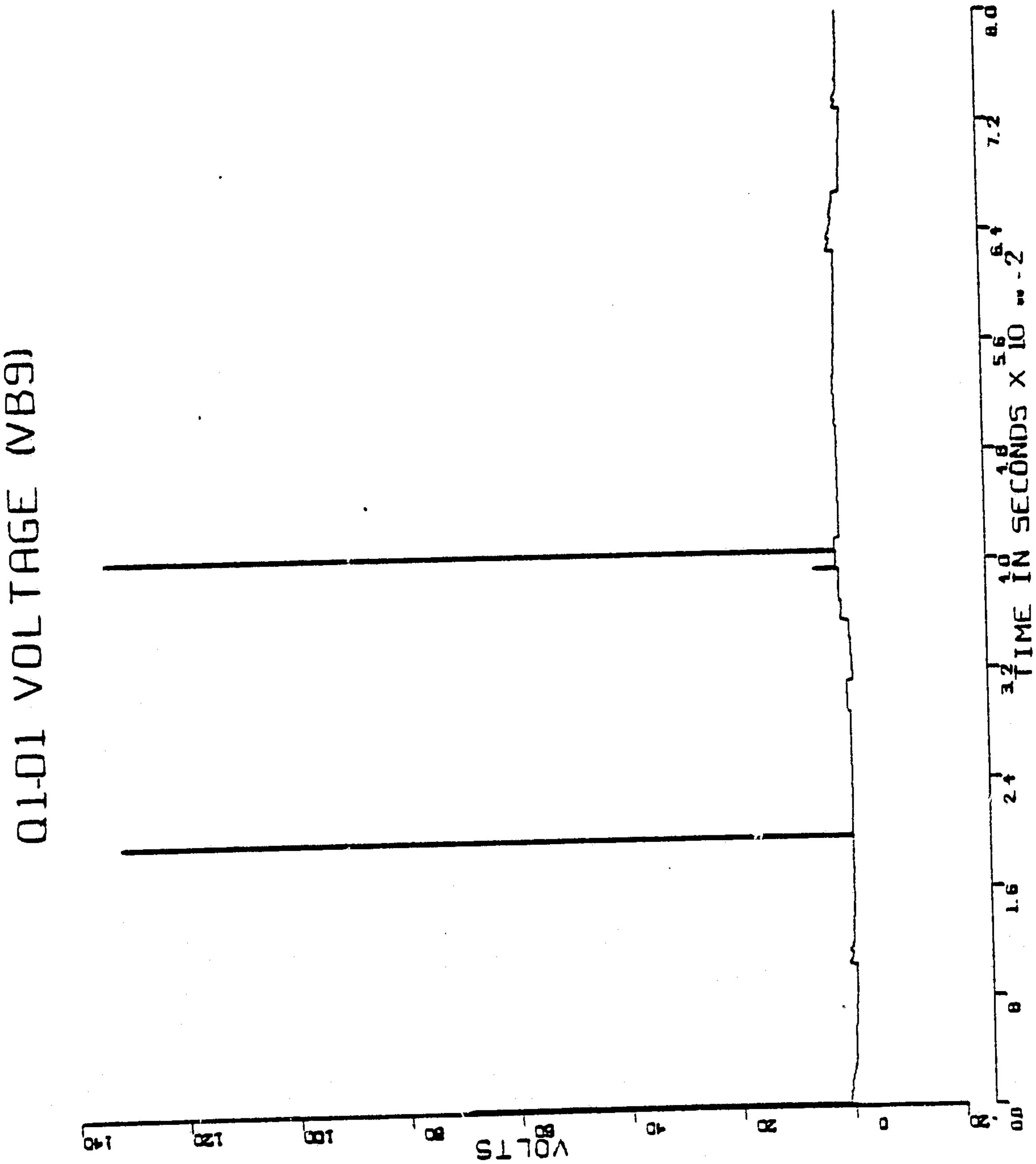
Q1-D1 VOLTAGE (VB9)
VOLTS
-20
0
20
40
60
80
100
120
140
TIME IN SECONDS X 10 ** -2
0.0
.8
1.6
2.4
3.2
4.0
4.8
5.6
6.4
7.2
8.0

Figure C.1-12

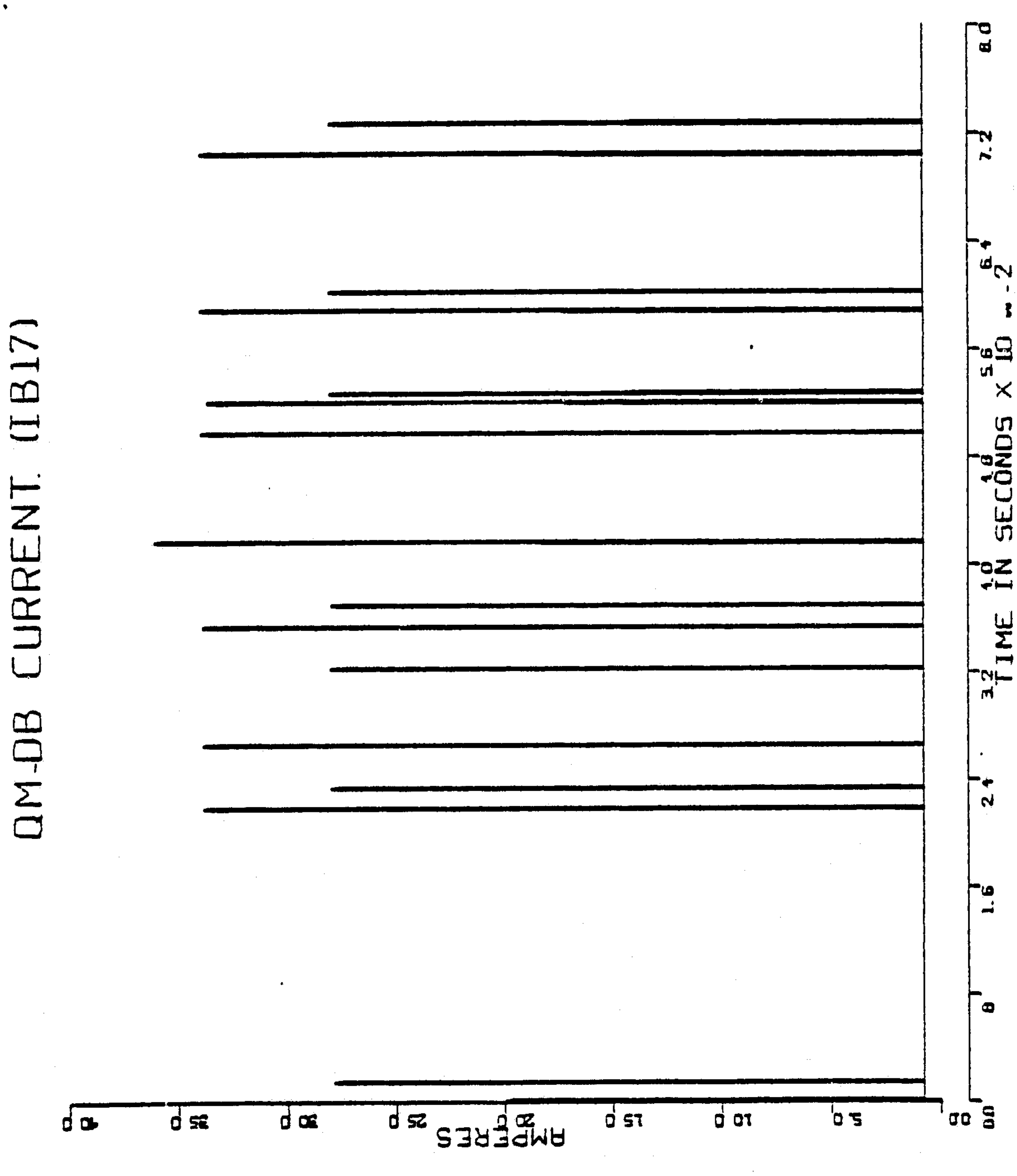

Figure C.1-13

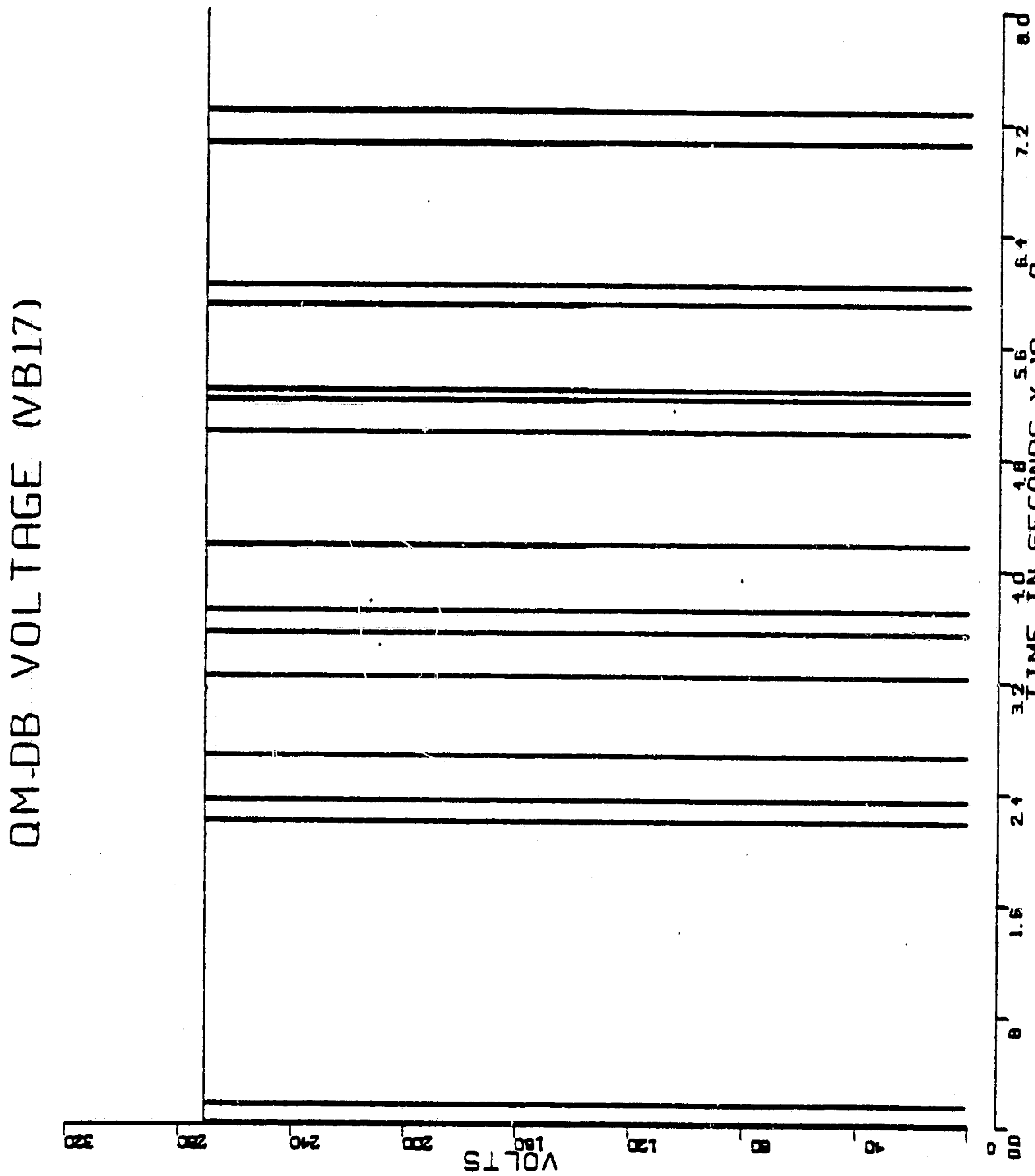
QM-DB VOLTAGE (VB17)
TIME IN SECONDS X 10 ** -2
VOLTS
0.0
0.8
1.6
2.4
3.2
4.0
4.8
5.6
6.4
7.2
8.0
0
40
80
120
160
200
240
280
320

Figure C.1-14

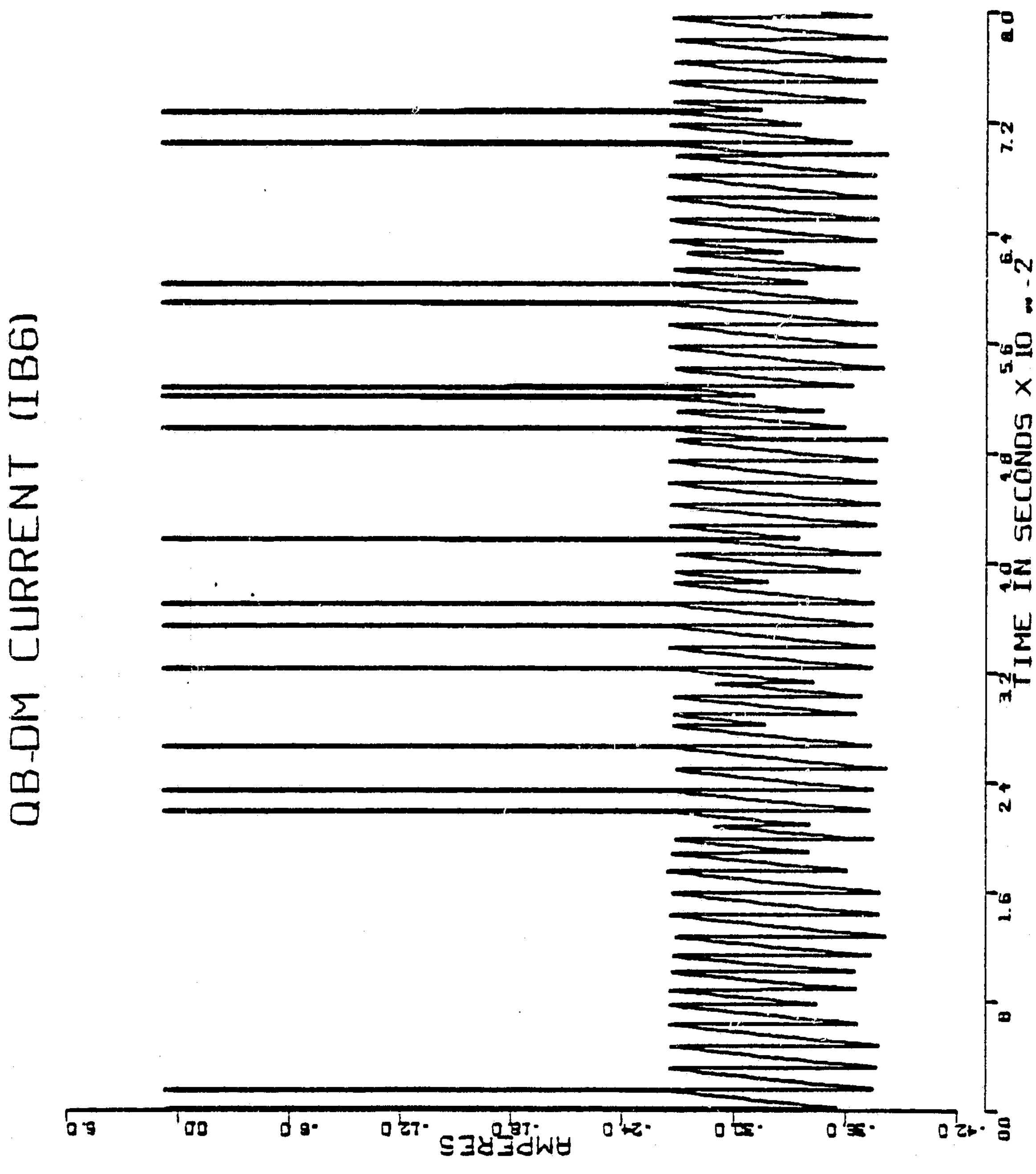

Figure C.1-15

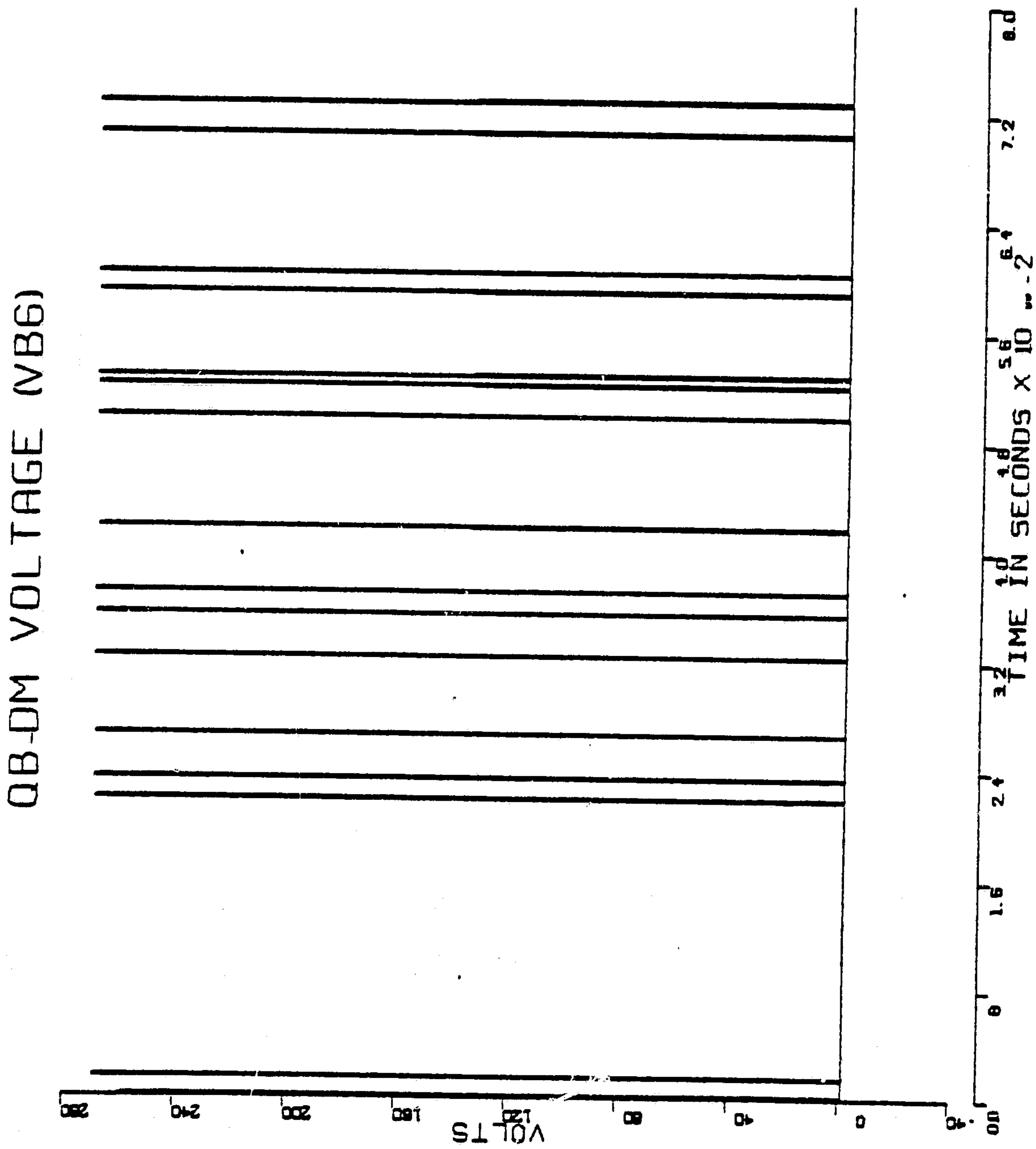
QB-DM VOLTAGE (VB6)
TIME IN SECONDS X 10 ** -2
VOLTS
0.0
0.8
1.6
2.4
3.2
4.0
4.8
5.6
6.4
7.2
8.0
-40
0
40
80
120
160
200
240
280

Figure C.1-16

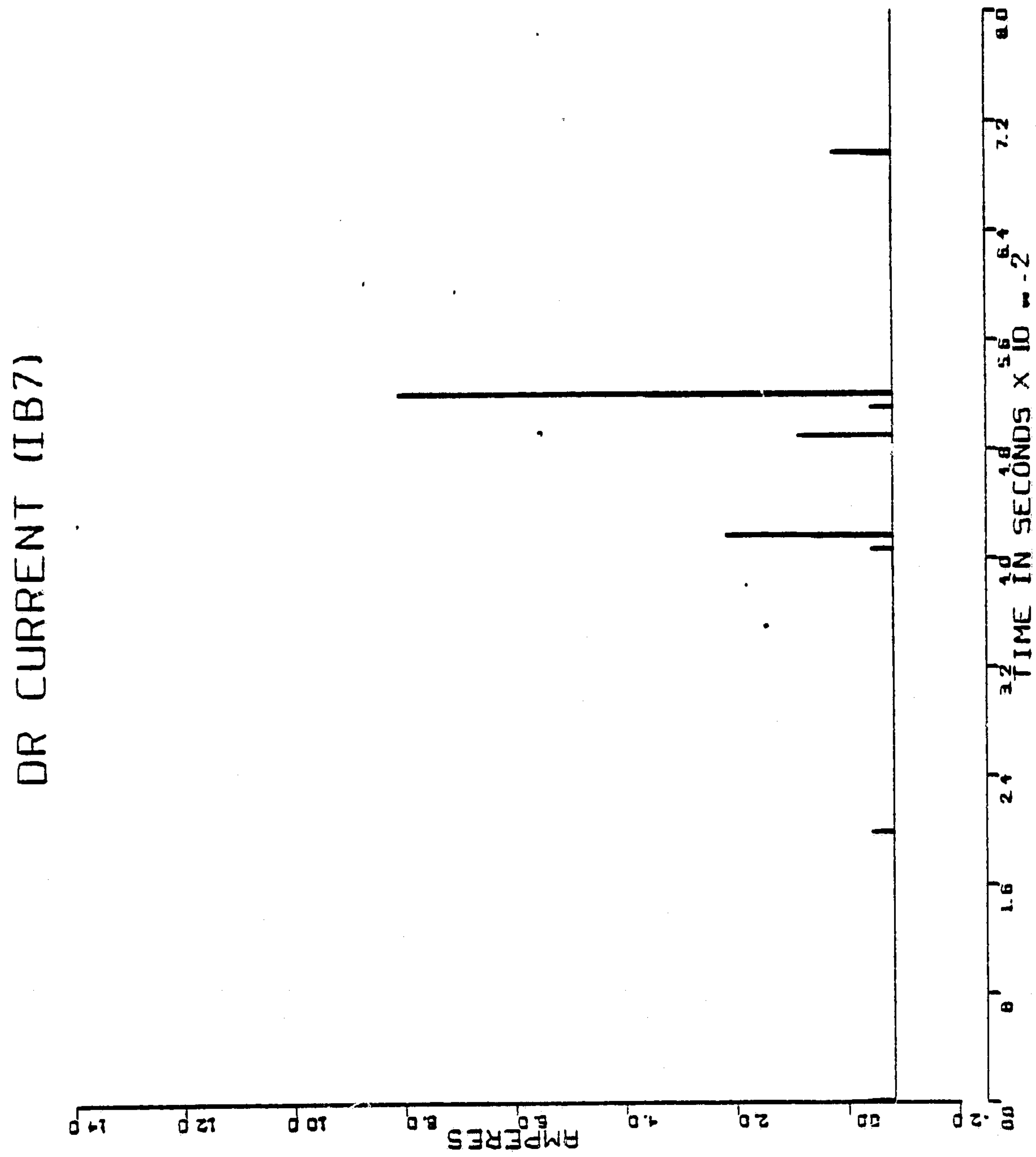

Figure C.1-17

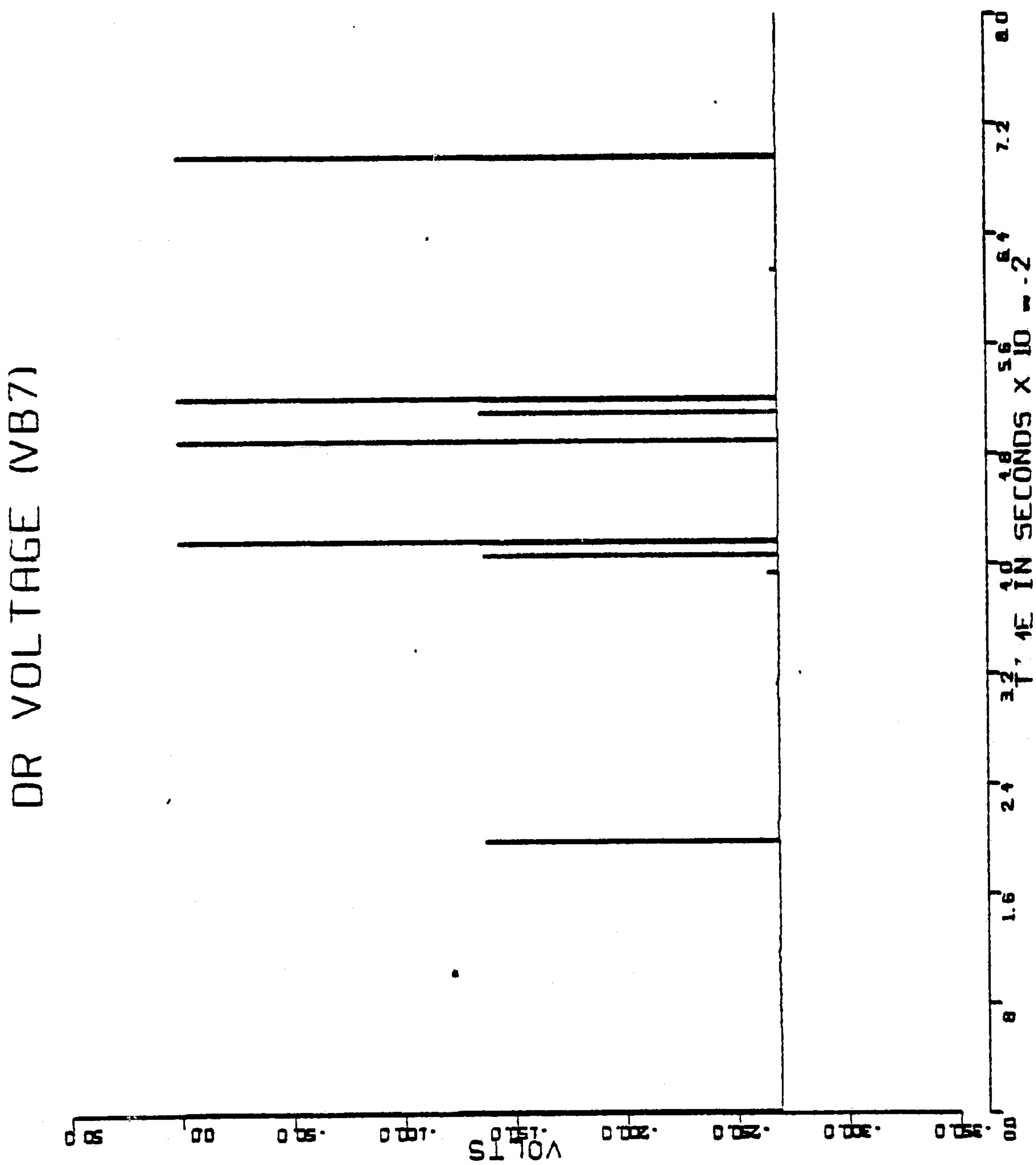

Figure C.1-18

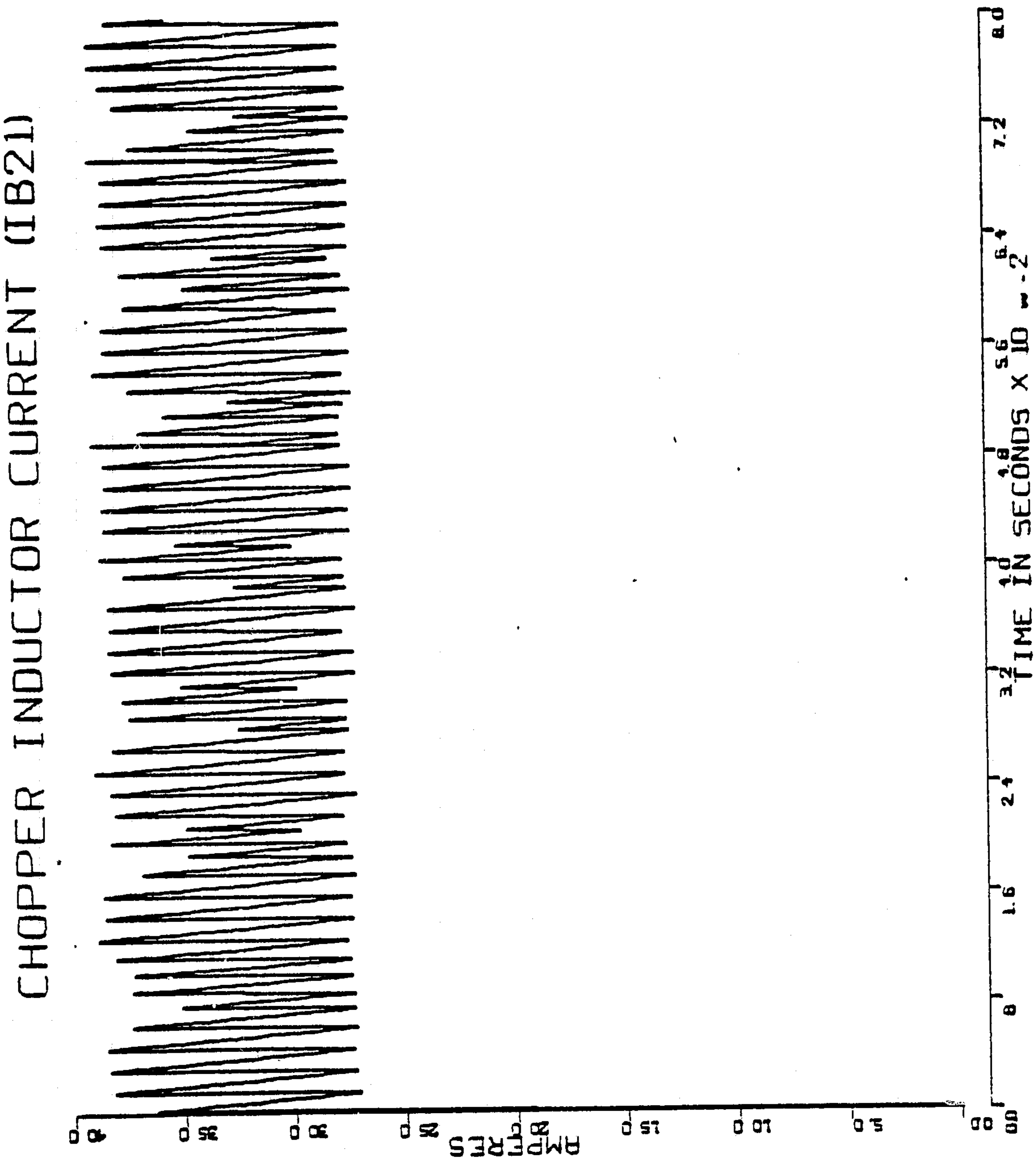
CHOPPER INDUCTOR CURRENT (IB21)
TIME IN SECONDS X 10 ** -2
AMPERES

Figure C.1-19

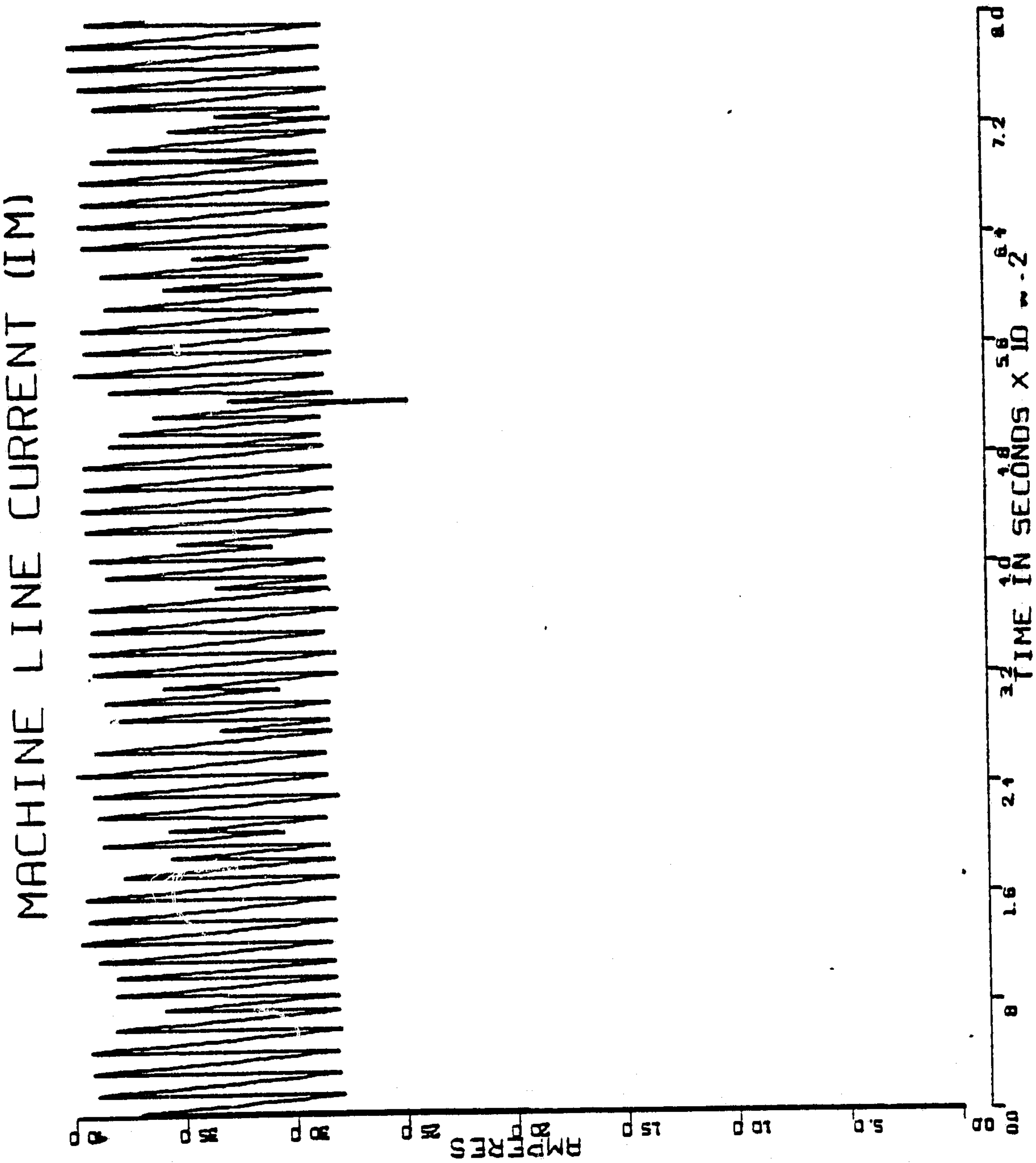
MACHINE LINE CURRENT (IM)
TIME IN SECONDS X 10 ** -2
AMPERES
0.0
.8
1.6
2.4
3.2
4.0
4.8
5.6
6.4
7.2
8.0
5.0
10.0
15.0
20.0
25.0
30.0
35.0
40.0

Figure C.1-20

APPENDIX C.2 CALCOMP PLOTS: PLUGGING 240 rpm 38° ADVANCE

RUN SUMMARY

MODE: PLUGGING

PROGRAM MODE: PGMODE = 1

CURRENT COMMAND: ICMD = 32.0 amps

TIME STEP: TSNET = 10 μs

COMMUTATION SHIFT: SHIFT = 0.0349066 mech rad

CURRENT THRESHOLD: ITOL = 4.0 amps

ROTOR VELOCITY: (240 rpm), (24.1327 rad/sec)

TOTAL NUMBER OF POINTS PLOTTED: NREC = 801

TOTAL NUMBER OF NETWORK CHANGES: NNETSW = 373

TOTAL NUMBER OF INTEGRATIONS: NUMINT = 8000

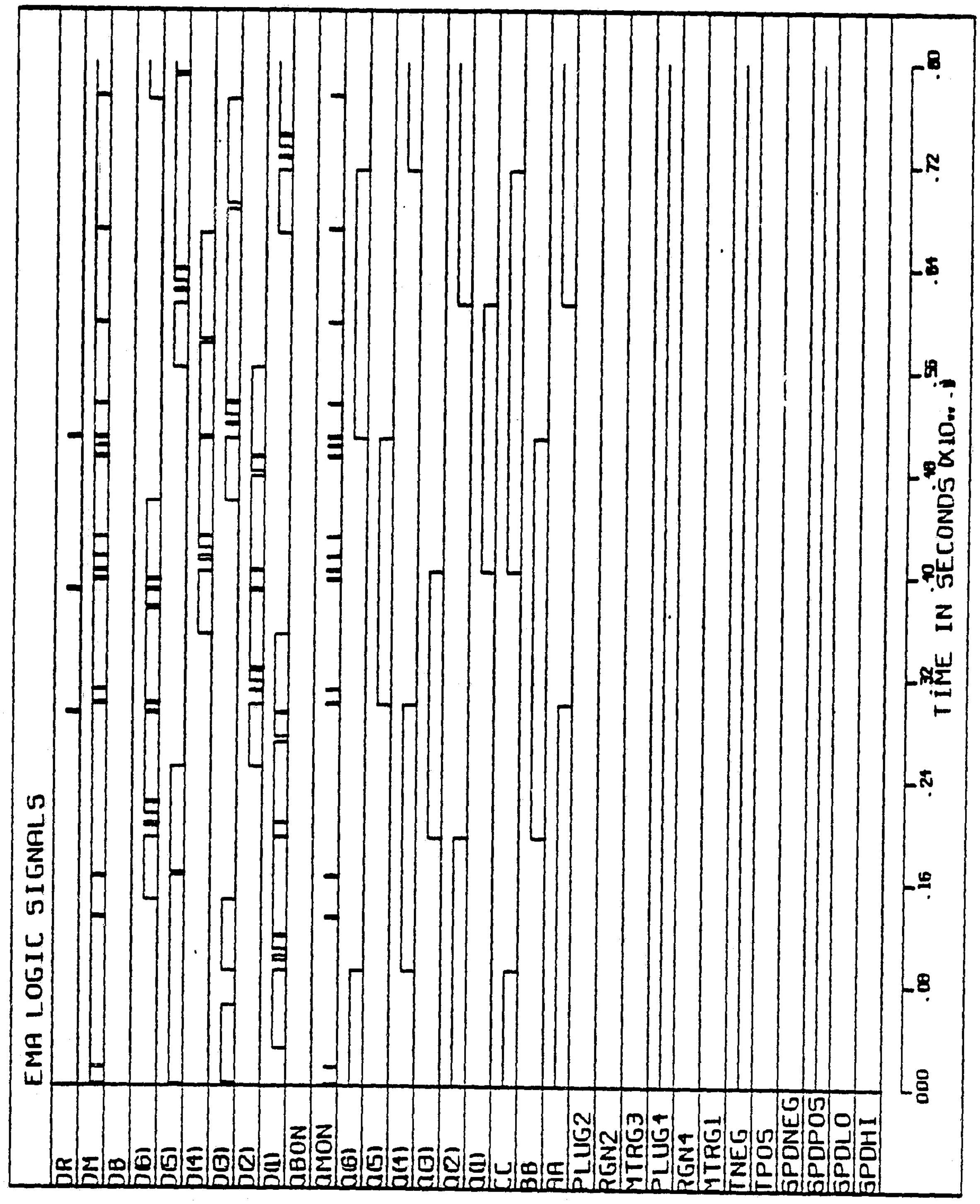
EMA LOGIC SIGNALS
DR
DM
DB
D(6)
D(5)
D(4)
D(3)
D(2)
D(1)
DBON
DMON
Q(6)
Q(5)
Q(4)
Q(3)
Q(2)
Q(1)
CC
BB
AA
PLUG2
RGN2
MTRG3
PLUG4
RGN4
MTRG1
TNEG
TPOS
SPDNEG
SPDPOS
SPDLO
SPDHI
.000
.08
.16
.24
.32
.40
.48
.56
.64
.72
.80
TIME IN SECONDS

Figure C.2-1

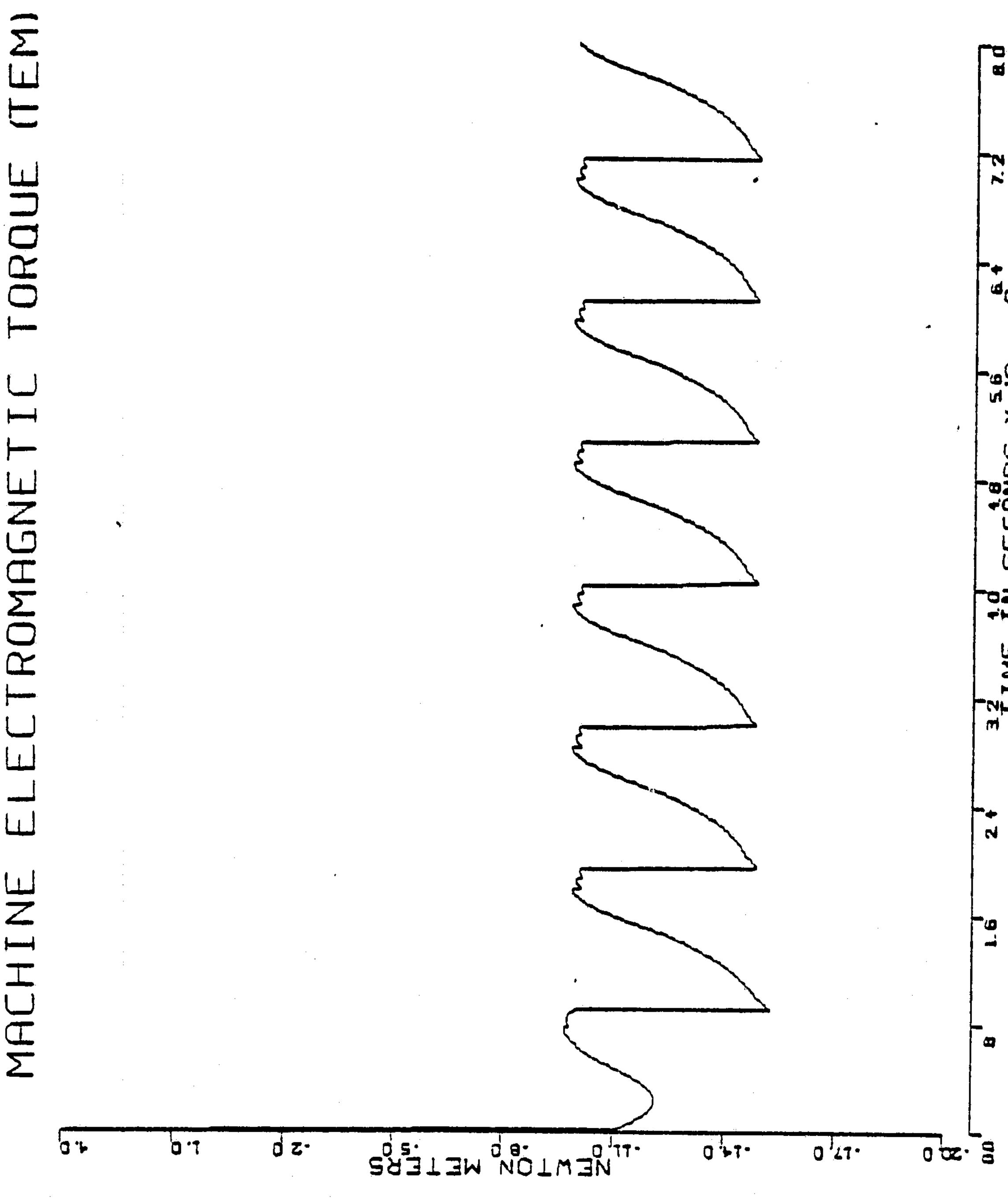
MACHINE ELECTROMAGNETIC TORQUE (TEM)
NEWTON METERS
TIME IN SECONDS X 10 ** -2

Figure C.2-2

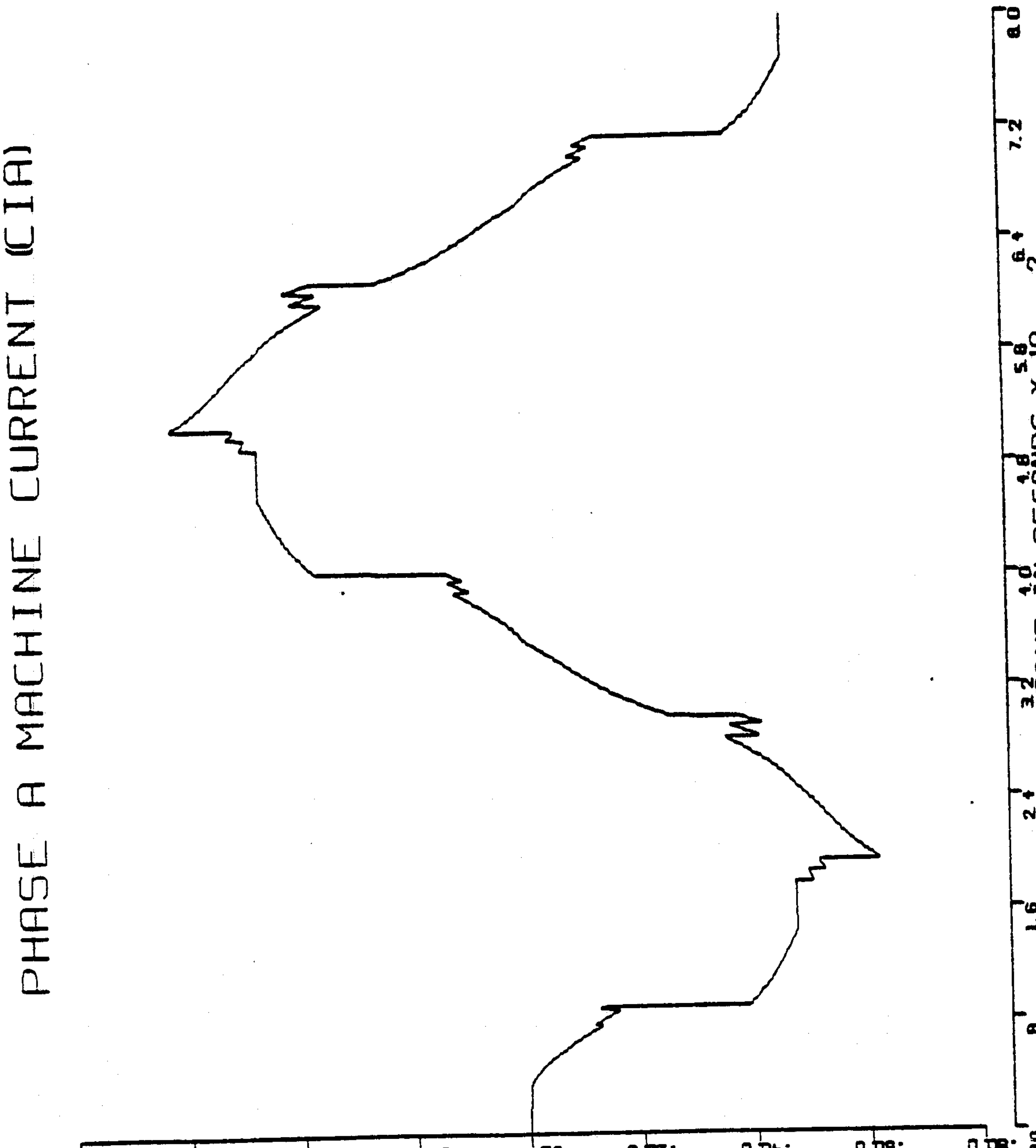

Figure C.2-3

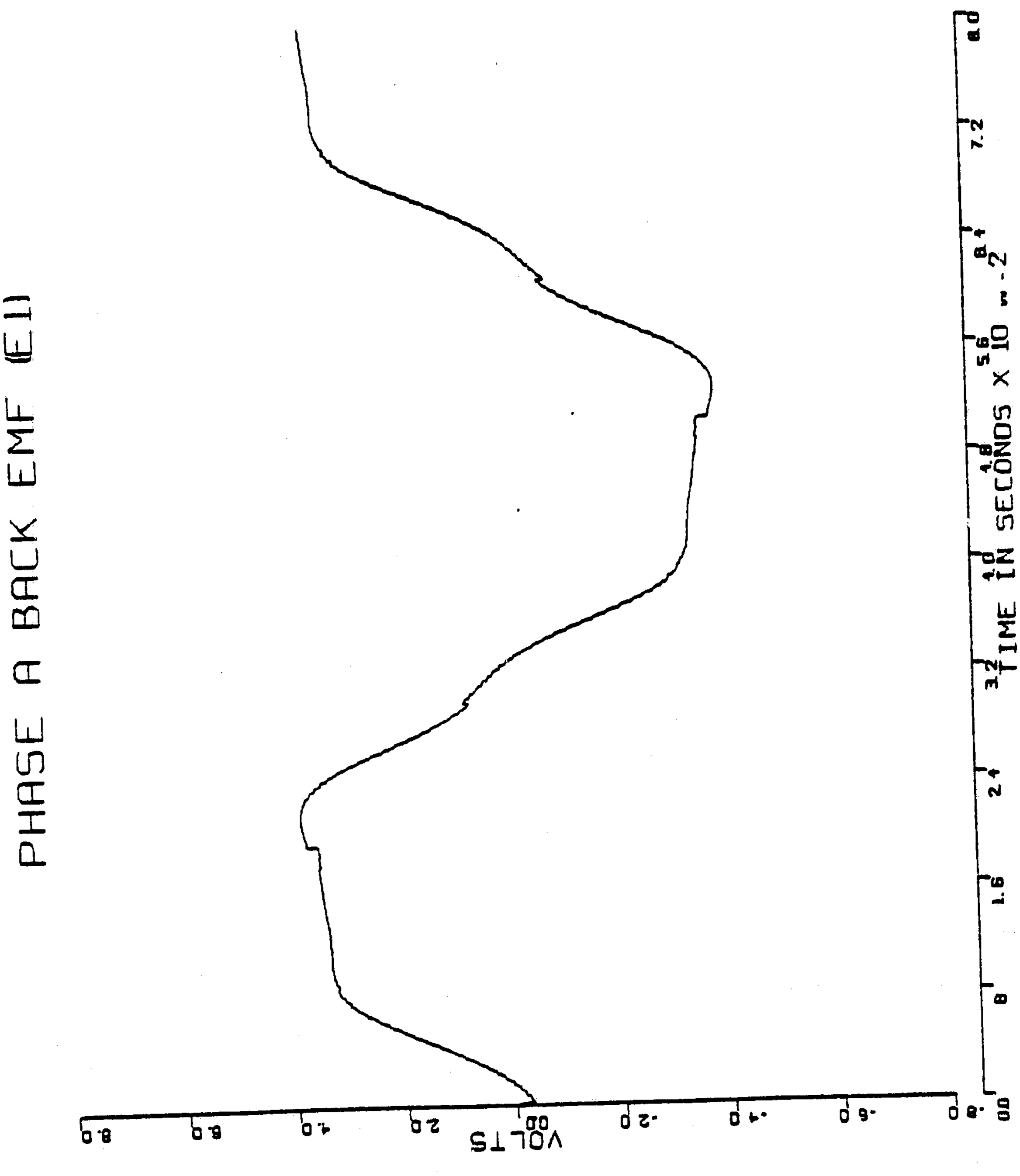

Figure C.2-4

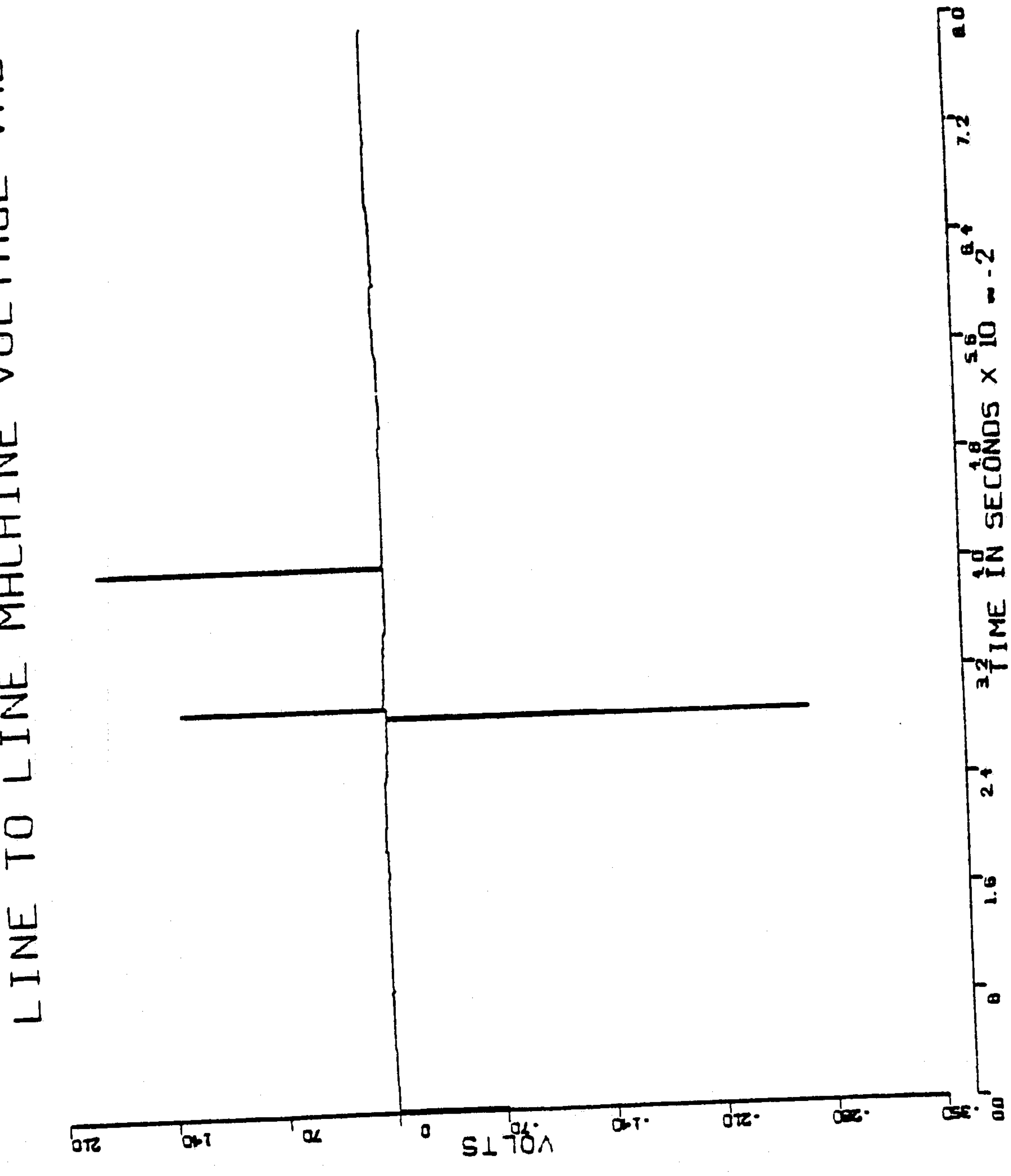
LINE TO LINE MACHINE VOLTAGE VAB
TIME IN SECONDS X 10 ** -2
VOLTS
0.0 0.8 1.6 2.4 3.2 4.0 4.8 5.6 6.4 7.2 8.0
-350 -280 -210 -140 -70 0 70 140 210

Figure C.2-5

APPENDIX C.3 CALCOMP PLOTS: PLUGGING 240 rpm 22° ADVANCE

RUN SUMMARY

MODE: PLUGGING

PROGRAM MODE: PGMODE = 1

CURRENT COMMAND: ICMD = 32.0 amps

TIME STEP: TSNET = 10 μs

COMMUTATION SHIFT: SHIFT = -0.0349066 mech rad

CURRENT THRESHOLD: ITOL = 4

ROTOR VELOCITY: (240 rpm), (25.1327 rad/sec)

TOTAL NUMBER OF POINTS PLOTTED: NREC = 801

TOTAL NUMBER OF NETWORK CHANGES: NNETSW = 372

TOTAL NUMBER OF INTEGRATIONS: NUMINT = 8000

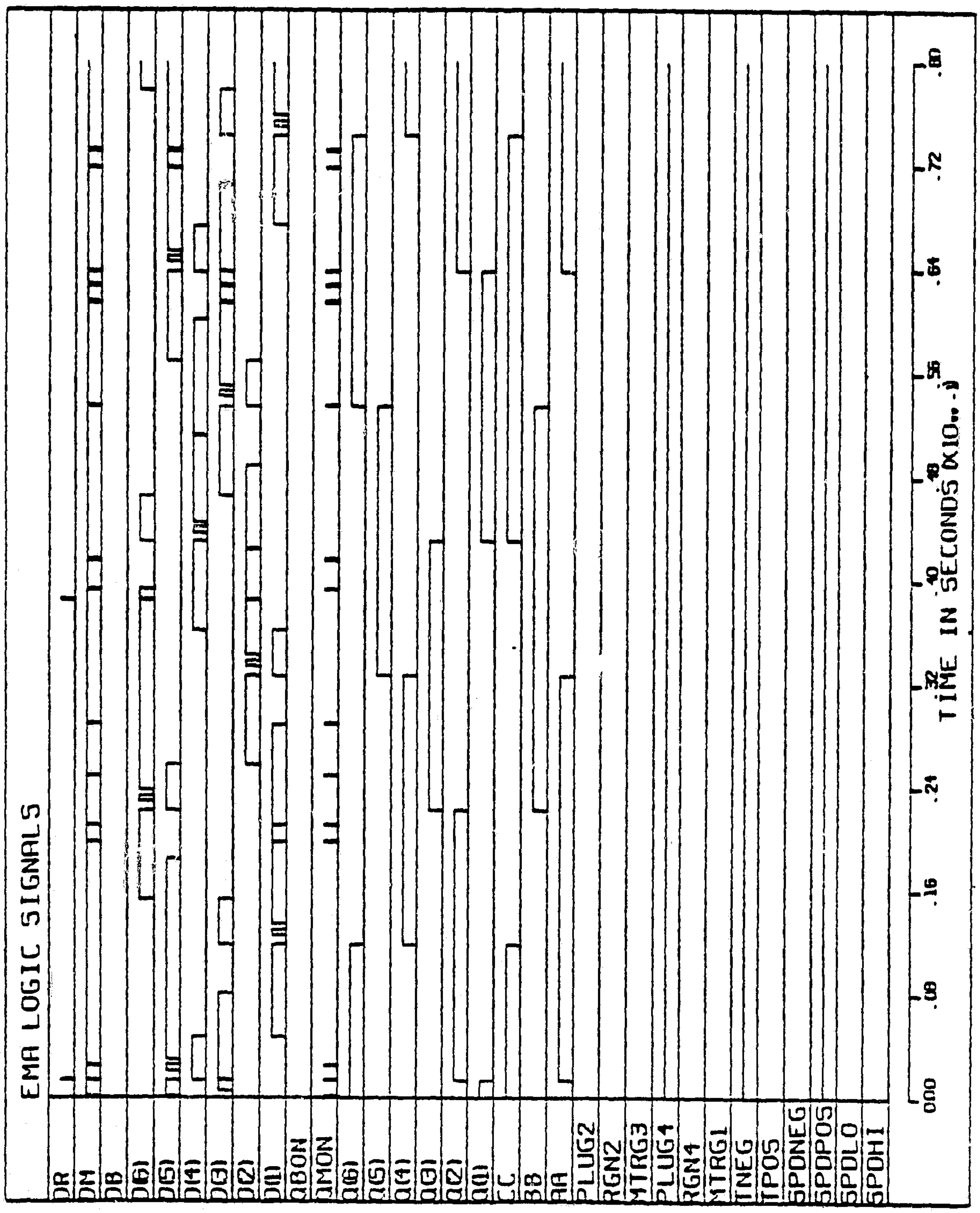
EMA LOGIC SIGNALS
DR
DM
DB
D(6)
D(5)
D(4)
D(3)
D(2)
D(1)
QBON
QMON
Q(6)
Q(5)
Q(4)
Q(3)
Q(2)
Q(1)
CC
BB
AA
PLUG2
RGN2
MTRG3
PLUG4
RGN4
MTRG1
TNEG
TPOS
SPDNEG
SPDPOS
SPDLO
SPDHI
0.00
.08
.16
.24
.32
.40
.48
.56
.64
.72
.80
TIME IN SECONDS (X10** -1)

Figure C.3-1

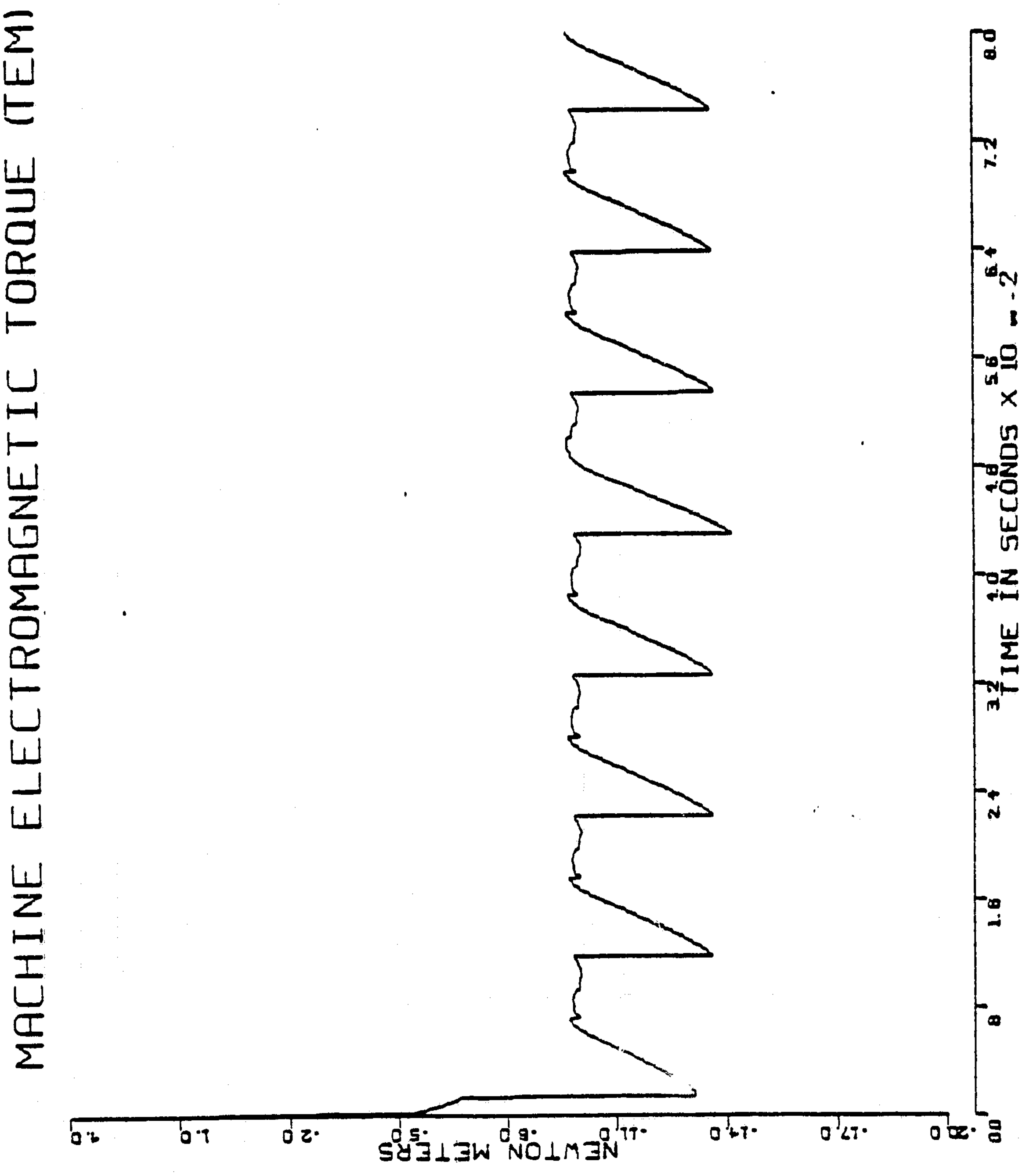
MACHINE ELECTROMAGNETIC TORQUE (TEM)
TIME IN SECONDS X 10 -2
NEWTON METERS

Figure C.3-2

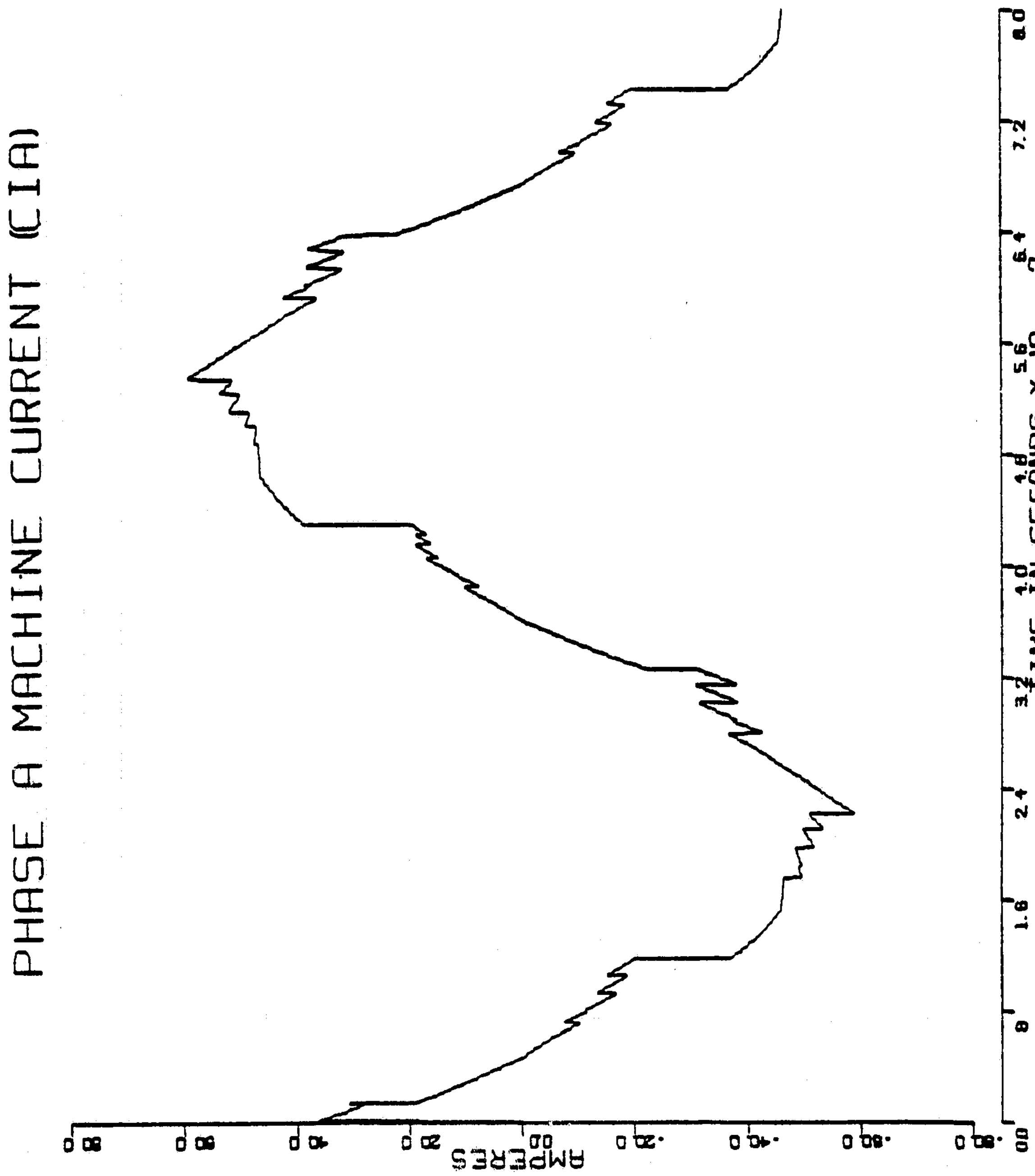

Figure C.3-3

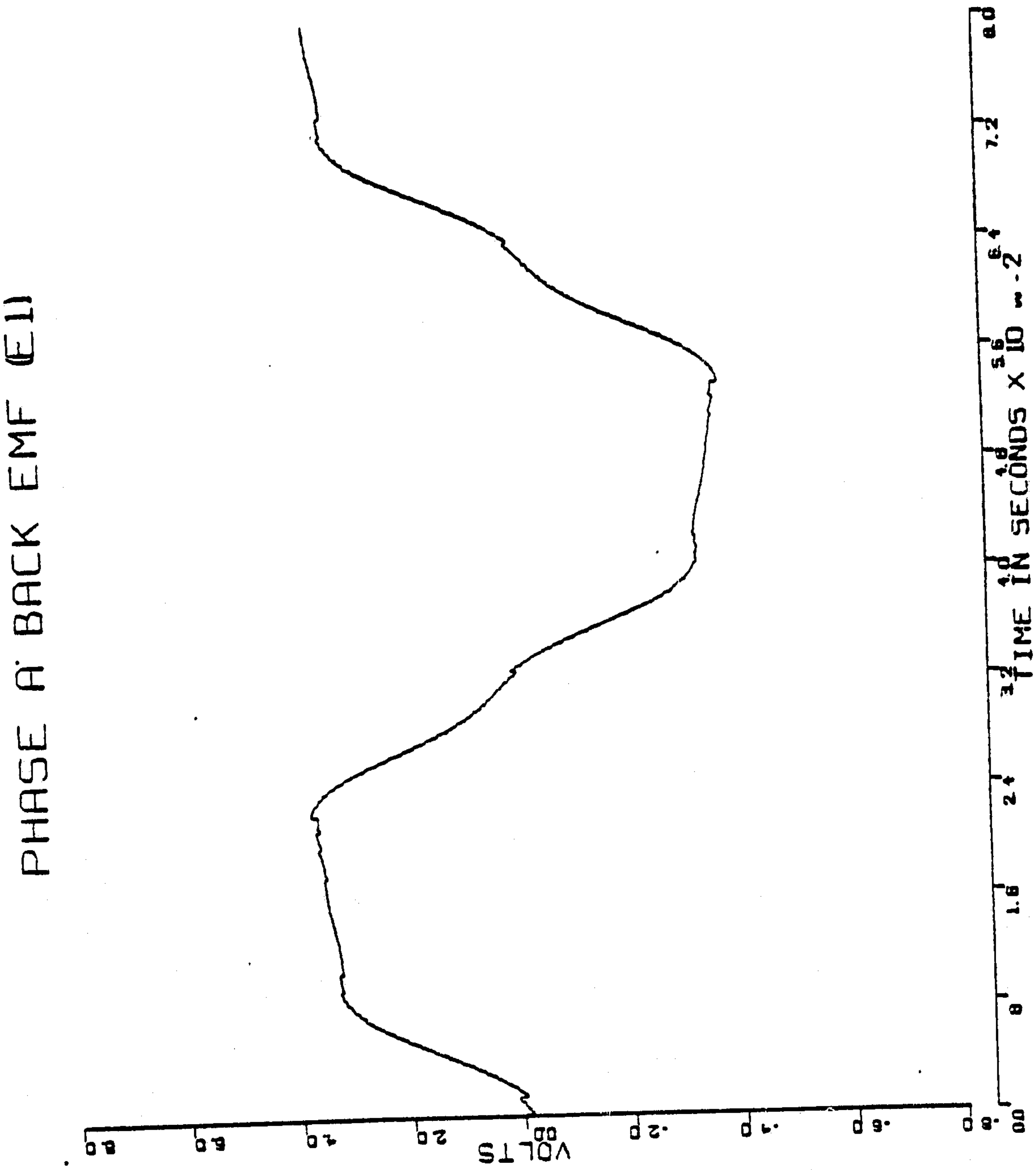

Figure C.3-4

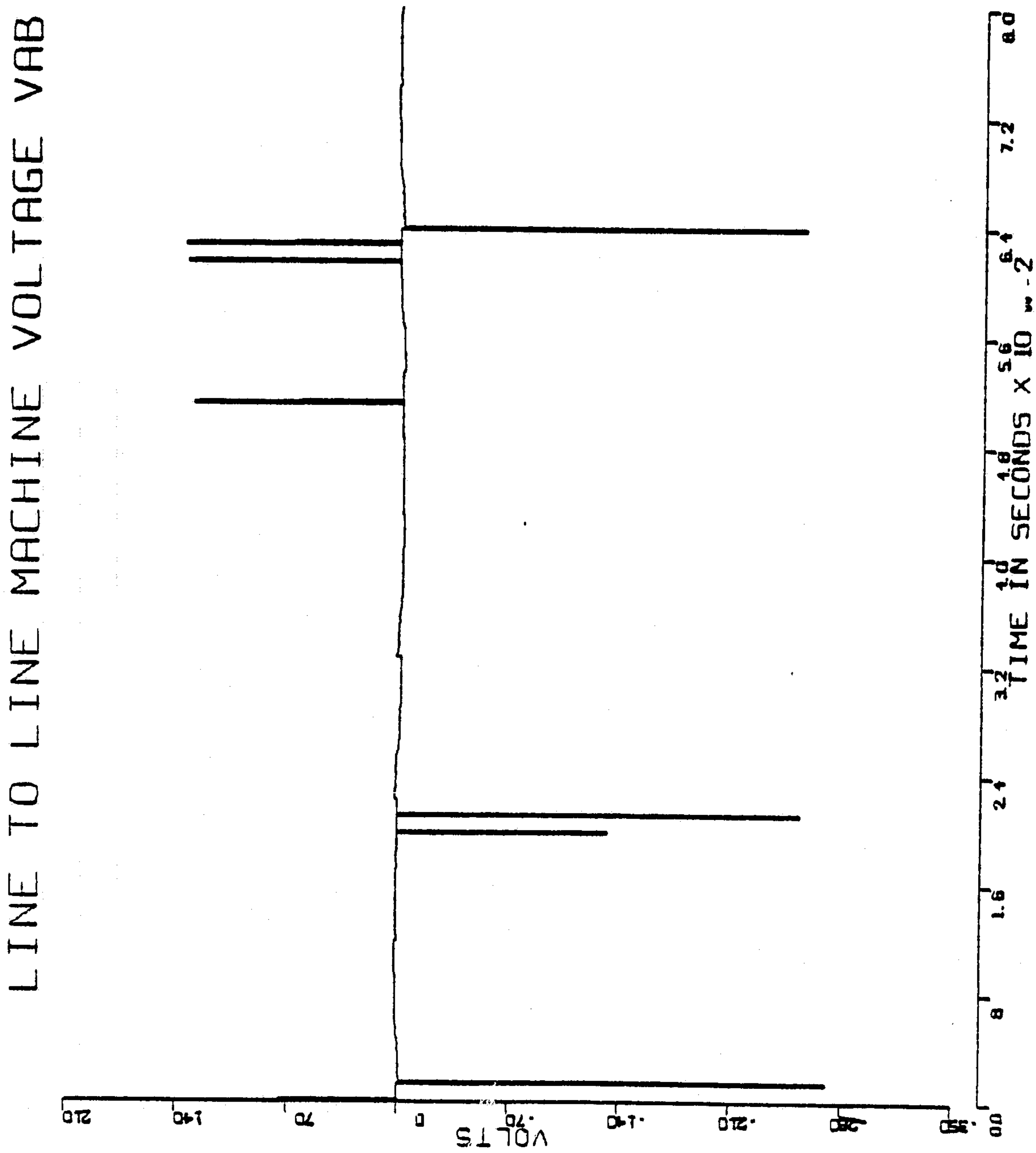

Figure C.3-5

APPENDIX D.1 CALCOMP PLOTS: 14^{th} Order EMA Model DC = 2.75°

RUN SUMMARY

MODE: 14^{th} ORDER EMA MODEL

PROGRAM MODE: PGMODE = 3

NUMBER OF MACHINES: NMACH = 2

DEFLECTION COMMAND: DC = 2.75 flap deg

TOTAL NUMBER OF INTEGRATIONS: NUMINT = 40000

TOTAL NUMBER OF MECHANICAL-POSITION LOOP INTEGRATIONS: NINTI = 2000

TOTAL NUMBER OF VELOCITY LOOP INTEGRATIONS: 8000

TOTAL SIMULATION TIME: 0.4 sec

TOTAL NUMBER OF POINTS PLOTTED: 1001

TOTAL NUMBER OF NETWORK CHANGES: 5811

TIME TO DC: .179 sec

TIME TO FIRST PEAK: .236 sec

PEAK DEFLECTION: 3.233 flap deg

MAXIMUM ROTOR SPEED: 10175 rpm

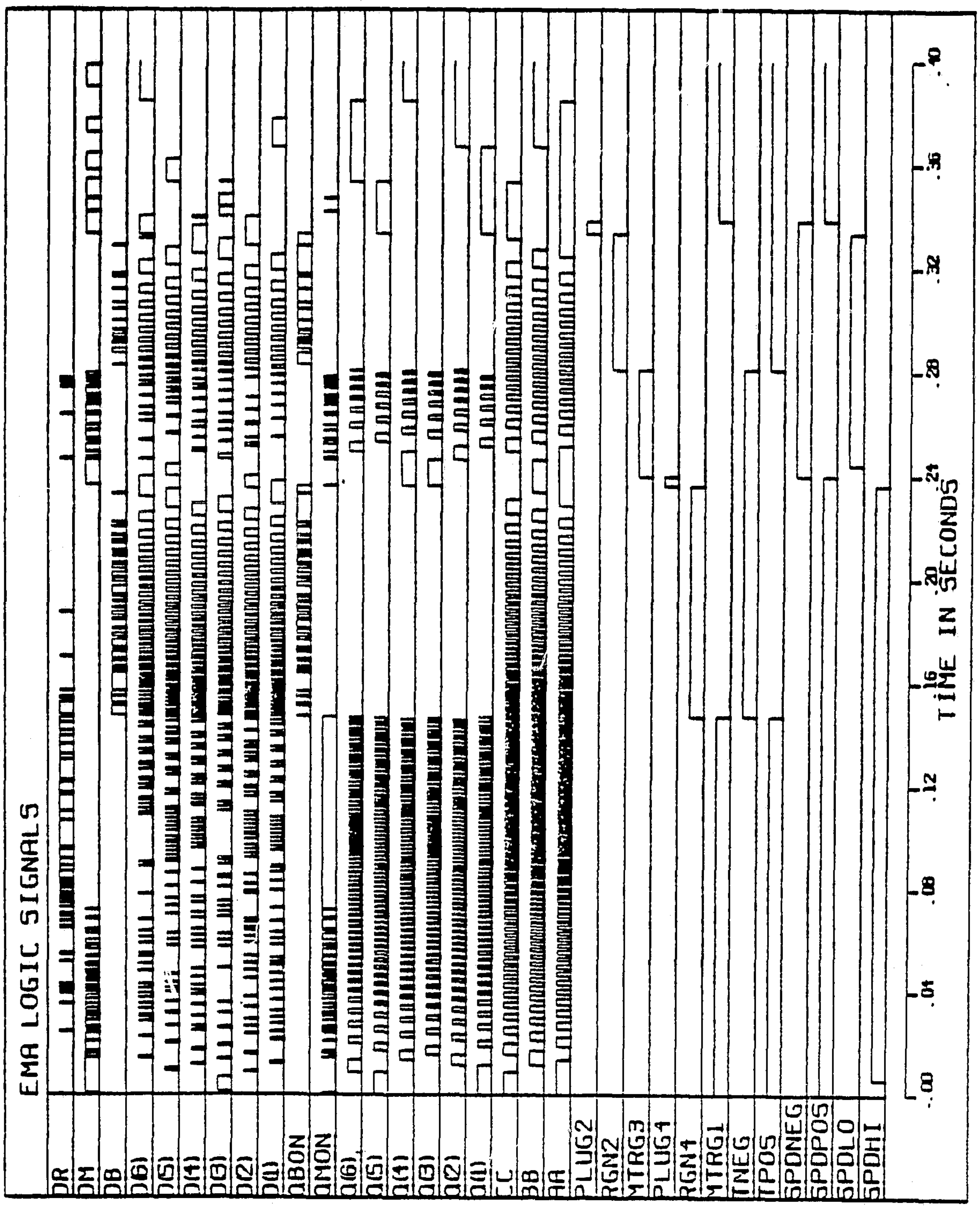
EMA LOGIC SIGNALS
DR
DM
DB
D(6)
D(5)
D(4)
D(3)
D(2)
D(1)
DBON
DMON
Q(6)
Q(5)
Q(4)
Q(3)
Q(2)
Q(1)
CC
BB
AA
PLUG2
RGN2
MTRG3
PLUG4
RGN4
MTRG1
TNEG
TPOS
SPDNEG
SPDPOS
SPDLO
SPDHI
.00
.04
.08
.12
.16
.20
.24
.28
.32
.36
.40
TIME IN SECONDS

Figure D.1-1

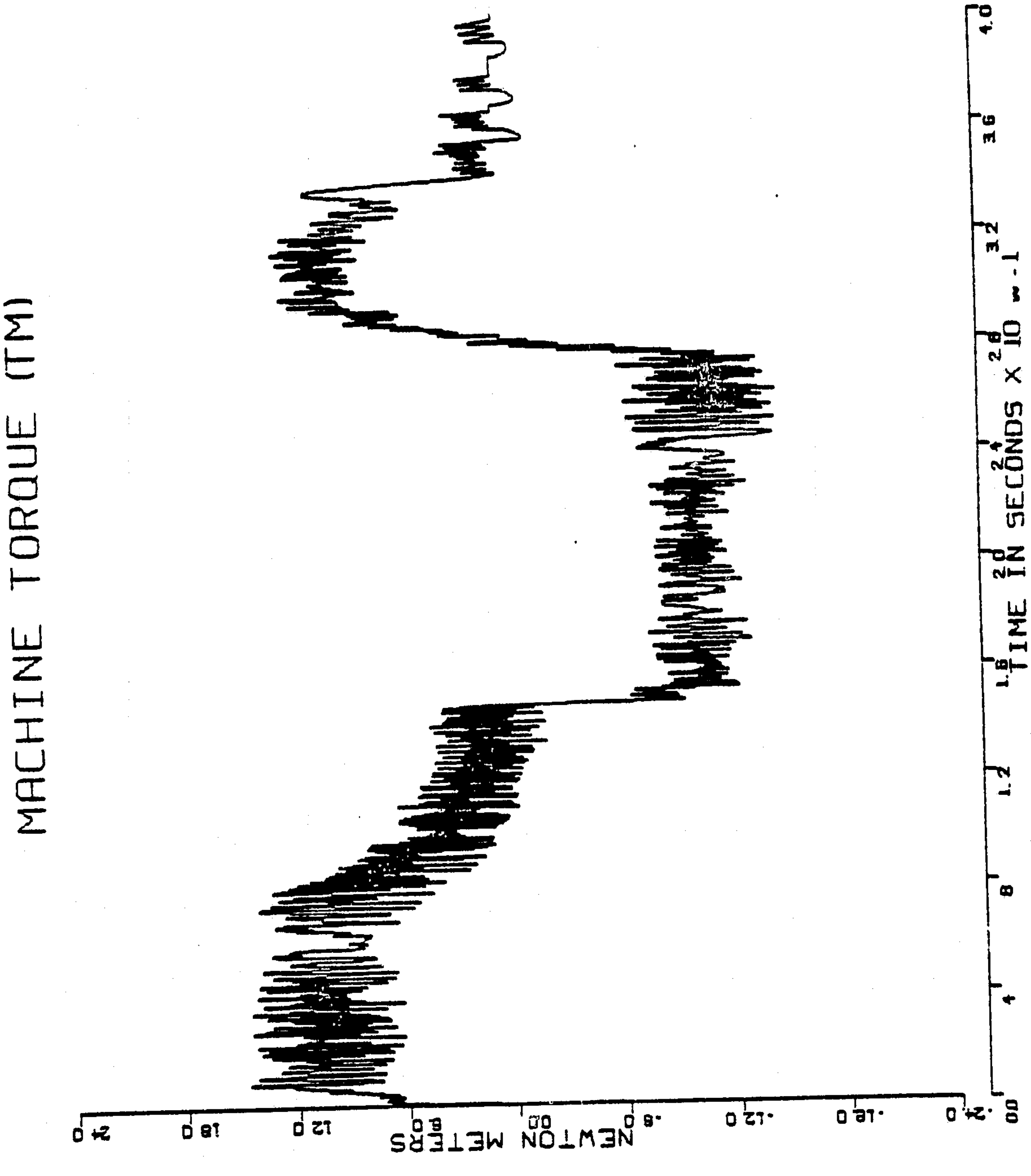

Figure D.1-2

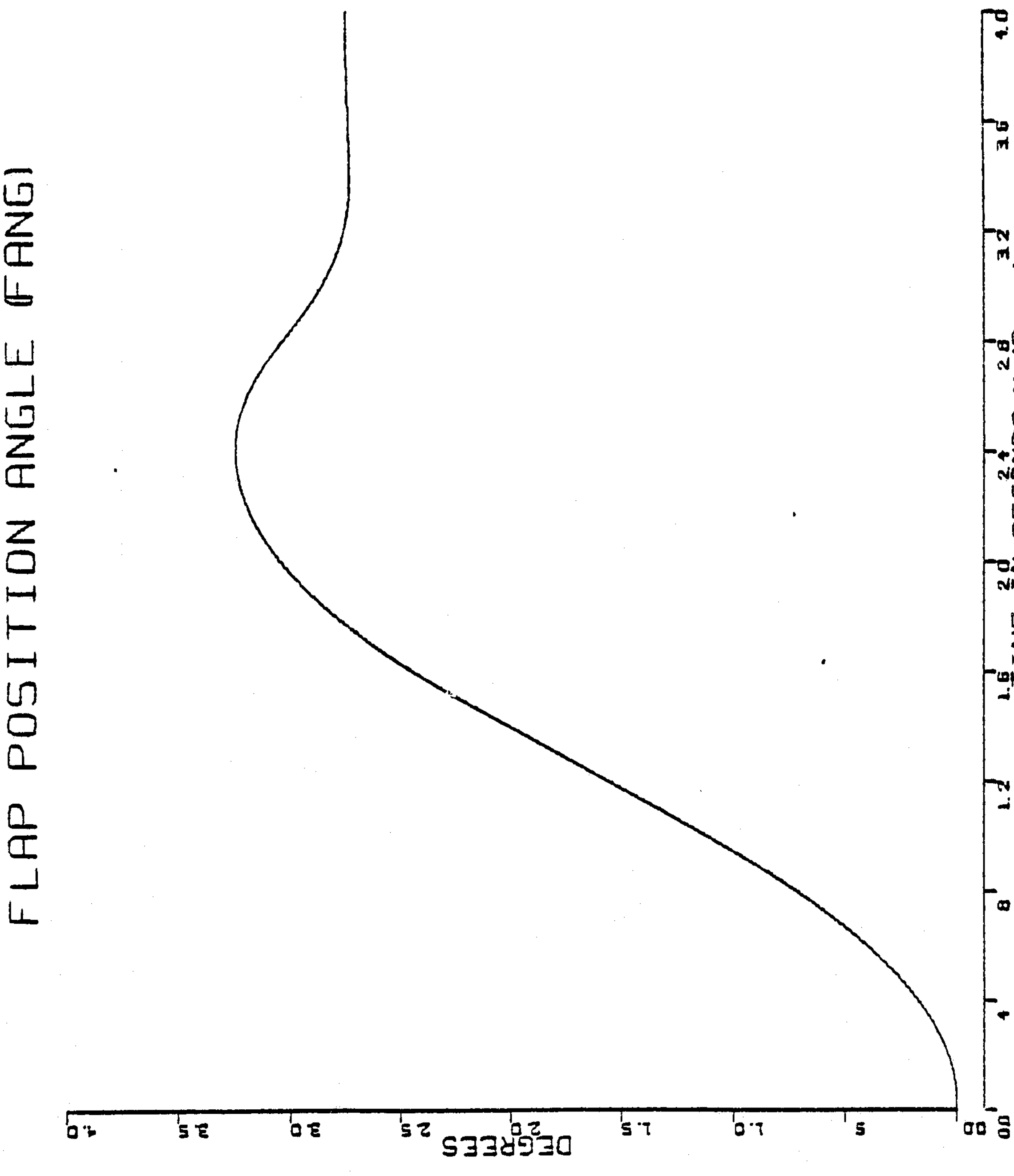
FLAP POSITION ANGLE (FANG)
TIME IN SECONDS X 10 ** -1
DEGREES
0.0
.4
.8
1.2
1.6
2.0
2.4
2.8
3.2
3.6
4.0
.5
1.0
1.5
2.5
3.0
3.5

Figure D.1-3

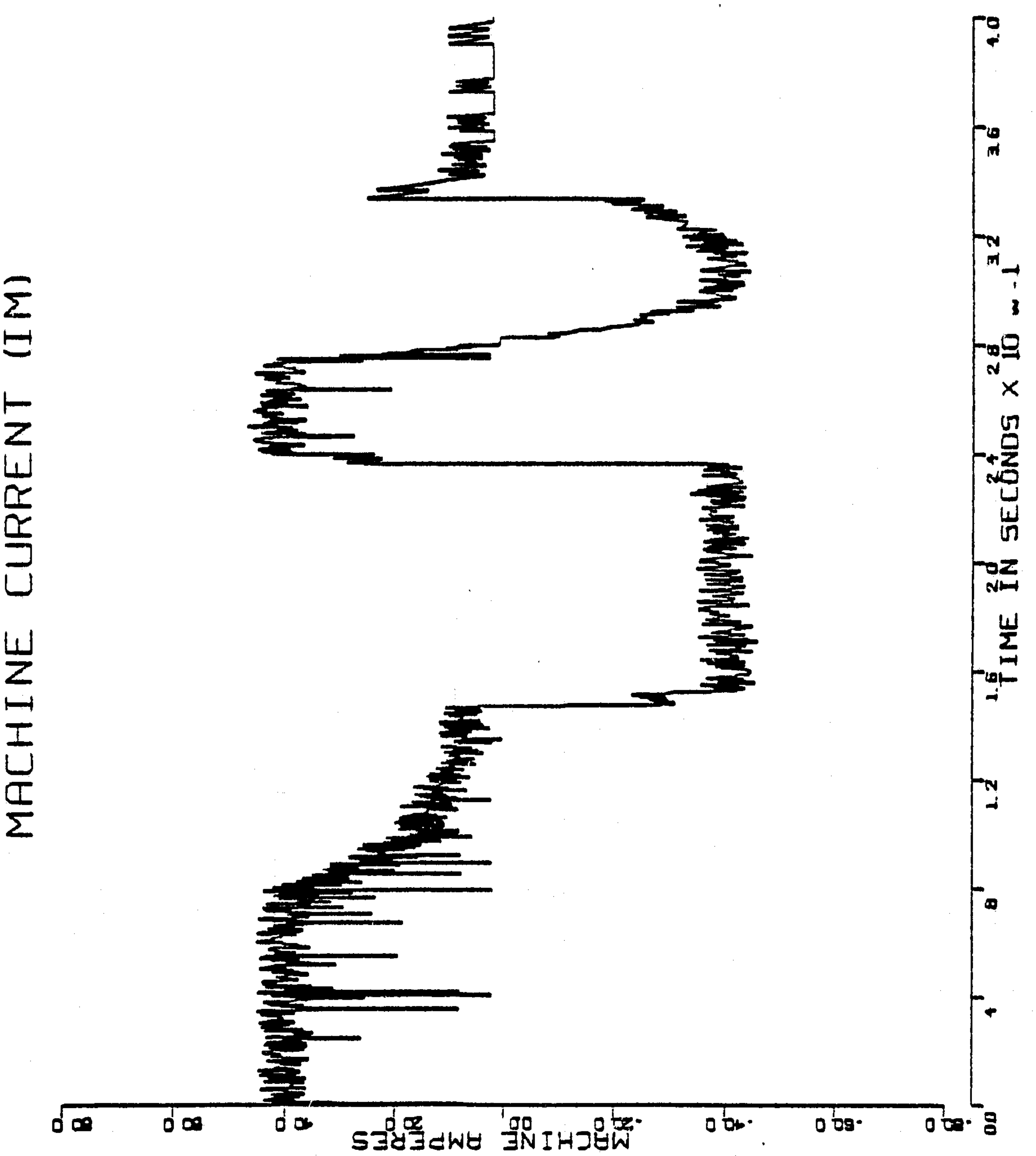

Figure D.1-4

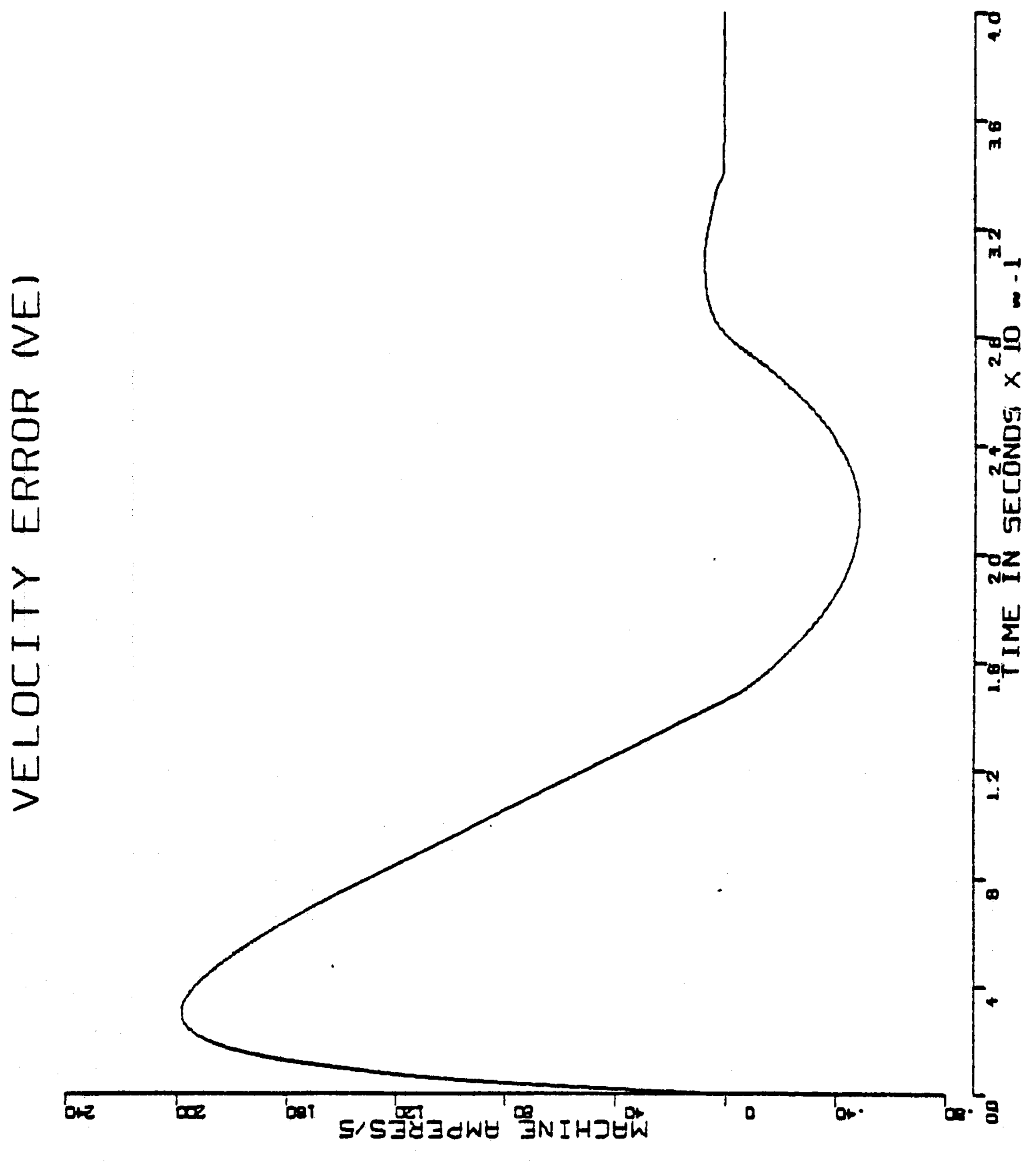
VELOCITY ERROR (VE)
MACHINE AMPERES/S
TIME IN SECONDS X 10 ** -1
240
200
160
120
80
40
0
-40
-80
0.0
.4
.8
1.2
1.6
2.0
2.4
2.8
3.2
3.6
4.0

Figure D.1-5

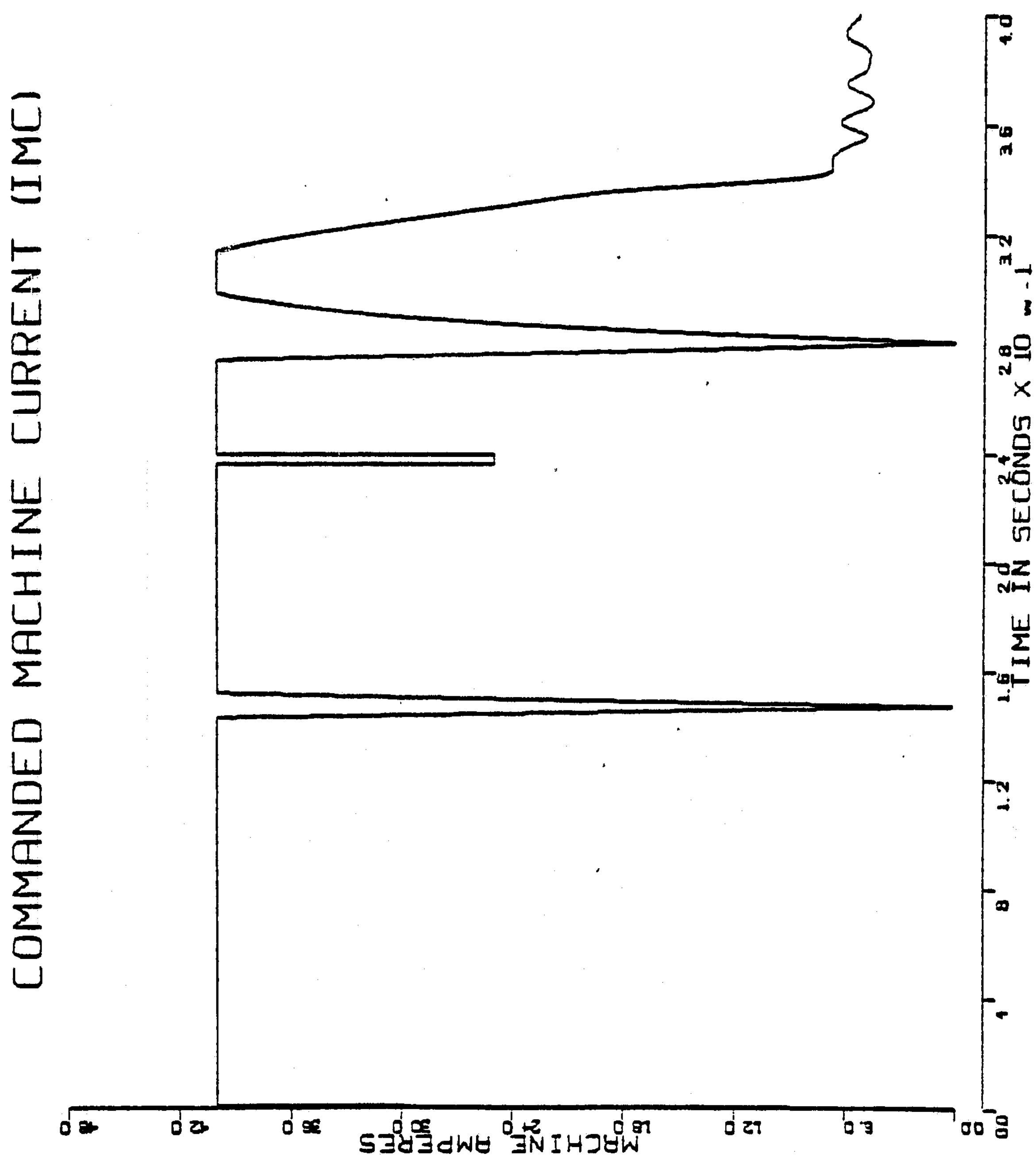
COMMANDED MACHINE CURRENT (IMC)
TIME IN SECONDS X 10 -1
MACHINE AMPERES
0.0
.4
.8
1.2
1.6
2.0
2.4
2.8
3.2
3.6
4.0
6.0
12.0
18.0
24.0
30.0
36.0
42.0
48.0

Figure D.1-6

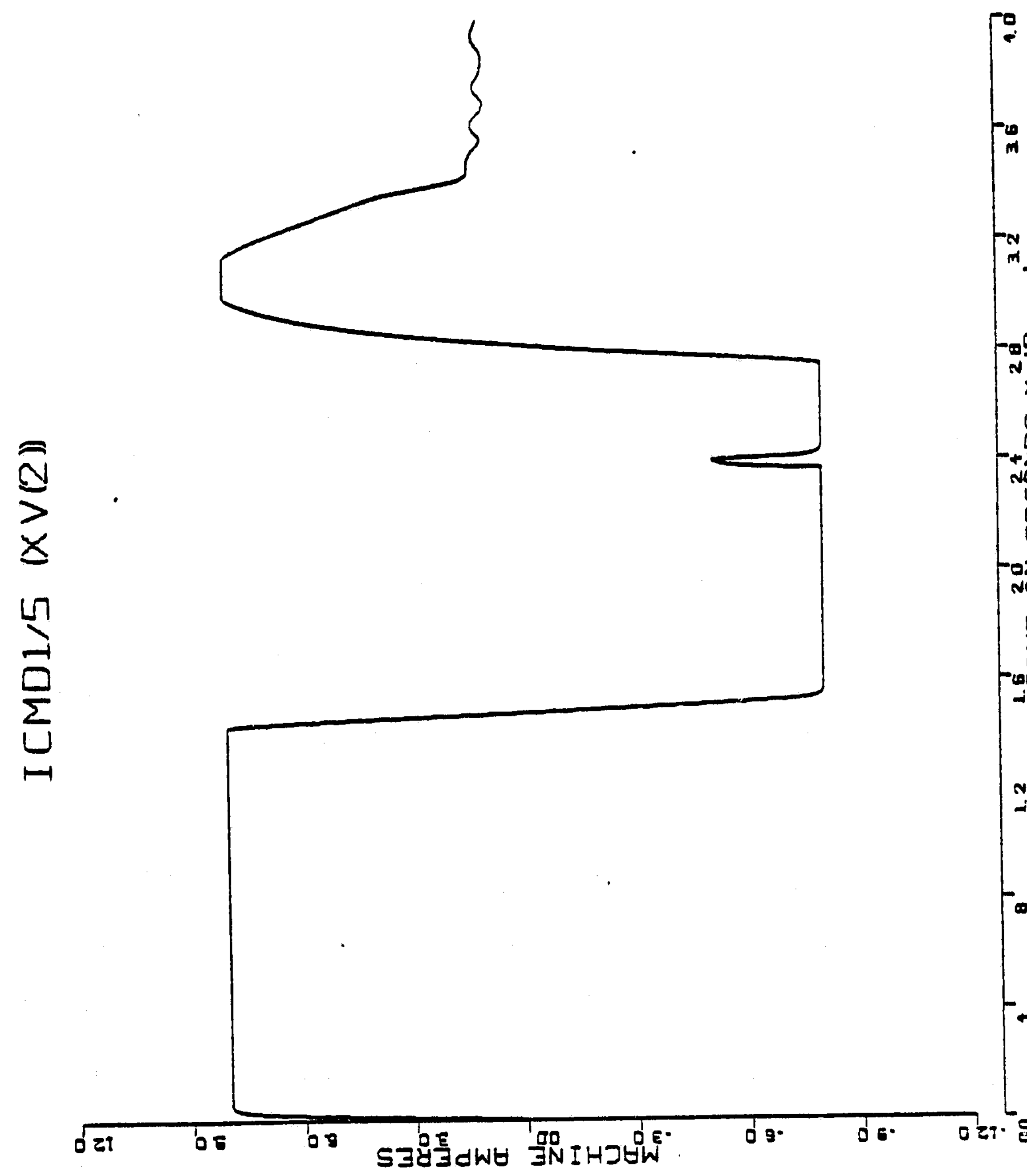
ICMD1/5 (XV(2))
TIME IN SECONDS X 10 ** -1
MACHINE AMPERES
0.0
.4
.8
1.2
1.6
2.0
2.4
2.8
3.2
3.6
4.0
-12.0
-9.0
-6.0
-3.0
0.0
3.0
6.0
9.0
12.0

Figure D.1-7

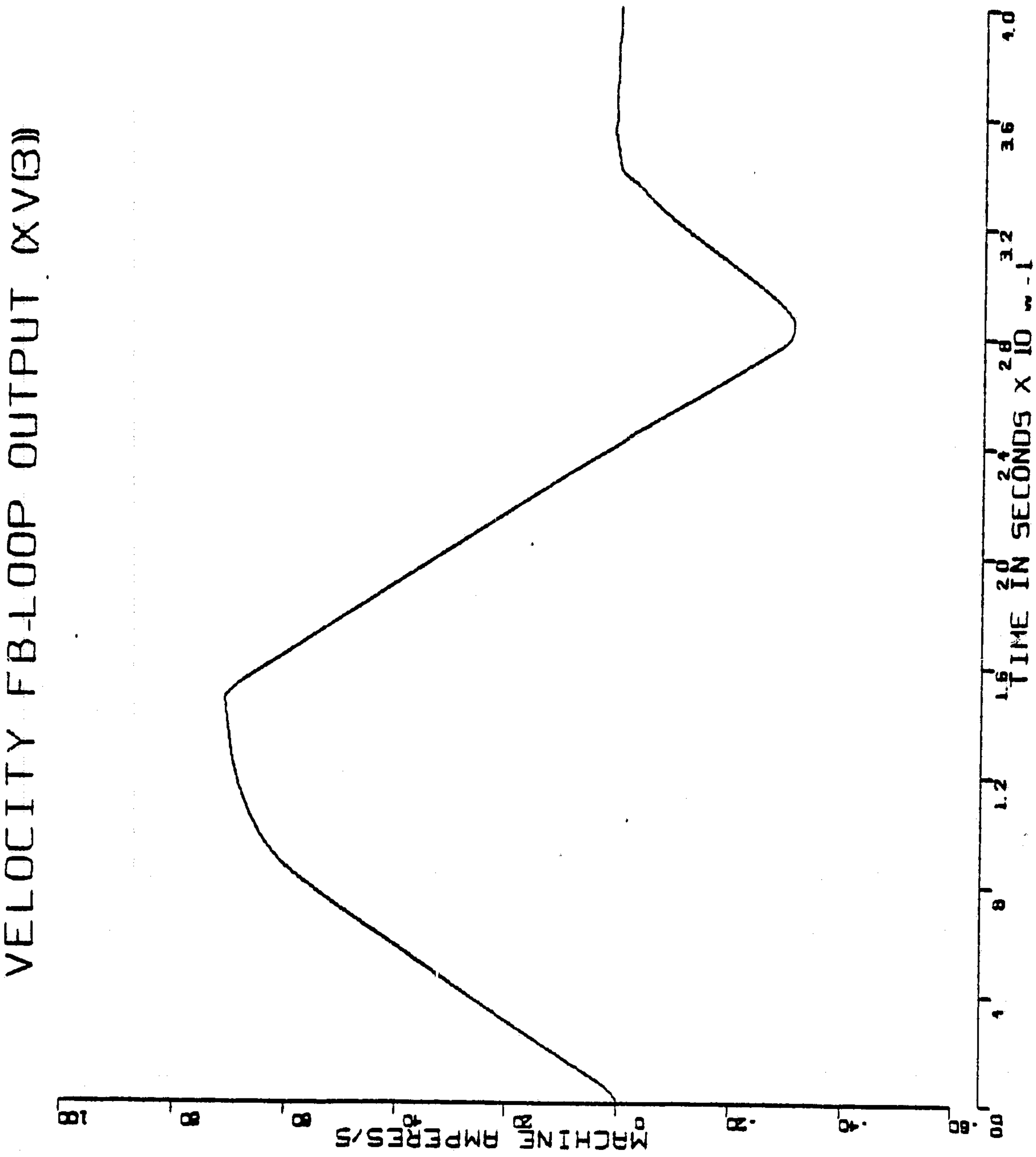
VELOCITY FB-LOOP OUTPUT (XV(3))
TIME IN SECONDS x 10
MACHINE AMPERES/S

Figure D.1-8

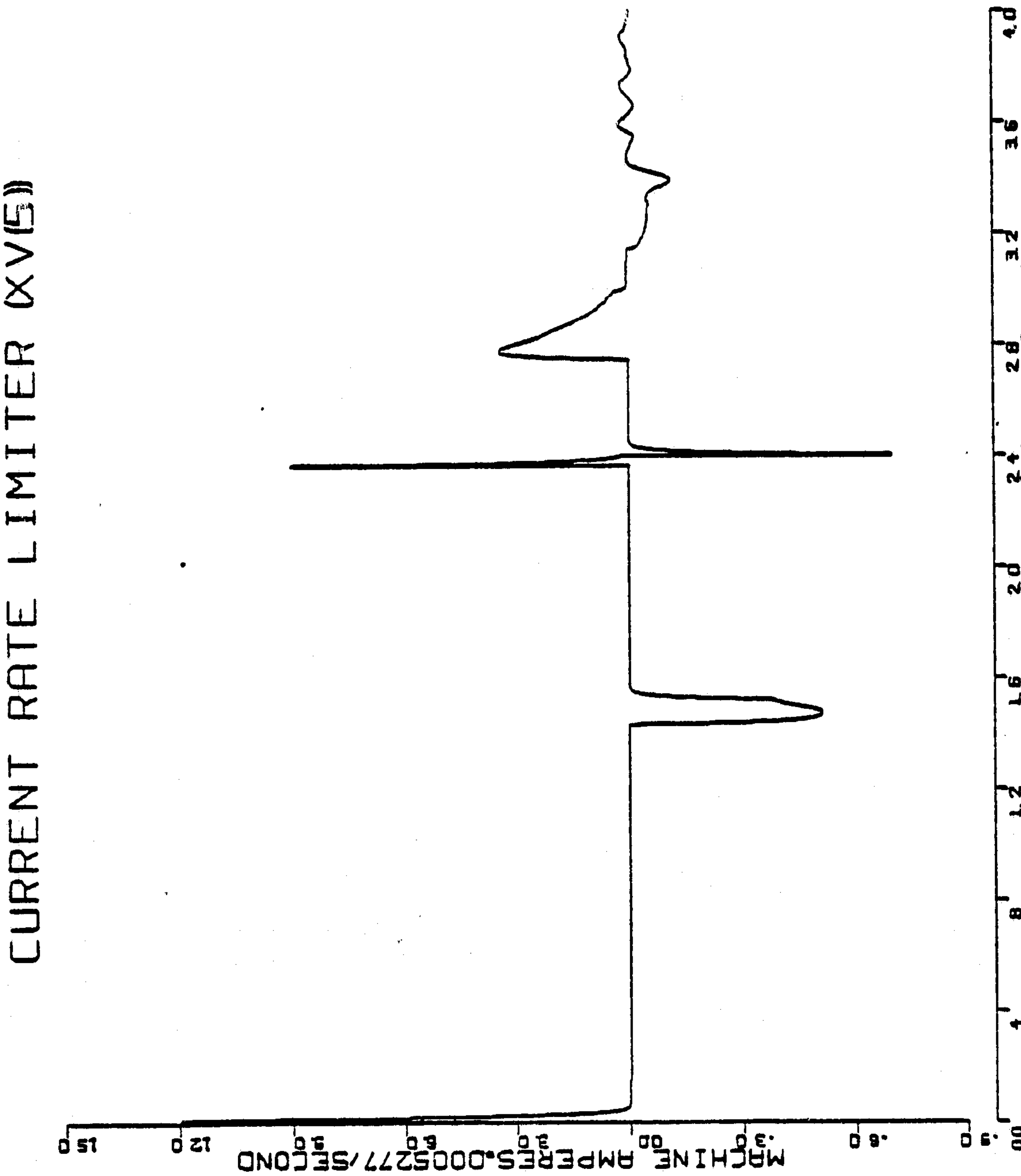
CURRENT RATE LIMITER (XV(5))
TIME IN SECONDS x 10 ** -1
MACHINE AMPERES.000527/SECOND
0.0
.4
.8
1.2
1.6
2.0
2.4
2.8
3.2
3.6
4.0
15.0
12.0
9.0
6.0
3.0
0.0
-3.0
-6.0
-9.0

Figure D.1-9

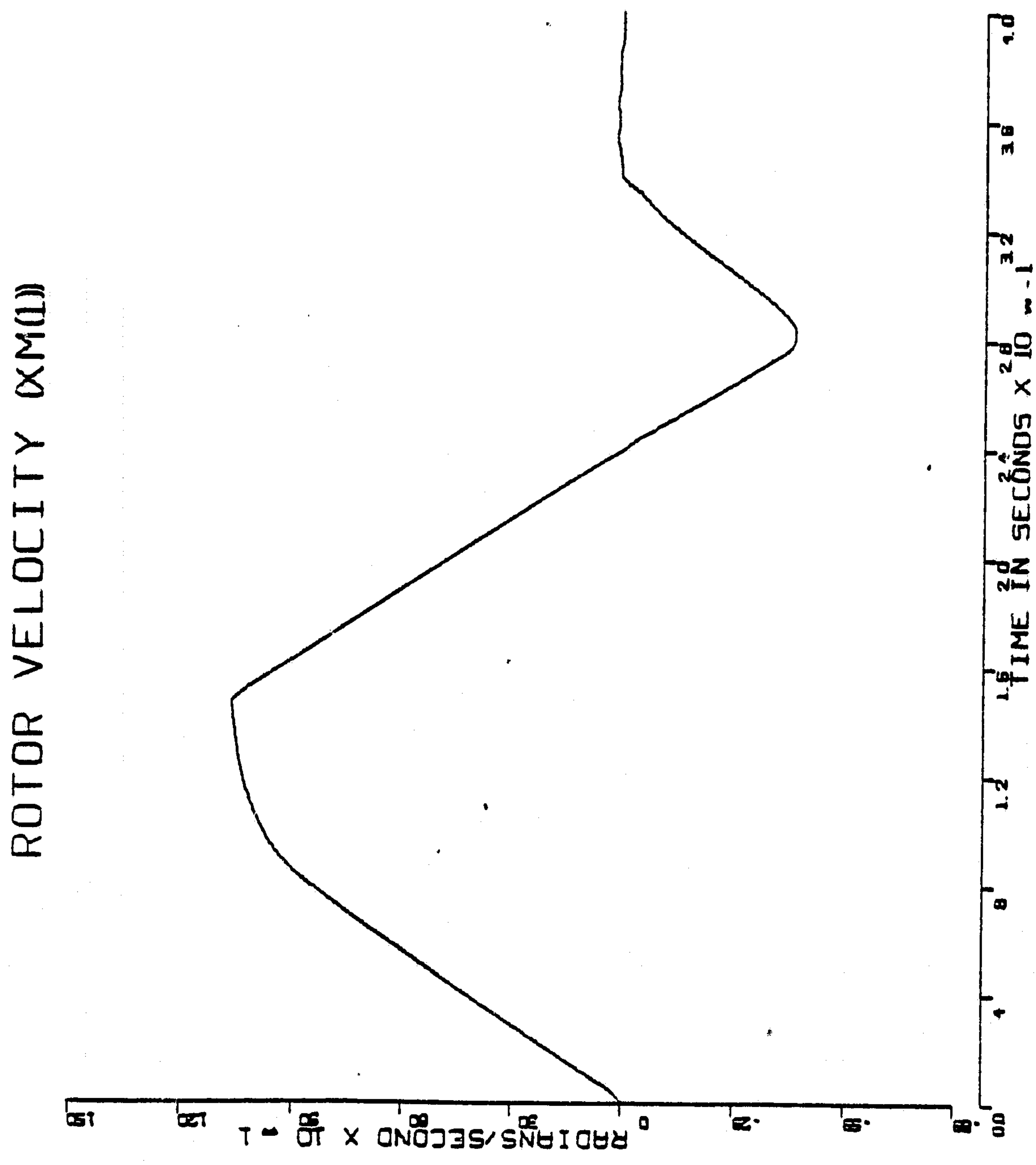
ROTOR VELOCITY (XM(1))
TIME IN SECONDS X 10 ** -1
0.0
.4
.8
1.2
1.6
2.0
2.4
2.8
3.2
3.6
4.0
RADIANS/SECOND X 10 ** 1
150
120
90
60
30
0

Figure D.1-10

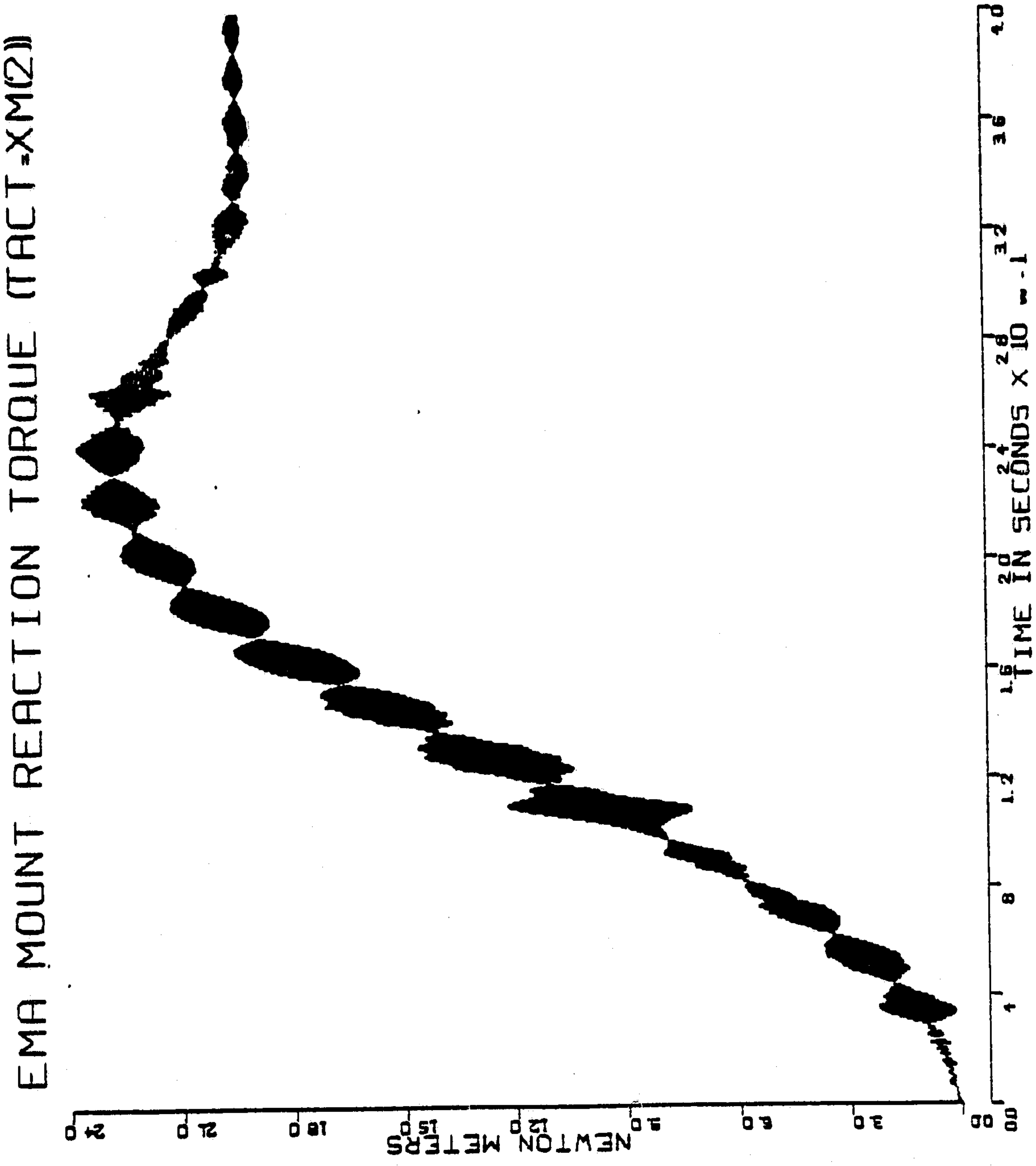
EMA MOUNT REACTION TORQUE (TACT-XM(2))
TIME IN SECONDS X 10 ** -1
NEWTON METERS

Figure D.1-11

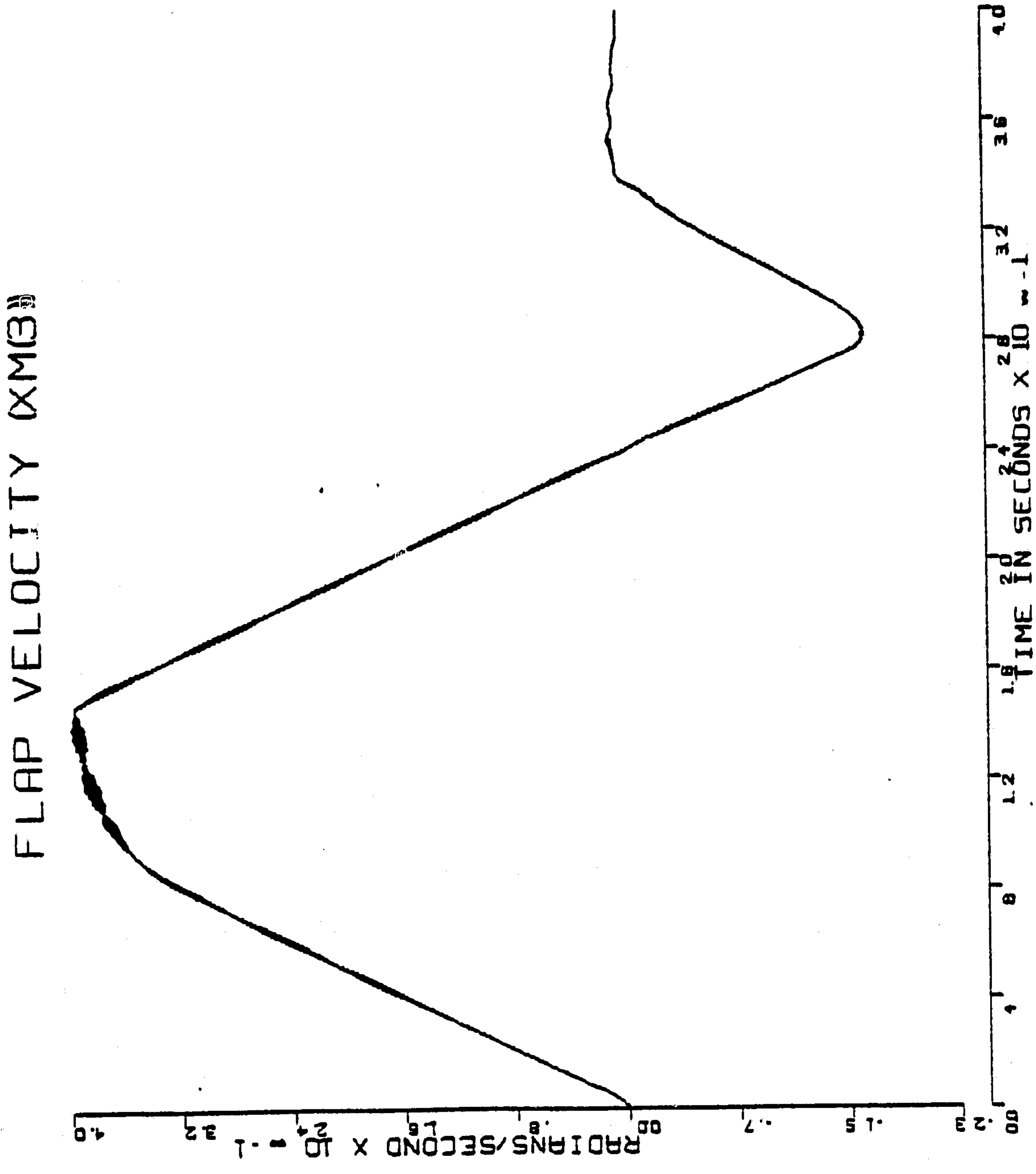

Figure D.1-12

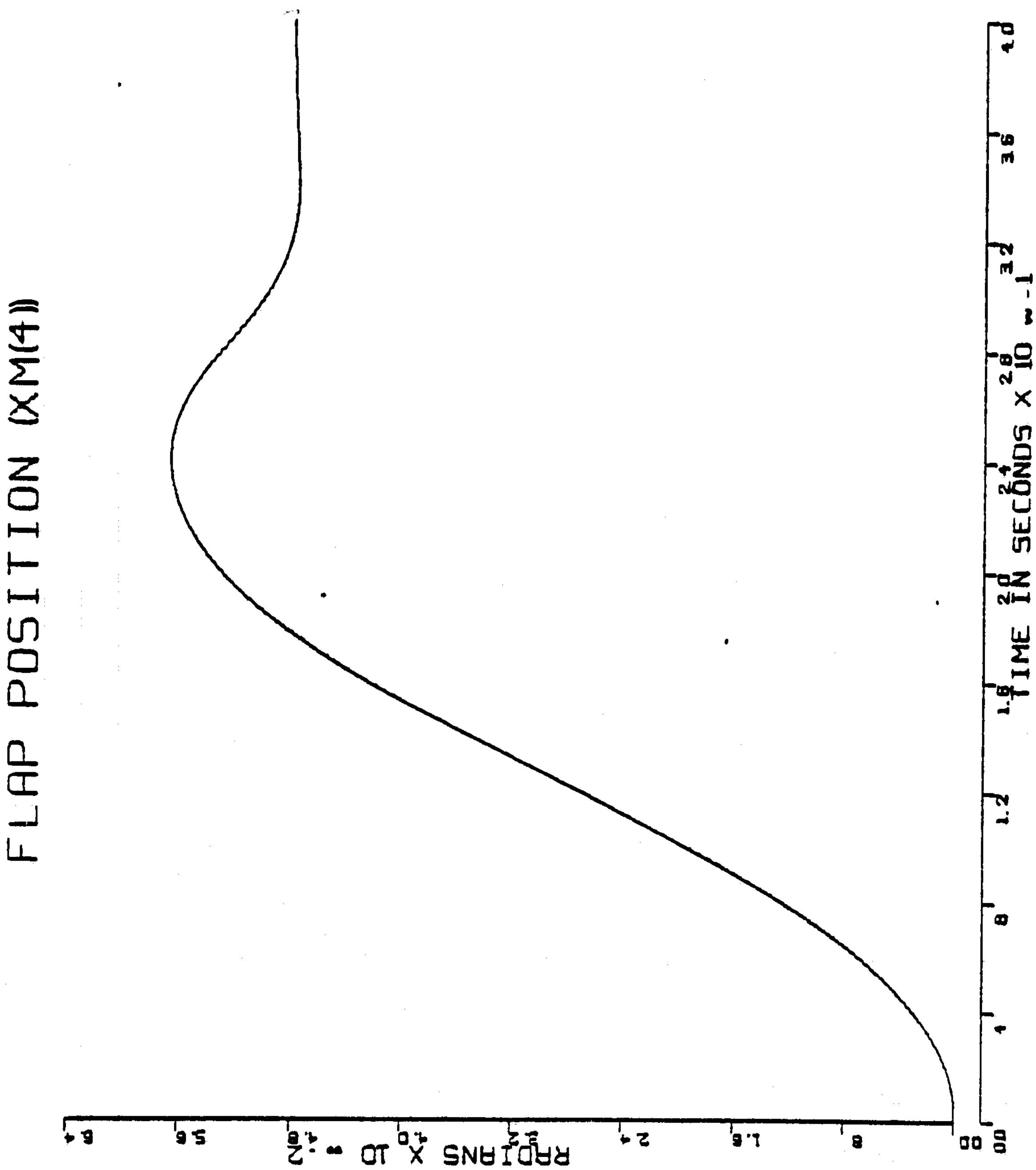

Figure D.1-12

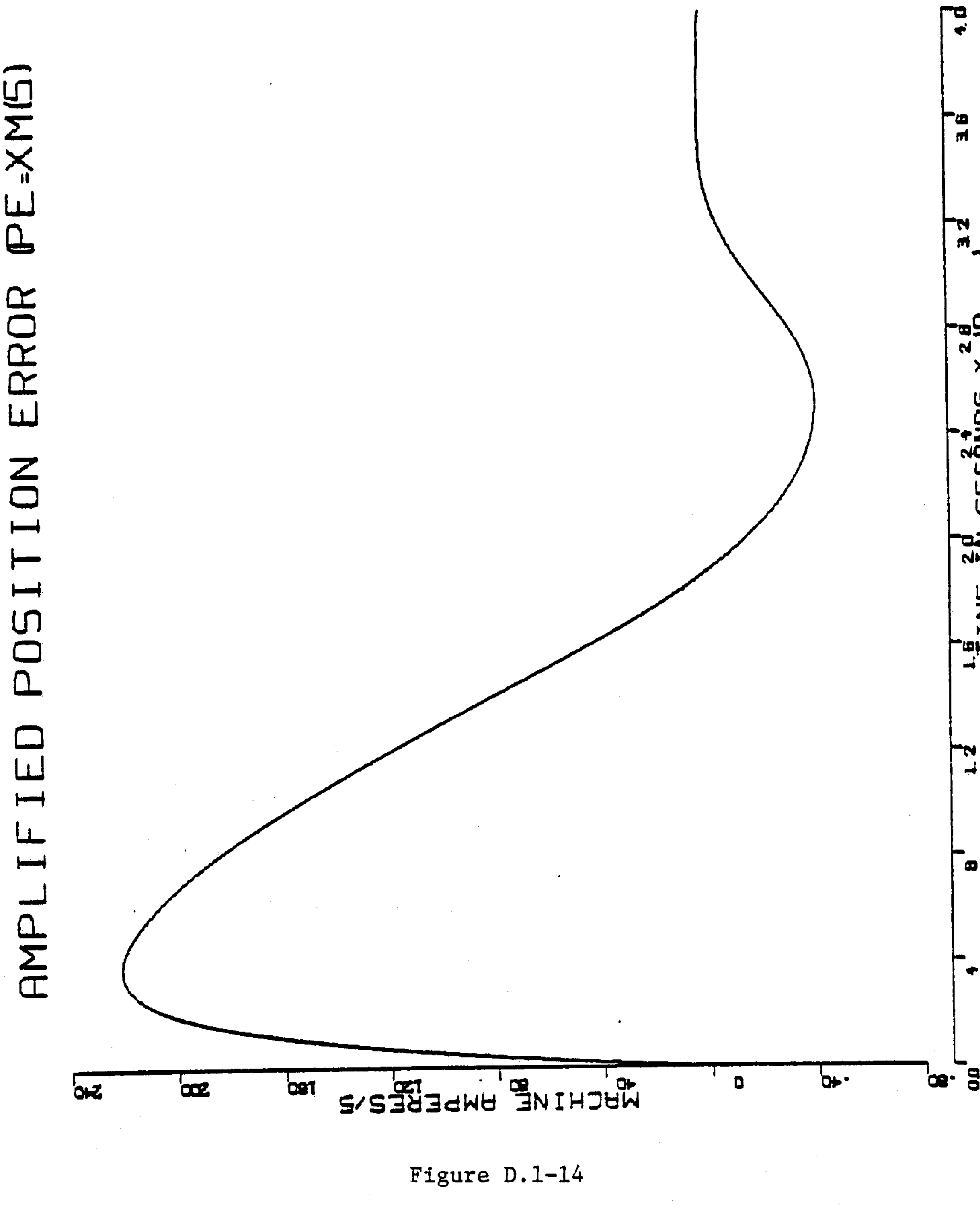

AMPLIFIED POSITION ERROR (PE=XM(5)
TIME IN SECONDS X 10 **-1
0.0
.4
.8
1.2
1.6
2.0
2.4
2.8
3.2
3.6
4.0
MACHINE AMPERES/5
-80
-40
0
40
80
120
160
200
240

Figure D.1-14

APPENDIX E.1 CALCOMP PLOTS: 10^{th} Order EMA Model DC = 1.1°

RUN SUMMARY

MODE: 10^{th} ORDER EMA MODEL

PROGRAM MODE: PGMODE = 2

NUMBER OF MACHINES: NMACH = 2

DEFLECTION COMMAND: DC = 1.1 flap deg

TOTAL NUMBER OF INTEGRATIONS: NUMINT = 2000

TOTAL NUMBER OF MECHANICAL-POSITION LOOP INTEGRATIONS: NINTI = 2000

TOTAL NUMBER OF VELOCITY LOOP INTEGRATIONS: 2000

TOTAL SIMULATION TIME: 0.4 sec

TOTAL NUMBER OF POINTS PLOTTED: 1001

TOTAL NUMBER OF NETWORK CHANGES: 0

TIME TO DC: .114 sec

TIME TO FIRST PEAK: .163 sec

PEAK DEFLECTION: 1.3329 flap deg

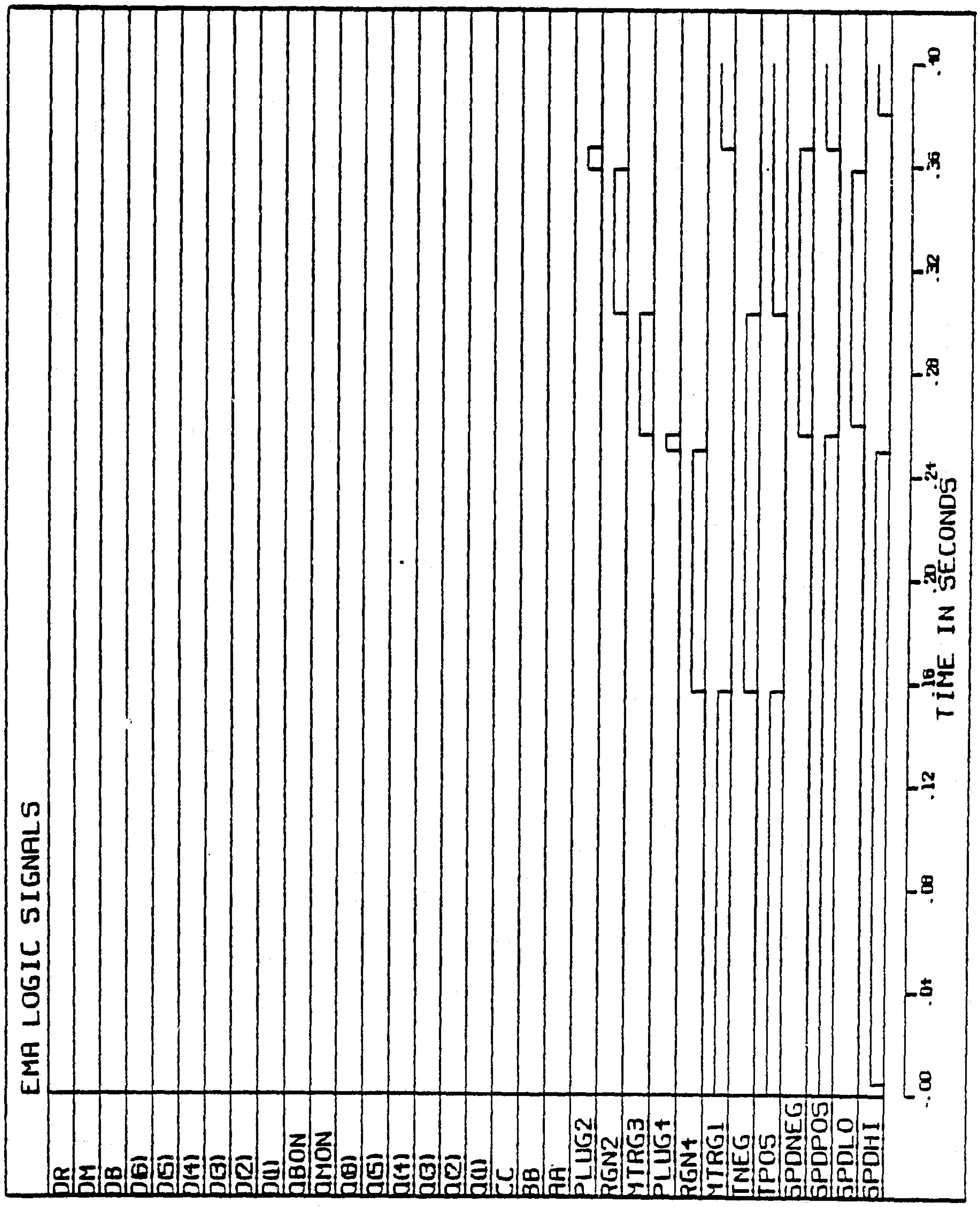
EMA LOGIC SIGNALS
TIME IN SECONDS
.00
.04
.08
.12
.16
.20
.24
.28
.32
.36
.40

Figure E.1-1

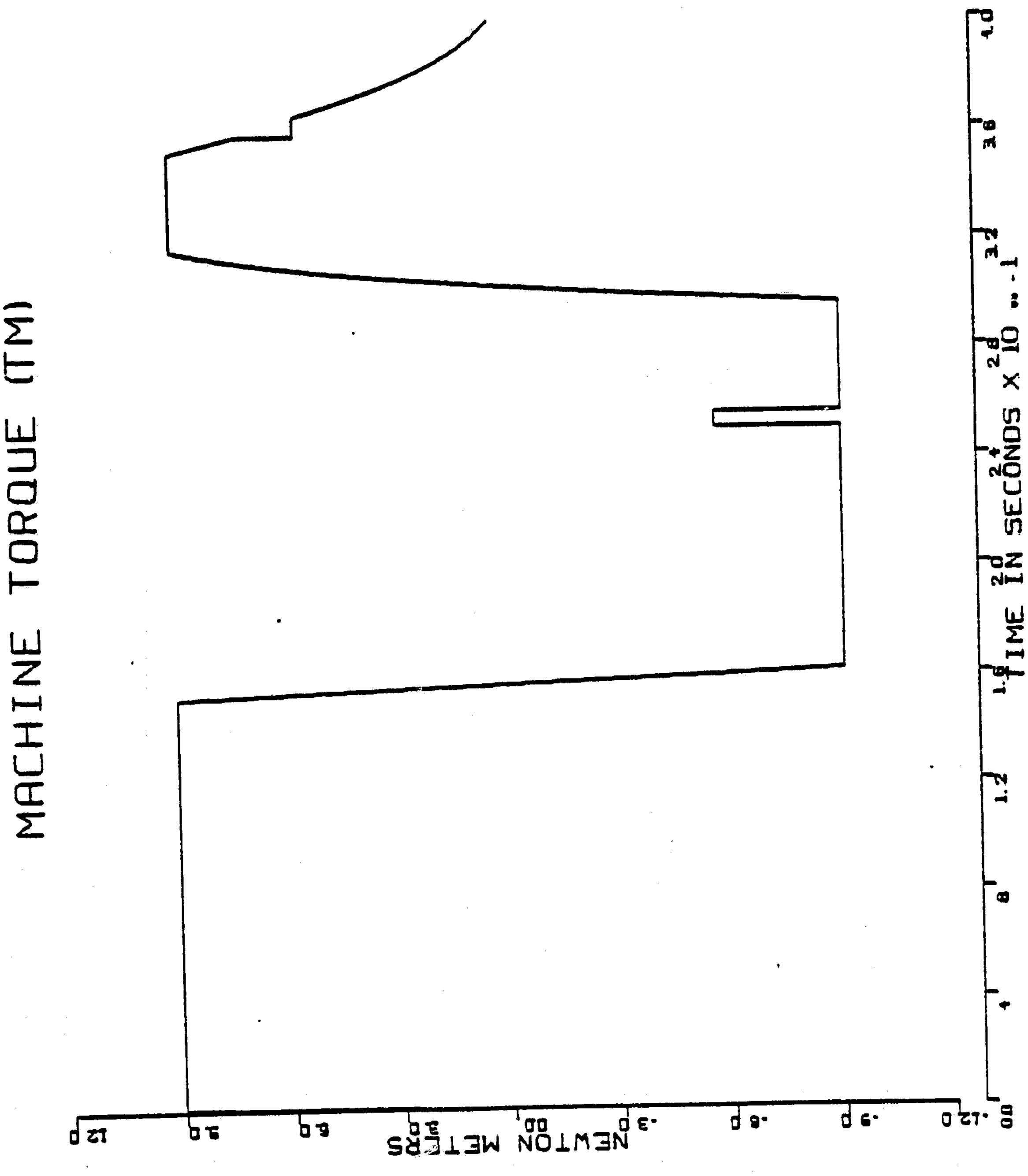

Figure E.1-2

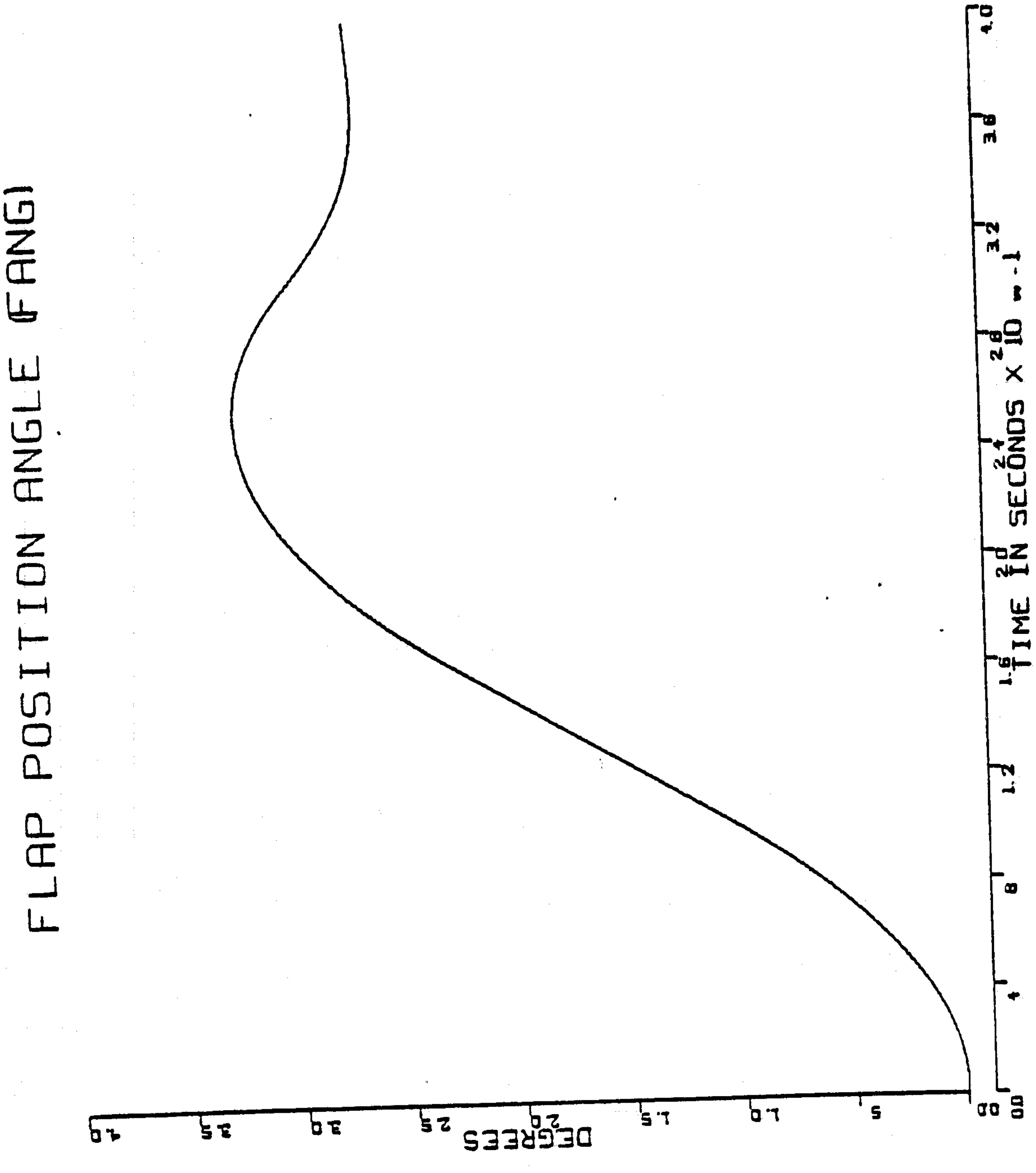
FLAP POSITION ANGLE (FANG)
TIME IN SECONDS X 10 ** -1
DEGREES
0.0
.4
.8
1.2
1.6
2.0
2.4
2.8
3.2
3.6
4.0
.5
1.0
1.5
2.0
2.5
3.0
3.5
4.0

Figure #.1-3

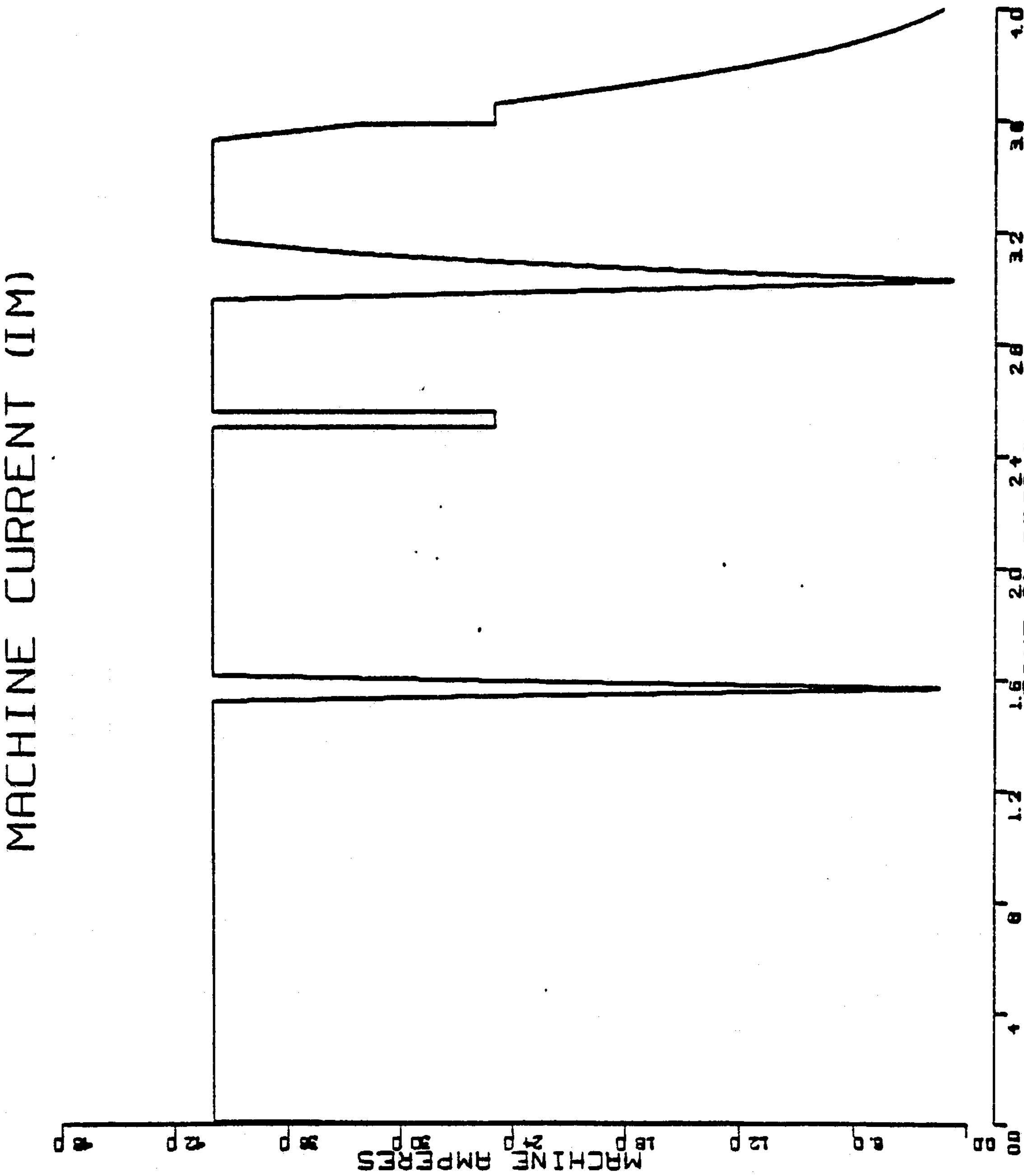

Figure E.1-4

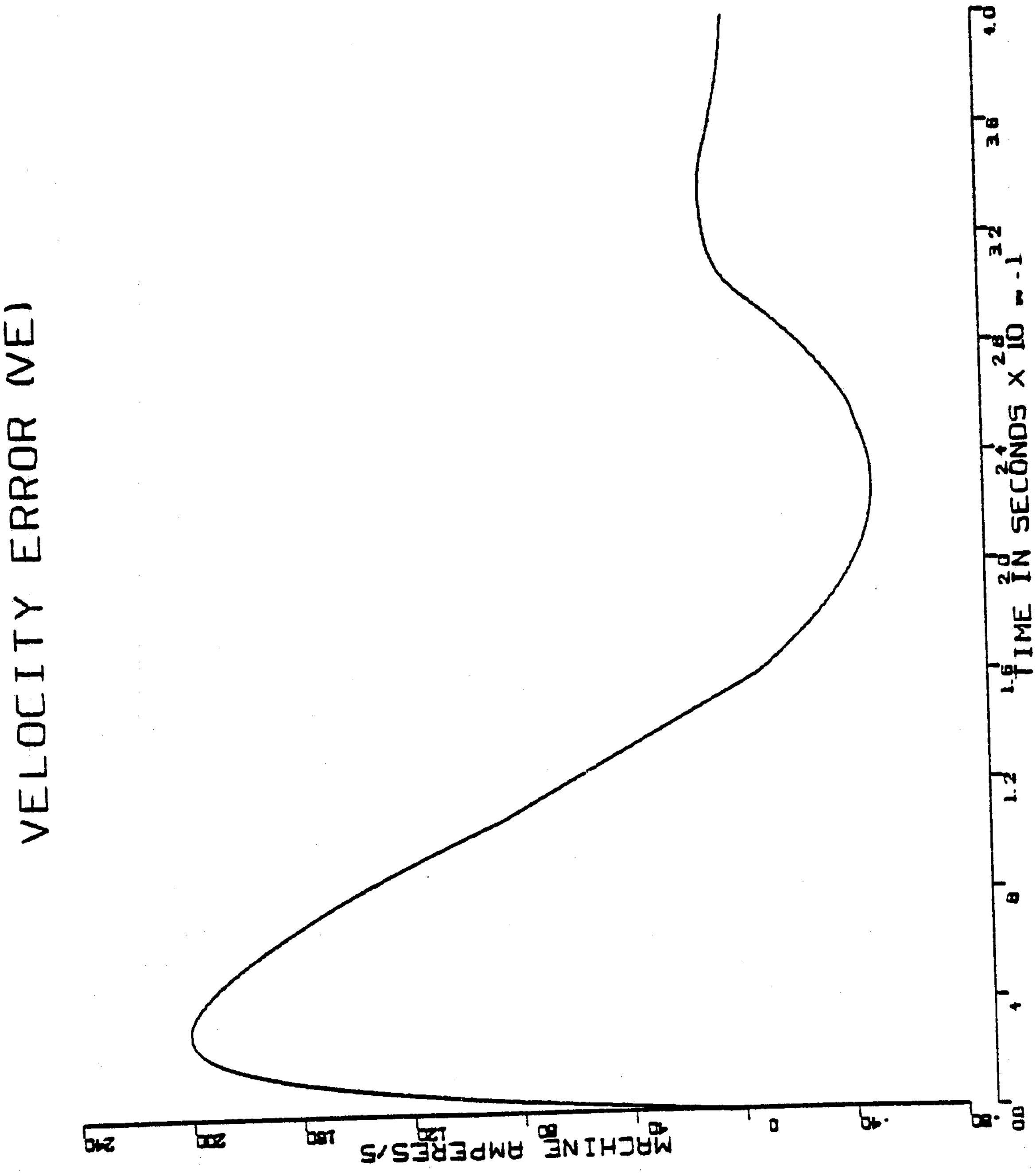
VELOCITY ERROR (VE)
TIME IN SECONDS X 10 ** -1
MACHINE AMPERES/S
0.0
.4
.8
1.2
1.6
2.0
2.4
2.8
3.2
3.6
4.0
-80
-40
0
40
80
120
160
200
240

Figure E.1-5

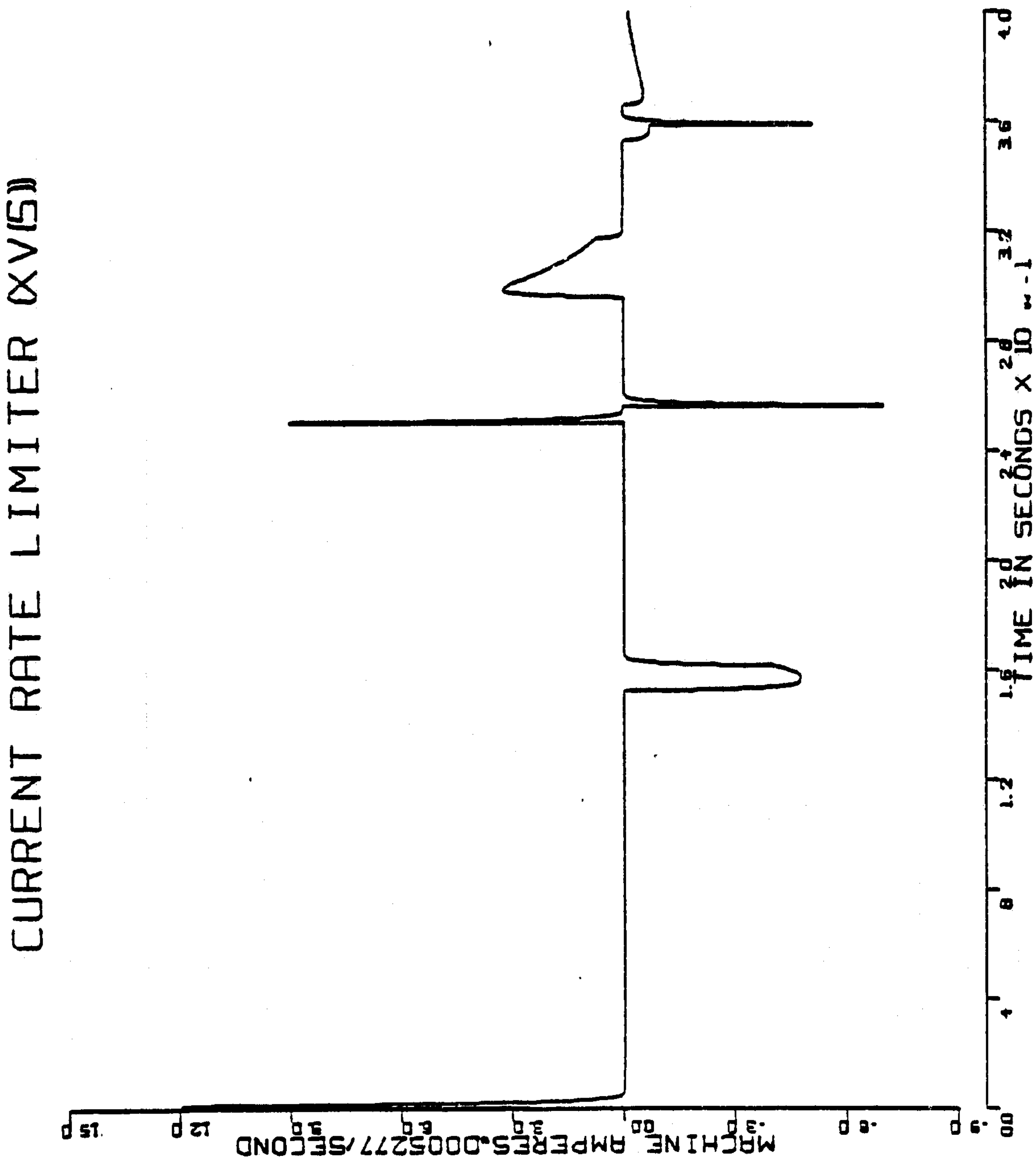

CURRENT RATE LIMITER (XV(5))
TIME IN SECONDS x 10 ** -1
MACHINE AMPERES.0005277/SECOND

Figure E.1-6

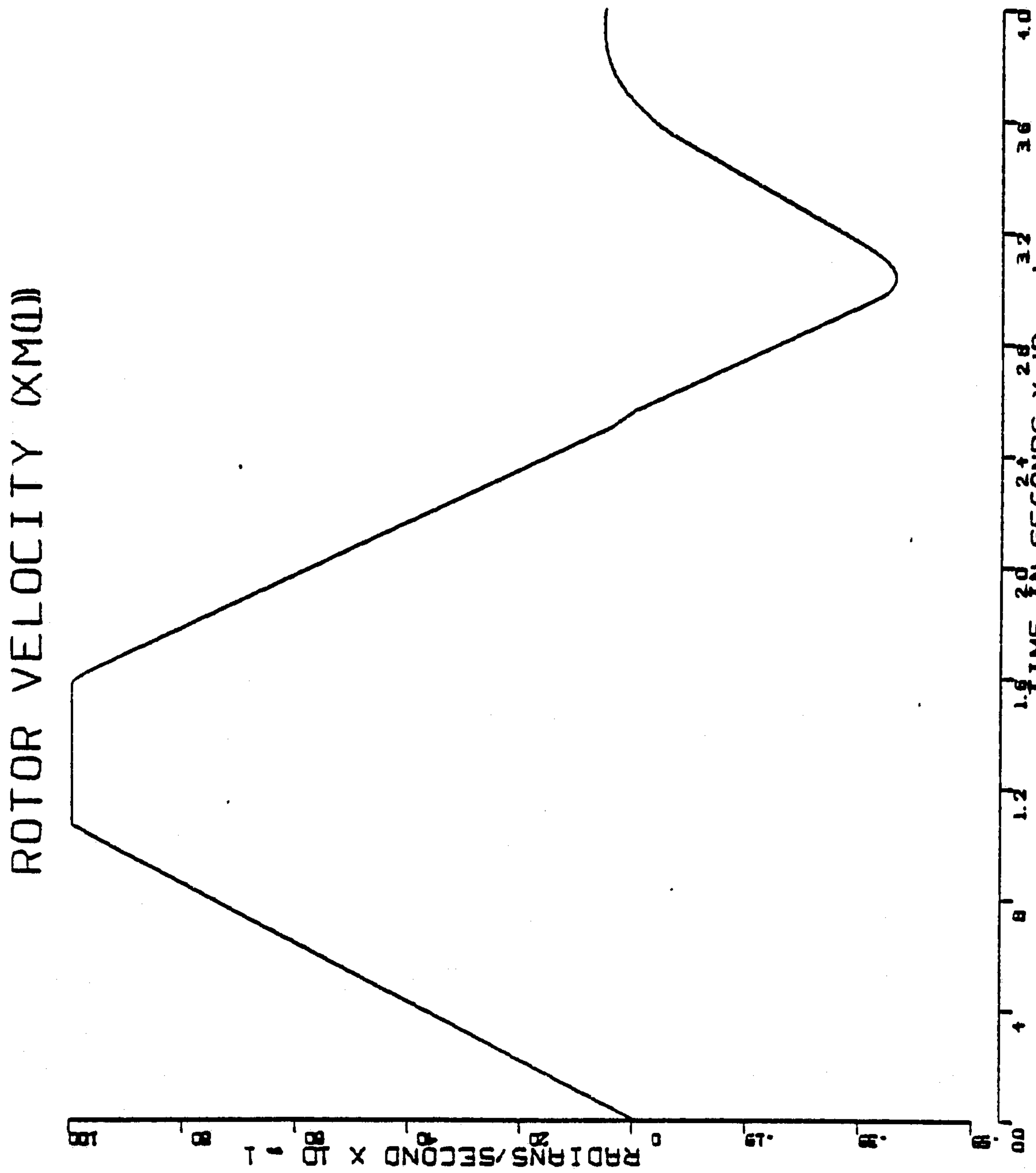
ROTOR VELOCITY (XM(1))
TIME IN SECONDS X 10 ** -1
RADIANS/SECOND X 10 ** 1
0.0
.4
.8
1.2
1.6
2.0
2.4
2.8
3.2
3.6
4.0
100
80
60
40
20
0

Figure E.1-7

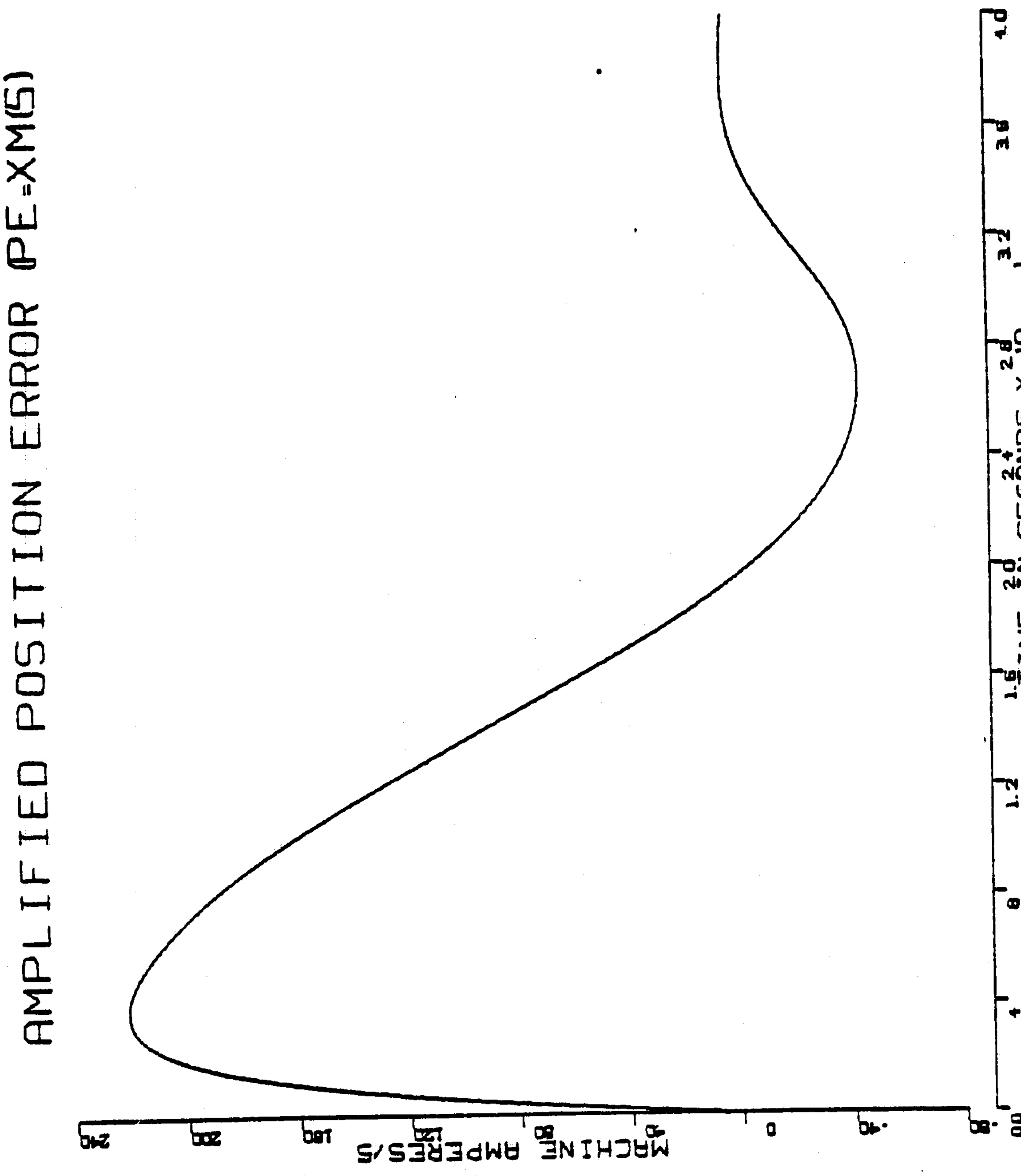
AMPLIFIED POSITION ERROR (PE=XM(5))
TIME IN SECONDS X 10 ** -1
0.0
.4
.8
1.2
1.6
2.0
2.4
2.8
3.2
3.6
4.0
MACHINE AMPERES/S
-80
-40
0
40
80
120
160
200
240

Figure E.1-8

APPENDIX E.2 CALCOMP PLOTS: 10^{th} Order EMA Model DC = 1.65°

RUN SUMMARY

MODE: 10^{th} ORDER EMA MODEL

PROGRAM MODE: PGMODE = 2

NUMBER OF MACHINES: NMACH = 2

DEFLECTION COMMAND: DC = 1.65 flap deg

TOTAL NUMBER OF INTEGRATIONS: NUMINT = 2000

TOTAL NUMBER OF MECHANICAL-POSITION LOOP INTEGRATIONS: NINTI = 2000

TOTAL NUMBER OF VELOCITY LOOP INTEGRATIONS: 2000

TOTAL SIMULATION TIME: 0.4 sec

TOTAL NUMBER OF POINTS PLOTTED: 1001

TOTAL NUMBER OF NETWORK CHANGES: 0

TIME TO DC: .139 sec

TIME TO FIRST PEAK: .204 sec

PEAK DEFLECTION: 2.14 flap deg

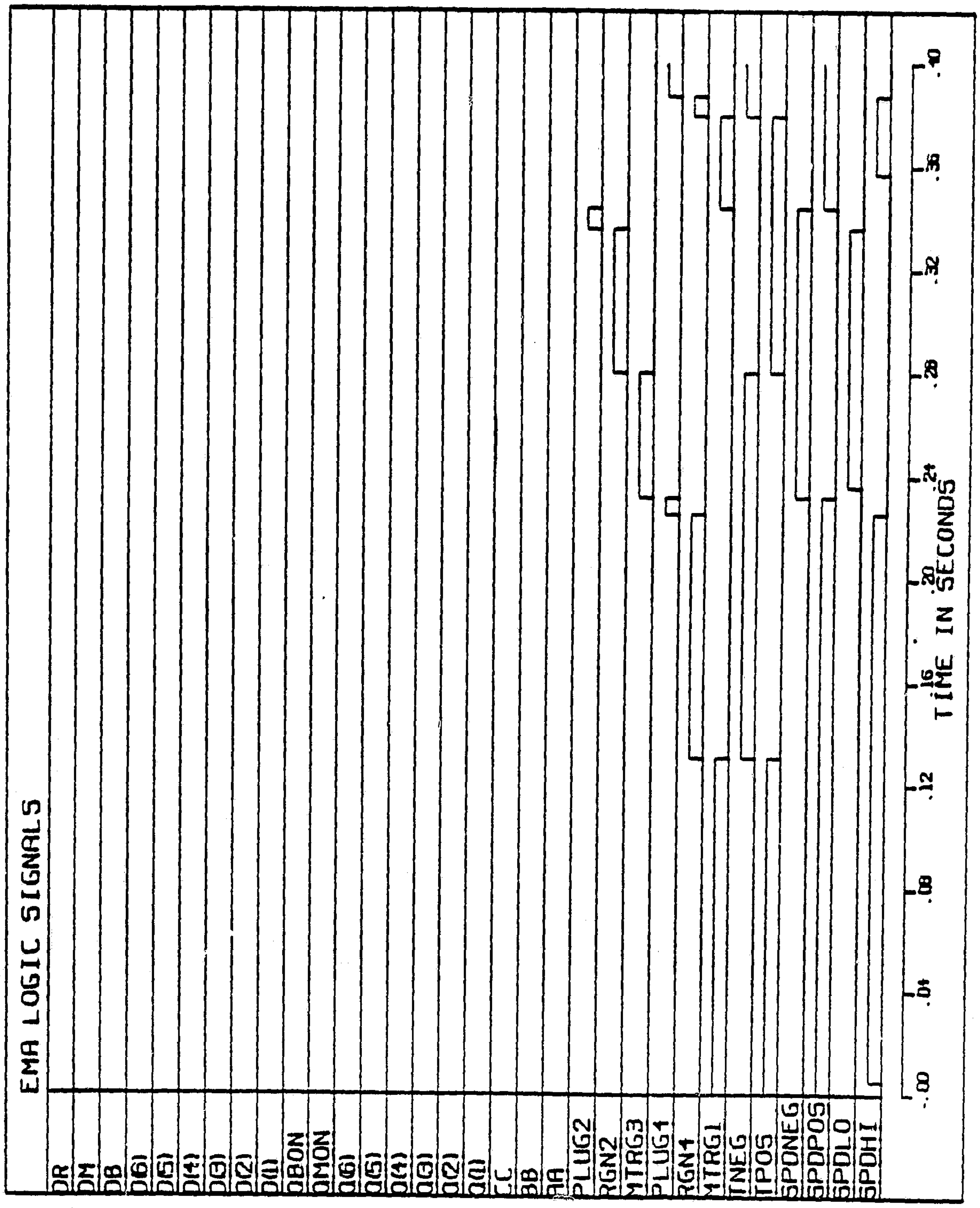
EMA LOGIC SIGNALS
DR
DM
DB
PLUG2
RGN2
MTRG3
PLUG1
RGN4
MTRG1
TNEG
TPOS
SPDNEG
SPDPOS
SPDLO
SPDHI
.00
.04
.08
.12
.16
.20
.24
.28
.32
.36
.40
TIME IN SECONDS

Figure E.2-1

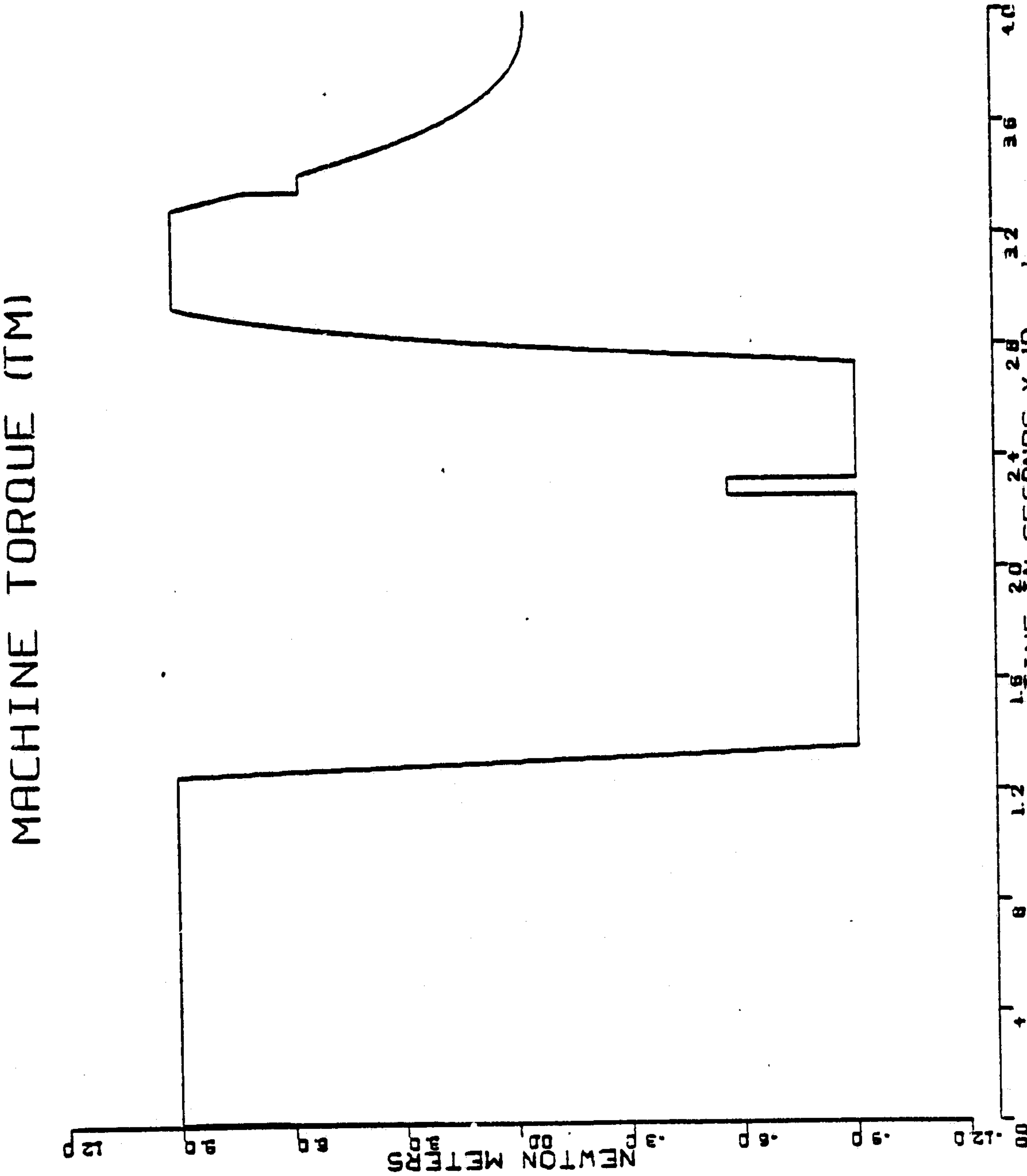

Figure E.2-2

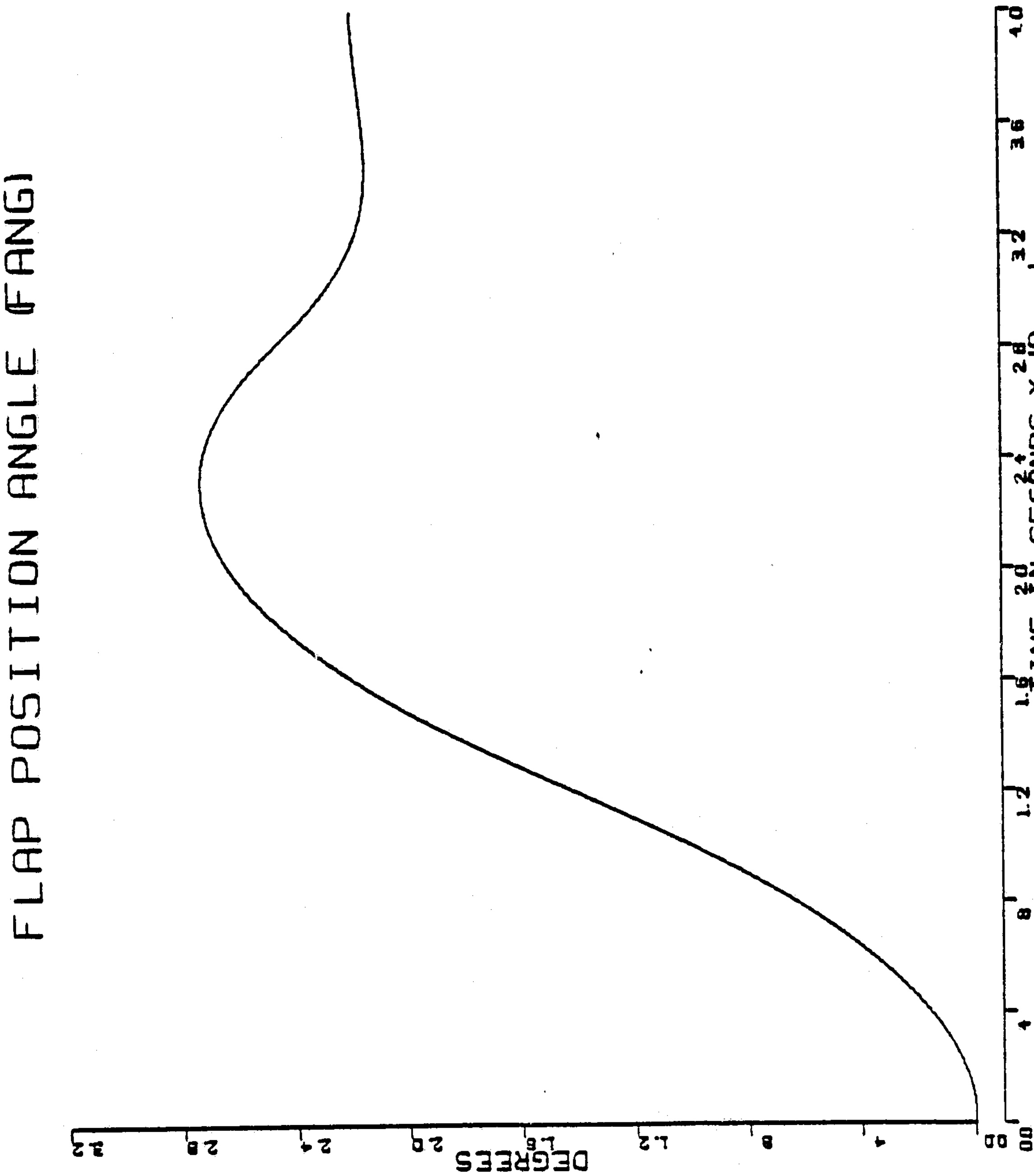
FLAP POSITION ANGLE (FANG)
DEGREES
TIME IN SECONDS X 10 ** -1
.0
.4
.8
1.2
1.6
2.0
2.4
2.8
3.2
3.6
4.0

Figure E.2-3

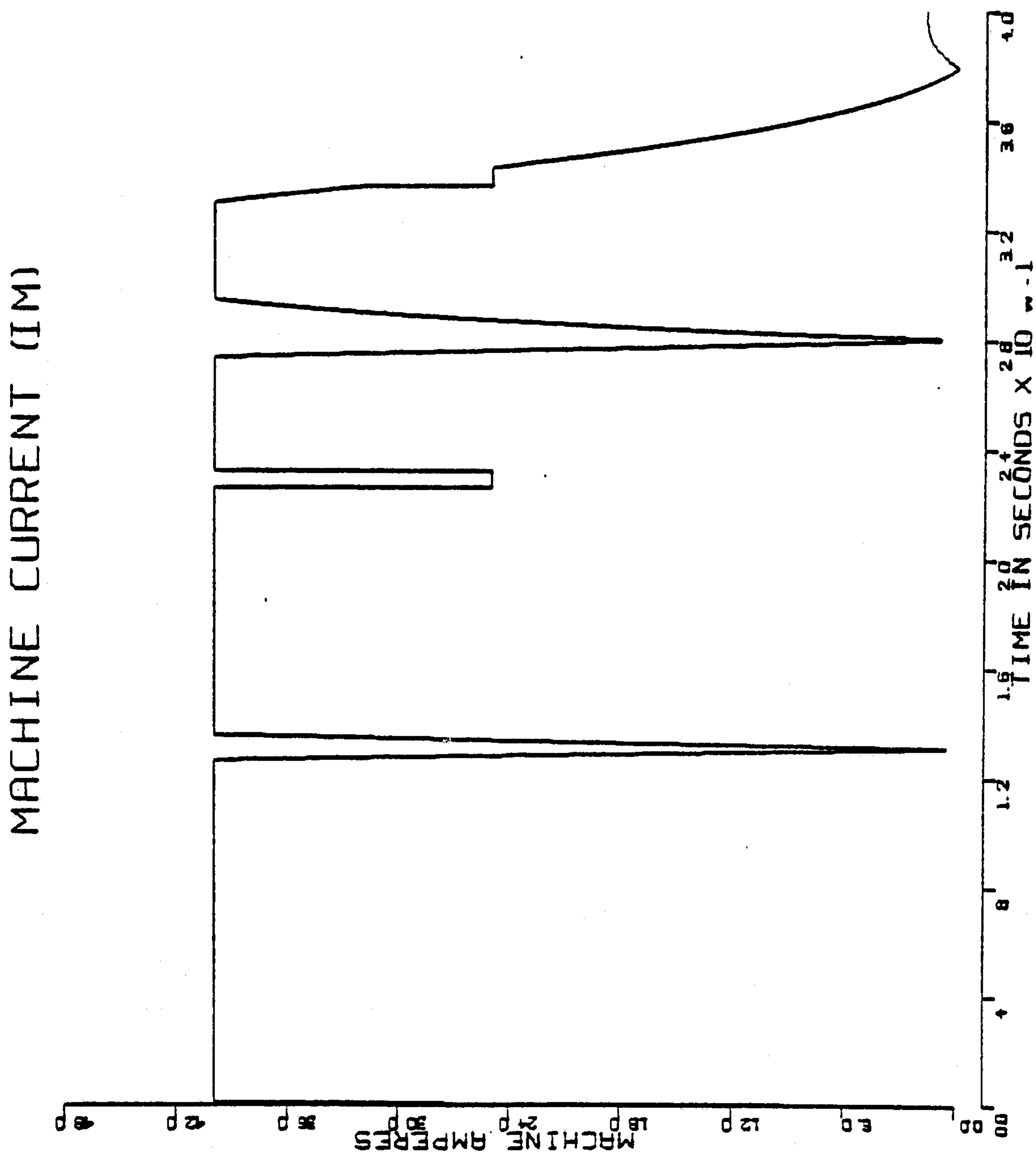

Figure E.2-4

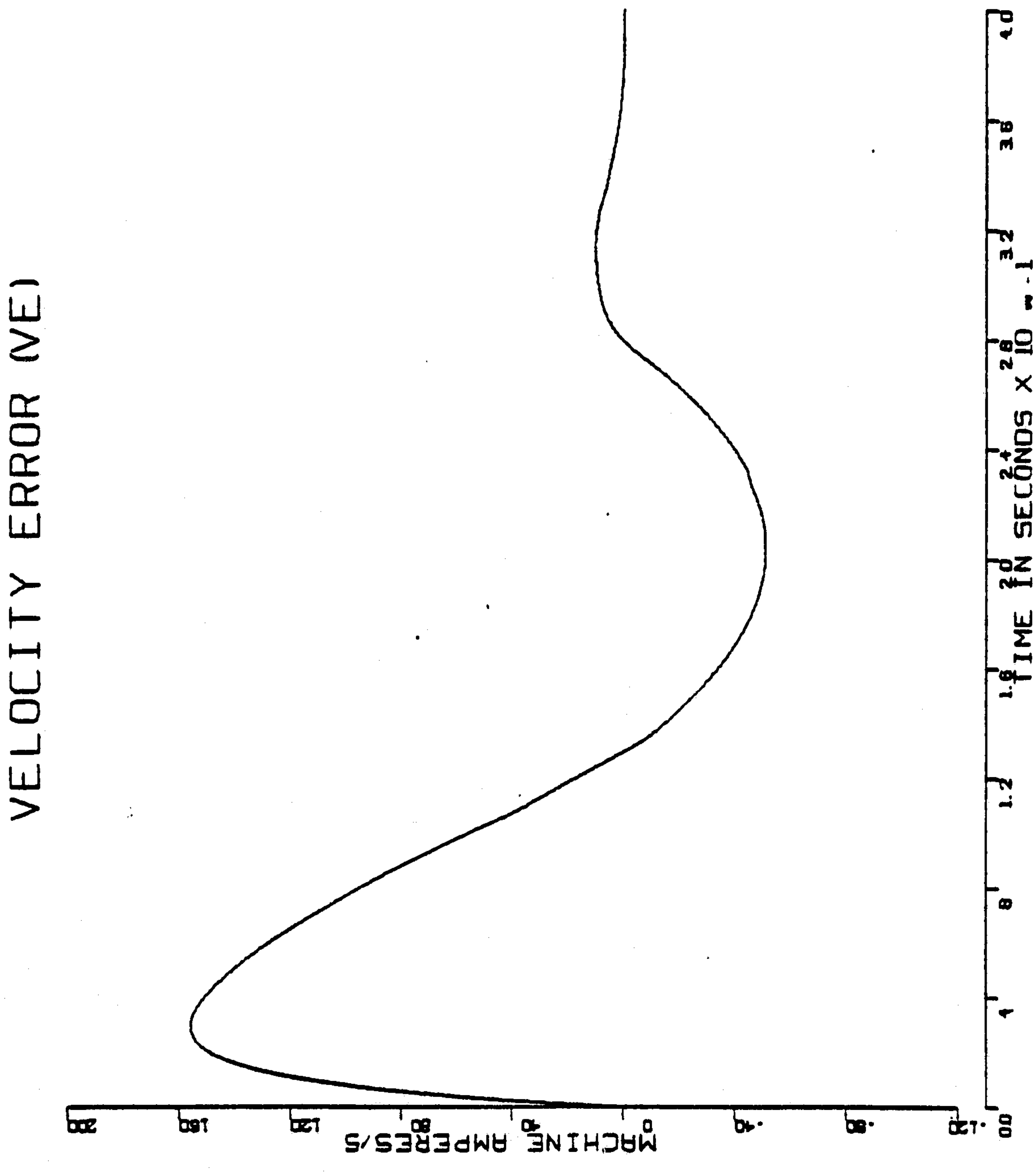

Figure E.2-5

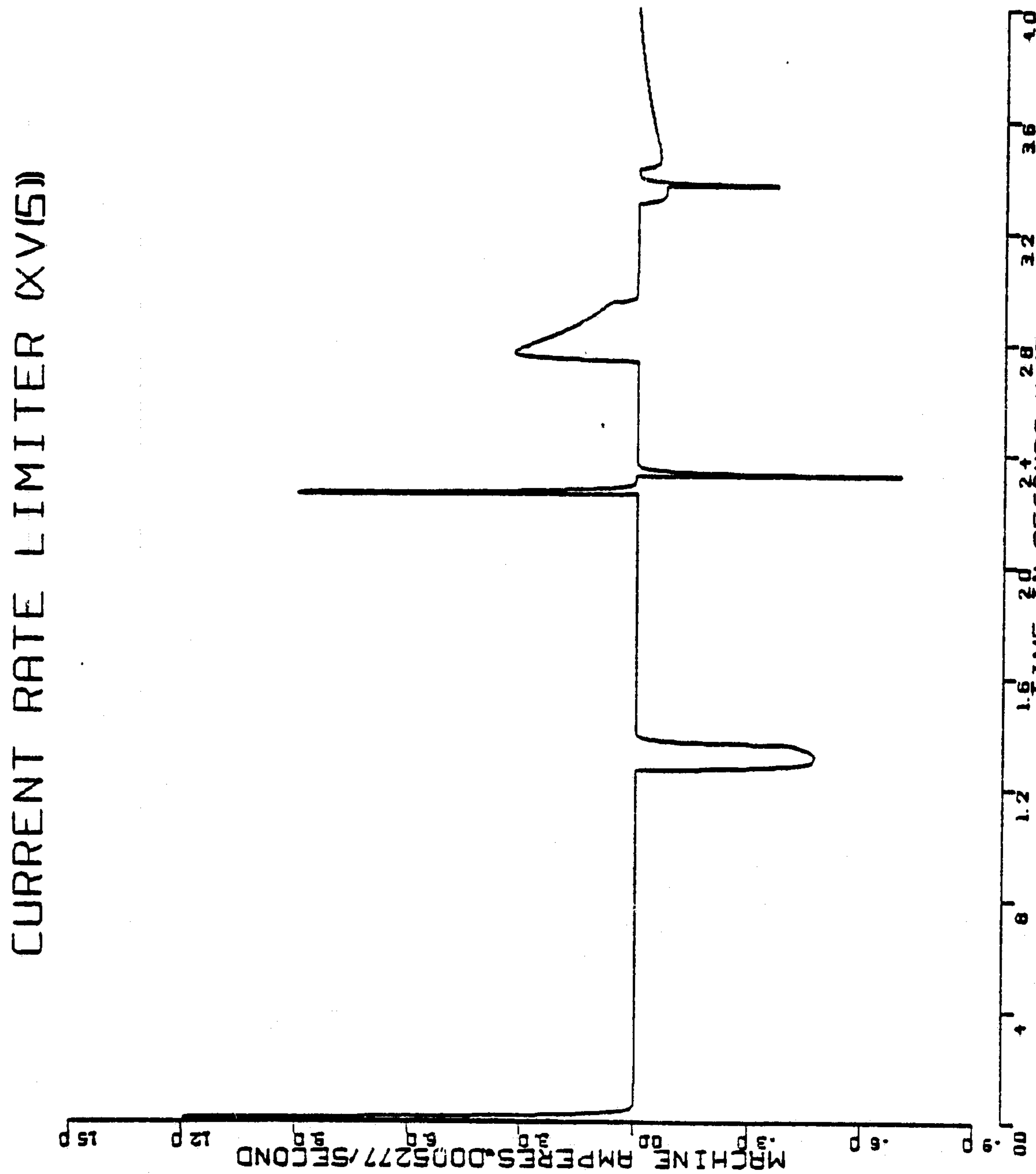

Figure E.2-6

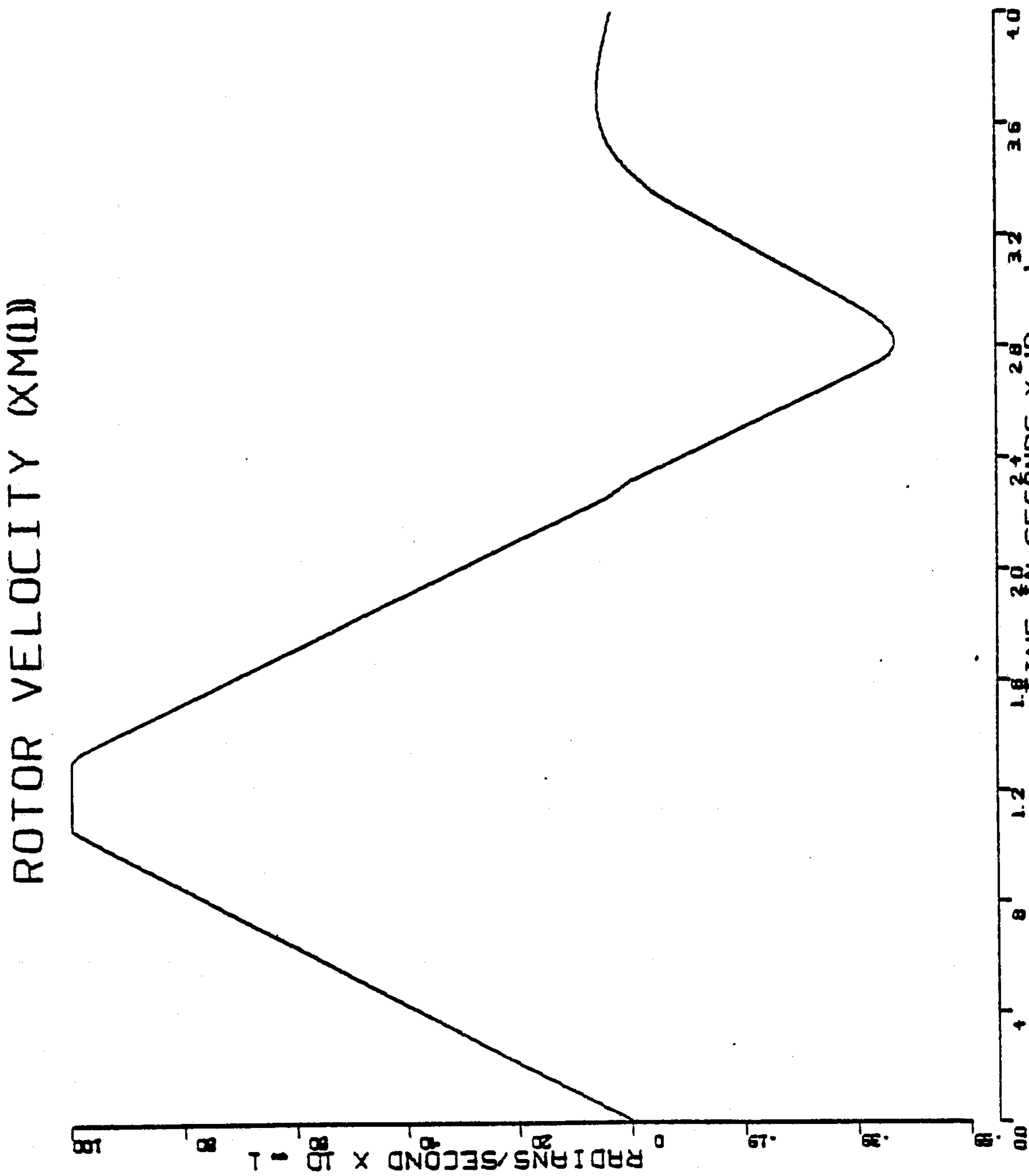
ROTOR VELOCITY (XM(1))
TIME IN SECONDS X 10 ** -1
RADIANS/SECOND X 10 ** 1

Figure E.2-7

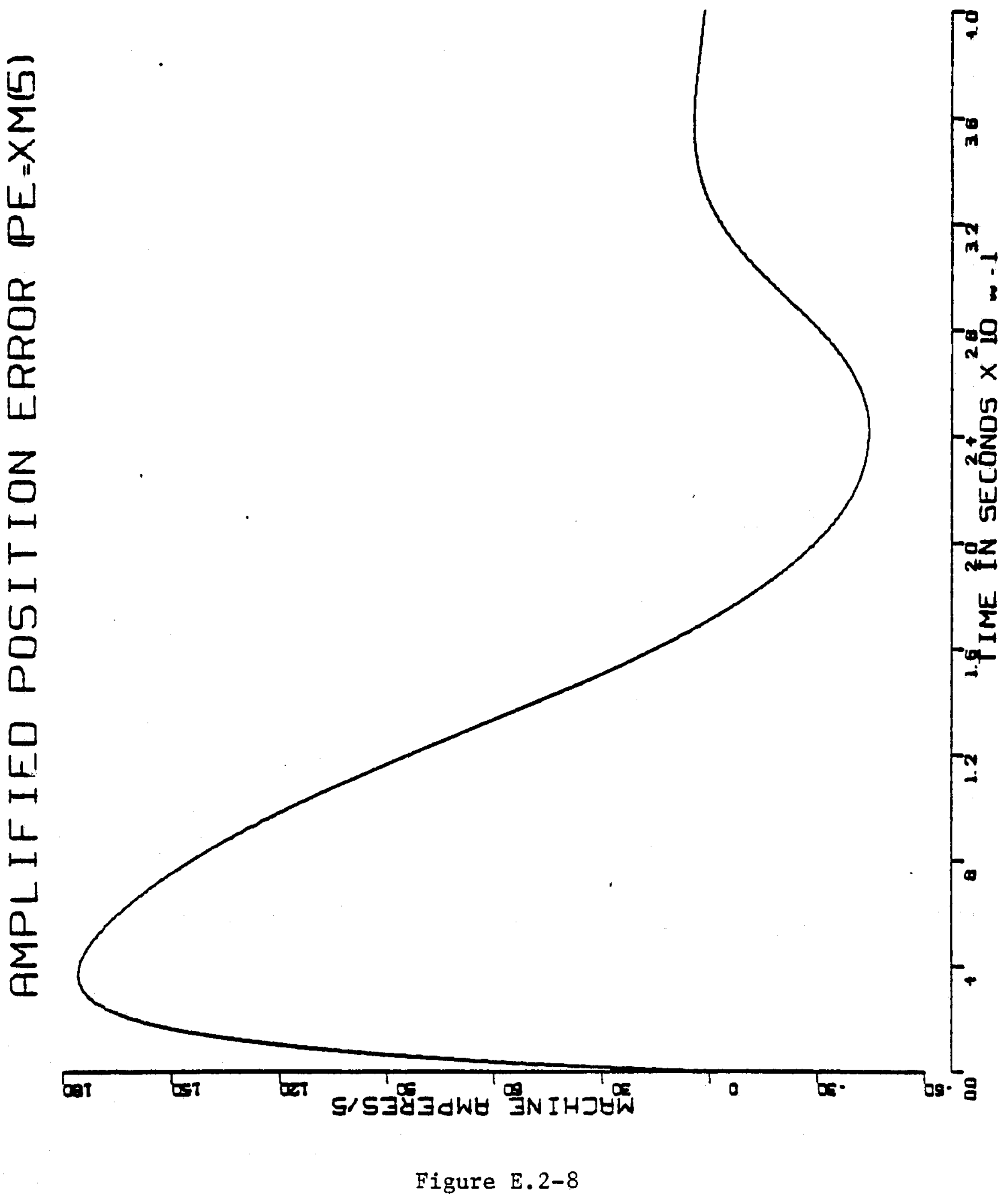
AMPLIFIED POSITION ERROR (PE=XM(5))
TIME IN SECONDS X 10 ** -1
0.0 .4 .8 1.2 1.6 2.0 2.4 2.8 3.2 3.6 4.0
MACHINE AMPERES/S
-60 -30 0 30 60 90 120 150 180

Figure E.2-8

APPENDIX E.3 CALCOMP PLOTS: 10^{th} Order EMA Model DC = 2.2°

PROGRAM SUMMARY

MODE: 10^{th} ORDER EMA MODEL

PROGRAM MODE: PGMODE = 2

NUMBER OF MACHINES: NMACH = 2

DELFECTION COMMAND: DC = 2.2 flap deg

TOTAL NUMBER OF INTEGRATIONS: NUMINT = 2000

TOTAL NUMBER OF MECHANICAL-POSITION LOOP INTEGRATIONS: NINTI = 2000

TOTAL NUMBER OF VELOCITY LOOP INTEGRATIONS: 2000

TOTAL SIMULATION TIME: 0.4 sec

TOTAL NUMBER OF POINTS PLOTTED: 1001

TOTAL NUMBER OF NETWORK CHANGES: 0

TIME TO DC: .163 sec

TIME TO FIRST PEAK: .229 sec

PEAK DELFECTION: 2.73 flap deg

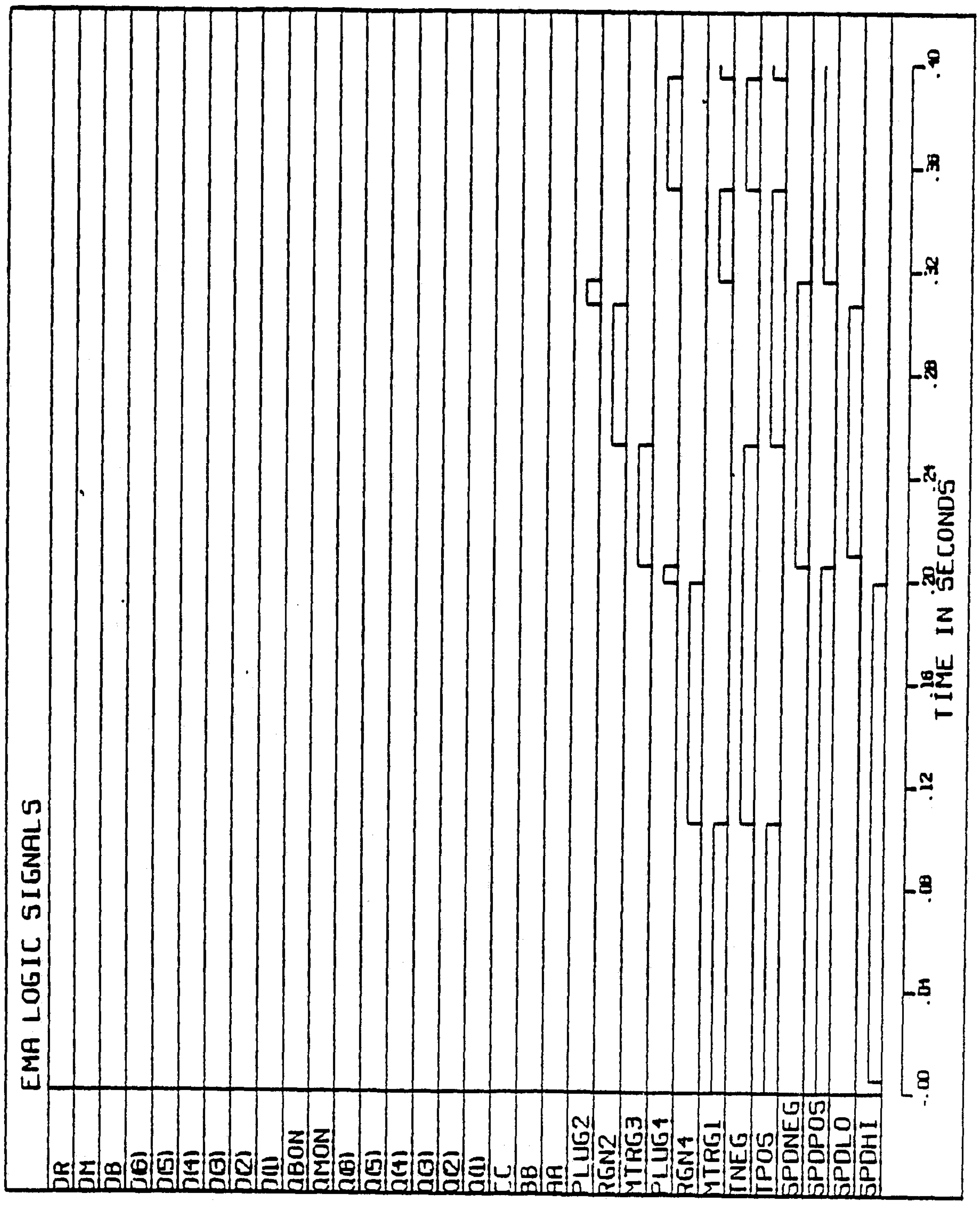
EMA LOGIC SIGNALS
DR
DM
DB
D(6)
D(5)
D(4)
D(3)
D(2)
D(1)
QBON
QMON
Q(6)
Q(5)
Q(4)
Q(3)
Q(2)
Q(1)
LC
BB
AA
PLUG2
RGN2
MTRG3
PLUG4
RGN4
MTRG1
TNEG
TPOS
SPDNEG
SPDPOS
SPDLO
SPDHI
-.00
.04
.08
.12
.16
.20
.24
.28
.32
.36
.40
TIME IN SECONDS

Figure E.3-1

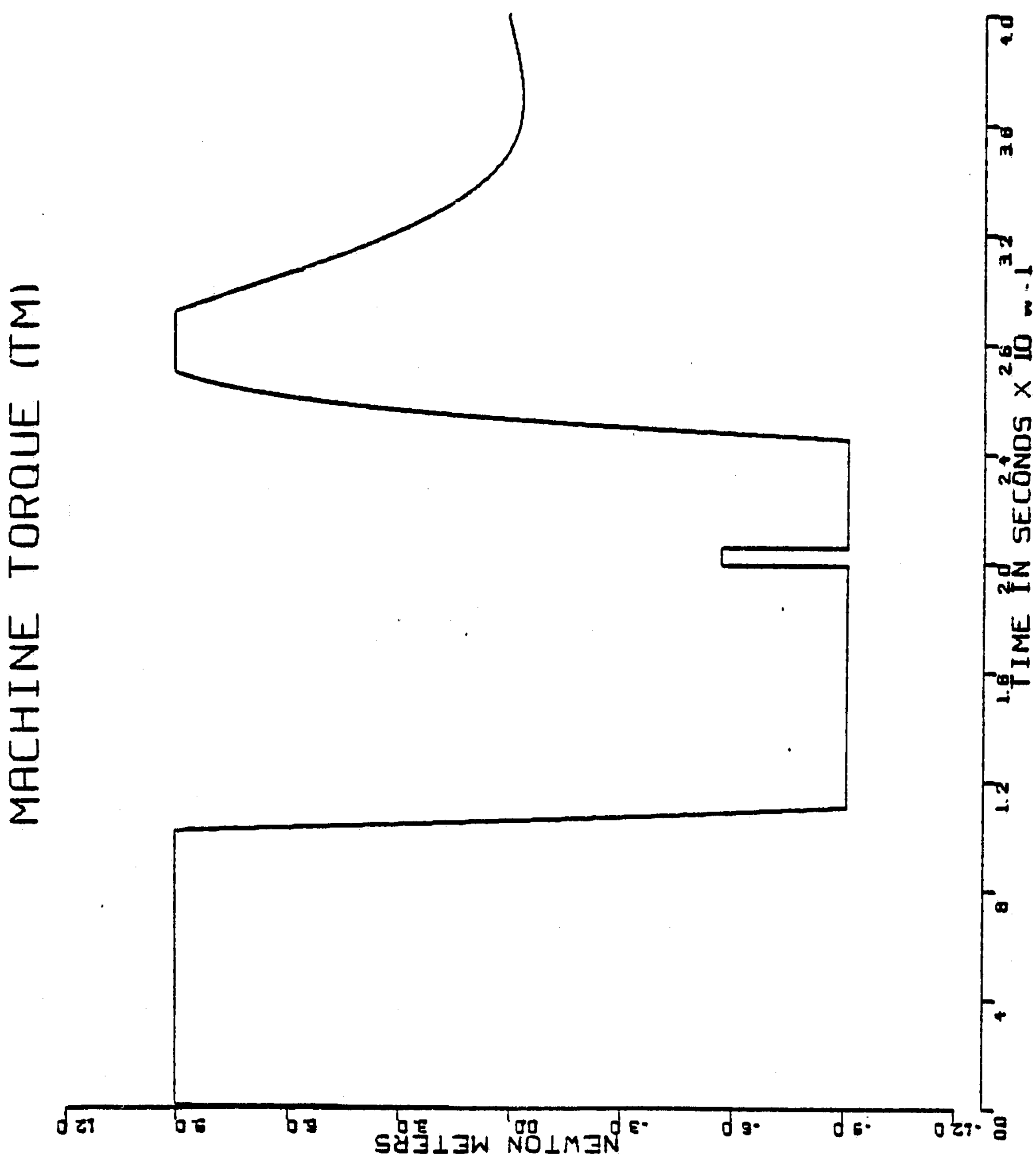
MACHINE TORQUE (TM)
TIME IN SECONDS x 10 -1
NEWTON METERS
12.0
9.0
6.0
3.0
0.0
-3.0
-6.0
-9.0
-12.0
0.0
.4
.8
1.2
1.6
2.0
2.4
2.8
3.2
3.6
4.0

Figure E.3-2

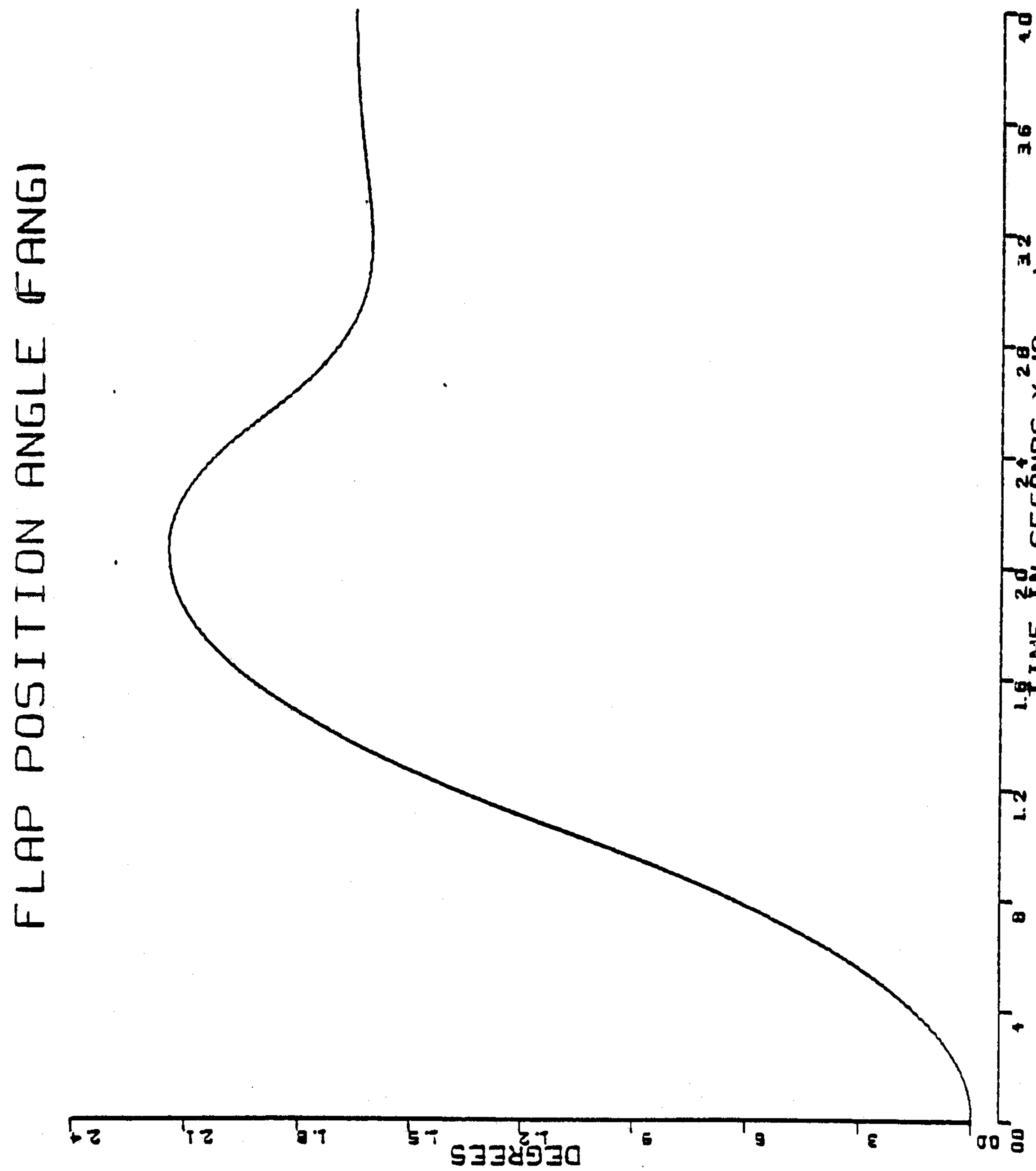
FLAP POSITION ANGLE (FANG)
TIME IN SECONDS × 10 ** -1
DEGREES
0.0
.4
.8
1.2
1.6
2.0
2.4
2.8
3.2
3.6
4.0
.3
.6
.9
1.2
1.5
1.8
2.1
2.4

Figure E.3-3

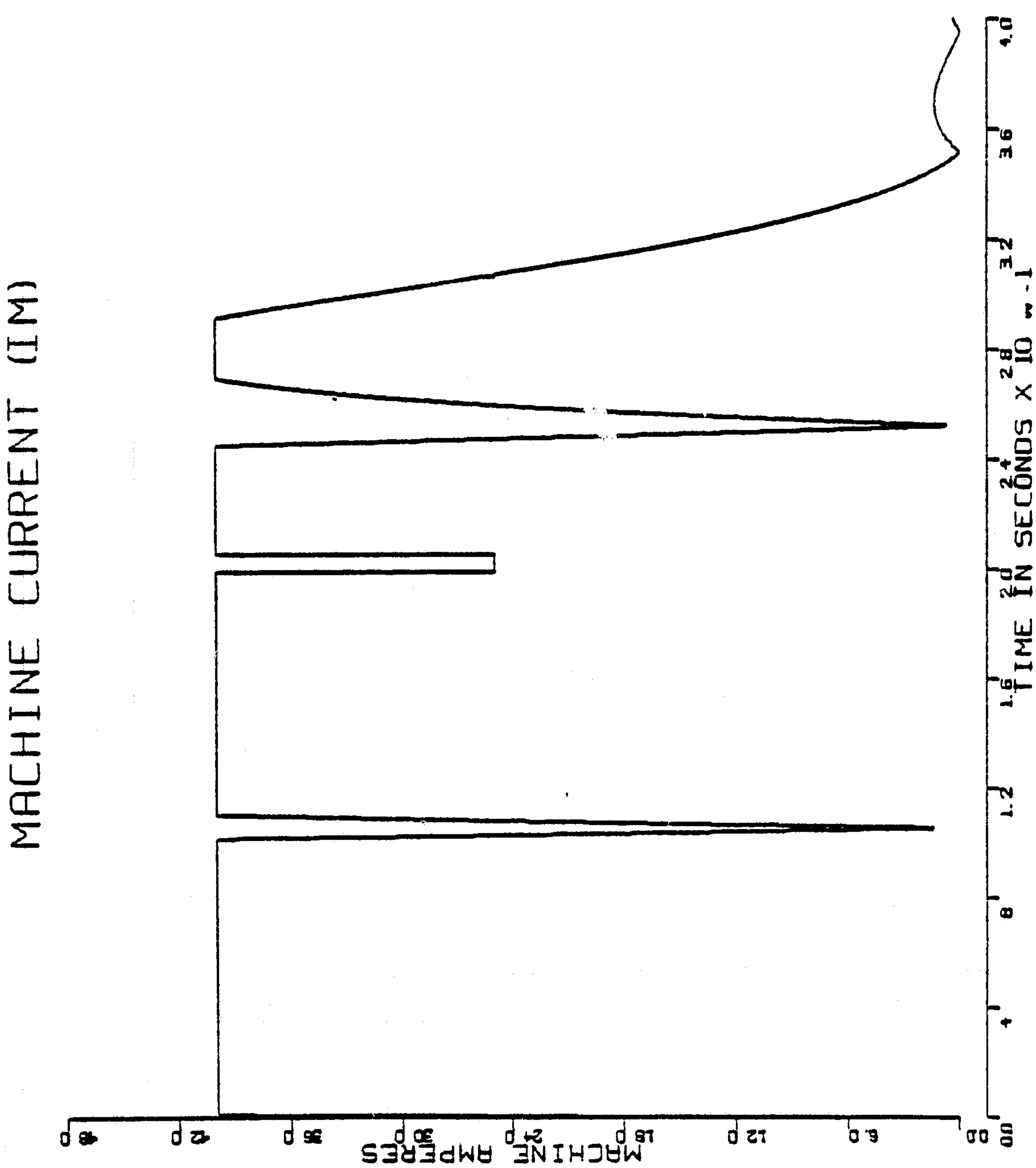

Figure E.3-4

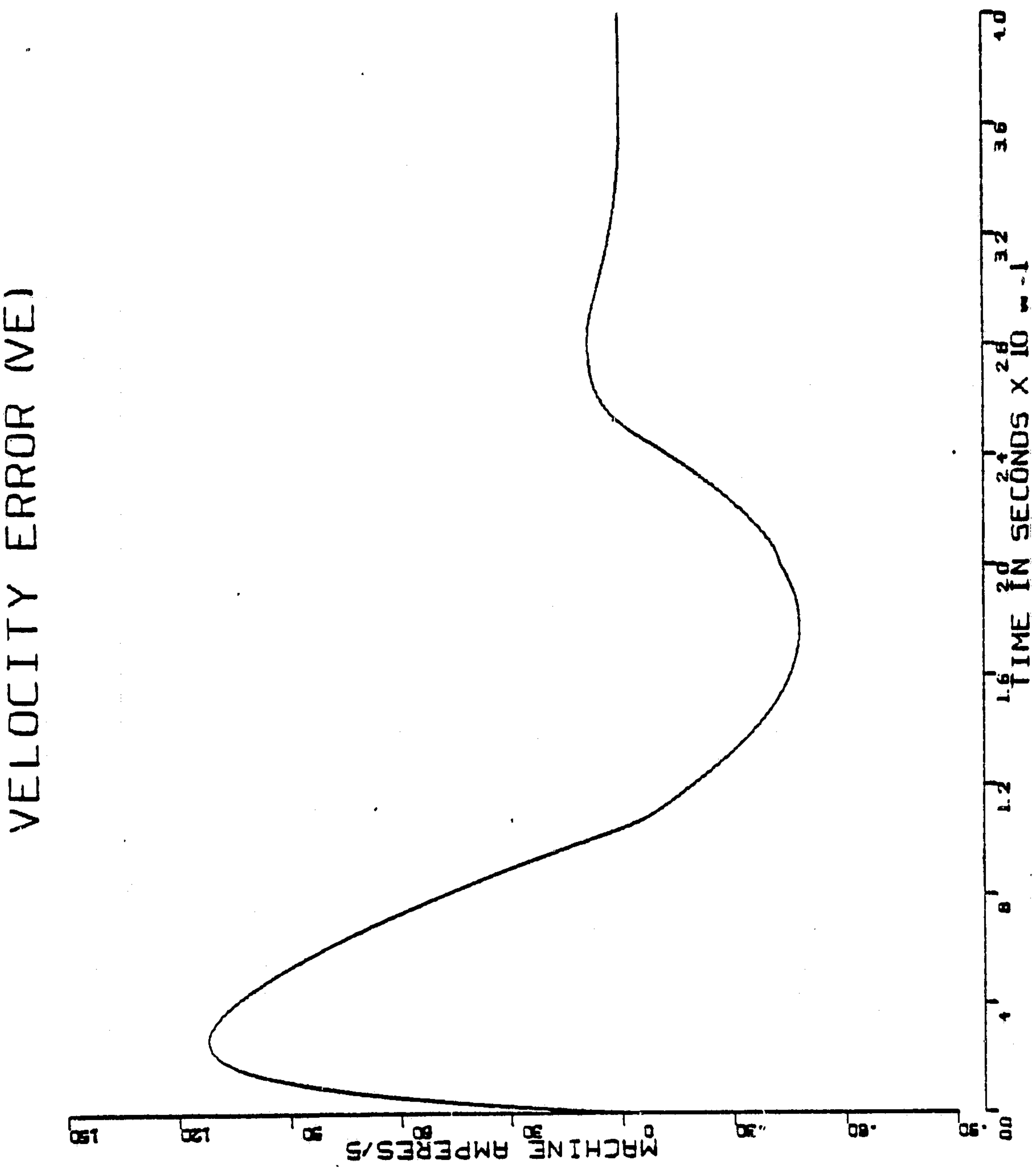

Figure E.3-5

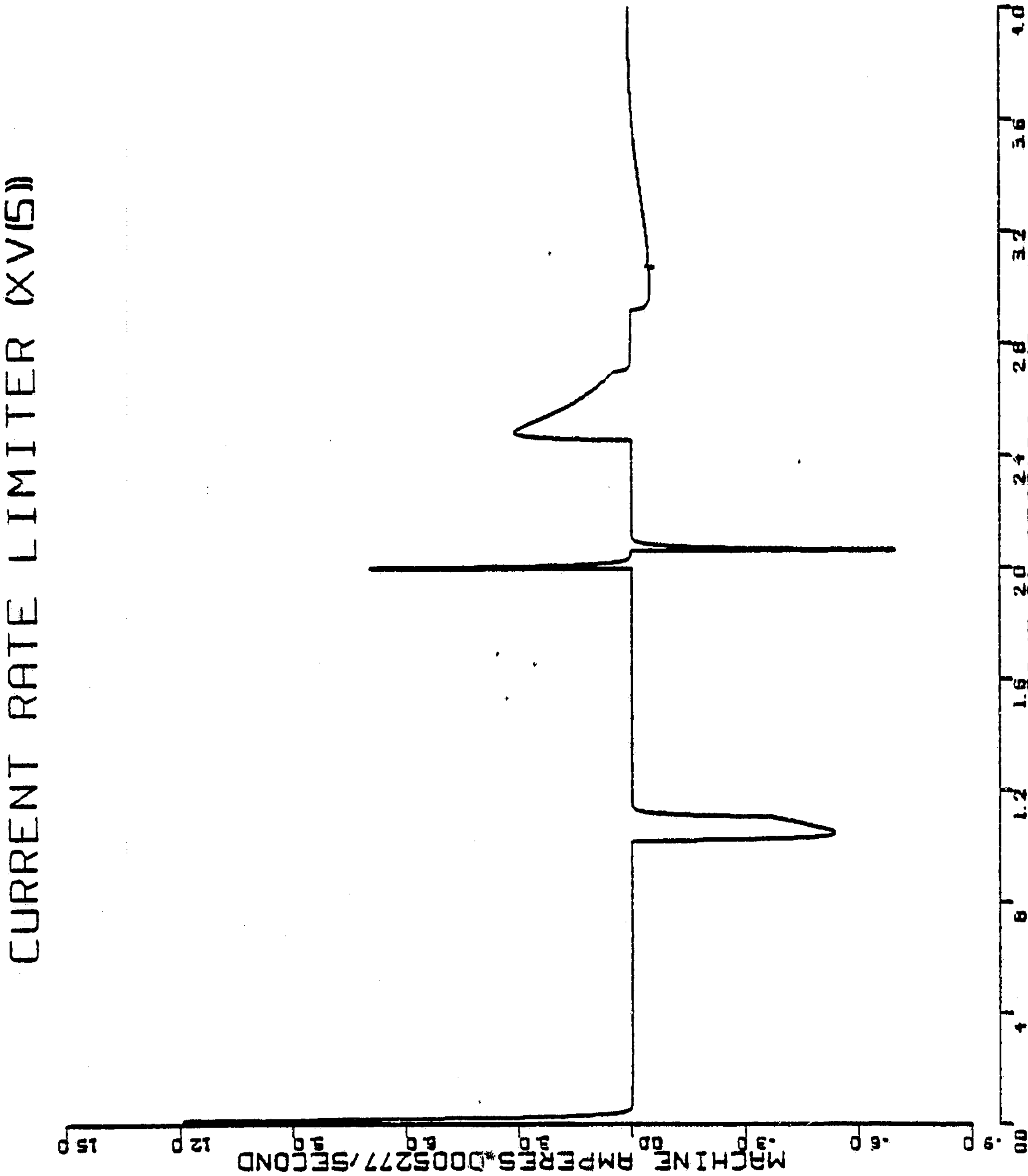
CURRENT RATE LIMITER (XV(5))
TIME IN SECONDS X 10 ** -1
MACHINE AMPERES*.0005277/SECOND
.0
.4
.8
1.2
1.6
2.0
2.4
2.8
3.2
3.6
4.0
-9.0
-6.0
-3.0
.0
3.0
6.0
9.0
12.0
15.0

Figure E.3-6

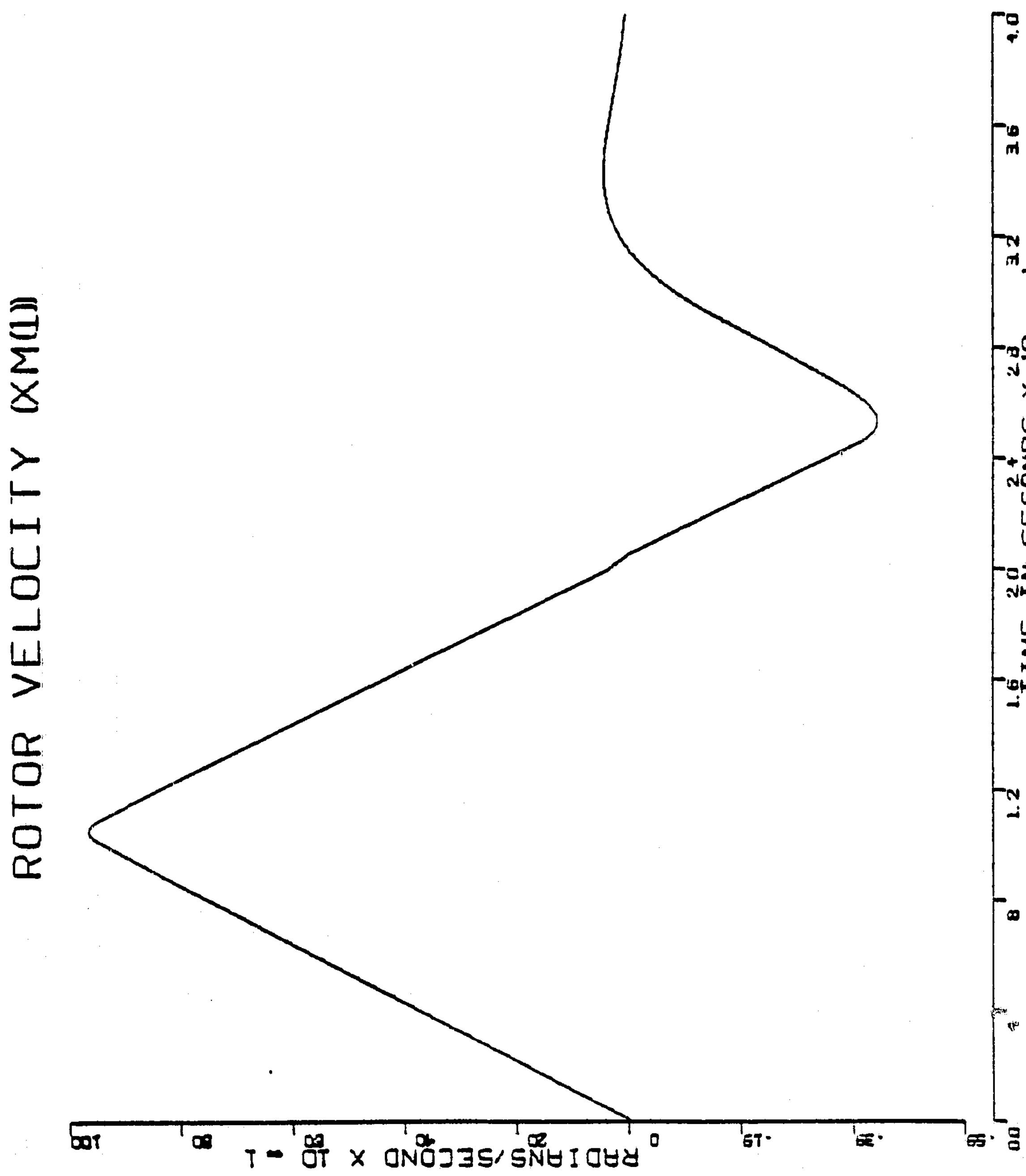
ROTOR VELOCITY (XM(1))
TIME IN SECONDS X 10 ** -1
RADIANS/SECOND X 10 ** 1

Figure E.3-7

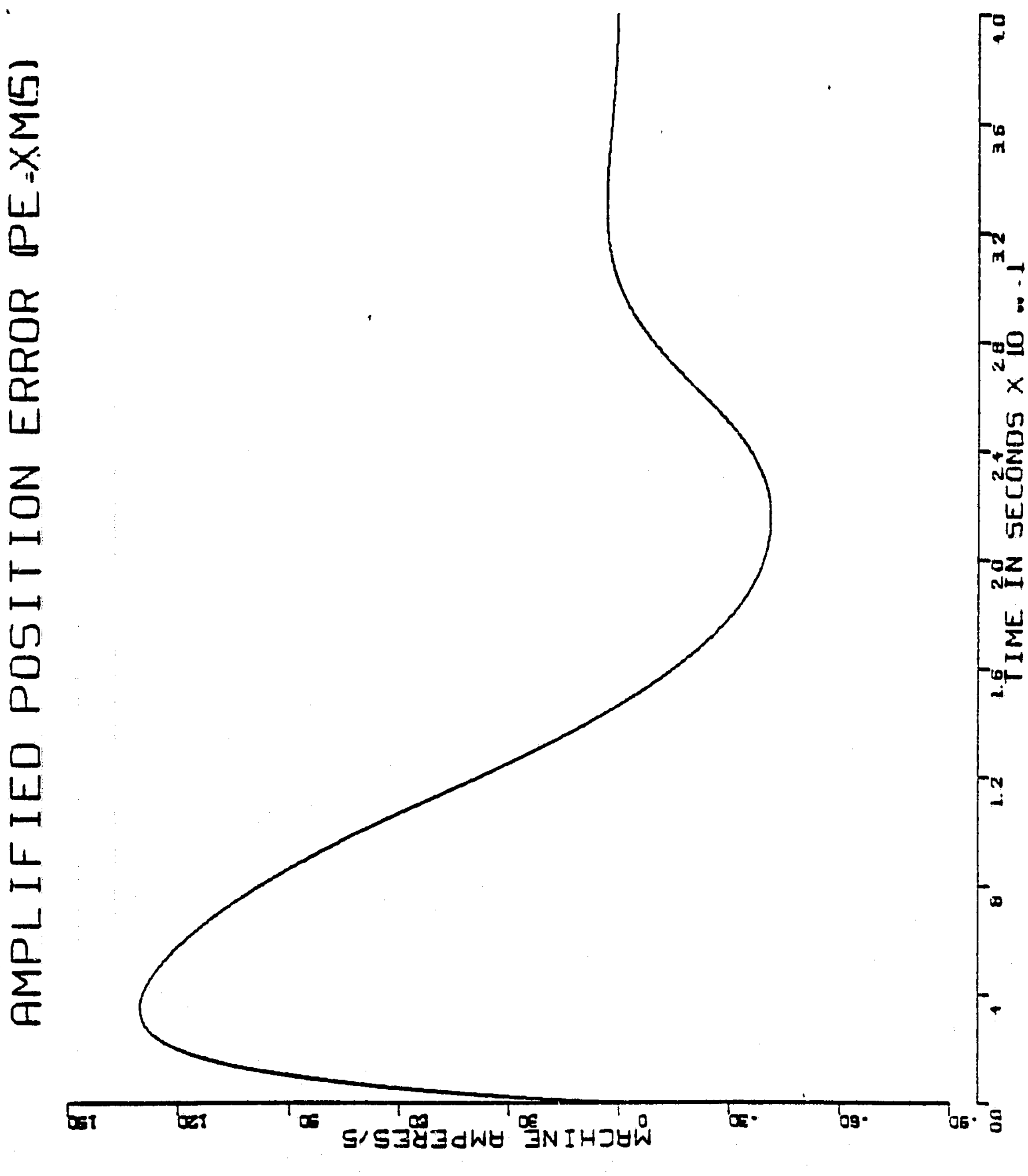
AMPLIFIED POSITION ERROR (PE-XM(5))
TIME IN SECONDS x 10 ** -1
MACHINE AMPERES/S
0.0
.4
.8
1.2
1.6
2.0
2.4
2.8
3.2
3.6
4.0
-90
-60
-30
0
30
60
90
120
150

Figure E.3-8

APPENDIX E.4 CALCOMP PLOTS: 10^{th} Order EMA Model DC = 2.75°

RUN SUMMARY

MODE: 10^{th} ORDER EMA MODEL

PROGRAM MODE: PGMODE = 2

NUMBER OF MACHINES: NMACH = 2

DEFLECTION COMMAND: DC = 2.75 flap deg

TOTAL NUMBER OF INTEGRATIONS: NUMINT = 2000

TOTAL NUMBER OF MECHANICAL-POSITION LOOP INTEGRATIONS: NINITI = 2000

TOTAL NUMBER OF VELOCITY COOP INTEGRATIONS: 2000

TOTAL SIMULATION TIME: 0.4 sec

TOTAL NUMBER OF POINTS PLOTTED: 1001

TOTAL NUMBER OF NETWORK CHANGES: 0

TIME TO DC: .187 sec

TIME TO FIRST PEAK: .253 sec

PEAK DEFLECTION: 3.26 flap deg

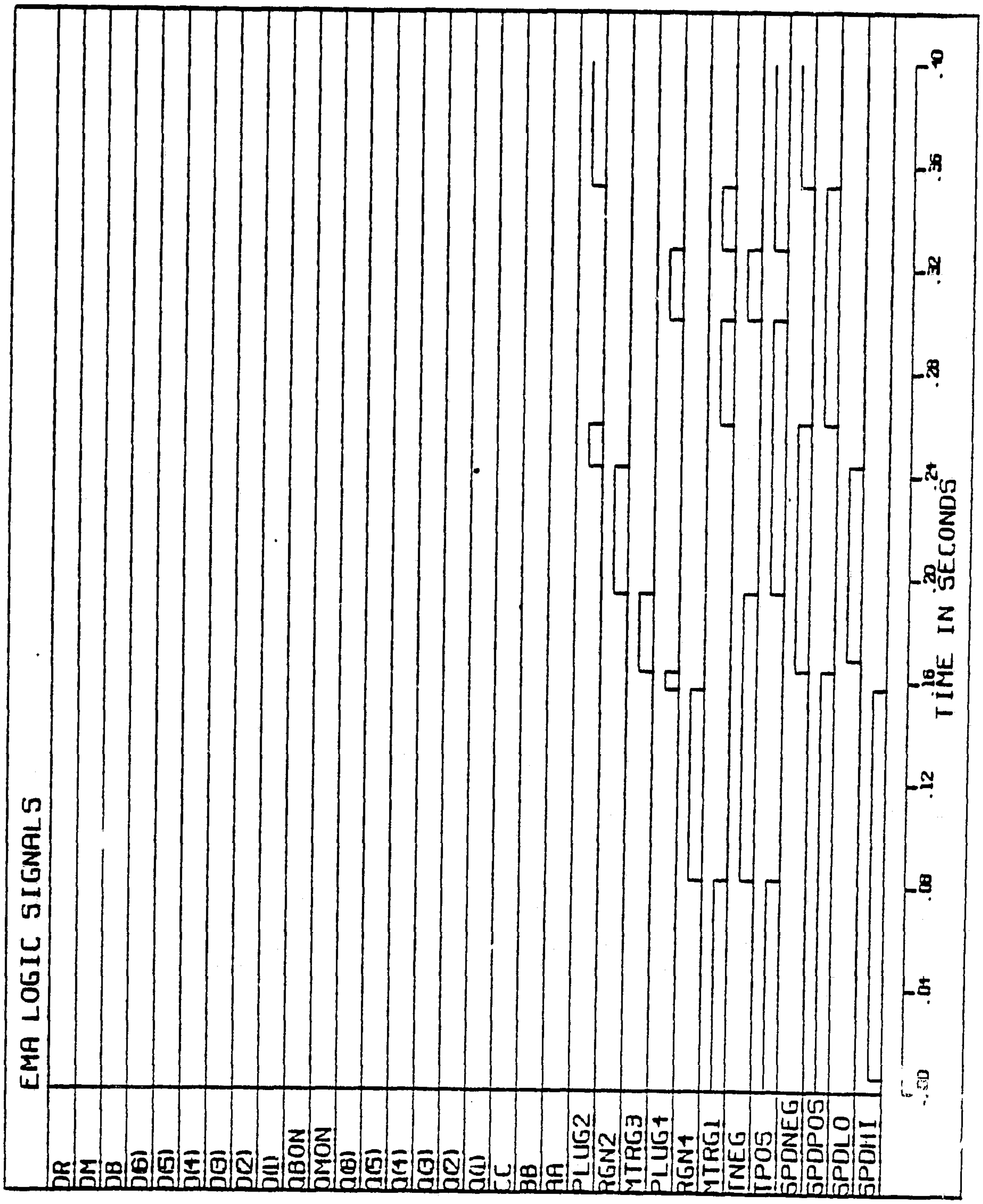
EMA LOGIC SIGNALS
PLUG2
RGN2
MTRG3
PLUG4
RGN4
MTRG1
TNEG
TPOS
SPDNEG
SPDPOS
SPDLO
SPDHI
.04
.08
.12
.16
.20
.24
.28
.32
.36
.40
TIME IN SECONDS

Figure E.4-1

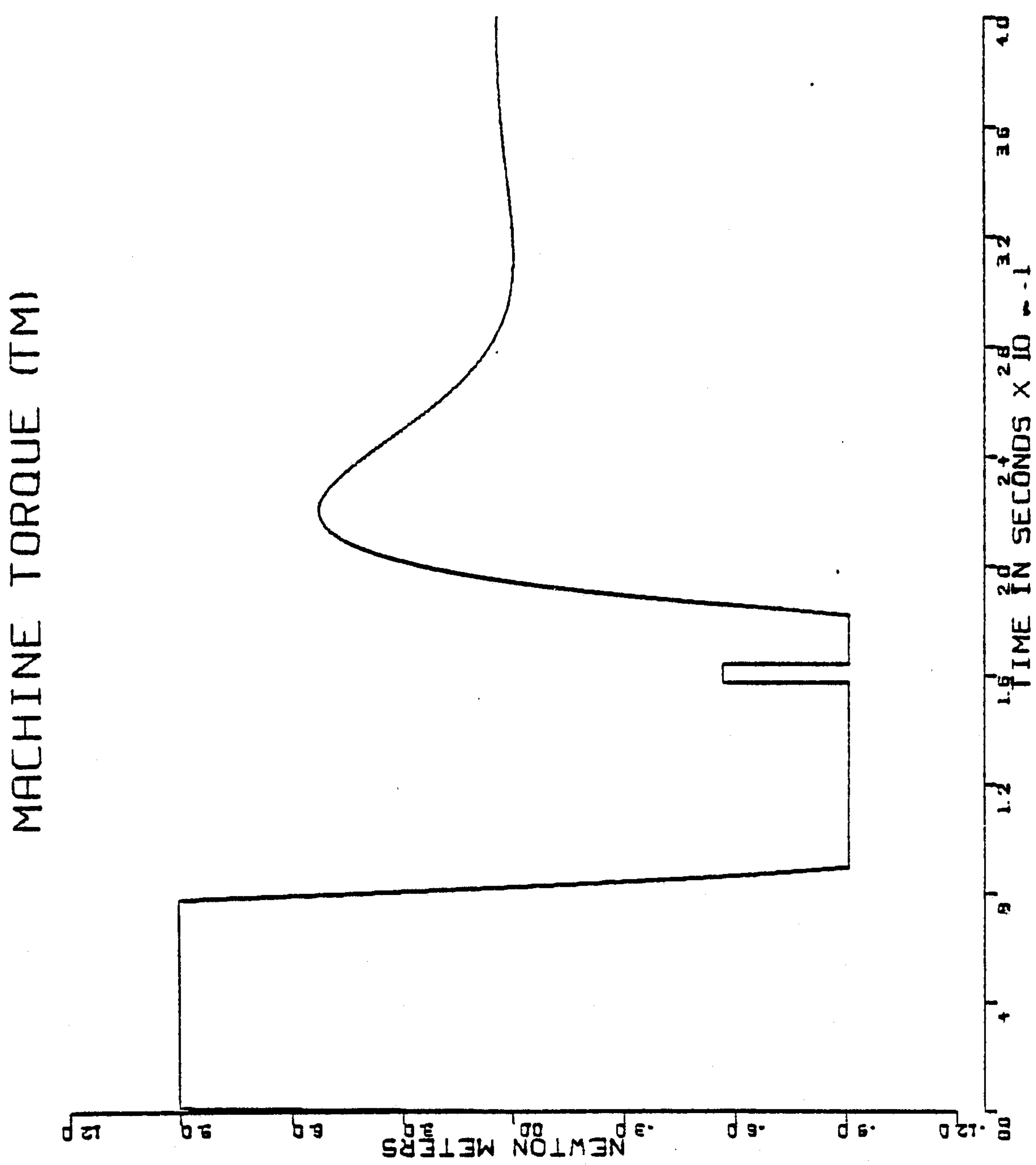

Figure E.4-2

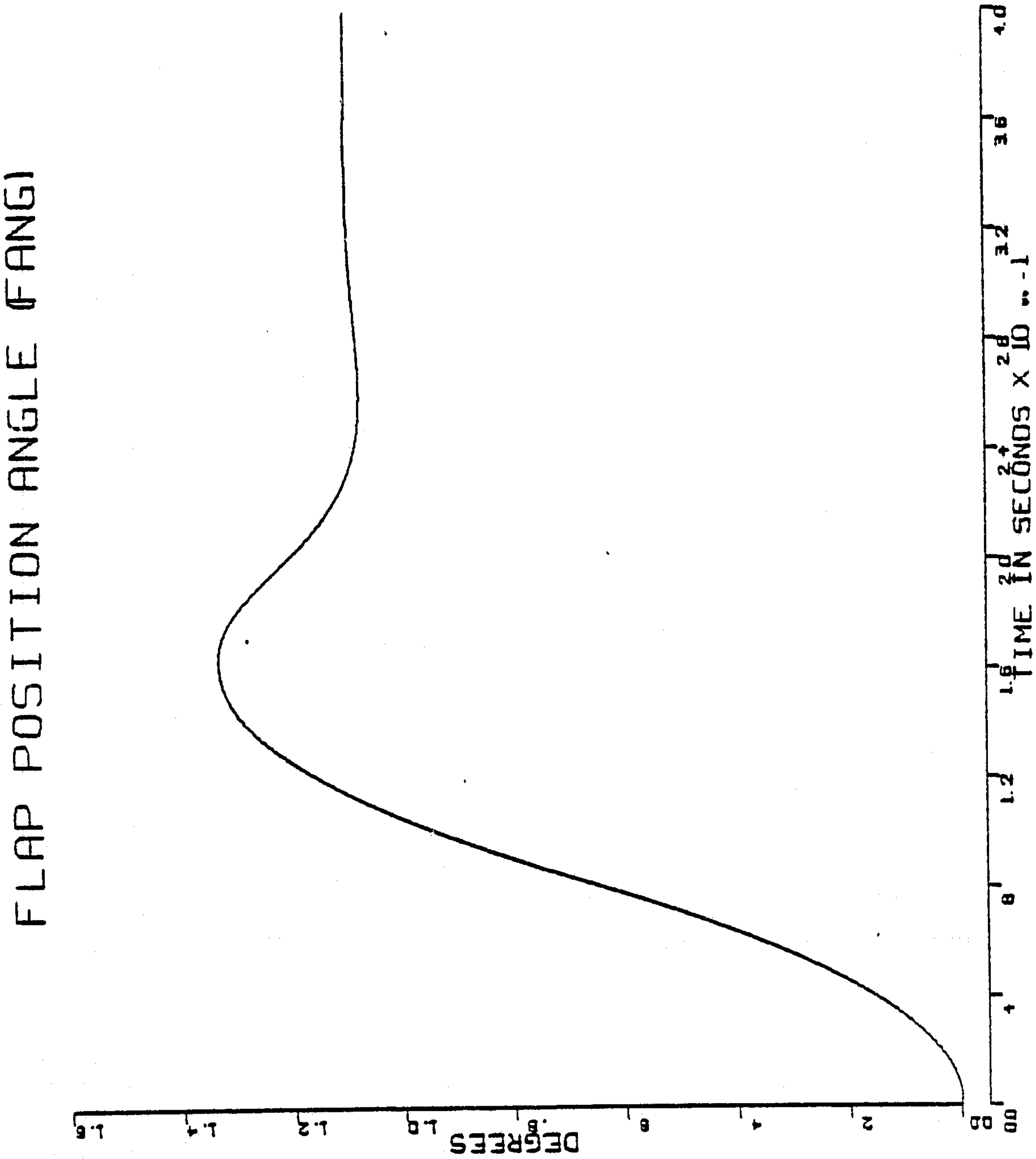

Figure E.4-3

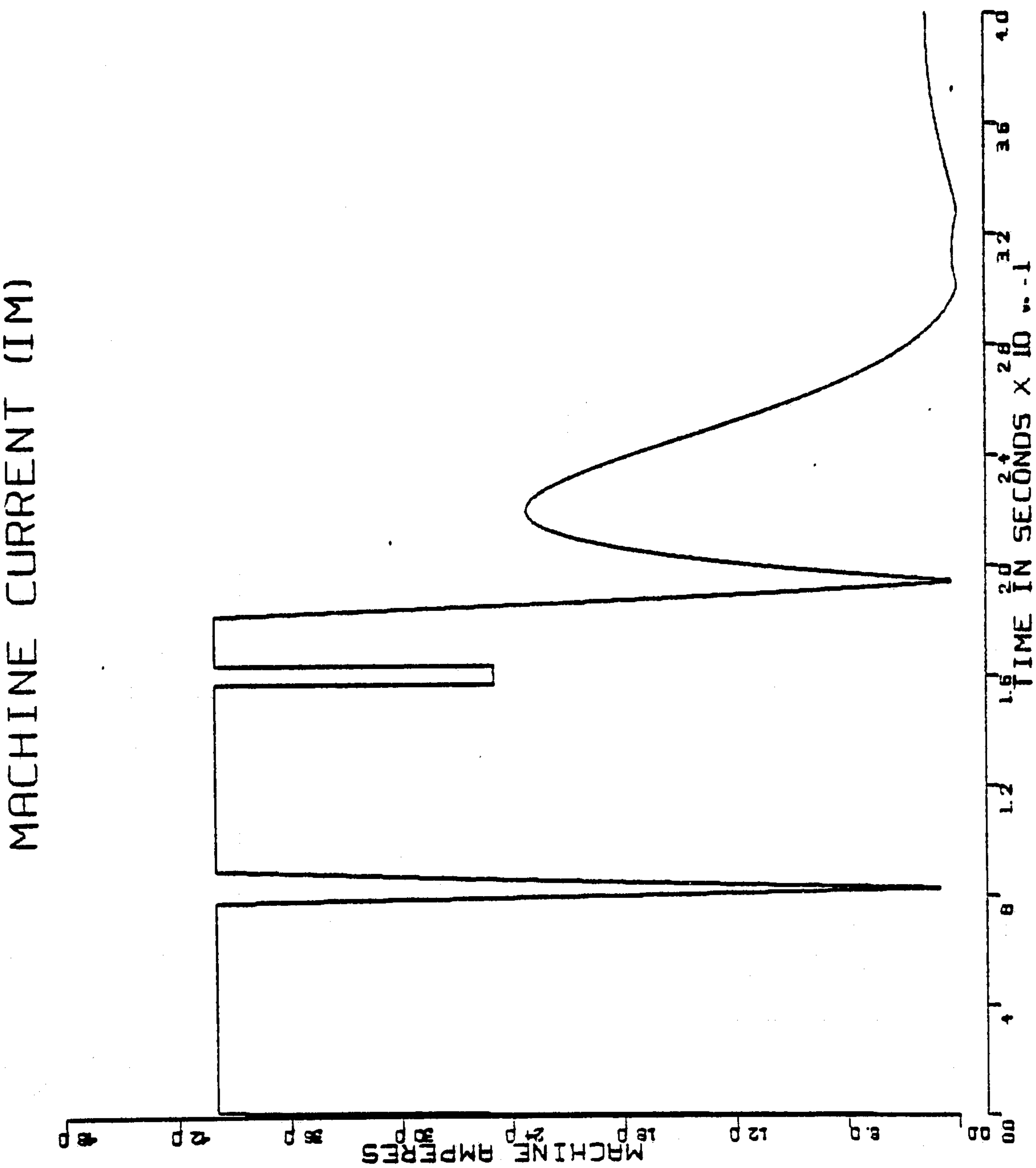

Figure E.4-4

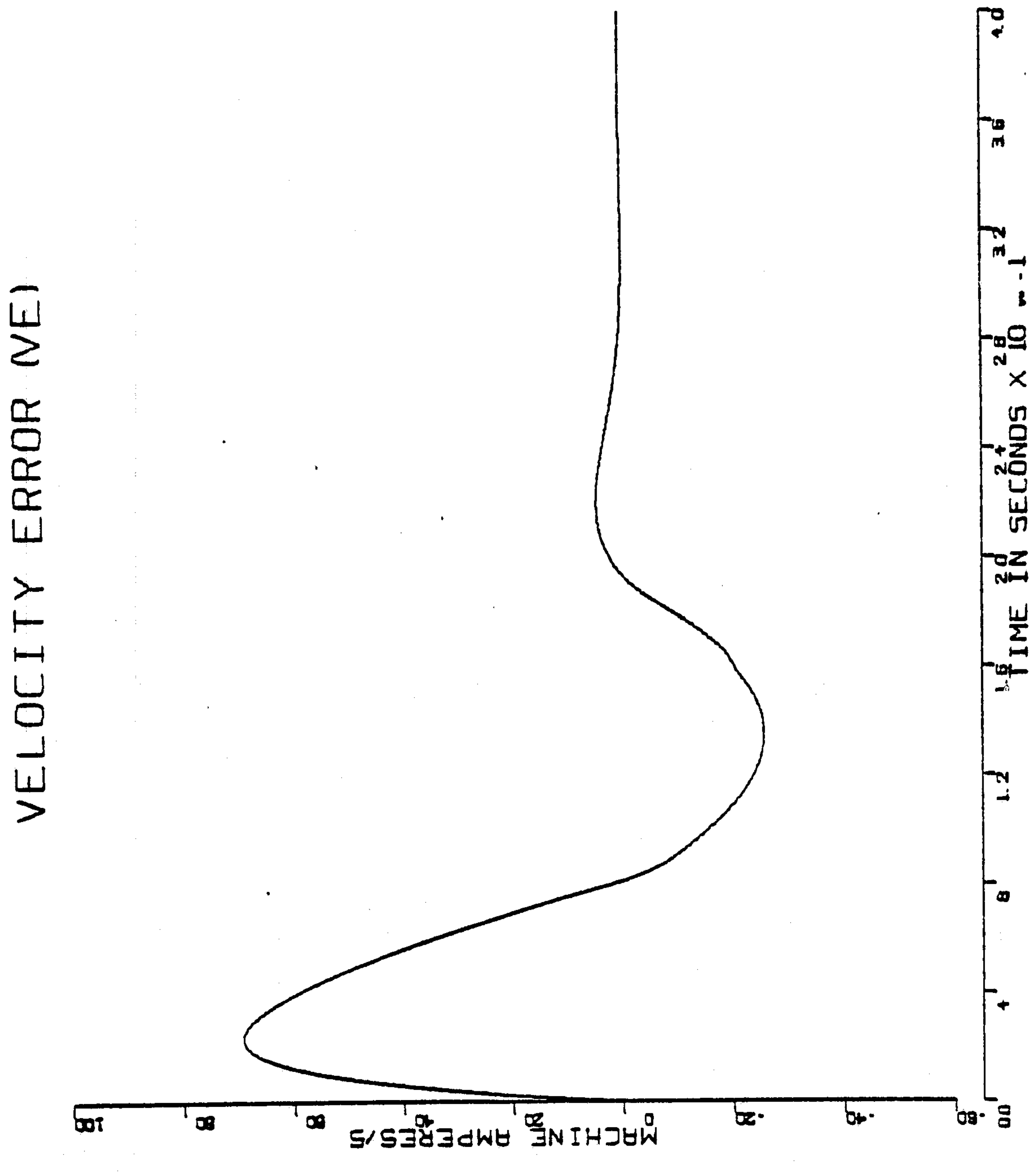
VELOCITY ERROR (VE)
TIME IN SECONDS X 10 ** -1
MACHINE AMPERES/S
0.0
.4
.8
1.2
1.6
2.0
2.4
2.8
3.2
3.6
4.0
-60
-40
-20
0
20
40
60
80
100

Figure E.4-5

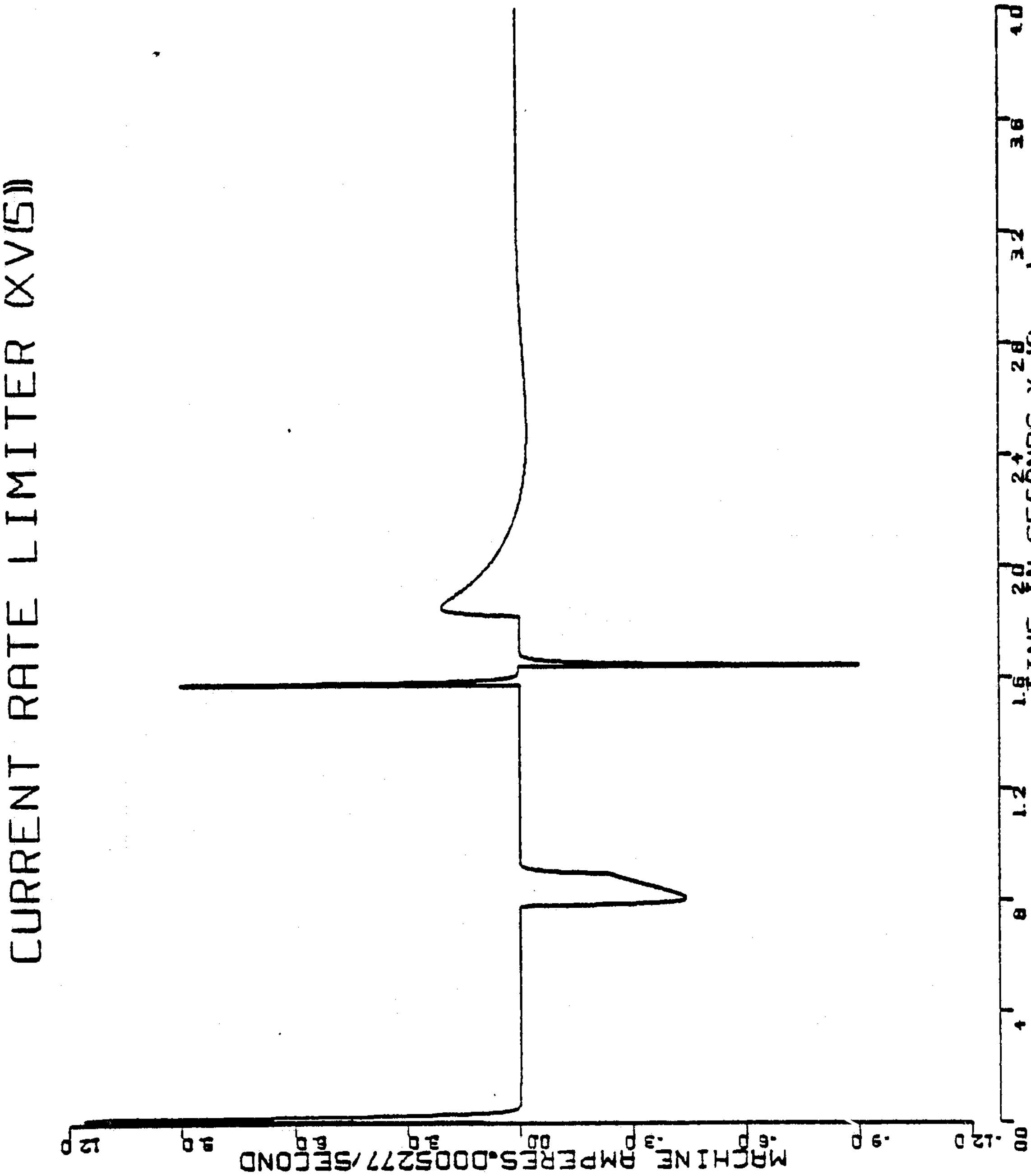
CURRENT RATE LIMITER (XV(5))
TIME IN SECONDS X 10 ** -1
0.0
.4
.8
1.2
1.6
2.0
2.4
2.8
3.2
3.6
4.0
MACHINE AMPERES.0005277/SECOND
-12.0
-9.0
-6.0
-3.0
0.0
3.0
6.0
9.0
12.0

Figure E.4-6

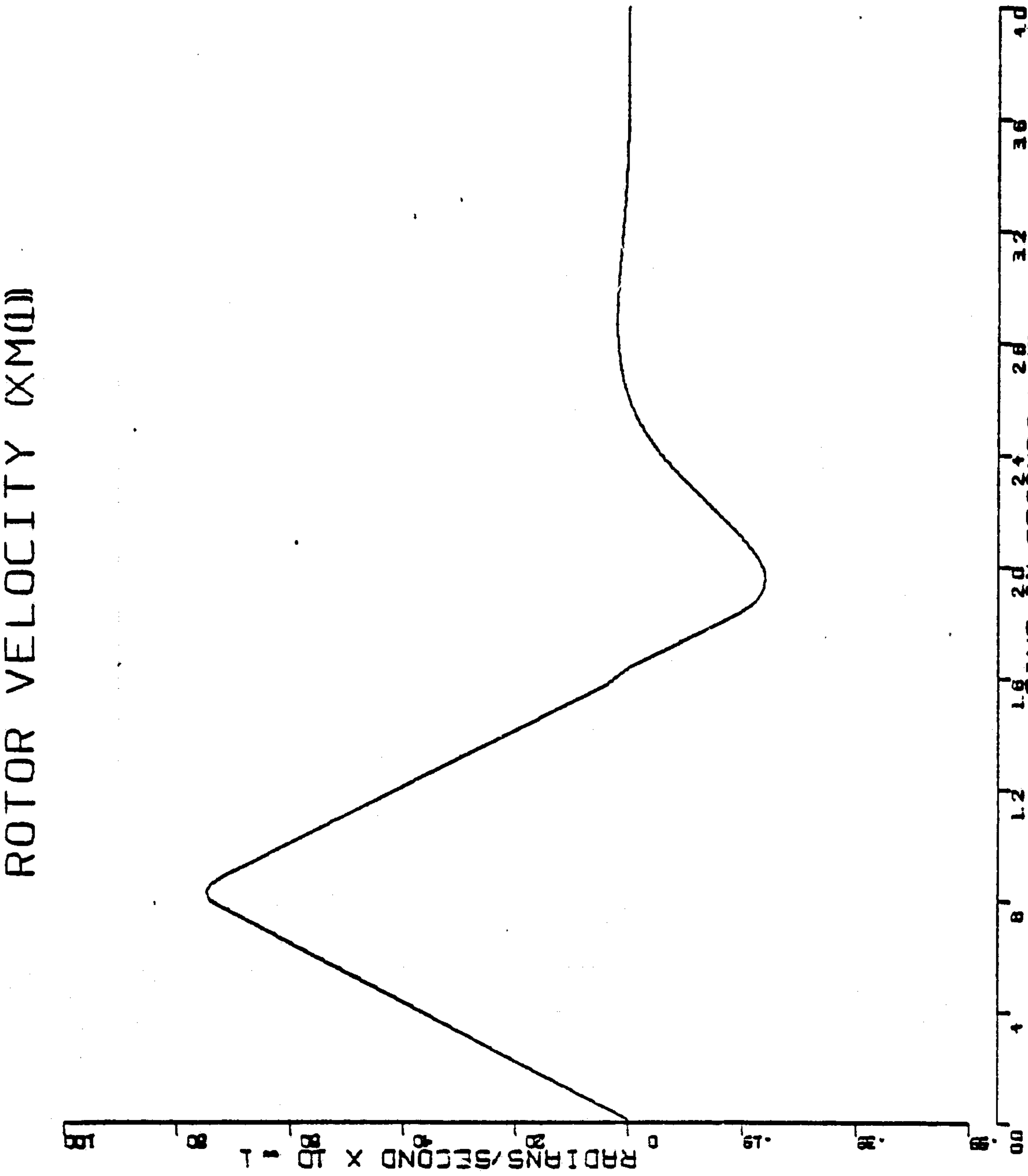
ROTOR VELOCITY (XM(1))
TIME IN SECONDS X 10 ** -1
RADIANS/SECOND X 10 ** 1
0.0
4
8
1.2
1.6
2.0
2.4
2.8
3.2
3.6
4.0

Figure E.4-7

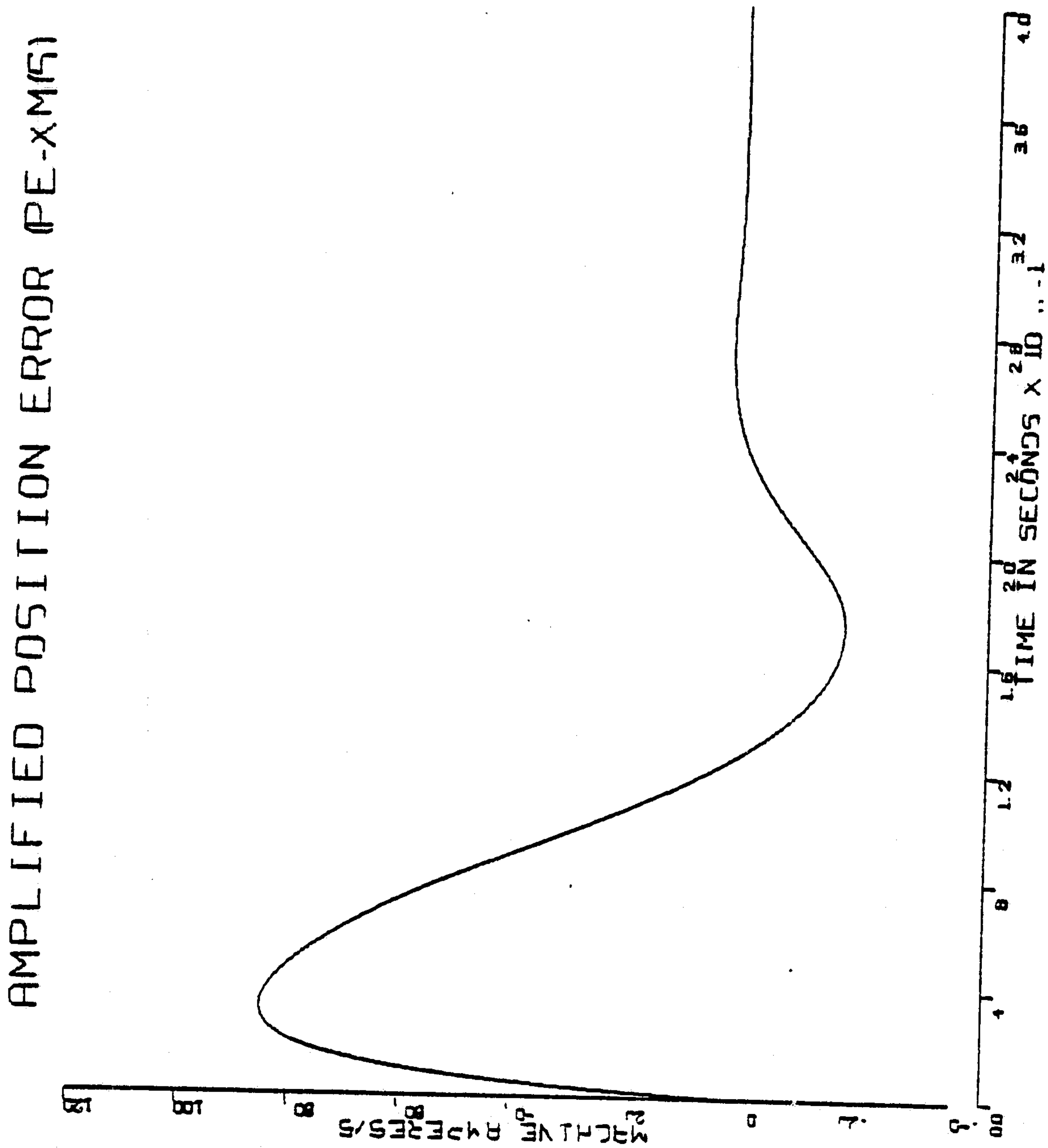
AMPLIFIED POSITION ERROR (PE-XM(5)
TIME IN SECONDS x 10 ^-1
0.0
4
8
1.2
1.6
2.0
2.4
2.8
3.2
3.6
4.0

Figure E.4-8

LIST OF REFERENCES

1. Nehl, T. W. "Ph.D Dissertation," Department of Electrical Engineering, Virginia Polytechnic Institute and State University, Blacksburg, Virginia, expected June 1979.

2. Delco Electronics, "Final Report on the Electromechanical Flight Control Actuator," Final Report on Contract No.: NSA 9-14952, General Motors Corporation, Delco Electronics Division, Santa Barbara Operations, Goleta, CA, Volume 1, January 1978.

3. Delco Electronics, "Final Report on the Electromechanical Flight Control Actuator," Final Report on Contract No.: NAS 9-14952, General Motors Corporation, Delco Electronics Division, Santa Barbara Operations, Goleta, CA, Volume 2, January 1978.

4. Delco Electronics, "Final Report on the Electromechanical Flight Control Actuator," Final Report on Contract No.: NAS 9-14952, General Motors Corporation, Delco Electronics Division, Santa Barbara Operations, Goleta, CA, Volume 3, January 1978.

5. Balabanian, N. and Bickart, T. A., "Electrical Network Theory," Syracuse University, New York, John Wiley and Sons, Inc. 1969.

6. McCaig, Malcolm, "Permanent Magents," Halsted Press, New York, N.Y.

7. Nehl, T. W., "Comparison between Finite Element and Finite Difference Method for Numerical Solutions of Electromagnetic Fields in Power Apparatus," M.S. Thesis, Department of Electrical Engineering, Virginia Polytechnic Institute and State University, Blacksburg, Virginia, Dec. 1976.

8. Demerdash, N. A. and Nehl, T. W., "An Evaluation of the Methods of Finite Elements and Finite Differences in the Solution of Nonlinear Electromagnetic Fields in Electrical Machines," IEEE Transactions on Power Apparatus and Systems, Jan./Feb. 1979.

9. Shah, M. R., "A New Approach to Short Circuit Studies of Large Turbogenerators," M.S. Thesis, Department of Electrical Engineering, Virginia Polytechnic Institute and State University, Blacksburg, Virginia, April 1977.

10. Demerdash, N. A. and Shah, M. R., "A Practical Approach to Inclusion of Electromagnetic Field Nonlinearities in Dynamic Modeling of Large Turbogenerators - Part (I): Basic Principles for Inclusion of Instantaneous Magnetic Saturation," A Paper Submitted (August 10, 1978) for Review by IEEE for Presentation and Publication at the PES 1979 Winter Meeting, New York (F79-153-8).

11. Shah, M. R. and Demerdash, N. A., "A Practical Approach to Inclusion of Electromagnetic Field Nonlinearities in Dynamic Modeling of Large Turbogenerators - Part (II): Derivation and Calculation of Machine Parameters," A Paper Submitted (August 10, 1978) for Review by IEEE for Presentation and Publication at the PES 1979 Winter Meeting, New York.

12. Demerdash, N. A. and Shah, M. R., "A Practical Approach to Inclusion of Electromagnetic Field Nonlinearities in Dynamic Modeling of Large Turbogenerators - Part (III): Transformed Model Formulation, Numberical Algorithm and Applications," A Paper Submitted (August 10, 1978) for Review by IEEE for Presentation and Publication at the PES 1979 Winter Meeting, New York.

13. Demerdash, N. A. O., "Analytical Modeling of the Dynamics of Brushless DC Motors for Aerospace Applications: A Conceptual Framework," Johnson Sapce Center, Houston, Texas, August 18, 1976.

14. Demerdash, N. A. O and Nehl, T. W., "Second Progress Report on Contract No.: NAS 9-15091," Department of Electrical Engineering, Virginia Polytechnic Institute and State University, Blacksburg, Va., May 15, 1977.

15. Demerdash, N. A. O. and Nehl, T. W., "Final Progress Report on Contract No.: NAS 9-15091," Department of Electrical Engineering, Virginia Polytechnic Institute and State University, Blacksburg, Va.